PKM2 regulation of metabolism but not transcription is important for natural killer cell responses

A dissertation submitted to Trinity College Dublin in candidature for the degree of Doctor of Philosophy

School of Biochemistry and Immunology
Trinity College, Dublin

2020

By Jessica Walls

Under the supervision of Dr. David Finlay, Dr. Clair Gardiner and Dr. Daniel McVicar

Declaration

I declare that this thesis has not been submitted as an exercise for a degree at this or any other university and it is entirely my own work.

I agree to deposit this thesis in the University's open access institutional repository or allow the library to do so on my behalf, subject to Irish Copyright Legislation and Trinity College Library conditions of use and acknowledgement

For my Mam and Dad

Publications

Nutrient sensing, signal transduction and immune responses

Seminars in Immunology **Vol. 29**, Issue 5 October 2016

Jessica Walls, Linda Sinclair and David Finlay

Glucose represses dendritic cell-induced T cell responses

Nature Communications **Vol. 8**, 30 May 2017

Simon J. Lawless*, Nidhi Kedia-Mehta*, **Jessica F. Walls**, Ryan McGarrigle, Orla Convery, Linda V. Sinclair, Maria N. Navarro, James Murray ,David K. Finlay
**These authors contributed equally to this work*

Table of Contents

Table of Figures

List of Tables

Summary

Natural Killer (NK) cells are cytotoxic lymphocytes that are crucial for defence against viruses and cancer. Our knowledge of murine NK cell metabolism has evolved over recent years and has revealed that NK cell effector functions are integrally linked to metabolism. NK cells predominantly use glucose to fuel their metabolism through glycolysis, however nothing is known of the direct enzymatic regulation of this pathway in NK cells. One key metabolic regulators of glycolysis in other immune cells is the enzyme Pyruvate Kinase Muscle (PKM). PKM is the last enzyme of glycolysis and converts phosphoenolpyruvate to pyruvate. Two isoforms exist, PKM1 and PKM2. Data suggests that PKM1 exists primarily as a tetramer that is fully active. In contrast, PKM2 can adopt two configurations, active tetramers or relatively inactive mono/dimers. Thus, PKM2 has the ability to adopt different activity levels whereas PKM1 does not. In cancers, inactive monomers limit the rate of pyruvate production resulting in accumulation of upstream glycolytic intermediates to support biosynthesis and cell growth. Monomeric/dimeric PKM2 has a relatively low affinity for its substrate, but plays other roles such as phosphorylating other proteins, and regulating activity of transcription factors. Therefore, PKM2 can function as both a regulator of both metabolic biosynthesis and the transcriptome. Here we have investigated the role of PKM2 in murine NK cell biology.

Our data show that *in vitro* cytokine stimulated murine NK cells and *in vivo* Poly(I:C) activated NK cells up-regulated their expression of PKM2. In order to dissect the role of PKM2 in NK cell physiology, we generated an NK cell specific PKM2 knock out mouse line ($Ncr1^{Cre}$ x $Pkm2^{fl/fl}$). Our data show that NK cells lacking PKM2 are functionally and

metabolically normal, both with *in vivo* activation with Poly(I:C) and with a model of murine cytomegalovirus. Similarly, cytokine activation of NK cells *in vitro* upregulate metabolism normally, and make normal levels of pro-inflammatory cytokines. Interestingly, NK cells lacking PKM2 also have a normal transcriptome, indicating that PKM2 is not a transcriptional regulator in NK cells.

Metabolically, $PKM2^{KO}$ cells are normal due to genetic compensation by the alternate PKM isoform, PKM1. Expression of this isoform allows them to maintain normal pyruvate kinase activity, even in the absence of PKM2.

To overcome this genetic compensation we utilised a pharmacological activator of PKM2, TEPP-46. We find that in NK cells, TEPP-46 promotes PKM2 enzymatic activity and acutely increases glycolytic flux. TEPP-46 treatment of IL-2/12 stimulated NK cells over 18 hours leads to reduced NK cell effector functions, reduced blastogenesis and impaired mitochondrial metabolism. This is accompanied by increased cellular reactive oxygen species indicating that inactive PKM2 may play an oxidative defence role in NK cells. Taken together our data indicate that PKM2 does not regulate the transcriptome of NK cells, and that tight regulation of pyruvate kinase enzymatic activity is required for optimal NK cell metabolism and function.

Abbreviations

2-DG	2-deoxyglucose
ADP	Adenosine diphosphate
ATP	Adenosine triphosphate
AML	Acute Myeloid Leukaemia
BrDU	Bromodeoxyuridine
CAR	Chimeric antigen receptor
CMS	Citrate-malate shuttle
DC	Dendritic cell
ECAR	Extracellular acidification rate
EAE	Experimental autoimmune encephalomyelitis
FACS	Fluorescent activated cell sorting
FADD	Fas-Associated Death Domain
$FADH_2$	Flavin adenine dinucleotide
GAPDH	Glyceraldehyde 3-phosphate dehydrogenase
HIF1a	Hypoxia inducible factor 1 alpha
Hex2	Hexokinase 2
HLA	Human leukocyte antigen
IFNγ	Interferon gamma
ITAM	Immunoreceptor tyrosine-based activation motif
ITIM	Immunoreceptor tyrosine-based inhibition motif
JAK	Janus Kinase
Ldha	Lactate dehydrogenase

MHC	Major Histocompatibility Complex
MAPK	Mitogen activated protein kinase
MCMV	Murine cytomegalovirus
mTORC1	Mammalian target of rapamycin complex 1
NADH	Nicotinamide adenine dinucleotide
NADPH	Nicotinamide adenine dinucleotide phosphate
NCR	Natural cytotoxicity receptors
NFAT	Nuclear factor of activated T cells
NK cell	Natural Killer cell
OCR	Oxygen consumption rate
OxPhos	Oxidative Phosphorylation
PEP	Phosphoenolpyruvate
PKM	Pyruvate Kinase muscle
Poly(I:C)	Polyinosinic:polycytidylic acid
Rplp0	Ribosomal protein lateral stalk subunit P0
S6	Ribosomal protein S6
SREBP	Sterol regulatory element binding protein
STAT	Signal transduced and activator of transcription
TCA cycle	Tricarboxylic acid cycle
TCR	T cell receptor
TLR	Toll like receptor
TRAIL	TNF-related apoptosis inducing ligand
ROS	Reactive oxygen species

Acknowledgements

I will start out this acknowledgements section by saying that I have a lot of people to thank. The opportunity to carry out my PhD in two different countries has allowed me to meet so many people, which has been the most enjoyable part of this PhD, but it also means that I have an extra-long acknowledgements section.

First things first. I need to thank all three of my PhD supervisors. To Dave and Clair, thank you both for giving me the chance to go for this amazing studentship back when I was 4th year of my undergrad. It has been such an amazing opportunity and I will be eternally grateful to you both.

Dave, thanks for being a fantastic supervisor, I've learned so much about immunometabolism from you and always enjoyed talking science.

Clair, thanks so much for your help over the past few years. I promise going forward I will be much more positive. Thanks especially for your help over the past few weeks, you have really helped me get through this writing process.

Dan, when I moved to the States almost 2 and half years ago, I was honestly very daunted to be working with a mentor that never had a graduate student. That notion flew out the window within the first week. I am so grateful for your guidance over the past few years. Thank you so much for being such a great listener and mentor. The Dude abides.

To the past members of the Finlay and Gardiner labs: Thanks to Ray and Simon for giving great advice at the beginning of the PhD. Thanks to Roisin for teaching me so many techniques and for forewarning Katie and I what the write up 'syndrome' would be like. Thanks to Nadine for always being great fun.

Nidhi, thank you so much for everything. Starting out in the lab during my undergrad, I never would have predicted how good of a friend I would gain in you. You are one of the most honest people I know, and also one of the best listeners I know. Whether I was sitting in the reading room, or 3000 miles away in the states I knew I could always count on you for a chat if I needed it. Thanks for being the best lab counsellor!

Katie, I'm so glad we got to start our PhD's together. The time we almost killed all of our cells in our first week looked like a bad omen, but look at where we are now! I will be eternally grateful for your positivity and friendship throughout this whole process and I can't wait to see all of the amazing things you achieve!

Thanks to Vanessa and Elena for always being so nice to be around in TC. Thanks to Karen for making me so many cups of tea the last few weeks and always being a listening ear to my complaints. To everyone in the 5th floor reading room. Thanks for a fun 2 years! Big thanks to all the people who stared this PhD at the same time as me: Aisling, Emma, Peter and Louise. Thanks also to Ji and Laura, Natalie, Darren, Paul, Ryan, Anna and anyone else I've forgotten. It was so hard leaving behind such a great group of people. Coming back and seeing how the people in the reading room change but the support and atmosphere is always the same is so amazing.

To my US lab!

First I want to thank Chris! You were such a pleasure to work with and so much fun. I learned so much from you and I have to thank you for getting me into running! It honestly got me through the tough times of my PhD.

To Luke. Thanks for letting me sit at the end of your bench for a year and a half. I know it must have been annoying having someone there all the time but I always knew I could

turn around and ask you a question if needed. It was a pleasure to learn science from you.

To Marieli and Erika. You girls have been the best people to be around these past few years. Thanks so much Marieli for always being so positive and teaching how to balance science and life. You are a great scientist but also a great mentor and friend. Thanks especially for the covfefe breaks. Erika, you are one of the brightest people I know and yet so incredibly humble. Thanks for always being patient with me and saying it how it is. You are going to do such great things.

Jeff, thank you for teaching me how to argue! And for showing me that there are a lot of good things about the US (although I will never admit it to your face!). Even if you think American bread, chocolate, everything is better than Europe! (You're wrong!). Seriously though, I want to thank you for always listening to my ideas and my ranting.

Jon. Helloooo! Thanks for always being a great resource to turn to when I need science or career advice. But also thanks for always having fun in the lab and telling me when there are snacks (apart from the apple pie! Ew!)

Thanks so much to my fellow Wellcome PhD student, Andrew. Living with you for almost two years was so beneficial to me both personally and scientifically. Not only were you my housemate and friend, but you were always a pleasure to chat to about anything metabolism. You are a powerhouse of a person!

Ryan, thanks for putting up with the ups and downs of the PhD over the last few months. The past two years of this PhD have been so tough but you kept me sane and kept life fun. I promise I'll be normal again soon and I can't wait to go on all the trips we have planned over the next few months!

I also want to thank my grandparents. Three of them aren't here anymore, but they were/are some of the most influential people I have had in my life. I want to thank Alice McIntyre, Maureen and Maurice Walls who made me who I am and who will always be missed. To my grandad, Charles McIntyre. Thanks so much for your support over the past few years, I am truly lucky to have you as my grandad.

To my Mam and Dad, Glynis and Tony Walls. I definitely don't say it enough, but I am so grateful that I have you two as my parents. You always say you were only lucky enough to have one child where in reality I was lucky that I had you both all to myself. Thanks for always supporting me. I promise I'm finally done(ish) with college now!!

Chapter 1: Introduction

1.1. Natural Killer cells

Natural killer (NK) cells are crucial part of the innate immune system that were discovered in the early 1970's [1]. They were initially recognized to be important for the detection and elimination of both virally infected and transformed cells but have now been identified to have a broader range of functions such as in pregnancy [2]. NK cells act as a first line of defence against immunological threats but are also uniquely placed to regulate adaptive arms of immunity through cytokine signalling and cell-cell interactions. NK cells are potent producers of cytokines such as IFNγ which is important for control of cancer and required for the activation of other immune cells such as macrophages [3]. NK cells can also directly kill their targets via the production of cytotoxic molecules that can kill or lyse the target cell [4]. They are different from adaptive lymphocytes in that they do not undergo gene rearrangement of receptors and do not require prior exposure to antigen to become activated. NK cells are found in both humans and mice, and for the most part have the same functional roles although their surface marker expression, method of activation and classification can differ slightly between each species [5].

1.2. NK cell development

Haematopoietic stem cells in the bone marrow have different lineages which will ultimately give rise to a common lymphoid progenitor cell (CLP) and a common myeloid progenitor (CMP) [6]. NK cells are derived from a CLP precursor in the bone marrow which is common to other lymphocytes such as T cells and B cells [7]. However, NK cells are distinct from T cells and B cells as they comprise a main subset of innate lymphoid cells (ILC). ILC are a subset of immune cells arising from an ILC progenitor that later form three distinct classes of ILC's (ILC1, ILC2, ILC3). NK cells comprise one of two subsets of ILC1 with other subsets characterized by different expression of transcription factors and cytokine production signatures. ILC1 cells produce IFNγ but don't produce Th2 and Th17 associated cytokines. The most significant difference between NK and ILC1 is differential expression of the transcription factor eomesdermin (EOMES) [8].

Murine NK cells form several distinct subsets in their development. Initially, they are derived from a CLP in the bone marrow. The formation of a committed NK cell intermediate is classified as being $CD122^{+}NK1.1^{-}DX5^{-}$ [9].The acquirement of CD122 expression is critical in NK cell development as it is the IL-2/IL-15 receptor common β subunit (CD122) which is associated with NK cell precursor formation [10]. This receptor is common to both IL-2 and IL-15 signalling pathways. Early studies identified that CD122 was required for normal NK cell development. Mice lacking CD122 showed a reduction in NK cell in the circulation and had no NK cytotoxic activity *in vitro* [11]. CD122 acquisition marks stage 1 of NK cell development with stage 2 being characterized by acquisition of NK1.1, CD94/NKG2, and NKG2D [12]. Immature and mature NK cells are classified based on expression of Ly49 and integrin α2 (DX5) (Fig. 1.1) [12].

Once NK cells are differentiated they can be found as either circulating or tissue resident NK cells. NK cells in human blood represent as much as 2-18% of circulating lymphocytes and 2% or 10% in the mouse spleen and lung respectively [13]. Most NK cells are characterised as being $CD3^{-}CD56^{+}$ cells in humans and $CD3^{-}NK1.1^{+}$ $NKp46^{+}$ cells in C57Bl/6 mice [14].

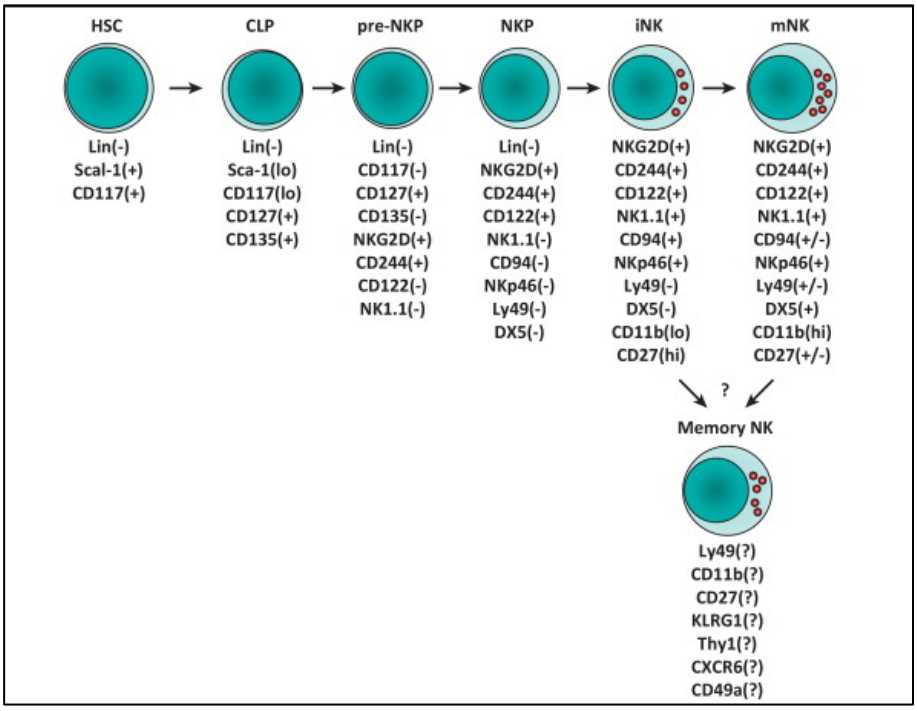

Figure 1. 1 Murine NK cell development :
Murine NK cells have three developmental intermediates derived from the common lymphoid progenitor with the eventual formation of a mature NK cell. Mature NK cells are proficient at both cytotoxicity and cytokine production. Image [7]

1.3. NK cell functions

The primary function of NK cells is to recognize and eliminate virally infected cells and cancer cells. Although, it has recently become apparent that NK cells play multiple other physiological roles including a crucial role in pregnancy. Uterine NK cells (uNK) are required for normal placental development after implantation. NK cells have also been shown to play roles in control of bacterial infections and in clearing senescent cells [15, 16].

NK cell effector functions are first dependent on target recognition. NK have specialised ways of achieving this, particularly in relation to virally infected cells. Many viruses have evolved to evade T cell responses through down regulation of MHC-I [17], the key mechanism of T cell recognition. However, NK cells are efficient at recognising this MHC loss on the surface of infected cells [18]. Indeed, the importance of NK cells in viral clearance is made evident by studies in NK deficient humans or mice. One seminal study demonstrated severe susceptibility to Herpesvirus infection in an adolescent without NK cells [19]. Similarly depletion of NK cells from mice using anti-NK1.1 or anti-asialo-GM1 antibodies led to decreased ability to clear murine cytomegalovirus (MCMV), herpes simplex virus 1 (HSV-1) and vaccinia virus [20]. These studies implicate a crucial role for NK cells in anti-viral immunity.

NK cells also play a crucial role in control of cellular transformation, particularly in the control of leukaemia. Indeed, mice depleted of NK cells were shown to have a higher number of metastases in a B16 clearance assay *in vivo* [21]. In humans, there have been correlative studies showing that people with low peripheral blood NK cell activity show

an increased risk of cancer [22]. Thus, NK cells clearly play an important role in anti-cancer immunity *in vivo.*

There are numerous other roles for NK cells, however, most commonly they exert their functions in three main ways (Fig. 1.2): Firstly, NK cells can release cytotoxic granules which directly kill target cells. Secondly, they can cause target cell death through interaction with cell surface receptors. Thirdly, they can produce cytokines and chemokines.

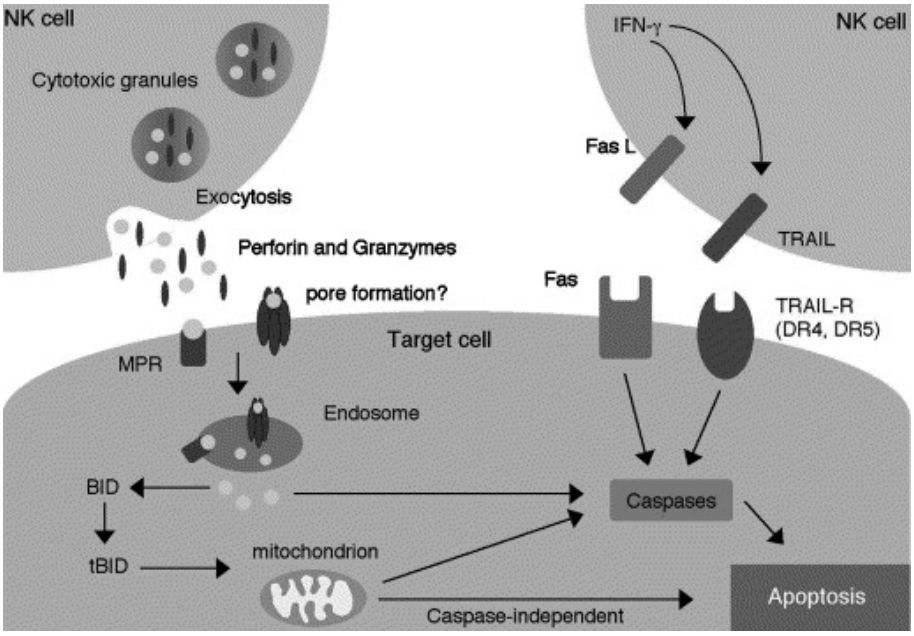

Figure 1. 2. Overview of three key NK cell effector functions

1) NK cells can release cytotoxic granules to mediate target cell death. 2) NK cells can induce apoptosis of target cells through death receptor signalling 3) NK cells can produce pro-inflammatory cytokines to activate other immune cells and can produce interferon to limit viral spread [23]

1.4. NK cell mediated cytotoxicity

NK cells can kill target cells through the exocytosis of cytotoxic granules, a process that is balanced by a variety of inhibitory and activating signals. NK cell cytotoxic granules are a type of organelle that contain perforins and granzymes [23]. There are 11 known isoforms of granzymes that are all structurally related; ten of which are found in mice and five that are found in humans [23]. Granzymes are proteases, with granzyme A and B being indispensable for the control of ectromelia, a poxvirus in mice [24]. Granzyme B is known to be a serine protease (it cleaves after serine residues on target cell peptides) which is able to induce apoptosis of target cells through direct cleavage of pro-caspases [25]. It is widely accepted that granzymes can enter the target cell with the assistance of pore forming proteins called perforins [26]. Perforin forms an opening in the target cell through which granzymes can enter after exocytosis from the NK cell. NK cell cytotoxicity generally causes death of the target cell, through either apoptotic or necrotic means [27, 28]

1.5. Death Ligands

NK cells can also directly induce death of target cells through the use of death receptor pathways. TRAIL (TNF-related apoptosis-inducing ligand) is a transmembrane protein that belongs to the TNF superfamily. TRAIL can induce death of target cells through death receptors TRAIL-R1 (DR4) and TRAIL-R2 (DR5) which are members of the TNF receptor superfamily [29]. There are two more death receptors, TRAIL-R3 and TRAIL-R4; however binding of TRAIL to these receptors does not induce apoptosis in humans [29]. Mice express only one isoform of TRAIL-R which shows homology to human DR5 [30]. DR4 and DR5 have a death domain present in their cytoplasmic region. Ligation of these

receptors by TRAIL results in formation of a death-inducing signalling complex (DISC) at the death domain which in turn causes recruitment of an adaptor molecule called FADD (Fas-Associated Death Domain) [31]. FADD leads to activation of caspase-8 and caspase-10 which causes cleavage of caspase 3 which then activates apoptosis pathways within the target cell [31]. Some studies have proposed the use of soluble TRAIL as a cancer therapy [31].

Similarly, another mechanism of NK cell induced target cell apoptosis is through the cell surface expression of Fas ligand (FasL). FasL works similarly to TRAIL in that it causes recruitment of adaptor proteins to the death domain present on the Fas receptor in the target cell, and causes downstream activation of apoptosis activator caspase-3 [32].

1.6. NK cell cytokine and chemokine production

NK cell also play a role in producing cytokines. This can activate other members of the immune system or directly limit cancer and viral spread. Key examples of cytokines produced by activated NK cells are: tumour necrosis factor-α (TNFα), interferon-γ (IFNγ) and granulocyte-macrophage colony stimulating factor (GM-CSF). IFNγ can directly activate other mechanisms of anti-viral defence, and also directly limit viral spread to surrounding cells [33]. IFNγ is a key cytokine for the activation of macrophages, but it also plays a key role in activating the adaptive immune response. Indeed, IFNγ is a key cytokine for polarising CD4 T cells into proinflammatory Th1 cells [34]. IFNγ has even been shown to play a protective role in cancer [35]. NK cells can also activate myeloid cells. NK cell derived GM-CSF production is important for differentiation and activation of DC and macrophages [36]. NK cells also robustly produce chemokines such as macrophage inflammatory protein-1α (MIP1α) and

macrophage inflammatory protein-1β (MIP1β) to recruit other immune cells to a site of infection or inflammation [37].

1.7. NK cell receptor signalling

NK cells can be regulated in multiple ways. This is achieved mainly through a balance of activating and inhibitory receptors. NK cells do not express immunoglobulin receptors such as T cell receptor or antibodies, and so are different to their lymphocyte counterparts. NK cells highly express high levels of natural cytotoxicity receptors (NCR) [38]. For both humans and mice, a key method of NK cell target cell identification is based on 'missing self'. NK cells can kill cancer cells that lack MHC class I, but will spare cells that express it at their surface [39]. The ability of an NK cell to recognize MHC is physiologically important as virally infected and cancer cells can have reduced expression of MHC I at the cell surface as an evasion mechanism from CD8+ T cells [40]. Inhibitory receptors therefore play a significant role in the regulation of NK cell responses, as healthy cells expressing MHC I will not be targeted by NK cells. One of the main classes of inhibitory receptors expressed on human NK cells are killer cell immunoglobulin-like receptors (KIR). KIR recognise different variants of human leukocyte antigen (HLA) [41]. KIR mediated recognition allows human NK cells to distinguish transformed or virally infected cells from healthy cells [42].

The mouse counterpart to KIR is the Ly49 gene family. Ly49 is a C-lectin type family of receptors and they are mainly inhibitory and recognize MHC I [43]. Although functionally similar to KIR, they are structurally unrelated and appear to have evolved convergently [44]. Ly49 can require peptide binding in the MHC groove although the specificity of peptide binding varies among the Ly49 receptors [43, 45]. An example of

an inhibitory Ly49 receptor is Ly49I. Ly49I expressed on NK cells from 129/J mice will recognise murine cytomegalovirus antigen m157. This is a viral evasion mechanism as ligation of Ly49I by m157 will inhibit NK cell recognition of the virally infected cell [46].

Inhibitory receptors signal through a common immunoreceptor tyrosine-based inhibitory motif (ITIM). When receptors containing an ITIM are activated, a tyrosine residue in the motif becomes phosphorylated and recruits the lipid phosphatase SHP-1 [47]. Engagement of inhibitory receptors has been shown to prevent intracellular Ca^{2+} release caused by phospholipase C, thus preventing second messengers within a cell.

NK cells also express activating receptors. NK activating receptors include the natural cytotoxicity receptors (NCRs); NKp30, NKp44 and NKp46 [41].

Activating NK cell receptors contain immunoreceptor tyrosine-based activation motifs (ITAM) [47]. Studies have shown that ITAM based signalling is mediated predominantly by phospholipase Cγ1 and phospholipase Cγ2 in CD16 stimulated NK cells [48]. Activation of phospholipases is associated with release of intracellular Ca^{2+} which can be used to activate other signalling molecules such as NFAT (nuclear factor of activate T cells). A key example of an activating NK cell receptor in viral control is Ly49H. Ly49H can directly bind virally encoded proteins exposed on the target cell surface. Similar to Ly49I, Ly49H recognises MCMV viral antigen m157. But unlike Ly49I, Ly49H will recognize it as a viral ligand and will lead NK cell expansion and target cell killing [44].

Another key activating NK cell receptor is NKG2D. This receptor is highly specialised for cells expressing markers of stress on their cell surface [49]. Murine ligands for this receptor include MULT-1 (murine ULBP-like transcript-1), RAE-1 (retinoic acid early inducible-1), three different isoforms of a protein called H60 (histocompatibility 60) [50]. NKG2D will recognise cells undergoing stress and will use cytotoxicity to kill them.

1.8. NK cell cytokine signal transduction

Along with receptor mediated NK cell activation, NK cells are also robustly activated by cytokines. These include IL-2, IL-12, IL-15, IL-18 and IL-21 and type I interferons. However, the hallmark cytokine known to be involved in NK cell development is IL-15 [14]. IL-15 is a protein of 14kDa that shares 19% sequence homology with IL-2 [51]

As described previously, NK cell expression of IL-2Rβ/CD122 chain (which is common to IL-15 and IL-2 signalling) is a defining moment in NK cell development. IL-15 signalling through this receptor is important for NK cell development and proliferation. Indeed, IL-15 has been utilized in some studies for NK cell culture expansion, as it will cause NK cell proliferation in a mixed population of lymphocytes [52]. It is produced by DC and is trans-presented by IL-15Rα which is expressed by the DC [53]. IL-15 signals through a heterotrimeric receptor consisting of a unique α chain, CD122, and a the common-γ subunit [53].

Signalling mediated by the common-γ subunit is shared by IL-2, IL-7, IL-4, IL-9 and IL-21 cytokine pathways [54]. IL-2 signals through the same subunit as IL-15, CD122, and the common-γ subunit, however it has a higher affinity to the heterotrimeric combination of IL-2Rα-CD122-γc whereas IL-15 has a higher affinity for the heterotrimetic complex of IL-15Rα-CD122-γc [54, 55]. Both of these signalling pathways use Janus Kinase 1 and Janus Kinase 3 (Jak1, Jak3) for signal transduction (Fig.1.3).

Engagement of the IL-15Rα or IL2Rα with the CD122 and common-γ subunit leads to the phosphorylation of the receptor and recruitment of JAK1 and JAK3. This leads to recruitment of STAT5 which itself becomes phosphorylated on a tyrosine residue causing it to form homodimers [55]. Dimerization of STAT5 leads to its dissociation from the receptor and its translocation to the nucleus to transcribe target genes such as c-

Myc and Bcl-2 [55, 56]. Transcription of STAT5 target genes then supports NK cell survival, proliferation and cytotoxicity [57]. Indeed, murine NK cells deficient in STAT5 have significantly decreased viability [56]. IL-2 is also an activator of mammalian target of rapamycin complex 1 (mTORC1) which can coordinate metabolism and blastogenesis in murine NK cells, and is required for IFNγ production [52]. IL-2 will also drive mitogenic signals through the mitogen activated protein kinase (MAPK) pathway [58].

NK cells can also respond to IL-12. Indeed, IL-12 was first named 'NK cell stimulating factor' based on its ability to induce IFNγ by NK cells [59]. Later, it was identified that IL-12 activates NK cells in a STAT4-dependent manner which will lead to downstream activation and IFNγ production [60]. IL-12 will also induce the expression IL-2Rα on murine NK cells, which will allow them to more robustly respond to the adaptive cytokine IL-2 [52]

This indicates that NK cells are primed to respond to both innate (IL-12) and adaptive (IL-2) cytokines, which are capable of modulating NK cell immunological functions and also metabolism.

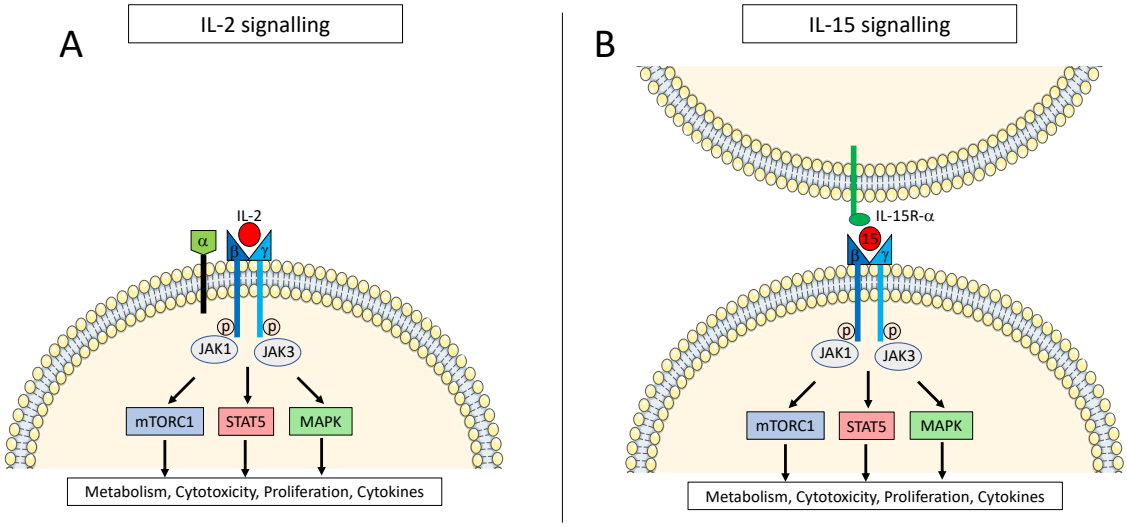

Figure 1. 3. IL-2 and IL-15 Signalling

IL-2 and IL-15 signal through similar mechanisms using both CD122 (β) chain and the common γ chain. (A) IL-2 is a key adaptive cytokine that will drive activation of key signalling pathways in NK cells. IL-2 receptor consists of IL-2Rα, CD122 and the common gamma chain. (B) Unlike IL-2 signalling, IL-15 signalling does not require the expression of IL-2α Instead IL-15 is transpresented from another cell (such as DC) through the IL-15Rα IL-2 or IL-15 binding to their respective receptors causes recruitment of JAK1 and JAK3 to the cytoplasmic region of the receptor. JAK1 and JAK3 will lead to downstream activation of mTORC1, MAPK and STAT5 signalling. IL-2 and IL-15 signalling can result in in increased metabolism, proliferation, cytotoxicity and effector molecule production.

1.9. NK cell control of cytomegalovirus

A specific pathogen example that showcases the importance of NK cells is cytomegalovirus. Cytomegalovirus (CMV) is a double stranded DNA virus of the β-herpes family [61]. It is a ubiquitous infection, with current estimations setting worldwide prevalence at 83% of the population [62]. This virus is generally asymptomatic but can profound effects in immunocompromised individuals [61]. CMV is highly opportunistic towards the unborn foetus causing congenital and developmental defects. Indeed, CMV is the leading cause of congenital birth defects in the United States [61, 63]. NK cells have distinct roles in the control of CMV. The vast majority of NK cell receptors are inhibitory. However, certain viruses can cause antigens to be expressed on the cell surface which will trigger NK cell activating receptors, indeed this is the case for CMV.

CMV is classically studied in a murine model (murine cytomegalovirus or MCMV). Mouse studies show that NK cells play a crucial role in early responses to MCMV before that adaptive arm of immunity is activated after which cytotoxic T lymphocytes are involved. As previously discussed, NK cells express the Ly49 receptor family (murine NK cell gene complex) which is responsible for NK cell recognition of MCMV. Indeed, C57/Bl6 mice have innate resistance to MCMV due to their expression of the receptor Ly49H [64] . Other mouse strains such as BALB/c are susceptible to the virus [65]. Ly49H has the ability to recognize an MCMV encoded protein called m157 [66]. Ly49H signals through a DAP12, a signalling protein that contains an ITAM and will lead to downstream activation [67]. MCMV is an interesting viral model as it induces a type of clonal expansion of these Ly49H positive NK cells. Early infection with MCMV (2 days) in

C57Bl/6 mice is characterised by increased serum cytokines such as IFNγ , IL-12, and TNF but Ly49H cell numbers are normal in the spleen, liver and blood [68]. However, at this early timepoint they are starting to cell cycle. Dokun et. al showed that DNA replication is occurring by assessing incorporation of thymidine analogue BrDU into NK cells [69]. Interestingly, by day 6 there is a 20% increase in total Ly49H positive NK cells in the spleen indicating that they have undergone expansion. NK cell control of MCMV is relatively quick as by day 14, Ly49H cells have undergone contraction and fall back to normal frequencies. At this two week timepoint, the virus is undetectable in spleen, liver and blood of wild type C57Bl/6 mice [70]. Selective depletion of Ly49H positive NK cells has shown uncontrolled viral titres at this timepoint indicating that they are absolutely required for control of MCMV [64]

1.10. Human NK cell biology and immunotherapies

Human NK cells have similar development and functions to murine NK cells and develop from a CLP in the bone marrow. They go through numerous developmental stages, until they acquire the expression of CD56 at stage 4 and 5 of their development. Human NK cells can be classified based on the expression of this CD56 antigen, as being $CD56^{bright}$ or $CD56^{dim}$. $CD56^{dim}$ cells comprise 90% of NK cells and are predominantly found in the circulation. $CD56^{bright}$ cells are mostly found in secondary lymphoid organs and are make up only a small proportion of NK cells in the periphery [71]. $CD56^{bright}$ cells are potent producers of cytokine and $CD56^{dim}$ being cytotoxic and having expression of the FcγRIII (CD16) for recognition of opsonized target cells. $CD56^{dim}$ cells comprise 90% of NK cells and are predominantly found in the circulation [71].

NK cells are a key immune component with huge potential to harness for clinical therapies in humans. Indeed, the numerous effector functions of NK cells such as direct cytotoxicity and the generation of proinflammatory cytokines and chemokines make them prime targets to develop for clinical use. Much of the focus for NK cell therapies has been on harnessing their anti-cancer functions. The first anti-cancer strategies for NK cells in humans involved *ex vivo* IL-2 activation of autologous NK cells and reinfusion into patients [72]. However these trials showed limited clinical efficacy due to IL-2 induced expansion of regulatory T (Treg) cells and sustained inhibition of NK cells by the hosts own human leukocyte antigen (HLA) molecules [73]. This has led to adoptive transfer strategies using allogeneic NK cell infusions from haploidentical donors, as this affords increased responses inherently due to alloreactivity. For example, one study trialled the use of haploidentical NK cell transplantation for the treatment of Acute

Myeloid Leukaemia. This strategy demonstrated a reduced risk of relapse of this disease [74, 75].

One of the main immunotherapies being utilised against B cell malignancies utilises NK cell antibody dependent cellular cytotoxicity (ADCC) [76]. Rituximab is a monoclonal antibody against CD20 which essentially opsonizes the target cell for ADCC. NK cells are key mediators of this as they express FcγRIIIa (CD16) which recognizes the Fc portion of IgG, an thus can kill target cells labelled with the anti-CD20 mAb [77]. Other cells such as macrophages can also kill rituximab labelled cells [78].

Recent studies have shown that chimeric antigen receptor expressing NK cells (CAR-NK) are showing huge promise for anti-cancer functions. CAR-NK cells can be engineered such that they express a receptor that will recognise a cancer specific antigen. CAR-NK cells have an advantage over CAR-T cells in that they are not long lived, and will have less off target cytotoxic effects [79]. The downside of CAR-NK cells is that is challenging to get sufficient primary cell numbers from human donors, and it is hard to transfect the receptor of interest [80]. However, recent studies have showed that CAR-NK cells can be generated from induced pluripotent stem cells (iPSC), which means that it is possible to generate sufficient numbers for therapeutic use [79].

Therapeutic strategies have also turned to using the NK Cell line NK-92, as they are highly proliferative and easier to transfect with a 50% transfection efficacy [81]. One clinical study showed that use of NK-92 cells showed a positive response in three-quarters of patients with solid tumours or leukaemia, and with limited toxicity [82]. CAR-NK cells may show even more promise as clinical trials progress and CAR technology advances.

1.11. Immunometabolism

Most normal cells and tissues have a fixed environment and a constant supply of nutrients. However, immune cells such as lymphocytes, circulate the body and encounter a number of challenges such as pathogens and cancer cells in a multitude of different conditions. Indeed, inflammation and infection can lead to altered nutrient homeostasis [83]. Therefore, this requires immune cells to be highly dynamic and adaptable. Immune cells have the primary job of recognizing an immunological threat and eliminating it. The main way that immune cells do this is by producing effector molecules, which can be cytokines (to amplify an immune response) or cytotoxic molecules (that directly kill the threat) or direct engulfment of the pathogen (phagocytosis). These processes are energetically demanding, requiring the synthesis and exportation of new proteins and cytoskeletal rearrangement. Thus, immunologists have started to take an interest in the metabolism of immune cells, with a specific interest in how immune cell metabolism is configured to allow them to carry out their specialised functions. Aside from growth and energy production, it is becoming clear that metabolism can be directly required for immune function. This newly evolved field of study is termed immunometabolism.

1.11.1. Metabolism for energy production

Metabolism is a dynamic process that allows cells to adapt to any given environment. The two main outputs of metabolism are the generation of energy and the supply of biosynthetic precursors for cell growth and blastogenesis. In normal physiological settings nutrients are in abundant supply in the form of glucose, amino acids and free fatty acids, which are all metabolized in cells through different but integrated metabolic

pathways. These pathways can be broadly categorized into six main arms - glycolysis, pentose phosphate pathway (PPP), tricarboxylic cycle (TCA), amino acid metabolism, fatty acid synthesis and fatty acid oxidation [84].

One key fuel utilised for cellular metabolism is glucose, which is first metabolised by glycolysis into pyruvate, which then enters the mitochondria to fuel a process called oxidative phosphorylation (OxPhos). Fuels for OxPhos are called reducing equivalents and they are traditionally generated from the TCA cycle. However, other pathways have been shown to generate reducing equivalents, such as the malate-aspartate and citrate-malate shuttle [85, 86]. The main energy currency generated by OxPhos is adenosine triphosphate (ATP), which has the benefit of a high-energy phosphate bond, which can be used to fuel processes such as protein phosphorylation, transporters, cytoskeletal arrangement and protein trafficking.

Glycolysis is relatively inefficient at ATP production, producing only 2 net ATP molecules per molecule of glucose. However, it generates pyruvate which can fuel oxidative phosphorylation. Glycolysis can occur in hypoxia. Oxidative phosphorylation, which requires oxygen, is very efficient at energy production, as it can generate up to 36 molecules of ATP per molecule of glucose metabolized by glycolysis [84]. As OxPhos requires oxygen, under hypoxic conditions cells rely on glycolysis to produce ATP.

1.11.2. Metabolism for biosynthesis

Glycolysis

Glycolysis is not only a catabolic pathway that generates ATP, it is also an important pathway for biosynthesis. While glycolysis is an inefficient way to generate ATP, some cells such as cancer and immune cells can preferentially utilise glycolysis even under normoxic conditions, when they could utilize OxPhos. This metabolic configuration provides the cells with a biosynthetic advantage. This preferential use of glycolysis is called 'aerobic glycolysis' and results in the generation of lactate from pyruvate, instead of fuelling OxPhos [87]. Lactate production from pyruvate generates NAD+ which is a crucial cofactor for the upstream glycolytic enzyme GAPDH. This NAD+ generation from pyruvate is therefore required to sustain high levels of glycolytic flux. Aerobic glycolysis also means that cells need to take up more glucose to sustain ATP production compared to utilising OxPhos exclusively. This has the added benefit of generating a large pool of glycolytic intermediates that can be used for biosynthetic processes [87]. Therefore, aerobic glycolysis is generally utilized by highly proliferative cells such as immune cells and cancer.

Glycolysis can also be used to make amino acids for protein synthesis. It can specifically fuel *de novo* serine synthesis through the serine biosynthesis pathway. The glycolytic metabolite, 3-phosphoglycerate, can undergo three sequential enzymatic reactions to generate serine [88] . Thus, glycolysis is an important ATP generating pathway but can also be used as a reservoir for biosynthetic molecules.

Pentose Phosphate Pathway

Glycolytic intermediates such as glucose-6-phosphate can be used to make macromolecules for biosynthesis. Indeed, glucose-6-phosphate is utilized by the pentose phosphate pathway (PPP), a major biosynthetic pathway. The PPP can be utilized to produce reduced nicotinamide adenine dinucleotide phosphate (NADPH) and precursors for the synthesis of nucleotides [84]. Nucleotides are important in proliferating cells for the synthesis of DNA and RNA. NADPH is a reducing agent that is a crucial cofactor for anabolic reactions such as lipid synthesis and is important for antioxidant production [89].

TCA and Citrate-Malate Shuttle

Glycolysis is coupled to OxPhos through the final glycolytic metabolite, pyruvate. As previously mentioned, OxPhos is highly efficient at ATP production. Pyruvate can enter the mitochondria and be metabolized further by pyruvate dehydrogenase to produce NADH and Acetyl-CoA. Acetyl-CoA then enters the mitochondria and forms citrate, where depending on the cell type, it will be further metabolised through the TCA cycle, or exported as citrate to fuel the CMS. Both the TCA cycle and the CMS will generate reducing equivalents in the form of reduced nicotinamide adenine dinucleotide (NADH) or flavin adenine dinucleotide ($FADH_2$) for OxPhos. The TCA and CMS also generate intermediates which can be used for anabolic process. One of the key metabolites that both the TCA and CMS generate is citrate, which is exported from the mitochondria and used for the generation of lipids [90]. The TCA cycle has an element of plasticity in that it can utilize numerous fuels. Glutamine can enter the TCA cycle as alpha-ketoglutarate and similarly acetyl CoA can also be obtained through fatty acid oxidation [91]. The CMS

does not utilise glutamine as a fuel. This means that unlike glycolysis and the CMS, the TCA cycle can generate biosynthetic precursors from fuels other than glucose.

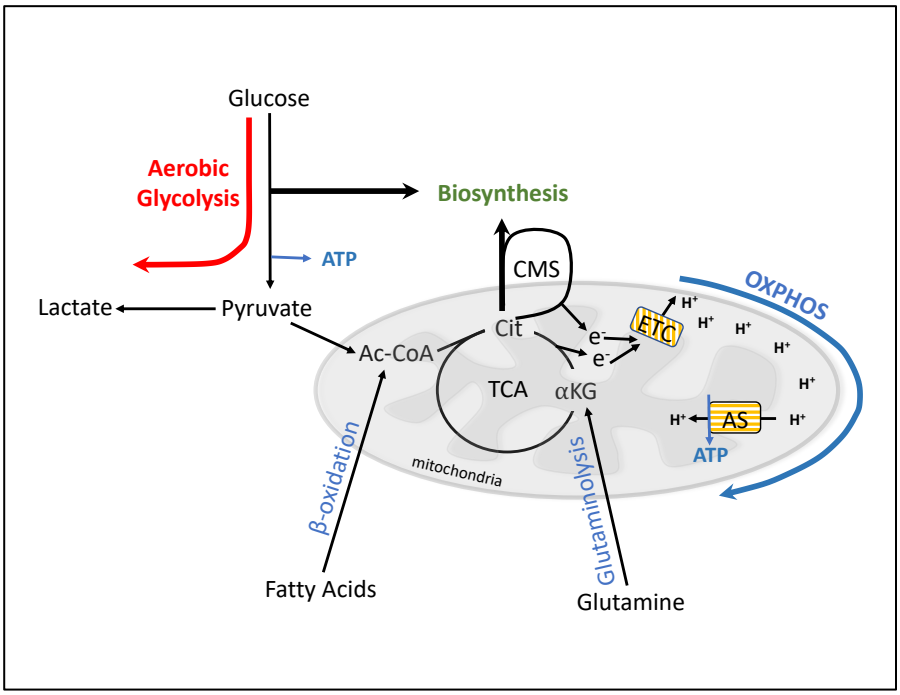

Figure 1. 4. Metabolism balances energy production with biosynthesis

Metabolism is important for generating energy (ATP) but also for cell growth. Glycolysis involves the breakdown of glucose into pyruvate. The breakdown of glucose makes numerous intermediates (not shown) that can fuel other pathways for biosynthesis. The process of aerobic glycolysis leads to the production of lactate, which will allow the cells maintain a higher rate of glycolysis. If the pyruvate is imported into the mitochondria it will be converted into acetyl CoA (Ac-CoA) which will be converted to citrate to fuel either the TCA cycle or the CMS. Citrate production will also be used for the synthesis of lipids. The CMS and TCA will form reducing equivalents (depicted as e^-) which will fuel the electron transport chain for OxPhos and energy production. Other fuel sources can also be used such as glutamine or fatty acids.

1.11.3. Metabolic configurations of immune cells

Immune cells adopt distinct metabolic configurations depending on their function. For example, naïve T cells that have been newly formed from the thymus have the sole purpose of migrating through secondary lymphoid tissue in search of cognate antigens in a process termed immunosurveillance [92]. These cells do not undergo much proliferation until activated, so therefore do not require biosynthetic precursors for growth and proliferation. However, these migrating cells generally undergo cytoskeletal remodelling while trafficking, which requires ATP [93]. Naïve T cells therefore prioritize energy generation over biosynthesis. As previously discussed, the most efficient way for a cell to generate ATP is through OxPhos so it is therefore not surprising that these cells utilize this arm of metabolism [94].

Effector T cells also undergo clonal expansion when activated. This process requires the generation of large amounts of biomolecules for biosynthetic purposes. As previously mentioned, glycolysis acts as a reservoir of biosynthetic molecules, so it is therefore not surprising that CD8+ effector T cells have high levels of aerobic glycolysis when activated [95, 96]. As these are effector cells, they synthesize cytotoxic granules to directly kill target cells. This an energetically demanding process that requires the synthesis of new proteins. Indeed, non-effector molecule producing regulatory T cells (Tregs) that are FoxP3+ utilize oxidative phosphorylation more than glycolysis [97]. Whereas their FoxP3- (Tr1) counterparts that do produce effector molecules granzyme B and perforin have comparatively elevated levels of glycolytic flux [98]. There is clearly a dynamic balance between glycolysis and oxidative metabolism for the regulation of energy production and biosynthesis.

Memory T cells which are formed after effector T cells have carried out their function use OxPhos. These cells are relatively inert, and so maintain energy homeostasis over biosynthesis. Their primary role is also immunosurveillance, and when they encounter a previously eliminated antigen they undergo rapid expansion and proliferation to eliminate their TCR-restricted target. However, a significant difference between memory T cells and naïve T cells is the speed of their expansion. For this reason, memory T cells continuously synthesize fatty acids under homeostatic conditions [99]. These fatty acids are generated from glucose-derived citrate. When the cells need to make ATP they oxidise the fatty acids to generate substrate for the TCA cycle and OxPhos [99]. This essentially allows them to have a reservoir of fatty acids for oxidation which can be utilized immediately when activated and that is not dependent on having a microenvironment that is replete with glucose. Fatty acid oxidation is an extremely energetically efficient method of generating ATP in that it generates approximately 106 ATP per molecule of palmitate in contrast to 36 ATP per molecule of glucose [99]. Direct comparison of naïve T cells and memory T cells demonstrated that memory T cells have a greater mitochondrial mass than their naïve counterparts. This means that they are essentially primed to upregulate oxidative metabolism upon activation [99].

As previously mentioned, memory T cells rapidly proliferate when reactivated. Although their ability to up regulate oxidative metabolism facilitates increased ATP production, it does not generate all the required biomolecules for growth and proliferation. Memory T cells have also been shown to rapidly increase glycolytic flux when activated in a manner which is dependent on their elevated mitochondrial mass. Hexokinase 2, a rate limiting ATP dependent enzyme in glycolysis, has been shown to directly interact with mitochondria in activated memory T cells. In this way hexokinase 2 can easily access

ATP from OxPhos to fuel the first stage of glycolysis, which can be used to facilitate their growth and proliferation [100].

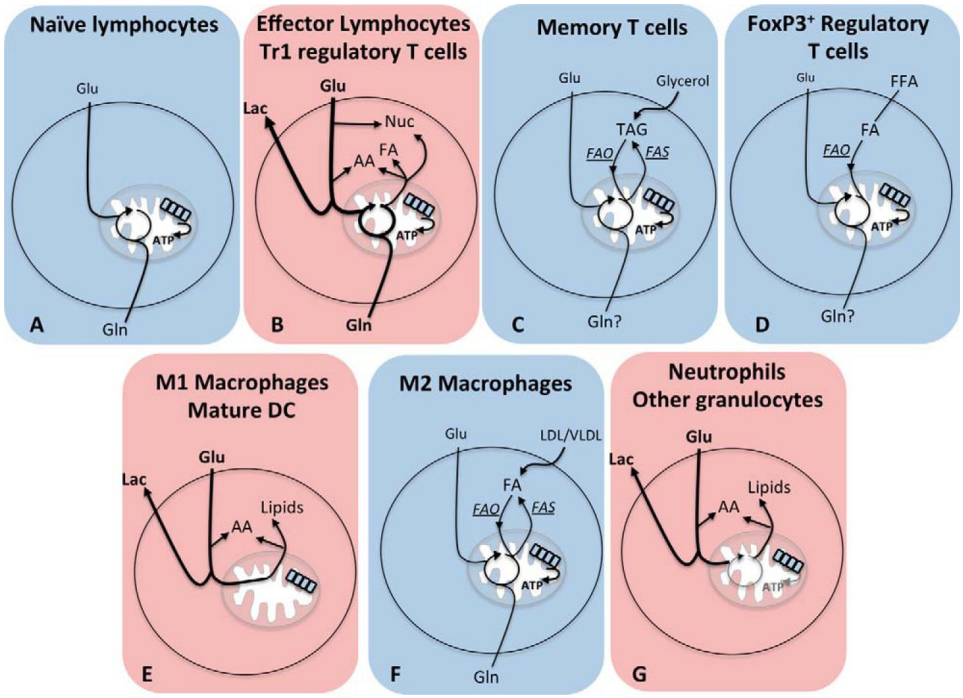

Figure 1. 5. Immune cells adopt metabolic configurations

Panels in red represent cells with glycolytic metabolism, panels in blue represent cells with oxidative metabolism (A) Naïve lymphocytes use small amounts of glucose and glutamine to fuel ATP production (B) Effector T cells and Tr1 use aerobic glycolysis to fuel biosynthesis and ATP production (C) Memory cells make fats as storage mechanism which they can later oxidise for energy upon antigen stimulation (D) FoxP3^{+} cells use exogenous fatty acids to fuel mitochondrial metabolism (E) M1 macrophages use aerobic glycolysis (F) M2 macrophages oxidise fatty acids for energy (G) Neutrophils predominantly use glucose as a fuel source. Glu: Glucose, Lac: Lactate, Nuc: Nucleotides, FA: Fatty acids, Gln: Glutamine, TAG: Triacylglycerol, FAO: Fatty acid oxidation, FAS: Fatty acid synthesis, AA: Amino Acids, LDL/VLDL: Low density lipoprotein/Very low density lipoprotein.

1.11.4. Direct metabolic regulation of immune function

Aside from biosynthesis and energy production, immune metabolism is directly required for immune effector functions. Indeed, metabolites and metabolic enzymes can directly regulate immune cell function.

One of the classic examples of metabolite modulation of immune function is succinate. Succinate is a TCA intermediate which has also been shown to be an important regulator of immune responses in macrophages. Lipopolysaccharide (LPS) activated macrophages greatly increase their rates of glycolysis and down regulate OxPhos-associated genes [101]. Simultaneously, these cells demonstrate increased levels of succinate. This metabolite is required for the induction of IL-1β. The authors found that succinate could stabilize HIF1α protein and that this was required for mature IL-1β production [101].

One recent example of this is the metabolite itaconate. Itaconate is a metabolite that is robustly generated by inflammatory macrophages from the TCA cycle. This metabolite has been shown to be unable to support respiration, but rather acts as an anti-inflammatory signalling molecule [102]. Indeed, macrophages deficient in the enzyme required for itaconate synthesis, immune responsive gene 1 (*Irg1*), have heighted levels of pro-inflammatory cytokine production in response to lipopolysaccharide (LPS).

Thus, this shows that metabolites can directly regulate immune cell function.

1.12. Natural Killer cell metabolism

In terms of immunometabolism, our knowledge of NK cells has been accelerated in recent years. Like most quiescent, naïve immune cells, freshly isolated splenic NK cells utilise more OxPhos than glycolysis for energy production [103]. NK cells similarly to effector T cells undergo robust changes in their metabolism when activated [104].

NK cell metabolism has been extensively studied in our lab in response to adaptive cytokines such as IL-2. NK cells that are stimulated with cytokines overnight show heightened levels of metabolism and function. Indeed, Donnelly et. al have demonstrated that IL-2/12 stimulated murine NK cells vastly increase in size over 20 hours and they increase the expression of IFNγ and granzyme B [52]. These cells utilize aerobic glycolysis and OxPhos and increased expression of the metabolic markers CD71 (transferrin receptor) and CD98 (Slc3a2) to facilitate increased nutrient uptake. These metabolic changes are crucial for NK cell functional responses. Indeed, pharmacological inhibition of glycolysis and OxPhos has been shown to be detrimental to NK cell function. This is true for humans and mice, as use of the glycolytic inhibitor, 2-deoxyglucose (2-DG) or OxPhos inhibitor, oligomycin, severely blunted IFNγ production in both species [105]. This suggests that metabolism is not only important for NK cell energy production, but it is also critical for effector molecule production.

1.13. Regulation of NK cell metabolic reprogramming

1.13.1. mTORC1

Coordination of NK cell metabolic reprogramming requires the synthesis of metabolic machinery. Therefore it is important to consider the signalling molecules behind this. The serine/threonine kinase mammalian target of rapamycin complex 1 (mTORC1) has been shown in numerous immune cells such as T cells to regulate both metabolism and effector functions [106]. mTORC1 is a known regulator of cellular processes such as protein synthesis, metabolism, cell cycle progression and is a negative regulator of processes such as autophagy [107]. It is a member of the phosphoinositide 3-kinase related family. When activated, mTORC1 turns off autophagy and turns on anabolic processes such as lipid synthesis, protein synthesis and metabolism. mTORC1 rapidly responds to growth factors and alterations in the metabolic microenvironment. It is acutely sensitive to the availability of certain nutrients such as amino acids and is responsive to growth factors such as cytokines. This kinase has been shown to be a key regulator of NK cell metabolism and function.

Murine NK cells show activation of mTORC1 when stimulated with IL-2/12 [52]. mTORC1 can be inhibited using a pharmacological agent called rapamycin. IL-2/12 stimulated murine NK cells that are treated with rapamycin fail to undergo blastogenesis, cannot upregulate glycolysis and have defective effector functions, including IFNγ and granzyme B production [52]. This requirement for mTORC1 activity is also conserved in human NK cells [105]. This indicates that mTORC1 is a crucial regulator of NK cell effector functions and is an example of how a metabolic regulator can directly impact upon immune cell function.

1.13.2. c-Myc

Data from the Finlay lab has shown that the transcription factor c-Myc also plays a fundamental role in murine NK cell metabolic reprogramming and effector functions. c-Myc is a basic helix loop helix transcription factor that when activated binds to the promoters of glycolytic genes and initiates their transcription. It is indispensable for T cell growth and proliferation [108]. Indeed, the same is true for activated murine NK cells as c-Myc knock outs are metabolically dysfunctional with reduced mitochondrial mass and an inability to express glycolytic genes [109]. c-Myc is regulated on a number of levels. On a transcriptional level c-Myc is transcribed by STAT5 thus meaning that it can be induced by IL-2 [110]. However, c-Myc is also dynamically regulated on a protein level. Sinclair et. al found that c-Myc protein expression is acutely sensitive to amino acid uptake by the transporter Slc7a5 in T cells activated through their T cell receptor (TCR) [111]. The authors show that in Slc7a5-null T cells, c-Myc protein expression is blunted and that this is probably due to the relatively short half-life of c-Myc protein and that continuous amino acid uptake is required for the re-synthesis of this protein [111]. The same is true in NK cells, whereby glutamine withdrawal significantly inhibits cMyc protein expression [109]. Loss of cMyc in IL-2/12 activated NK cells is causes reduced granzyme B and IFNγ production. This indicates that cMyc dependent metabolism is required for cytokine activated NK cell functional responses.

1.13.3. SREBP

Another key regulator of NK cell metabolism are sterol regulatory element binding proteins (SREBP). SREBP are a family of transcription factors that are generally associated with control of lipid and cholesterol synthesis pathways. Indeed, SREBP are required for CD8 T cell cholesterol synthesis [112]. However, in NK cells these transcription factors have a dual role. SREBP also controls glucose metabolism and OxPhos in cytokine activated NK cells. NK cells do not utilise a traditional Krebs/TCA cycle to fuel OxPhos. They use an alternate cycle for NADH generation in the form of the citrate-malate shuttle. This involves the export of mitochondrial citrate into the cytoplasm, and the import of cytoplasmic malate into the mitochondria. Malate is then converted to oxaloacetate, and in doing so it generates mitochondrial NADH to fuel OxPhos. The expression of this citrate-malate antiporter (SLC25A1) is controlled by SREBP. Not only does SREBP control OxPhos but it also controls NK cell glycolysis. When citrate gets exported from the mitochondria it is cleaved by another SREBP target enzyme called ATP citrate lyase (ACLY) into oxaloacetate and acetyl co A. This oxaloacetate is then converted to malate and in doing so it generates cytosolic NAD+. This NAD+ is required for proper functioning of glycolysis as it is a cofactor for the key glycolytic enzyme glyceraldehyde-3-phosphate dehydrogenase (GAPDH).

Metabolic tracing experiments with C13 labelled glucose and glutamine showed that this citrate-malate shuttle is predominantly fuelled by glucose [86]. Short term withdrawal of the other fuel source for OxPhos, glutamine, does not significantly impair NK cell mitochondrial metabolism [109]. Interestingly, inhibition of SREBP is highly detrimental to NK cell cytokine production and tumour killing *in vivo* [86].

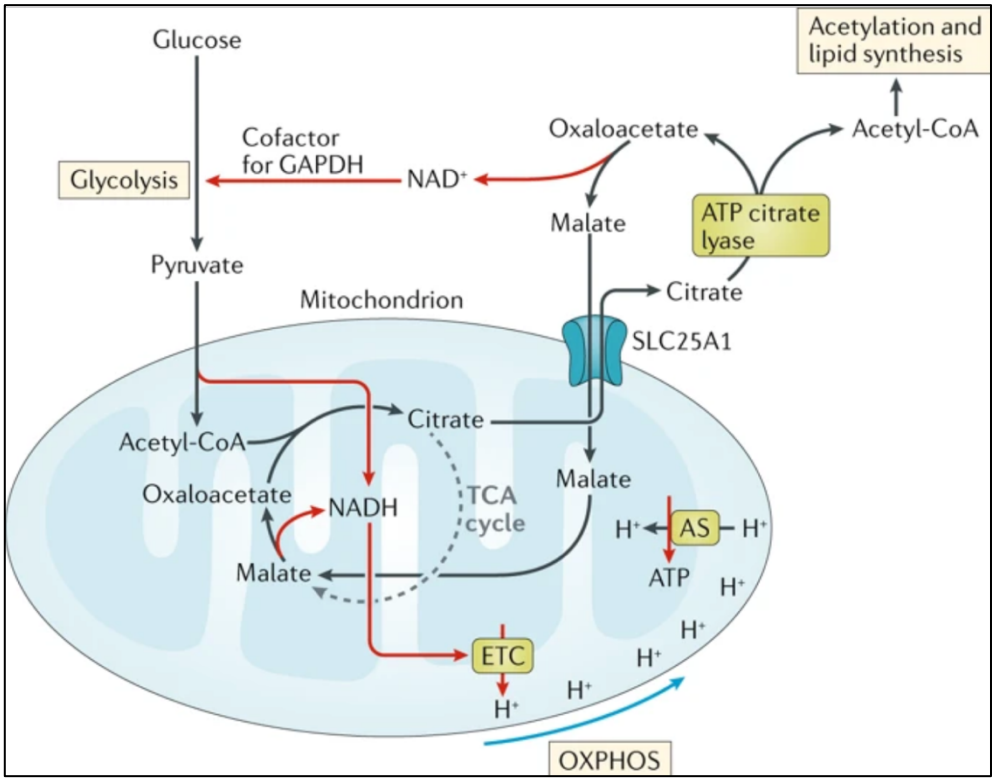

Figure 1. 6. NK cell oxidative metabolism is fuelled by the citrate-malate shuttle

Unlike most cells, NK cells utilise the citrate malate shuttle to generate NADH for oxidative phosphorylation. Glucose is metabolised through glycolysis to pyruvate, pyruvate enters the mitochondria and is converted to acetyl co A. Acetyl co A is then converted to citrate and exported to the cytosol through SLC25A1. SLC25A1 is an antiporter and requires malate to be imported into the mitochondria. Malate is then converted back to oxaloacetate. This step also produces NADH which can be used to fuel the electron transport chain for ATP generation. CMS derived citrate is also required for biosynthesis of lipids [113].

1.14. Glycolytic regulation of immune function

One of the key pathways that is required for NK cell function is glycolysis. Indeed, fuelling of the NK citrate-malate shuttle is maintained by glucose. However not much is known about the enzymatic regulation of NK cell glycolysis. Glycolysis is a key pathway for the generation of energy in the form of ATP and for biomolecule production. Glycolysis involves the breakdown of glucose through 10 enzymatic steps. Glucose breakdown results in the generation of two molecules of pyruvate and ATP per molecule of glucose. This pathway is traditionally regulated by 3 main enzymes: glucokinase (hexokinase), phosphofructokinase 1 and pyruvate kinase [114]. (**Fig. 1.7)**

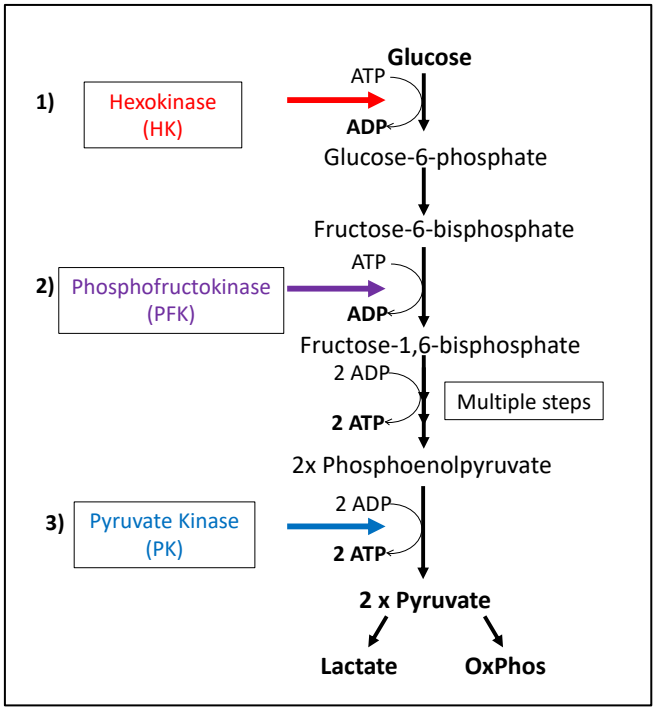

Figure 1. 7. Glycolysis is regulated by 3 main enzymatic steps

Glycolysis involves the breakdown of glucose through 10 sequential steps to form two molecules of pyruvate and two molecules of ADP. Glycolysis also contributes metabolites to biosynthesis. Glycolytic flux is regulated by 3 main enzymes: 1) Hexokinase (HK), 2) phosphofrucktokinase (PFK) and 3) pyruvate kinase (PK). Pyruvate kinase is responsible for generating ATP from glucose and for generating pyruvate for downstream metabolism.

As previously discussed, glucose breakdown through this pathway is crucial for cellular biosynthesis but it also plays a key role in regulating immune function. Indeed, both glycolytic metabolites and glycolytic enzymes can control effector functions of immune cells. Inhibition of glycolysis in both human and murine NK cells inhibits IFNγ and granzyme B production, indicating that this pathway is directly required for function. However, nothing is known of which glycolytic metabolites or enzymes are directly required for NK cell function. There is some evidence for this in other immune cells which are discussed below.

Glycolytic metabolite control of immune cell function

The glycolytic intermediate phosphoenolpyruvate (PEP) has been shown to directly regulate T cell function. PEP is the second last metabolite in glycolysis and is the substrate for pyruvate kinase. Ho et. al found that PEP was required for sustaining TCR mediated NFAT (nuclear factor of activated T cells) signalling, through its role in preventing Ca^{2+} reuptake through Sarco/ER Ca^{2+}ATPase (SERCA) [115]. The authors demonstrated that IFNγ production was directly dependent on the levels of PEP in anti-CD3-CD28 activated T cells.

Glycolytic enzyme control of immune cell function

Interestingly, glycolytic enzymes have also been demonstrated to directly regulate immune cell function. The glycolytic enzyme glyceraldehyde-3-phosphate dehydrogenase (GAPDH) has been shown to regulate Th1 cytokine production independently of its role in glycolysis. When there are low levels of glycolytic flux,

GAPDH binds to the 3'-UTR of IFNγ mRNA, thus preventing it's translation [116]. However, when the cell is undergoing a high rate of glycolytic flux GAPDH is active in glycolysis and is unbound from IFNγ mRNA. These two processes are mutually exclusive, meaning that GAPDH can directly inhibit Th1 IFNγ production when glucose is limited [116]. This indicates that GAPDH, a glycolytic enzyme is required for IFNγ production in T cells, although it is unknown whether this is true in other immune cells.

Similarly, the glycolytic enzyme enolase is required for Foxp3 transcription factor expression [117]. This enzyme can bind to regulatory regions on the gene and promote the expression of Foxp3-E2 thus promoting regulatory T cell formation.

Other glycolytic enzymes with a role in immune regulation include hexokinase 1 (HK1) and pyruvate kinase M2 (PKM2). Hexokinase 1 has been demonstrated to regulate inflammasome activation in macrophages. In glycolysis, hexokinase functions to convert glucose from to glucose-6-phosphate. This enzyme has been shown to be directly required for normal NLRP3 inflammasome activity in M1 macrophages [118]. The authors demonstrated that HK1 directly associates with a voltage dependent ion channel (VDAC1) in the mitochondria, which is required for NLRP3 activation [91]. Knock down of HK1 using shRNA resulted in significant decreases in IL-1β and IL-18 (which are both NLRP3 dependent), while TNFα remained unchanged.

The last enzyme is glycolysis is pyruvate kinase. This enzyme is particularly interesting it is crucially important for metabolism for the synthesis of pyruvate (which is a key fuel for fuelling the TCA and CMS) , however, it also plays a direct role in regulating immune cell function. This enzyme has been shown to play a direct signalling and regulatory role in macrophage function [119, 120]. Macrophages that are deficient in PKM2 do not undergo normal HIF1α signalling and have impaired cytokine production in response to

LPS. Similarly, PKM2 is directly required for Th17 polarisation [121]. To date there is no knowledge of whether any of these glycolytic enzymes play an immune regulatory role in other cells such as NK cells. As PKM2 is important for fuelling OxPhos and glycolysis, aswell as having signalling roles, it is likely that it will be important for NK cell function as well.

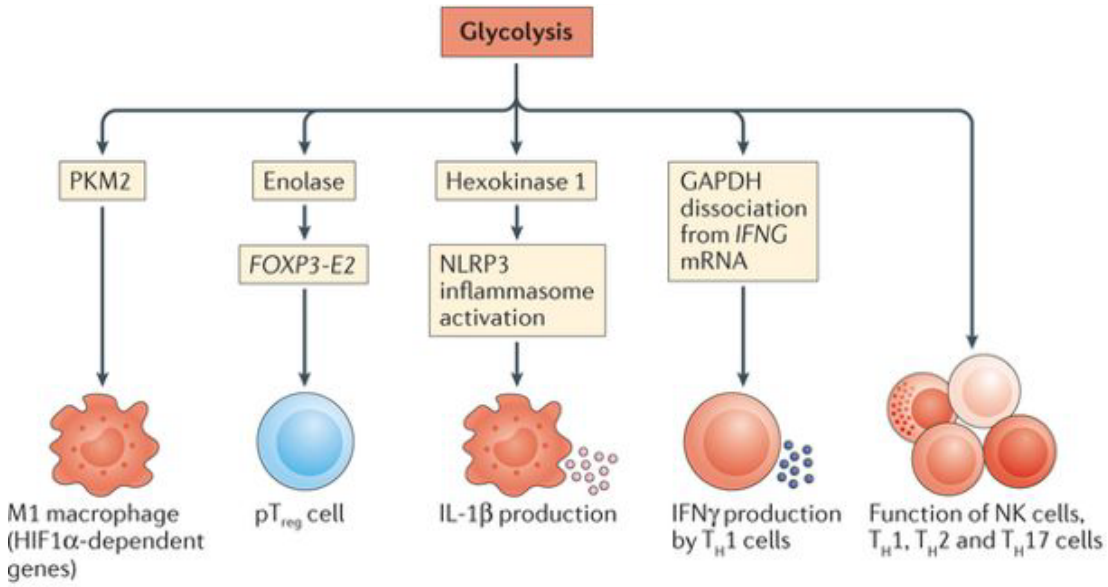

Figure 1. 8. Metabolic enzymes can directly regulate immune cell function

Enzymes involved in glycolysis such as PKM2, enolase and GAPDH can regulate immune cell function and differentiation independently of their role in metabolism. Direct enzymatic regulation by glycolytic enzymes has been observed in Th1 cells and macrophages, however it is not known whether glycolytic enzymes directly play a role in the function of NK cells. [84]

1.15. Pyruvate Kinase and Glycolysis

The last enzyme in glycolysis is pyruvate kinase. This enzyme generates pyruvate and ATP from PEP. As briefly mentioned previously, this enzyme has been shown to play a role in regulation of immune function. This is due to the fact that this enzyme exists in numerous isoforms which have distinct properties.

1.15.1. Isoforms

There are four isoforms of pyruvate kinase expressed in mammalian tissues, PKL, PKR, PKM1 and PKM2. PKL and PKR are expressed in liver and erythrocytes respectively [122]. However, pyruvate kinase muscle 1 and 2 are both expressed in most differentiated tissues, with PKM1 preferentially expressed by catabolic tissues such as muscle, and PKM2 being preferentially expressed in tissues that are highly proliferative such as immune cells and cancer cells. PKM1 and PKM2 are expressed from the same gene, but undergo mutually exclusive alterative mRNA splicing [123]. PKM1 incorporates exon 9 of the PKM gene, whereas PKM2 incorporates exon 10 [124]. Indeed, these two isoforms differ only by 23 amino acids out of a total of 531 [123]. The ratio of PKM1:PKM2 is controlled by a group of heterogenous ribonucleoproteins (hnRNP) and polypyrimidine tract binding protein (PTB). These proteins binds to regions of PKM pre-mRNA surrounding exon 9, repressing its inclusion into the mature mRNA transcript and promoting the inclusion of exon 10 which will form PKM2 [124]. hnRNP expression is controlled by the transcription factor c-Myc. Therefore, it is not surprising that a high PKM2:PKM1 ratio has been found in c-Myc expressing cancer cells [124]

1.15.2. Conformations

The role of PKM2 in immune regulation is directly related to its oligomeric conformation. It can be found as a highly catalytically active tetramer with a low Km for phosphoenolpyruvate whereas monomeric PKM2 and dimeric PKM2 have a high Km for PEP and thus are not very catalytically active [119, 120].

Characterisation of PKM2 activity in MCF-7 breast cancer cell lines revealed that active tetrameric PKM2 has a Km for PEP of 0.03mM whereas the inactive dimeric form of the enzyme has a Km of 0.46 mM which indicates that tetrameric PKM2 is the most catalytically active isoform [125]. Therefore, the relative ratio of these isoforms will control the rate of glycolysis i.e. tetrameric PKM2 should result in increased rates of glycolysis. PKM1, unlike PKM2, is only found in one conformation, tetrameric and as a result it can result in high rates of glycolysis, but it is not known to have any direct immune regulatory roles.

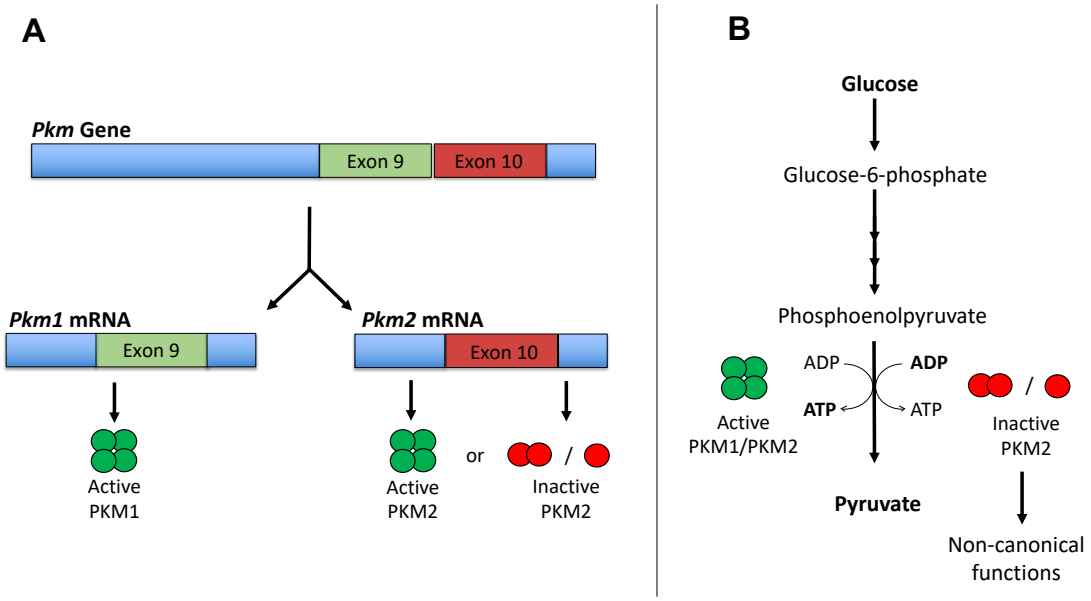

Figure 1. 9. *Pkm1* and *Pkm2* form from differential splicing and can regulate glycolytic flux

(A) The *Pkm* gene can form two distinct isoforms, *Pkm1* and *Pkm2.* These isoforms develop from differential splicing of the same gene. *Pkm1* mRNA includes exon 9 but not exon 10, and forms a constitutively highly active tetramer. *Pkm2* includes exon 10 but not exon 9 and can form an active tetramer or inactive monomer/dimers. (B) Pyruvate kinase is the last enzyme in glycolysis and generates pyruvate and ATP from phosphoenolpyruvate ADP. PKM1 and active tetrameric PKM2 are highly active and generate pyruvate. Inactive PKM2 is relatively inactive and has low pyruvate generating potential. Inactive monomeric/dimeric PKM2 also has non-canonical functions outside of pyruvate synthesis through transcriptional regulation and acting as a protein kinase.

1.16. Regulation of PKM2 conformation

1.16.1 Allostery

The switch between oligomeric conformations of PKM2 is dynamically regulated; by allostery, post translational modifications and reactive oxygen species [126]. The formation of active tetramers is promoted by upstream metabolites such as fructose-1,6-bisphosphate, serine and phosphoribosylaminoimidazolesuccinocarboxamide (SAICAR). These upstream metabolites represent a feedback mechanism of PKM2 activity as they are each metabolites directly associated with glycolysis (F-1,6-BP) or are metabolites associated with branch pathways from glycolysis; *de novo* serine synthesis from 3-phosphoglycerate and SAICAR synthesis from de novo purine synthesis (Fig. 1.10) [127]. In this way it acts as a finely tuned sensor to the availability of upstream substrates. For example, if there are sufficient serine levels in the cell, serine will promote PKM2 tetramerisation and increase glycolytic flux, thereby draining glycolytic intermediates from the pathway and inhibiting serine biosynthesis. In this way, PKM2 conformation and activity is thought to regulate cellular biosynthesis.

1.16.2. Post-translational modifications

Post-translational modifications can also regulate PKM2 conformation. Indeed, upstream growth factor signalling by tyrosine kinases is associated with inactive PKM2 formation. Phosphorylation of PKM2 on particular sites can drive the formation of inactive dimers in human cancer. One of the most predominant phosphorylation sites is tyrosine 105 (Y105) [128]. Hitosugi et. al identified that Y105 phosphorylation results in inactive PKM2 formation as it causes release of the allosteric activator fructose-1,6-

bisphosphate, which is required for formation active tetramers (Fig. 1.8). Although the upstream kinase that is responsible for tyrosine phosphorylation of PKM2 has not been definitively defined, there have been studies that have investigated the phosphatase that is capable of dephosphorylating PKM2 in cancers such as hepatocellular carcinoma [129]. SH2 domain-containing phosphatase 1 (SHP1) is a phosphatase that was first identified in haematopoetic cells, and is generally implicated in integrating inhibitory signals in immunoreceptor tyrosine based activation motif signalling [129]. Tai et. al have demonstrated that SHP1 can selectively dephosphorylate tyrosine 105 and thus drives PKM2 into tetrameric form.

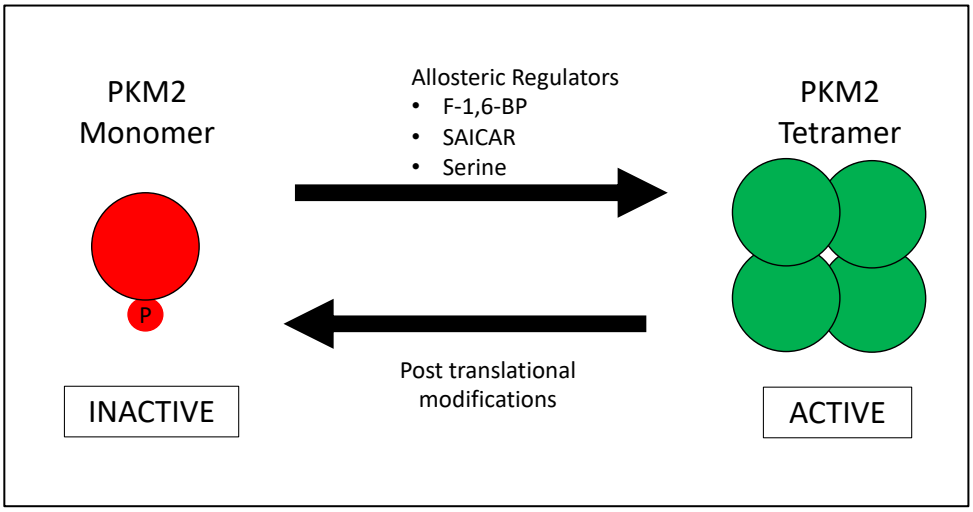

Figure 1. 10. PKM2 conformation is dictated by allostery and post-translational modifications

Metabolites that are present upstream from PKM2 in glycolysis can drive formation of catalytically active tetramers these include fructose-1,6-bisphosphate (F-1,6-BP, SAICAR and serine. Post translational modifications such as Y105 phosphorylation can cause the formation of catalytically inactive monomer/dimers.

1.17. Non-canonical functions of PKM2

Aside from pyruvate generation, PKM2 has been implicated to have a number of non-canonical roles in the regulation of other proteins and transcription factors. This is conformation dependent in that only the catalytically inactive monomer/dimer are reputed to have these extra functions.

Indeed, dimeric PKM2 is required for the expression of oncogenes such as c-Myc in hepatocellular carcinoma indicating that PKM2 acts as signalling molecule in some human cell lines [129]. Similarly, PKM2 has been linked to proteins of immunological relevance such as signal transducers and activators of transcription (STAT) proteins e.g. a study in cancer cells has implicated that Akt can directly phosphorylate PKM2 on serine 202 and cause it to interact with STAT5A. This interaction causes nuclear translocation and transcription of STAT5 target genes such as Cyclin D1 [130]. Some studies in cancer cell lines have demonstrated that PKM2 can act as a protein kinase with a diverse range of functions. One particular study indicated that PKM2 phosphorylates STAT3 thus regulating its activity [131]. This is controversial, as a more recent study has observed no protein kinase activity of PKM2, indicating that there may be differences in PKM2 functionality between different cell types [132].

One of the main tools that allow investigators to investigate the role of PKM2 conformation are the pharmacological PKM2 activators TEPP-46 and DASA-58. These pharmacological compounds drive of the formation of catalytically active PKM2 tetramers. Therefore, these compounds effectively inhibit the non-canonical roles of PKM2 monomers/dimers. These activators bind to the PKM2 subunit interaction interface at a site distinct from allosteric activators of PKM2 [133]. Binding of these activators prevents PKM2 from being susceptible to inactivation by tyrosine

phosphorylation [133]. These compounds have been used to investigate the non-canonical roles of PKM2 in numerous immunometabolic studies. Tetramerisation of PKM2 using TEPP-46 and DASA-58 in macrophages prevents LPS-induced HIF1α stabilisation and prevents upregulation of HIF1α associated genes. This effect was accompanied by a decrease in levels of the inflammatory cytokine IL1β [119]. The authors demonstrated that inactive PKM2 entered the nucleus upon LPS stimulation and acts as a transcriptional co-activator. However, tetramerisation of PKM2 ablated this effect. [119]. A similar study was carried out in primary macrophages in the context of atherosclerosis. This study demonstrated that nuclear PKM2 was required to phosphorylate STAT3 and boost IL-6 and IL1β production. Indeed, inhibiting this non-canonical role through tetramerisation of PKM2 resulted in significantly decreased IL1β and IL-6 production [120]. These studies implicate a crucial role for PKM2 in myeloid derived immune cells; however the role of PKM2 in lymphocytes has not been as extensively explored. There is one study showing that TEPP-46 treatment of macrophages and T cells results in a downregulation of PD-L1 [134]. More recently, there was a study on mouse T cells showing that knockdown of PKM2 prevents CD4 T cell differentiation into Th1 and Th17 cells. Overexpression of PKM2 restored Th17 differentiation. This is interesting as the authors then showed that inhibition of PKM2 was found to be protective in a mouse model of experimental autoimmune encephalomyelitis, meaning that PKM2 could be targeted for inflammatory diseases in the future [121]. To date, there is no information on the role of PKM2 in controlling NK cell metabolism and function.

Aims

Hypothesis

NK cell glycolysis is required for normal NK cell effector functions. Pyruvate kinase M2 (PKM2) is a glycolytic enzyme that is reported to have key roles in the regulation of glycolysis and function in other immune cells. Therefore, we hypothesised that PKM2 would play key regulatory roles in NK cell glycolysis and would be directly required for NK cell effector functions.

Key Objectives

1) To investigate the role of *Pkm2* in regulating NK cell function *in vivo.*

2) To investigate into the dual metabolic and transcriptional roles of *Pkm2* in regulating NK cell function and metabolism *in vitro.*

3) To pharmacologically assess the NK cell requirement for regulated pyruvate kinase enzymatic activity *in vitro*

Chapter 2: Materials and Methods

2.1. Materials

2.1.1. Chemicals

RPMI 1640 + L-glutamine media, rapamycin, Dulbeccos phosphate buffered saline, penicillin-streptomycin 0.4% trypan blue (in PBS), DEPC water, phosphate buffered saline tablets and disuccinymydllsuberate (DSS), Fluoro-Carbonyl Cyanide Phenylhdrazone (FCCP), oligomycin, rotenone, Antimycin A Albumin from bovine serum, RPMI medium 1640 (1X) [+]L-Glutamine, Dulbecco's phosphate buffered saline, Cell Tak, Penicillin-Streptomycin, L-Glutamine solution (100X) NuPAGE 12-well SDS PAGE gels, NuPAGE Transfer Buffer (20X), NuPAGE Running Buffer (20X) and GeneJET RNA purification kit were purchased from Thermo Fisher. Heat inactivated foetal calf serum was purchased from Biosera and VWR. RNeasy Mini Kit was obtained from Qiagen. GeneJet RNA kit was obtained from Thermo Fisher. Molecular grade ethanol, β-mercaptoethanol, isopropanol, Tetramethylethylenediamine (TEMED), Acetic acid, Tween 20, D-Glucose, D-2 deoxyglucose, Sodium dodecyl-sulphate (SDS) Bovine Serum Albumin, ammonium persulfate, phosphate buffered saline tablets, Ponceau S, 40% acrylamide/bis-acrylamide, isopropanol and rotenone were purchased from Sigma Aldrich. Golgi Plug (Brefeldin A), Cytofix/Cytoperm, BrDU staining kit APC, Perm Wash was obtained from BD biosciences. NK cell isolation kit, NK cell isolation kit II and Interleukin-12 (IL-12) was purchased from Millltenyi biotech. TEPP-46 (ML-265) was obtained from Cayman Chemical or EMD Millipore. High molecular weight Poly(I:C) was obtained from Invivogen. Pre-made 50X TAE buffer was obtained from Thermo Fisher. Immobilon Western Chemiluminescent HRP Substrate from EMD Millipore. IL-2 was obtained from NCI preclinical repository. Recombinant murine IL-15 was obtained from Peprotech. IL-12 and NK cell isolation kit II were purchased from Miltenyi Biotech.

Tris(hydroxymethyl)aminomethane was obtained from Acros Organics.High Capacity reverse DNA synthesis kit was from Thermo FIsher Qscript cDNA supermix and PerfeCTa SYBR® Green SuperMix was obtained from Quanta biosciences. Eagle Taq qPCR Universal mastermix (ROX) was obtained from Sigma Aldrich. DNeasy DNA purification kit was obtained from Qiagen. Dithiothreitol DTT was obtained from Santa Cruz. Pyruvate Kinase assay kit was purchased from Biovision. Immobilon Western Chemiluminiscent HRP substrate was from Merck Millipore. Seahorse XF media and calibration buffer were obtained from Agilent Technologies. X-Ray films were from Fujifilm or Carestream. Cytometric bead array kits were obtained from BD for IL-12, IFNγ , IL-10, TNF, MIP1α and MIP1β. Methanol and Ethanol were purchased from TCD school stores or Sigma Aldrich. Ethidium Bromide (0.625mg/mL) was obtained from Amresco. GoTaq was from Promega.

2.1.2. Equipment

6 well plates, 12 well plates, 24 well plates, 48 well plates, 96 well plates were purchased from Sigma Aldrich CoStar or Thermo Fisher. Pipette tips filtered and non-filtered were purchased from Thermo Fisher or Rainin. Cell culture flasks (25cm and 75cm) ,Eppendorf tubes, Subcellular Protein Fractionation Kit for Cultured Cells and AB-1900 low profile PCR plates, Absolute qPCR seal, 7500 fast real-time PCR system, Heraeus Pico 17 microcentrifuge, and Eppendorf Model 5810R Centrifuge were obtained from Thermo Fisher. 7900HT Sequence detection system was from ABI. 3Prime personal thermal cycler was purchased from Techne. Vapoprotect thermocycler was purchased from Thermo Fisher. Power pack for electrophoresis gels was from Thermo Fisher.

5mL, 10mL and 25mL pipettes and 15mL and 50mL centrifuge tubes were obtained from Corning Incorporated . Immobillon PVDF blotting membrane was purchased from EMD Millipore. Transfer pipettes were purchased from Sarstedt. Microflex gloves were from Ansell. Grant JB Series Water Bath was obtained from Amlab. Seahorse X24 and x96e seahorse plates and cartridges were from Agilent technologies. P10, P20, P200 and P100 pipettes were from Gilson or Rainin. Luer lock 25G x 5/8' syringes for intraperitoneal injections were from BD. Transfer pipettes were from Sarstedt.

1500 Standard Fumehood was manufactured by Phoenix Controls Corporation. Bioair Topsafe Fumehood was manufactured by Crowthorne HiTec Services.

Steri-cycle CO_2 incubator was manufactured by Thermo Forma. Legend RT centrifuge was from Sorvall. FACS Canto and LSR Fortessa, 5 mL syringes, 5mL FACS tubes were from BD. LS Macs separation columns and AutoMacs Pro separator were obtained from Miltenyi Biotech. Brightline haemocytometer was from Hausser Scientific. Electrophoresis plates were from Atto and XCELL II Blot Module transfer system and NuPAGE Module was from Invitrogen. 300 V power source was obtained from VWR International or Thermo FIsher. GelDoc XR+ imaging system was manufactured by BioRad. Nanodrop Spectrophotometer ND-1000 from Labtech International

2.1.3. Animal Husbandry

C57BL/6 mice were purchased from Harlan (Bicester, U.K.) and maintained in compliance with Irish Department of Health and Children regulations and with the approval of the University of Dublin's ethical review board.

C57BL/6 were also obtained from the NCI Frederick Core and maintained according to Animal Care and Use committee guidelines.

Pkm2$^{fl/fl}$ mice were obtained from Dr. Matthew Vander Heiden at Massachusetts Institute of Technology, USA. Mice were fully backcrossed to C57BL/6 prior to experimental use.

Ncr1^{Cre} KI mice were obtained Dr. Eric Vivier at INSERM, France and were maintained on a C57BL/6 background.

2.1.4. Antibodies

Target	Clone	Supplier	Dilution	Species
PKM2	D78A4	Cell Signaling	1:2500, 5% Milk in PBST	Rabbit
PKM1	D30G6	Cell Signaling	1:2500, 5% Milk in PBST	Rabbit
c-Myc	D84C12	Cell Signaling	1:1000, 5% Milk in PBST	Rabbit
C-Myc	D3N8F	Cell Signaling	1:1000, 5% Milk in TBST	Rabbit
β - Actin	AC-74	Sigma Aldrich	1:10,000, 5% Milk in PBST	Mouse
β - Actin	AC-15	Abcam	1:10,000, 5% Milk in TBST	Mouse
phospho- S6 (Ser235/236)	D57.2.2E	Cell Signaling	1:2500, 5% BSA in PBST	Rabbit
Total S6	C-8	SantaCruz Biotechnology	1:800, 5% Milk in PBST	Mouse

Table 2. 1 Western Blot Antibodies

Target	Fluor	Supplier	Clone	Dilution
NK1.1	BV421	BioLegend	PK136	1/200
NK1.1	APC	Thermo Fisher	PK136	1/200
NKp46	PE	eBiosciences	29A1.4	1/50
NKp46	efluor 450	eBiosciences	29A1.4	1/100
NKp46	Percp-efluor-710	eBiosciences	29A1.4	1/100
CD3	FITC	eBiosciences	145-2C11	1/600
CD3	Pacific blue	BD	500A2	1/200
TCRβ	APC	BD	H57-597	1/200
TCRβ	PE	BD	H57-597	1/200
IFNγ	APC	BD	XMG1.2	1/200
IFNγ	eFluor450	eBiosciences	XMG1.2	1/100
Granzyme B	PeCy7	eBiosciences	NGZB	1/200
ATP5B	Alexa Fluor 647	Abcam	3D5	1/100
BrDU	APC	BD	B44	1/50
Annexin V	PE	BD	-	1/50
CD69	Percpcy5.5	BD	H1.2F3	1/50
CD98	PE	Biolegend	RL388	1/100
Ly49H	PE	Thermo Fisher	3D10	1/50
L/D Aqua	Aqua	Thermo Fisher	-	1/50

Table 2. 2 ***Flow Cytometry Antibodies***

2.1.5. Miscellaneous buffers:

Buffer	Components
RNA lysis Buffer	RLT buffer (Qiagen)or GeneJet Lysis buffer (Thermo), 1% β-mercaptoethanol
FACS Buffer	Dulbecco's PBS, 10% NK cell media
Celltak (Seahorse)	13µl Cell-Tak, 4180.5µl Sodium Bicarbonate (0.1M, pH 8), 6.5µl NaOH (1M)
Running Buffer	25mM Tris, 192mM Glycine, 0.1% SDS
Transfer Buffer	25mM Tris, 192mM Glycine, 5-10% methanol
W.B Stripping Buffer	0.7% β-mercaptoethanol, 2% SDS, 62.5mM Tris
Protein lysis buffer	100mM Tris/HCl pH 6.7, 20% Glycerol, 4% SDS, 5% β-mercaptoethanol, 0.1% bromophenol blue
Tail digestion Buffer	0.25% SDS, 10mM Tris-HCL pH8, 100mM EDTA pH8

Table 2. 3 ***Miscellaneous Buffers***

2.2. Methods

2.2.1. Cell Culture

2.2.1.1 Natural Killer Cell Culture Medium

Cell culture Medium was prepared by supplementing RPMI 1640 + L-Glutamine media with 10% Foetal Calf Serum, 1% of Penicillin/Streptomycin and 55 μM β-mercaptoethanol using sterile technique.

2.2.1.2 Splenocyte Isolation

A murine spleen was pushed through a 70μM cell strainer using a plunger from a 2mL syringe into 4mL of cold media in a six well plate (under sterile conditions). A sterile Pasteur pipette was used to pass the cells back through the filter until the solution was homogenous. The cell suspension was then transferred to a sterile 50mL falcon tube using a Pasteur pipette. The well was rinsed with 5 mL of RPMI media and transferred to the 50 mL falcon. The cells were centrifuged at 300g for 4 minutes. In the meantime, 2mL of autoclaved and filter sterilised water was added to a 15mL falcon tube and 13mL of media was added to another. The cells were removed from the centrifuge, the supernatant poured off and the pellet and resuspended in zero volume. The sterile water was then poured on the cells (to lyse erythrocytes), immediately followed by the media to prevent lysis of lymphocytes. The cells were centrifuged again at 300g for 4 minutes. The resulting pellet was white in appearance. The supernatant was poured off and the cells were resuspended in 25 mL of RPMI media. Cells were then counted using trypan blue and the cell concentration was adjusted to 2 x 10^6 cells per mL using media. 5 mL of the cell solution was added to each well of a 6 well plate (10 x 10^6 cells). Cells

were cultured in IL-15 at a range of concentrations from 5 – 25ng / mL based on titrations of IL-15 activity from different batches. Generally, 15ng/mL was found to be the optimum dose. Cells were re-supplemented with IL-15 on day 4.

2.2.1.3 Harvesting cultured NK cells

Cells were MACS purified on day 6 where indicated using NK Cell Isolation Kit II (Miltenyi Biotech) or NK cell Isolation Kit (Miltenyi Biotech) and AutoMacs pro separator, or Stem Cell technologies NK cell isolation kit according to manufacturer's instruction. Purity was routinely 95% or greater for NK1.1+NKp46+CD3- cells. Cells were then counted and harvested for stimulation with IL-2 (20ng/ml, NCI preclinical repository), IL-12 (10ng/ml, Miltenyi Biotech) plus treatment.

2.2.1.4 Cell Treatments

Treatment	Stock Concentration	Final Concentration
IL-15	20 μg/mL	5 ng/mL
IL-2	20 μg/mL	20 ng/mL (330U/mL)
IL-12	50 μg/mL	10 ng/mL
Rapamycin	1 mM	20 nM
TEPP-46	50mM	25 μM and 50 μM
Mitoquinol	1mM	50nM or 100 nM

Table 2. 4 ***Cell Treatments***

2.2.2. RNA Analysis

2.2.2.1. RNA Isolation

MACS purified NK cells were stimulated for 18 hours at 37°C . At the end of stimulation cells were transferred to sterile Eppendorf tubes and centrifuged at 500g for 3 mins. Cells were washed with 1mL of cold Dulbeccos's PBS and the supernatant was removed. The pellets were gently resuspended and lysed using Qiagen's RLT buffer supplemented with 1% β-mercaptoethanol or GeneJET Lysis buffer supplemented with 1% β-mercaptoethanol. Lysates were stored at -80°C. Lysates were then purified for RNA using RNeasy minikit or GeneJET as per manufacturer's RNA isolation protocol.

2.2.2.2. cDNA Synthesis

SYBR Green experiments:
mRNA concentrations were normalised using NanoDrop. 16 µL of normalised mRNA (made up in RNase free water) was placed in an 8-PCR tube Strip. 4 µL of 5X qScript cDNA supermix was then added to each RNA condition. Tubes were sealed and placed in a 3Prime Thermal Cycler for cDNA synthesis using the following protocol:

Time	Temperature
5 minutes	25°C
30 minutes	42°C
5 minutes	85°C
Final Hold	10°C

Table 2. 5 ***cDNA Synthesis for SYBR Green qPCR***

TaqMan experiments:
mRNA concentrations were normalised using NanoDrop. 10μL of normalised RNA was added to 10 μL of high capacity reverse DNA synthesis kit master mix. Tubes were sealed and added to an Eppendorf Vapoprotect thermocycler and DNA was synthesised by the following protocol:

Time	Temperature
10 minutes	25°C
60 minutes	37°C
5 minutes	85°C
Final Hold	10°C

Table 2. 6 ***cDNA Synthesis for TaqMan qPCR***

2.2.2.3 SYBR Green Primers

Primers for SYBR green quantitative PCR were designed using the Primer BLAST tool on the NCBI website (http://www.ncbi.nlm.nih.gov/tools/primer-blast/). Primers were designed to meet the following criteria:

- GC clamp at 3' end of primer
- Span exon-exon junction
- 40-60% GC content
- Less than 1 degree Celsius between melting temperatures
- Have at lease 3 mismatches with any other sequence in the gene of interest

Sequences were then verified using Ensembl (http://www.ensembl.org/index.htm)

SYBR Green Primer Sequences:

Rplp0 forward: 5'-CATGTCGCTCCGAGGGAAG-3'

Rplp0 reverse: 5'-CAGCAGCTGGCACCTTATTG-3'

Pkm2 forward: 5'- GCTATTCGAGGAACTCCGCC-3'

Pkm2 reverse: 5'- AAGGTACAGGCACTACACGC-3'

Hprt forward: 5' TGATCAGTCAACGGGGGACA-3'

Hprt reverse: 5'- TTCGAGAGGTCCTTTTCACCA -3'

18S forward: 5'- ATCAGATACCGTCGTAGTTCCC-3'

18S reverse: 5'-TCCGTCAATTCCTTTAAGTTTCAGC -3'

2.2.2.4 TaqMan Primers

Primers for TaqMan qPCR were bought from Thermo Fisher or Integrated DNA Technologies.

Integrated DNA Technologies

Pkm2: Probe: 5'-/56-FAM/TTATCGTTC/ZEN/TCACCAAGTCTGGCA/3IABkFQ/-3'
Primer 1: 5'TTCGAGTCACGGCAATGATAG-3'
Primer 2: 5'-TCCTTCAAGTGCTGCAGTG-3'

MCMV-IE: For: 5'-TGTGTGGATACGCTCTCA CCTCTAT-3'
Rev: 5'-GTTACACCAAGCCTTTCCTGGAT-3'

Thermo Fisher:

Hprt:	Proprietary Probe :	Mm01545399_m1 Cat: 4331182
MCMV-IE:	Probe:	5'-TTCATCTGCTGCCATACTGCCAGCTG-3'
β-Actin:	Proprietary Probe:	Mm02619580_g1 Cat: 4331182

2.2.2.5 Real Time-Polymerase Chain Reaction (RT-qPCR)

2.2.2.6 SYBR green qPCR

Quantitative PCR was carried out in a 96 well plate using the SYBR green detection system and the 9500 fast PCR system by Thermo Fisher. Each condition was carried out in triplicate with each well containing a final volume of 10 µL of the following:

Reagent	Volume
Forward Primer	0.4 µL
Reverse Primer	0.4 µL
SYBR Green FastMix	5 µL
Filtered H2O	3.7 µL
cDNA	0.5 µL

Table 2. 7 ***SYBR Green qPCR Master Mix***

The plate was sealed with qPCR seal (Thermo Fisher) and centrifuged at 300g for 30 seconds to ensure that the solution was not adhering to the sides of the wells. Each set of conditions was normalized to an internal control gene (RPLP0, 18S ribosomal protein, HPRT (Hypoxanthine-guanine phosphoribosyltransferase) and run under fast cycling conditions:

Thermal Cycling conditions:

Stage	Temperature	Time	Cycles
1	95°C	1min	1
2	95°C	1 seconds	35
2	57°C	20 seconds	35
3	95°C	15 seconds	1
3	55°C	30 seconds	1
3	95°C	15 seconds	1

Table 2. 8 ***Thermal Cycle conditions for SYBR Green qPCR***

2.2.2.7 TaqMan qPCR

Quantitative PCR was carried out in a 96 well plate using the TaqMan detection system and the 9500 fast PCR system by Thermo Fisher. Real-time PCR for MCMV-IE was carried out using the following protocol adapted from Tanaka et. al 2007. Each condition was carried out in triplicate with each well containing a final volume of 20 µL of the following:

Standard Master Mix:

Reagent	Volume
TaqMan Probe	1 µL
2X EagleTaq Master Mix	10 µL
Filtered H_2O	7 µL
cDNA	2 µL

Table 2. 9 ***Master Mix for TaqMan qPCR***

MCMV-IE Master Mix:

Reagent	Concentration
Forward Primer	900 nM
Reverse Primer	900 nM
Probe	200 nM
cDNA	50ng/μL
Eagle Taq Master Mix	1X

Table 2. 10 ***cDNA Synthesis for MCMV qPCR***

TaqMan Thermal Cycling conditions:

Thermal cycling conditions were the same for standard TaqMan or MCMV reactions:

Stage	Temperature	Time	Cycles
1	50°C	2 min	1
2	95°C	10 min	1
2	95°C	15 seconds	40
3	60°C	1 min	1

Table 2. 11 ***Thermal Cycle for TaqMan qPCR***

Each reaction was performed in duplicate/triplicate. The relative mRNA levels calculated using the following equation:

Rel. mRNA expression =2^(CTuc-CTus)/ 2^(CTrc-CTrs)

Ct= cycle number to threshold, u is the sample of interest, r is the reference sample ,uc is the sample every other sample is made relative to and s is every other sample.

2.2.2.8. RNA Sequencing

2 x 10^6 MACS purified NK cells were washed twice in cold PBS. Cells were then lysed using the Gene Jet lysis buffer. mRNA was purified using the Gene Jet RNA kit according to manufacturer's instructions. RNA was quantified using NanoDrop. RNA was then snap frozen in liquid nitrogen and sent on dry ice to the Frederick National Laboratory Sequencing facility for sequencing. RNA samples were first subjected to quality control analysis. RNA-Seq samples were then pooled and sequenced on HiSeq4000 using Illumina TruSeq Stranded Total RNA Library Prep and paired-end sequencing. The samples have 52 to 246 million pass filter reads with more than 90% of bases above the quality score of Q30. Reads of the samples were trimmed for adapters and low-quality bases using Cutadapt before alignment with the reference genome (Mouse - mm10) and the annotated transcripts using STAR. The average mapping rate of all samples was 95%. Unique alignment was above 81%. There were 2.71 to 10.47% unmapped reads. The mapping statistics were calculated using Picard software. The samples had 0.07% ribosomal bases. Percent coding bases were between 19-52%. Percent UTR bases were 13-32%, and mRNA bases were between 33-84% for all the samples. Library complexity was measured in terms of unique fragments in the mapped reads using Picard's Mark Duplicate utility. The samples had 56-77% non-duplicate reads. In addition, the gene expression quantification analysis was performed for all samples using STAR/RSEM tools. Both the normalized count and the raw count are provided as part of the data delivery. Data were then analysed using Partek software by Dr. Marieli Gonzalez Cotto, and judged significant based on a p value of 0.05. Pathway enrichment analysis was carried out using the Metascape database.

2.2.3. Flow Cytometry

2.2.3.1. Extracellular Staining:

At the end of stimulations, cells were transferred to labelled FACS tubes. 1mL of FACS buffer was then added to each tube to wash. Tubes were centrifuged at 300g for 3 minutes at 4 degrees and the supernatant was poured off. Pellets were resuspended. Fc Block was added to the pellet (1:200 final dilution in FACS buffer) to prevent non-specific Ab binding to CD16. Cells were then incubated for 10 minutes at 4°C. Extracellular antibodies were made up in FACS buffer. Exposure of tubes to light was kept at a minimum to prevent fluorophore activation. The FACS tubes were removed from the fridge after 20 minutes and washed at 300g for 3 minutes in 1mL of FACS buffer.

2.2.3.2. Intracellular Staining:

For intracellular FACS staining, cells were treated with BD GolgiPlug (Brefeldin A, 1:1000) to prevent protein export from the Golgi Apparatus, four hours before the end of stimulation. Cells were then treated as above for extracellular staining. After extracellular staining 150μL of BD Cytofix/Cytoperm was added to each tube and kept at 4 degrees for 20 minutes. Cells were then washed in 1 x Permwash. Intracellular antibodies were made up in in Permwash. Cells were then incubated at 4 degrees for 20 minutes. They were then washed in 1X Permwash at 300g for 3 minutes. Data were acquired on a FACS Canto, FACS Fortessa or LSR II (Becton Dickinson) and analysed using FlowJo software (TreeStar).

Cytometric bead array for cytokine/chemokine measurements

For cell supernatant measurements, cells were seeded at 2 x 10^6 per mL and treated with cytokines. After 18 hours, supernatants were harvested and frozen for later analysis. For serum measurements, blood was harvested from mice by cardiac puncture. Serum was harvested by centrifugation in column tubes at top speed for two minutes. CBA was performed as per manufacturers (Becton Dickinson) instructions using 50 mL of supernatant or serum per sample and analysed by flow cytometry.

2.2.3.3. BrDU Staining

Cells were treated with BD FC Block and then stained for extracellular antigens as above. After 20 minutes cells were washed and fixed using 100μL BD Cytofix/Cytoperm. Cells were incubated on ice for 20 minutes. Cells were then washed with BD Permwash. Supernatants were discarded and cells were resuspended in 100μL of BD Cytoperm permeabilisation buffer plus. Cells were incubated on ice for 10 minutes. Cells were then washed with BD Permwash. Cells were then re-fixed in 100μL of BD Cytofix/Cytoperm. Cells were left for 5 minutes on ice and then washed with BD Permwash. Cells were then treated with 100μL of DNase (300μg/mL). Cells were then incubated at 37°C for 1 hour. Cells were then washed in Permwash. Cells were then resuspended in 50μL of Permwash containing 1μL of anti BrDU antibody per sample. Cells were then incubated on ice for 20 minutes. Cells were washed and stored at 4°C in the dark until flow cytometric analysis.

2.2.3.4. Gating strategy

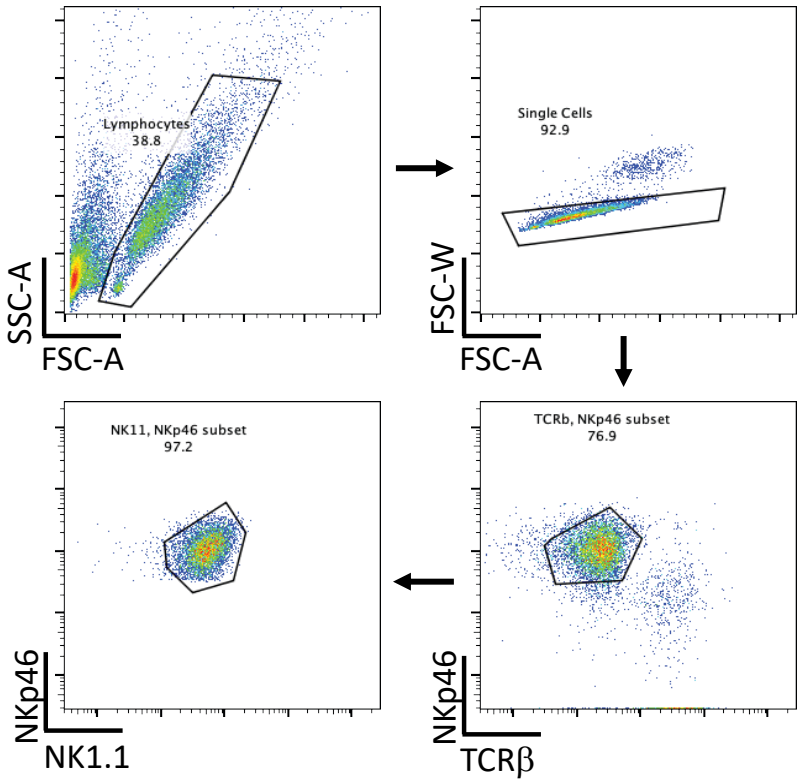

Representative gating strategy: Lymphocytes were gated based on their forward scatter and side scatter area. Doublets were excluded based on forward scatter width vs forward scatter area. NK cells were gated on 2 parameters – NK1.1+NKp46+CD3- or TCRβ– L/D stain was used in all *in vivo* experiments.

2.2.4. Protein Analysis

2.2.4.1. Protein Extraction:

MACS purified NK cells were stimulated at a concentration of 2 x 10^6 cells/mL for 18 hours. Cells were counted using the trypan blue exclusion method, and normalized to a concentration of 10 x 10^6 cells per mL. Cells were centrifuged at 500g for 3 minutes at 4°C. The supernatant was removed and 1 mL of PBS was added to wash. The cells were centrifuged again at 500g for 3 minutes and the PBS supernatant was removed. The pellet was then gently resuspended and lysed in 1X protein lysis buffer (Table 2.3) + 25 μM DTT. Samples were denatured at 95°C for 10 minutes prior to electrophoresis. Lysates were stored at -80°C.

2.2.4.2. Sodium dodecyl-sulfate polyacrylamide gel electrophoresis (SDS-PAGE)

SDS-PAGE was used to separate proteins based on size for Western blot analysis.

Gels were run using the AE6450 system from Atto Corporation or Novex NuPAGE system.. Gels were ran at 100V until proteins reached bottom of stacking gel. Voltage was then increased to 200V. Gels were made using pre-made NuPAGE gels from Thermo Fisher, or made according to the following recipe:

10% acrylamide gel recipe:

Reagent	Stacking gel	Resolving gel
1M Tris	0.625mL (pH 6.8)	2.25mL(pH 8.8)
1% SDS	500μL	600μL
40% acrylamide/bisacrylamide	500μL	1.5μL
1.5% APS	250μL	300μL
TEMED	5μL	6μL
ddH_20	3.12mL	1.344mL

Table 2. 12 ***10% acrylamide gel***

2.2.4.3. Western Blotting

For the transfer of proteins to PVDF membranes, membranes were first cut to size of gel and activated in methanol. 6 nylon sponges and 4 3mm Whatmann papers were soaked in transfer buffer. The gels were removed from the plates and assembled in the transfer apparatus with the Whatmann paper, PVDF and sponges as per manufacturer's instructions (XCELL II Invitrogen). The PVDF membrane was positioned on the side closest to the anode. Proteins were then transferred at 45V for 2 hours or at 15V overnight on ice. Once the transfer was complete membranes were stained with Ponceau S to locate unstained protein size marker and to assess if protein transfer was successful. Ponceau was then rinsed of with ddH20. Membranes were for 45 minutes at room temperature on a roller using 5% milk in PBST or 5% BSA in PBST. Membranes were then transferred to primary antibody and placed on a roller for 4 hours at room temperature or overnight at 4°C. After primary antibody incubation the membranes were washed 3 times for 5 minutes in PBST. Membranes were then placed in secondary antibody (1:5000 in 5% milk in PBST) for 1 hour at room temperature. The membranes were then washed again 3 three times in PBST for 5 minutes. HRP substrate was then added and the luminescence was assessed using a GelDoc system or XRay films .

2.2.4.4. Genotyping

50µl of tail lysis buffer and 5µl of 10mg/ml proteinase K was added to tail snip in 1.5ml Eppendorf tubes. Eppendorfs were placed in a heating block at 55°C for 4 hours to overnight, allowing the tails to become digested. Tails were then heated to 95°C for 10 minutes to inactivate proteinase K. 950µL of DNAse free water was then added to sample. DNA samples were stored at -20°C until use. DNA products were run on a 1.2% agarose gel stained with EtBr.

2.2.4.5. *Pkm2* Genotyping

Primers

Forward 5' TAG GGC AGG ACC AAA GGA TTC CCT 3'

Reverse 5' CTG GCC CAG AGC CAC TCA CTC TTG 3'

Reagent	Volume
2x GoTaq PCR Buffer	15µl
Pkm2 Primer- For	1µl
Pkm2 Primer-Rev	1µl
Tail DNA	1µl
ddH_20	12µl
Total	**30µl**

Table 2. 13 $PKM2^{fl/fl}$ Genotyping MasterMix

Pkm2$^{fl/fl}$ Genotyping Thermal Cycles:

Step	Temperature	Time
1	94°C	3 Min
2 (30 cycles)	94°C	30 Sec
3 (30 cycles)	59°C	30 Sec
4 (30 cycles)	72°C	30 Sec
5	72°C	2 Min
6	4°C	Hold

Table 2. 14 *PKM2*$^{fl/fl}$ *Thermal cycle conditions*

PCR products: *Pkm2*$^{fl/fl}$: 600bp ***Pkm2*$^{WT/WT}$:** 500bp

2.2.4.6 *Ncr1*^{Cre} genotyping

Primers

NKp46-cre F - 5′ GGA ACT GAA GGC AAC TCC TG

R (wt) - 5′ TTC CCG GCA ACA TAA AAT AAA

R (cre) - 5′ CCC TAG GAA TGC TCG TCA AG

Ncr1 ^{Cre} Master Mix:

Reagent	Volume
2x Gotaq PCR Buffer	15µl
NKp46-Cre For	2µl
NKp46- Rev (WT)	1µl
NKp46 - Rev (Cre)	1µl
Tail DNA	1µl
ddH_20	10µl
Total	**30µl**

Table 2. 15 *Ncr1 ^{Cre} Genotyping Master mix*

Step	Temperature	Time
1	94°C	3 Min
2 (32 cycles)	94°C	30 Sec
3 (32 cycles)	57°C	30 Sec
4 (32 cycles)	72°C	1 Min
5	72°C	3 Min
6	4°C	Hold

Table 2. 16 *Ncr1 ^{Cre} Genotyping Thermal Cycle Conditions*

PCR products: WT/WT: 340 bp, ***Ncr1^{Cre}*/WT:** 340 bp + 250 bp, ***Ncr1^{Cre}/Ncr1^{Cre}*:** 250 bp

2.2.5. Seahorse analysis

A Seahorse Extracellular Flux Analyser X24 or x96e was used for measurement of extracellular acidification rate (ECAR) and oxygen consumption rate (OCR). These measurements were used as an indicator of glycolysis and oxidative phosphorylation rates respectively.

2.2.5.1. 24 well

A 24 well seahorse cartridge was hydrated using Seahorse calibration buffer in a $-CO_2$ incubator at 37°C for 18 hours prior to analysis. 200μL for 24 well of prepared CellTak solution (BD) was placed in each well of a Seahorse cell culture plate for 20 minutes at room temperature. The wells were the washed twice with 500μL of sterile water. Seahorse media was supplemented with 10mM glucose and placed in a water bath at 37°C. For Seahorse analysis a minimum of 3 x 10^6 purified NK cells were required per condition (0.75 x 10^6 in quadruplicate). These cells were transferred to 15mL falcon tubes and washed twice in pre-warmed Seahorse media. Cells were then resuspended at 7.5 x 10^6 cells per mL in seahorse media supplemented with relevant treatments (TEPP-46). 100 μL of this cell solution was then added to designated wells in the Seahorse plate. The cell was then centrifuged at 100g without break for 3 minutes to allow cells to adhere to Celltak in the wells. The plate was then placed in a $-CO_2$ incubator for 20 minutes prior to cartridge loading. 70 μl of inhibitors were added to designate ports of the seahorse cartridge plate prior to calibration. Final concentrations of inhibitors were made up as follows in Seahorse media; oligomycin (2μM), fluoro-carbonyl cyanide phenylhdrazone (0.5μM), rotenone (100nM) plus antimycin (4μM) and 2-DG (30mM) (see table 2.8 for purpose of inhibitors). After 20 minutes of the cell plate incubation in $-CO_2$, 500μl of seahorse media containing relevant treatments was added

to each well, and 600μl seahorse media was put in the blank wells for background measurements. After calibration of the seahorse cartridge, the cell plate was placed in the Seahorse machine.

2.2.5.2. 96 well

A 96 well seahorse cartridge was hydrated using Seahorse calibration buffer in a $-CO_2$ incubator at 37°C for 18 hours prior to analysis. 25μL for of prepared CellTak solution (BD) was placed in each well of a Seahorse cell culture plate for 20 minutes at room temperature. The wells were the washed twice with sterile water. Seahorse media was supplemented with 10mM glucose and placed in a water bath at 37°C. For Seahorse analysis a minimum of 0.2 x 10^6 purified NK cells were required per condition (1 x 10^6 in quintuplicate). These cells were transferred to 15mL falcon tubes and washed twice in pre-warmed Seahorse media. Cells were then resuspended 400ml of seahorse media supplemented with relevant treatments (TEPP-46). 80 μL of this cell solution was then added to designated wells in the Seahorse plate. The cells were then centrifuged at 100g without break for 3 minutes to allow cells to adhere to Celltak in the wells. The plate was then placed in a $-CO_2$ incubator for 20 minutes prior to cartridge loading. 20 μl of inhibitors were added to designated ports of the seahorse cartridge plate prior to calibration. Final concentrations of inhibitors were made up as follows in Seahorse media; oligomycin (2μM), fluoro-carbonyl cyanide phenylhdrazone (0.5μM), rotenone (100nM) plus antimycin (4μM) and 2-DG (30mM) (see table X for purpose of inhibitors). After 20 minutes of the cell plate incubation in $-CO_2$, 100μl of seahorse media containing relevant treatments was added to each well, and 180μl seahorse media was

put in the blank wells for background measurements. After calibration of the seahorse cartridge, the cell plate was placed in the Seahorse machine.

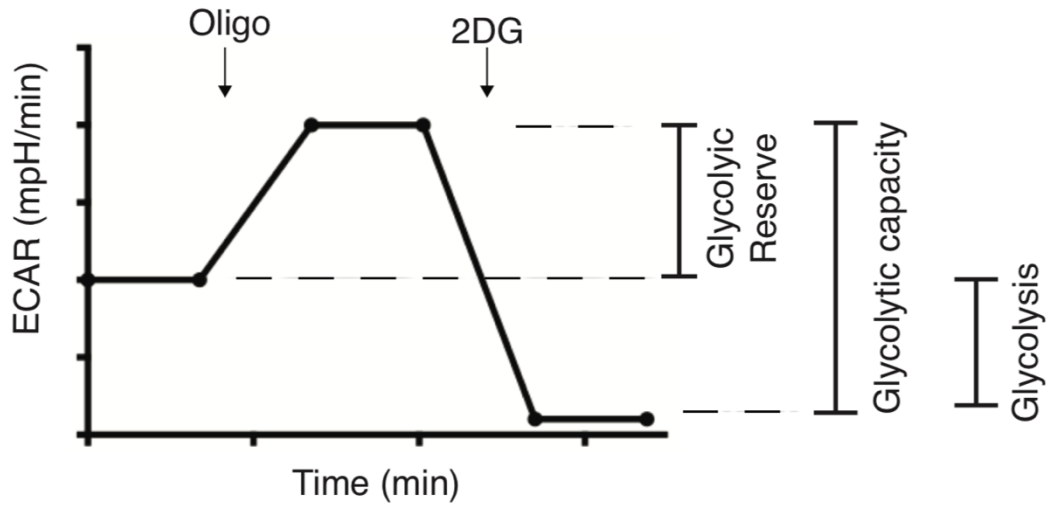

Figure 2. 1. Glycolytic measurements with seahorse analyser

Basal glycolysis can be measured by the extracellular acidification rate before the addition of oligomycin. The addition of oligomycin will inhibit ATP synthase and cause the cells to upregulate glycolysis to compensate. The measurement after this addition is the total glycolytic capacity of the cells. Addition of 2-DG inhibits glycolysis. Measurements after 2-DG will give background acidification. Therefore, this can be subtracted to give actual measurements of acidification due to glycolysis. Diagram from Loftus et. al 2018

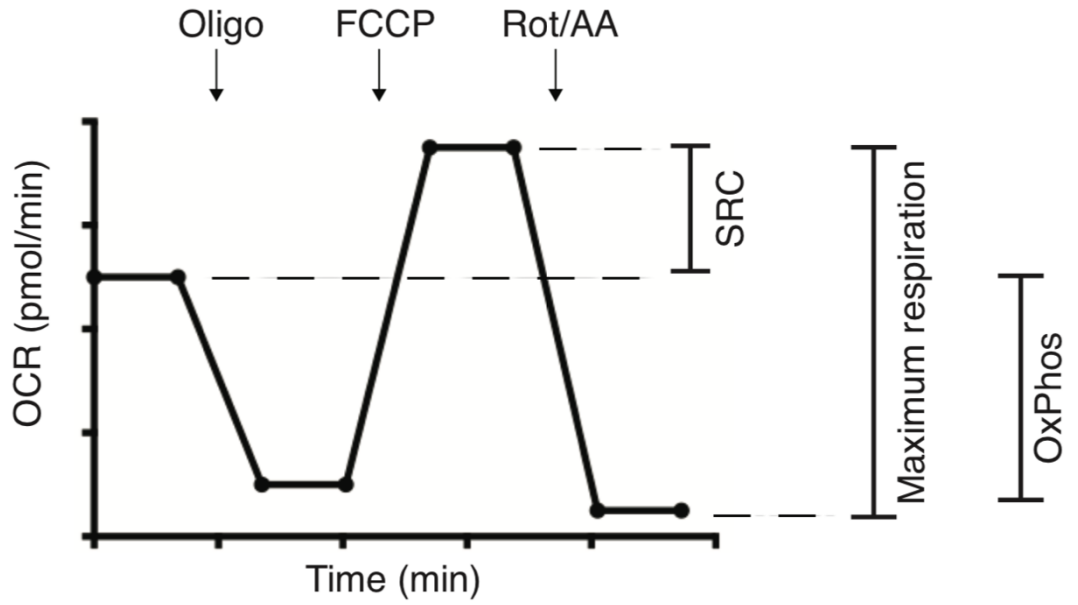

Figure 2. 2. OxPhos measurements using seahorse metabolic flux analyser

Measurements for OxPhos are based on the oxygen consumption rate (OCR) of cells. Basal OxPhos is measured before the addition of oligomycin. Oligomycin inhibits ATP synthase. FCCP disrupts the proton gradient across the inner mitochondrial membrane, which will uncouple OxPhos from energy production. This allows for the measurement of maximum respiration. The Spare Respiratory Capacity (SRC) can be calculated by subtracting the basal rate of OxPhos from the maximum rate of respiration. Antimycin A and Rotenone inhibit complex III and I of the electron transport chain respectively. This will shut down OxPhos so any measurements after this addition are just background. Diagram from Loftus et. al 2018

Seahorse injections:

Compound	Mechanism	Purpose
Oligomycin	ATP Synthase inhibitor	Inhibition of ATP Synthase by oligomycin leads to inhibition of mitochondrial ATP production. Therefore, This compound is used to determine the 'glycolytic capacity' of a cell as cells will increase glycolytic flux to maintain energy homeostasis in the absence of OxPhos.
FCCP	Mitochondrial uncoupler	FCCP is an ionophore that uncouples the mitochondrial membrane potential from ATP synthase. This results in increased oxygen consumption by Complex IV as there is a free flow of electrons through the ETC. This can be used to determine the 'maximal respiratory capacity' as it is an indicator of the maximal mitochondrial oxygen consumption that can be done by the cell.
Rotenone	Complex I inhibitor	Rotenone is used in Seahorse to inhibit complex I in order to assess background oxygen consumption in when OxPhos is inhibited. However, electrons can still be transported through complex II so this inhibitor is used in combination with Antimycin A.
Antimycin A	Complex III inhibitor	Antimycin A is used in combination with rotenone to inhibit OxPhos as it is a direct inhibitor of complex III. This allows for the measurement of oxygen consumption when OxPhos is inhibited.
2-DG	Phosphoglucose Isomerase inhibitor	2-DG is a glucose analogue that can be metabolized to 2-glucose-6-phosphate by hexokinase in glycolysis. However it cannot be metabolized any further and essentially inhibits glycolytic flux.

Table 2. 17 ***Seahorse Injection Summary***

2.2.6. Metabolomics

2.2.6.1 GC-MS Mass spectrometry Metabolomics

Untargeted mass spectrometry was carried out by West Coast Metabolomics at UC Davis. 10 x 10^6 MACS purified NK cells were washed 3 times in cold PBS. Samples were then snap frozen in liquid nitrogen. At UC Davis, samples were re-suspended with 1 ml of extraction buffer (37.5% degassed acetonitrile, 37.5% isopropanol and 20% water) at –20 °C, centrifuged and evaporated to complete dryness. Membrane lipids and triglycerides were removed with 50% acetonitrile in water. The extract was aliquoted into two equal portions and the supernatant evaporated again. Internal standards C08-C30 fatty acid methyl esters were added and the sample derivatized by methoxyamine hydrochloride in pyridine and subsequently by *N*-methyl-*N*-trimethylsilyltrifluoroacetamide for trimethylsilylation of acidic protons. Gas chromatography-time-of-flight analysis was performed by the LECO Pegasus IV mass spectrometer. Samples were additionally normalised using the sum of peak heights for all identified metabolites (mTIC Normalisation).

2.2.6.2. LC-MS Mass spectrometry Metabolomics

Cell pellets were washed and resuspended in -20°C 80% methanol. Phase separation was achieved by centrifugation at 4°C and the methanol-water phase containing polar metabolites was separated and dried using a vacuum concentrator. The dried metabolite samples were stored at −80°C and resuspended in Milli-Q water the day of analysis. An Agilent 6410 Triple Quadrupole mass spectrometer interfaced with a 1200 Series HPLC quaternary pump (Agilent) was used for ESI-LC–MS/MS analysis in multiple

reaction monitoring mode. Four concentrations of standards, processed under the same conditions as the samples, were used to establish calibration curves. The best fit was determined using regression analysis of the peak analyte area. Chromatographic resolution was obtained in reverse phase on a Zorbax SB-C18 (1.8μm; Agilent) for amino acids and an Eclipse Plus C18 (1.8μm; Agilent) for TCA intermediates, with a flow rate set at 0.4 ml/min. Data were normalised to protein concentration.

2.2.7. *In vivo* experiments

2.2.7.1. Polyinosinic:polycytidylic acid (PolyI:C)

Poly (I:C) experiments were carried out using high molecular weight Poly(I:C). Poly(I:C) was resuspended at 1mg/mL in saline. Poly(I:C) solution was then heated to 65°C for 10 minutes to dissolve. 200μg of Poly(I:C) in 200μL of saline was then administered to the left side of the peritoneum. Vehicle controls were administered 200μL of saline only. Spleens were harvested 24 hours post injection of Poly(I:C). Mice used were 7-10 weeks old.

2.2.7.2. Murine Cytomegalovirus (MCMV)

Stock of MCMV was a gift from the Brown lab at the University of Virginia. MCMV stock was obtained from salivary gland passage of MCMV infected BALB/c mice and titered on NIH3T3 or NIH3T12 monolayers. 1 x 10^5 PFU of virus in 100μL was injected into the left side of the peritoneum in saline. Vehicle controls were give 100μL of saline only. On day 4 post-infection, mice were euthanised and tissues harvested. DNA from spleen was digested overnight with DNeasy extraction kit for further downstream qPCR analysis. Mice used were 7-10 weeks old.

2.2.8. Statistical analysis

GraphPad Prism 8.11 for Macintosh (GraphPad Software) was utilized for statistical analysis of data. A one-way ANOVA with Tukey multiple comparison test was used when comparing two or more data sets. A two-way ANOVA with Sidaks post-test was used when comparing data with two variables. A students t-test was used when comparing two data sets.

Chapter 3: PKM2 is not required for NK cell activation *in vivo*

Introduction

NK cells respond to a plethora of immune stimuli *in vivo*. Specifically, NK cells are capable of robustly responding to viral infections and transformed cells. These NK cell functional responses are integrally linked to NK cell metabolism [113]. As previously discussed in chapter 1, control of NK cell metabolism has been investigated using genetic knock outs in *in vitro* models of activation. These studies have discovered a crucial role for SREBP and cMyc transcription factors in regulating NK cell metabolism [86, 109]. However, to date, studies investigating the role of NK cell metabolism *in vivo* have primarily relied on pharmacological inhibitors of metabolism. For example, it has been shown by the Cooper lab that NK cell glycolysis is required for NK cell responses to murine cytomegalovirus *in vivo* using the glycolytic inhibitor 2-deoxyglucose [135]. These data showed that pharmacological inhibition of glycolysis leads to impaired NK cell proliferation and activation in response to MCMV [135]. However, to date there have been no studies using a conditional knock out of a glycolytic enzyme in NK cells to assess function *in vivo.*

Pyruvate kinase M2 (PKM2) is a key glycolytic enzyme as it is responsible for the generation of pyruvate and ATP. However, aside from this metabolic role, PKM2 has also been ascribed diverse roles in transcriptional regulation of immune cell function in cells such as macrophages and T cells [119, 121]. Indeed, pharmacological manipulation of PKM2 significantly impaired macrophage responses to *Mycobacterium tuberculosis in vitro,* along with LPS-induced IL-1β production [119]. Glycolytic flux is hugely upregulated upon NK cell activation *in vitro* but not much is known about the glycolytic enzymes that facilitate this flux [52]. Given that PKM2 has been shown to be a key metabolic and functional regulator in other immune cells, it is likely that PKM2 could

play a crucial role in the regulation of NK cell glycolysis and function also. To date, there have been no studies on the role of PKM2 in NK cells. Therefore, the focus of this chapter is on the role of PKM2 in controlling murine splenic NK cell function *in vivo*. This will primarily be assessed using a genetic approach with an NK cell specific knockout for *Pkm2.*

3.1. PKM2 is induced in splenic NK cells by *in vivo* administration of poly(I:C)

PKM2 is expressed in a variety of immune cells such as macrophages, dendritic cells and T cells and is induced upon immune activation [122]. To investigate whether PKM2 is also induced in activated NK cells, wild-type C57Bl/6 mice were injected intraperitoneally with polyinosinic:polycytidylic acid (Poly(I:C)). Poly(I:C) is a synthetic double stranded RNA analogue that can directly activate NK cells through the melanoma differentiation-associated protein 5 (MDA-5) receptor and stimulates type I IFN responses [136].

Wild-type mice were injected into the peritoneum with two different doses of Poly(I:C); (100 μg and 200 μg). After 24 hours, mice were euthanised and spleens were harvested. Flow cytometry was then used to measure the fluorescence intensity of PKM2 staining. The data show that PKM2 protein is induced in splenic NK cells 24 hours post-poly(I:C) administration in a dose dependent manner **(Fig 3.1)**. This indicates that PKM2 is induced in response to immune stimulation *in vivo.*

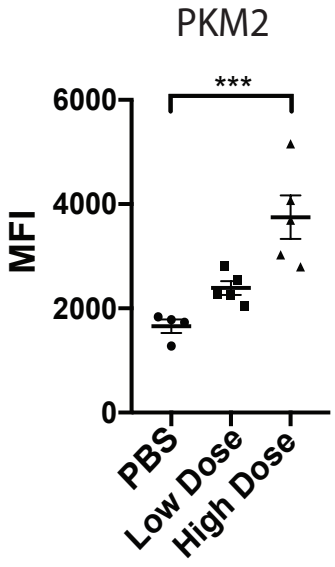

Figure 3. 1. Poly(I:C) administration induces PKM2 expression in splenic NK cells *in vivo*

C57Bl/6 mice were administered PBS, 100 μg (low dose) or 200 μg (high dose) of poly(I:C) by I.P injection. Spleens were harvested 24 hours post treatment. Splenocytes were isolated and PKM2 expression by $NK1.1^{+}NKp46^{+}$ cells was then quantified by flow cytometry (mean fluorescence intensity). Data are representative of two experiments. Data are displayed as mean +/- S.E.M for n=4-5 mice and were analysed by one-way ANOVA. (***$p<0.001$)

3.2. Generation of an NK cell specific *Pkm2* knock out mouse

PKM2 is induced in activated NK cells *in vivo*, therefore, it was next investigated whether PKM2 was required for NK cell metabolic and functional responses. To test this, an NK cell specific knock out for *Pkm2* was generated. This conditional knock out was achieved using a Cre recombinase and loxP system.

The Cre system used was *Ncr1*^{Cre}. The *Ncr1*^{Cre} mouse is a knock in mouse, whereby the gene encoding improved Cre recombinase (iCre) is inserted after the promoter for the *Ncr1* gene [137]. This mouse, which has been characterized elsewhere, has a caveat, in that it results in a downregulation of *Ncr1* protein (Nkp46) on the surface of NK cells. Although the *Ncr1*^{Cre} KI mouse results in lower surface expression of NKp46, it does not affect the overall percentage of NKp46 positive NK cells [137].

Initially, it was confirmed that *Ncr1*$^{Cre/Cre}$ homozygous mice had lower surface expression of NKp46 relative to *Ncr1*$^{WT/WT}$ mice (**Fig. 3.2 A).** The initial paper that characterised these mice decided to utilize *Ncr1*$^{Cre/WT}$ heterozygous mice, as it resulted in efficient deletion of floxed alleles and no overt phenotype of the NK cells. Therefore, for this study, *Ncr1*^{Cre} mice were also used as heterozygotes. Throughout the course of this study, *Ncr1*$^{Cre/WT}$ mice will be denoted as PKM2^{WT}.

In order to delete the gene for *Pkm2,* a *Ncr1*^{Cre} heterozygous mouse was crossed with a mouse containing loxP sites either side of exon 10 in the *Pkm* gene. This allowed for specific excision of the exon encoding *Pkm2.* Experimental mice were bred to be heterozygous for *Ncr1*^{Cre} and homozygous for *Pkm2*$^{fl/fl}$ (*Ncr1*^{Cre} *Pkm*$^{fl/fl}$). These experimental mice will henceforth be denoted as PKM^{KO}.

To ensure that this experimental setup was appropriately controlled, level of NKp46 expression was compared between $PKM2^{WT}$and $PKM2^{KO}$ mice. When assessed using flow cytometry, it was observed that they had comparable NKp46 expression and thus were properly controlled (**Fig. 3.2 B)**. For ease of comparison, respective genotypes for $PKM2^{WT}$ and $PKM2^{KO}$ NK cells can be visualised in figure 3.3.

In order to confirm that *Pkm2* was deleted from NK cells in these mice, NK cells were flow cytometrically sorted from spleens of wild type, $PKM2^{WT}$ (*Pkm2*$^{fl/fl}$) and $PKM2^{KO}$ (*Ncr1*^{Cre}*Pkm*$^{fl/fl}$) mice. Flow cytometric sorting resulted in a pure NK cell fraction. NK cells were then lysed and DNA was purified using a DNA extraction kit. PCR was then performed on NK cells from both genotypes ($PKM2^{WT}$ or $PKM2^{KO}$) for either the *Pkm2*$^{WT/WT}$ and *Pkm2*$^{fl/fl}$ allele. $PKM2^{KO}$ (*Ncr1*^{Cre}*Pkm*$^{fl/fl}$) NK cells showed efficient deletion of *Pkm2*, yielding only a 200kb fragment of the PKM gene (**Fig. 3.4)**.

This effect was specific to NK cells as the negatively flow sorted fraction of cells (splenocytes with NK cells removed) showed the regular 600kb floxed band. This indicates that the *Ncr1*^{Cre} *Pkm*$^{fl/fl}$ mouse successfully deleted the *Pkm2* gene in NK cells.

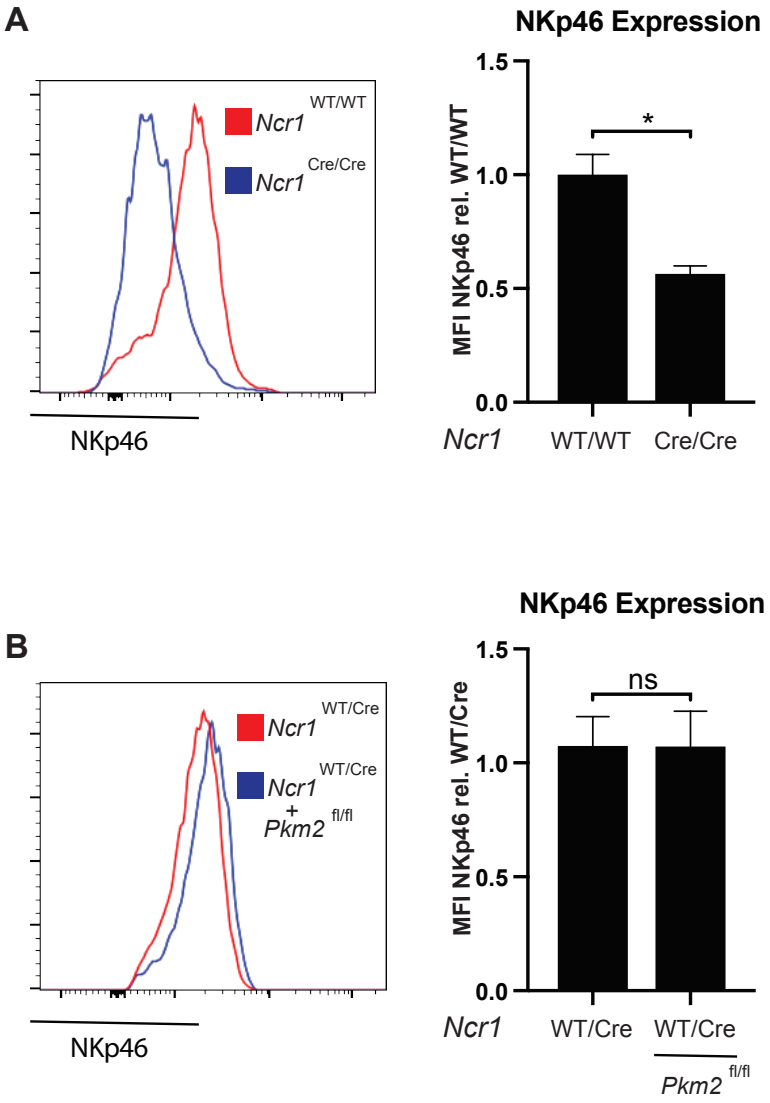

Figure 3. 2. NK cells from *Ncr1*$^{Cre/Cre}$ mice have less NKp46 than *Ncr1*$^{WT/WT}$ mice

Splenocytes were isolated from *Ncr1*$^{cre/cre}$ and *Ncr1*$^{wt/wt}$ mice and NK cells were identified as being NK1.1^{+}NKp46^{+}CD3^{-}. NKp46 expression was then analysed by mean fluorescence intensity. (A) Representative histogram and pooled data of relative NKp46 expression of *Ncr1*$^{WT/WT}$ mice or *Ncr1*$^{Cre/Cre}$ mice. (B) Splenic NK cells were identified by flow cytometry from *Ncr1*^{Cre}(PKM2^{WT}) and *Ncr1*^{Cre}*Pkm*$^{fl/fl}$ (PKM2^{KO}) mice. NK cells were then analysed for the expression of NKp46 by MFI. Representative histogram and pooled data of NKp46 expression of *Ncr1*$^{Cre/+}$(PKM2^{WT}) mice or *Ncr1*$^{Cre/+}$ x *Pkm2*$^{fl/fl}$ (PKM2^{KO}) mice. Data are mean +/- S.E.M. Bar graph is pooled data of 3 individual experiments. Data were analysed by paired students t-test (*$p < 0.05$, ns: non-significant)

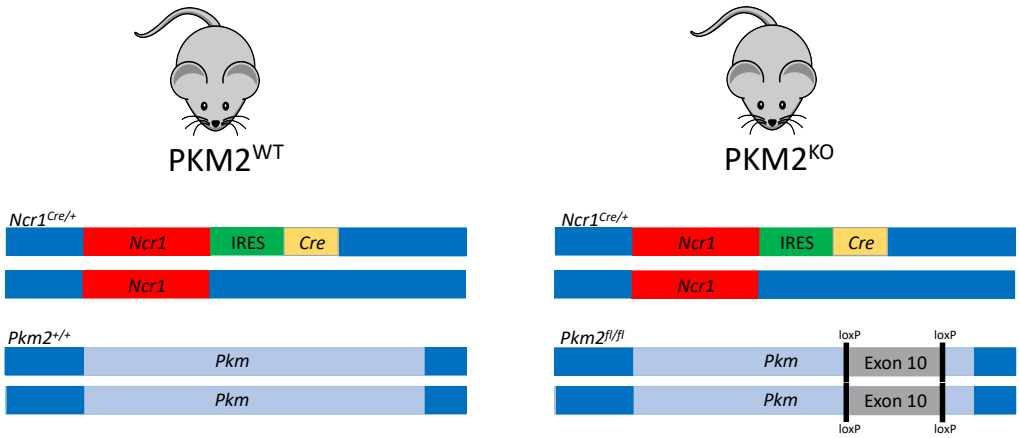

Figure 3. 3. Schematic of genotypes for PKM2^{WT} and PKM2^{KO} NK cells

Mice with PKM2^{WT} NK cells are *Ncr1$^{Cre/+}$ and Pkm2$^{+/+}$. Ncr1^{cre}* mice also contain and IRES (internal ribosome entry site) sequence. This allows for ribosomal entry of the Cre transcript for translation. Mice with PKM2^{KO} NK cells are *Ncr1$^{Cre/+}$* but contain two loxP sites at either side of exon 10 in the *Pkm* gene (*Pkm*$^{fl/fl}$). Expression of Cre recombinase in a mouse with floxed regions will lead to specific excision of the floxed gene of interest.

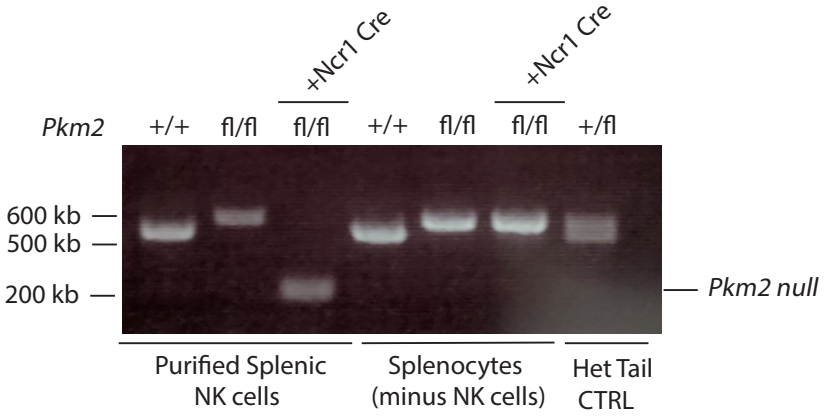

Figure 3. 4. The *Pkm2* gene is selectively deleted from NK cells of *Ncr1*$^{WT/Cre}$ x *Pkm2*$^{fl/fl}$ mice

Splenocytes from either *Pkm2*$^{WT/WT}$ (+/+), *Pkm2*$^{fl/fl}$ (fl/fl)or *Ncr1*^{Cre} *Pkm2*$^{fl/f}$ (PKM2^{KO})^{l} mice were flow cytometrically sorted into two fractions - NK cells (NK1.1^{+}CD3^{-} NKp46^{+}CD49b^{+}) and all other splenocytes. Cells were then lysed and DNA was isolated. PCR reactions were conducted for both the WT *Pkm2* gene and the loxP flanked *Pkm2* gene (*Pkm2*$^{fl/fl}$). Picture also displays a heterozygous control from mouse tail DNA with bands for both *Pkm2*$^{WT/WT}$ and *Pkm2*$^{fl/fl}$.

3.3. PKM2^{KO} Splenic NK cell numbers, frequencies and maturity are normal

The data show that *Pkm2* was efficiently deleted in murine splenic NK cells. Next, the functional impact of this deletion was evaluated. To test this, total splenic cell number, NK cell number and frequency were compared between PKM2^{WT} and PKM2^{KO} NK cells. Firstly, there was no difference in the total splenocyte number between PKM2^{KO} and PKM2^{WT} spleens **(Fig. 3.5 A)**. The frequency of NK cells (NK1.1^{+}NKp46^{+}CD3^{-}) in the spleen was evaluated using flow cytometry, and it was determined that there was no significant difference between PKM2^{WT} and PKM2^{KO} **(Fig. 3.5 B)**. The total number of NK cells in the spleen was also found to be normal **(Fig. 3.5 C)**.

NK cell maturation can be tracked by the expression of CD27 and CD11b. NK cells usually follow the developmental pattern of CD11b(low)CD27(low) to CD11b(low)CD27(high) to CD11b(high)CD27(high) to CD11b(high)CD27(low) [138]. Each step corresponds with acquiring different effector functions. When the expression of CD11b and CD27 was compared between PKM2^{WT} and PKM2^{KO} NK cells, it was found to be comparable (**Fig. 3.6).** Therefore it can be concluded that PKM2 is not required for splenic NK cell development or maturation.

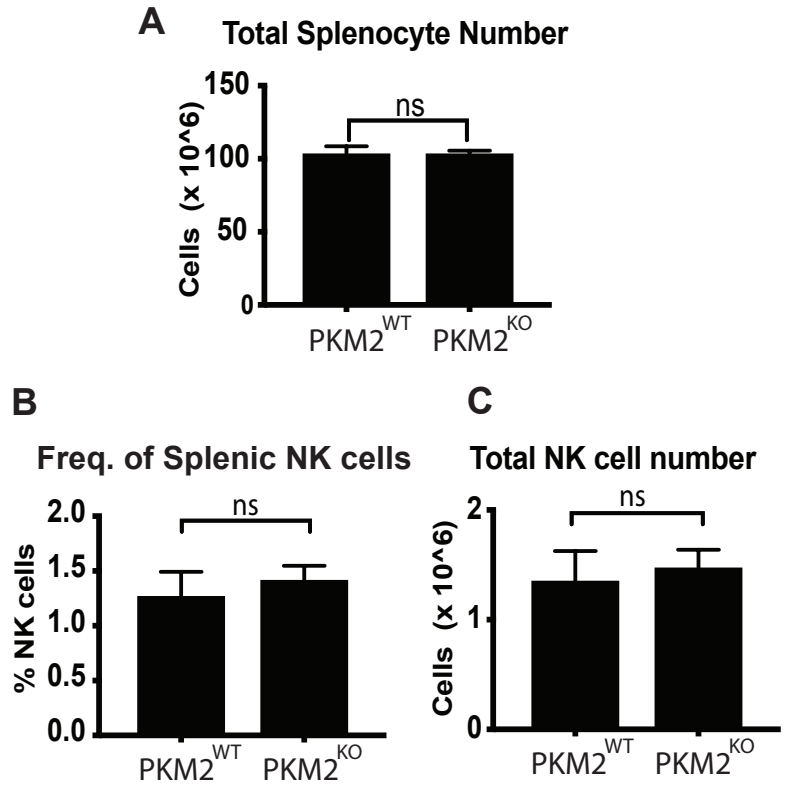

Figure 3. 5. Splenocyte numbers and NK cell frequency are normal between mice with *Pkm2*^{KO} NK cells and with *Pkm2*^{WT} NK cells

Splenocytes were isolated from mice with *Pkm2*^{WT} or *Pkm2*^{KO} NK cells (A) total splenic cells were counted and found to be normal between the two genotypes. (B) NK cells were stained for flow cytometry using NKp46^{+}NK1.1^{+}CD3^{-} gating strategy. NK cell frequency was then obtained by expressing number of NKp46^{+}NK1.1^{+}CD3^{-} cells as a percentage of total living splenocytes (C) Total NK cell number was obtained by using NK cell frequency and total NK cell numbers. Data are mean +/- S.E.M. Bar graphs are pooled data of 5 individual experiments. Data were analysed by paired students t-test (ns: non-significant)

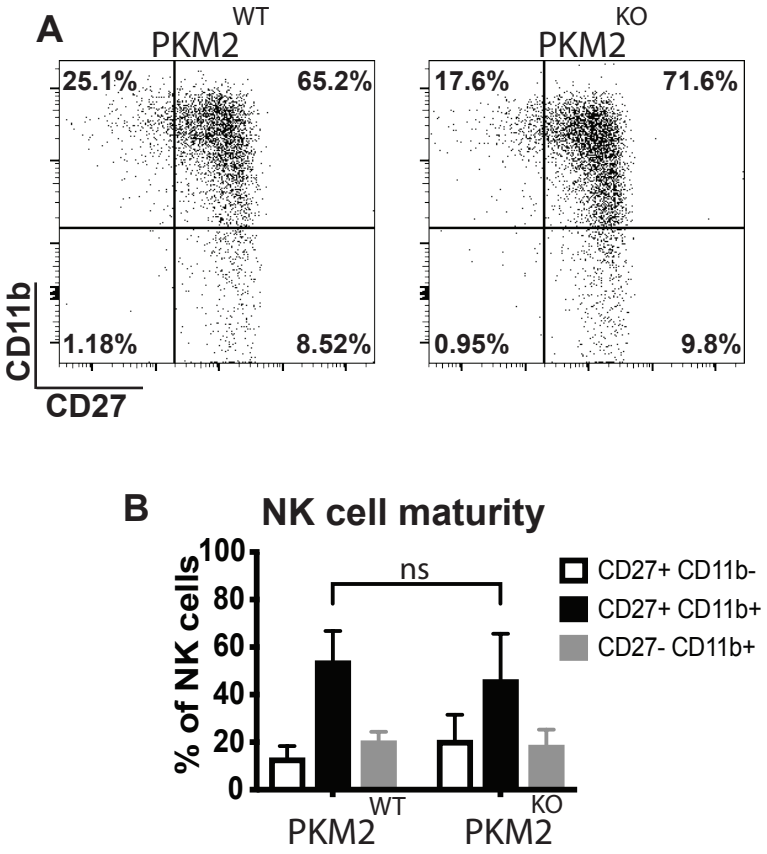

Figure 3. 6. Splenic PKM2^{KO} NK cells have normal expression of CD27 and CD11b

Splenocytes were isolated from PKM2^{WT} or PKM2^{KO} mice and analysed by flow cytometry for the expression of CD27 and CD11b (A) Representative dot plots for NK cells (NK1.1^{+}NKp46^{+}CD3^{-}) expressing CD27 or CD11b. Gates were drawn using FMO controls for CD27 or CD11b. (B) Pooled data for CD27 and CD11b expression on NK cells. Data are mean +/- S.E.M. Bar graphs is pooled data of 3 individual experiments. Data were analysed by two way ANOVA with Sidak post-test (ns: non-significant)

3.4. PKM2^{KO} NK cells are efficiently activated following Poly I:C injection

Previous data presented in this study has demonstrated that PKM2 protein is induced in response to poly(I:C) administration *in vivo.* Next, it was investigated whether *Pkm2* deletion would affect NK cell functional responses to poly(I:C) *in vivo.* Mice were injected intraperitoneally with 200μg of poly(I:C) (or saline) and spleens were harvested 24 hours later.

The expression of NK cell activation marker CD69 was evaluated to confirm that poly(I:C) was activating splenic NK cells. As predicted, poly(I:C) significantly increased expression of CD69 on the surface of PKM2^{WT} NK cells relative to the saline vehicle control (**Fig. 3.7 A).** Similarly, when the expression of CD69 on PKM2^{KO} NK cells was measured, it was comparable to that of PKM2^{WT} NK cells. This was observed for both CD69 MFI **(Fig. 3.7 B)** and in frequency of NK cells expressing CD69 **(Fig. 3.7 C).** This indicated that both PKM2^{WT} and PKM2^{KO} are comparably activated by poly(I:C) administration *in vivo.*

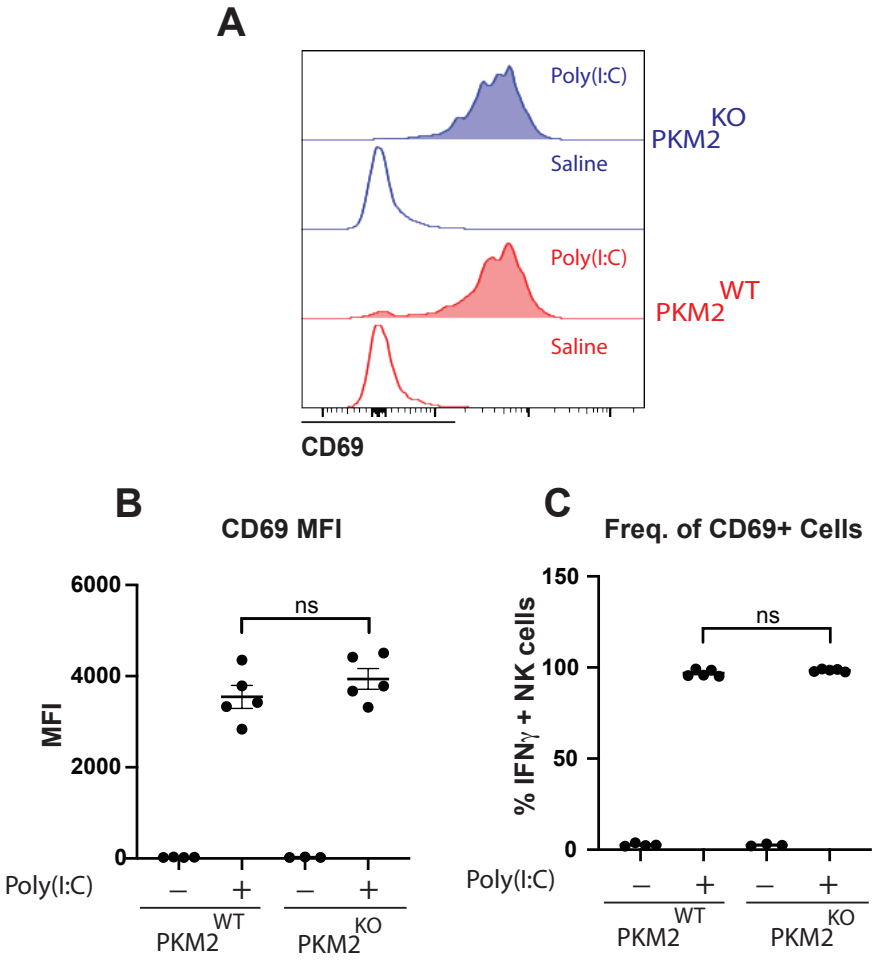

Figure 3. 7. Splenic PKM2^{WT} and PKM2^{KO} NK cells express similar amounts of CD69 to in response to 24 hour poly (I:C) treatment

Ncr1$^{Cre/+}$ (PKM2^{WT}) or *Ncr1*$^{Cre/+}$*Pkm2*$^{fl/fl}$ (PKM2^{KO}) mice were administered saline (-) or 200μg of poly(I:C) by i.p. injection and spleens harvested 24 hours post treatment. Splenocytes were isolated and NK1.1^{+}NKp46^{+}CD3^{-} cells were analysed by flow cytometry for CD69 expression. (A) NK cells were identified as NK1.1^{+}NKp46^{+}CD3^{-} cells and then assessed for the surface expression of CD69 by flow cytometry. Data shown is a representative histogram for CD69 expression. (B) pooled data of CD69 expression as measured by mean fluorescence intensity (C) pooled data for frequency of NK cells that are positive for CD69 relative to FMO control. Data are mean +/- S.E.M. Data are pooled data of 3-5 mice and is representative of one experiment. Data were analysed by two way ANOVA with Sidak post-test (ns: non-significant)

3.5. PKM2^{WT} and PKM2^{KO} NK cells increase IFNγ production comparably in response to poly(I:C) *in vivo*

In addition to CD69 expression, the number of NK cells expressing IFNγ in response to poly(I:C) treatment *in vivo* was also assessed. In general, activated NK cells will produce the effector molecule IFNγ as an anti-viral defence. PKM2^{WT} NK cells in poly(I:C) injected mice showed an increased percentage of IFNγ positive cells when compared with saline controls (**Fig. 3.8 A B).** PKM2^{KO} NK cells showed similar levels of IFNγ expression as PKM2^{WT} controls. These data indicated that splenic PKM2^{KO} NK cells demonstrate a normal IFNγ response to poly(I:C) activation in vivo .

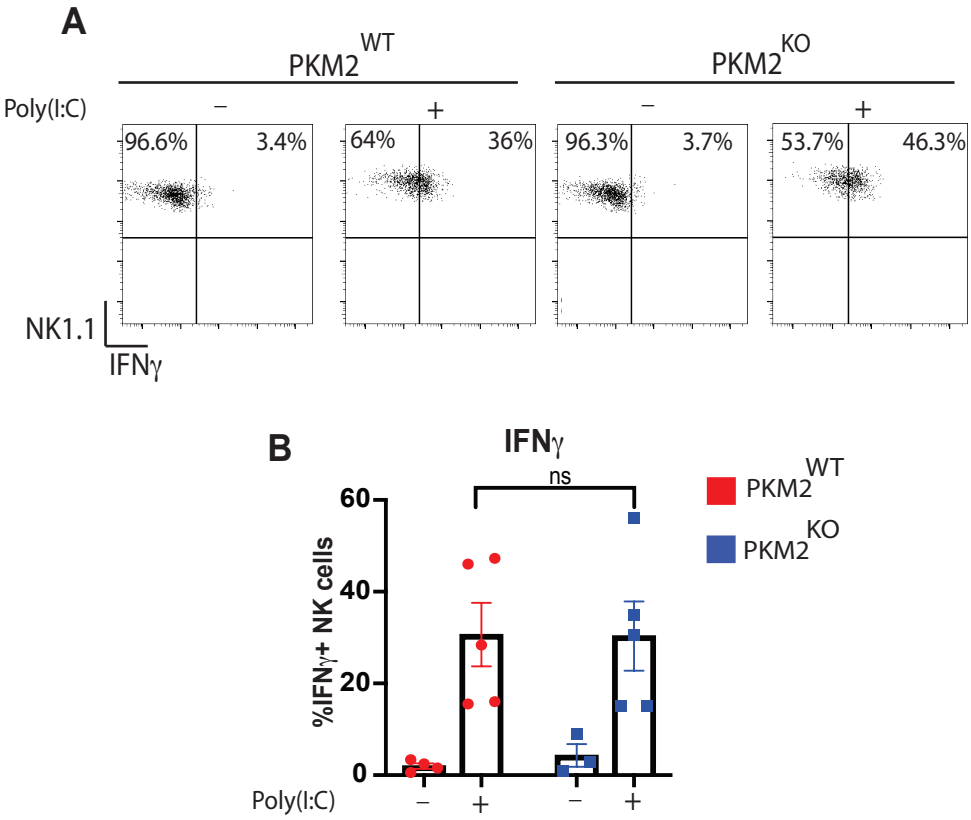

Figure 3. 8. . Deletion of PKM2 in splenic NK cells does not affect poly(I:C) induced expression of IFNγ *in vivo*

Mice from Ncr1$^{Cre/+}$ (PKM2^{WT}) or *Ncr1*$^{Cre/+}$*Pkm2*$^{fl/fl}$ (PKM2^{KO}) were administered saline (-) or 200μg of poly(I:C) (+) by i.p. injection and spleens harvested 24 hours post treatment. Splenocytes were isolated and NK1.1^{+}NKp46^{+}CD3^{-} cells were analysed by flow cytometry for IFNγ expression. (A) Data are representative of IFNγ positive cells from 4 mice (-) or 5 mice (poly(I:C)). (B) Data are mean +/- SEM of IFNγ positive NK cells from 4 mice (Veh.) or 5 mice (poly(I:C)). Each data point represents one individual animal. Data are from one experiment. Data were analysed using two-way ANOVA. ns: non-significant

3.6. Deletion of PKM2 in splenic NK cells does not affect poly(I:C) induced expression of CD98 *in vivo*

Next we assessed whether PKM2 deletion affects markers of NK cell metabolism such as the expression of CD98, a component of the L-amino acid transporters. CD98 can form heterodimers of two transporters Slc3a2 with other amino acid transporters such *Slc7a5* which controls cellular uptake of large neutral amino acids [111]. It has been previously demonstrated by the Finlay group that CD98 is acutely regulated by both mTORC1 and cMyc and is therefore a representative marker of global NK cell metabolism [52, 109, 139]. Therefore, this marker was evaluated in response to poly(I:C). Injection of 200μg poly(I:C) resulted in an equivalent increase in CD98 expression on both $PKM2^{WT}$ and $PKM2^{KO}$ NK cells compared to controls (**Fig. 3.9 A,B).**

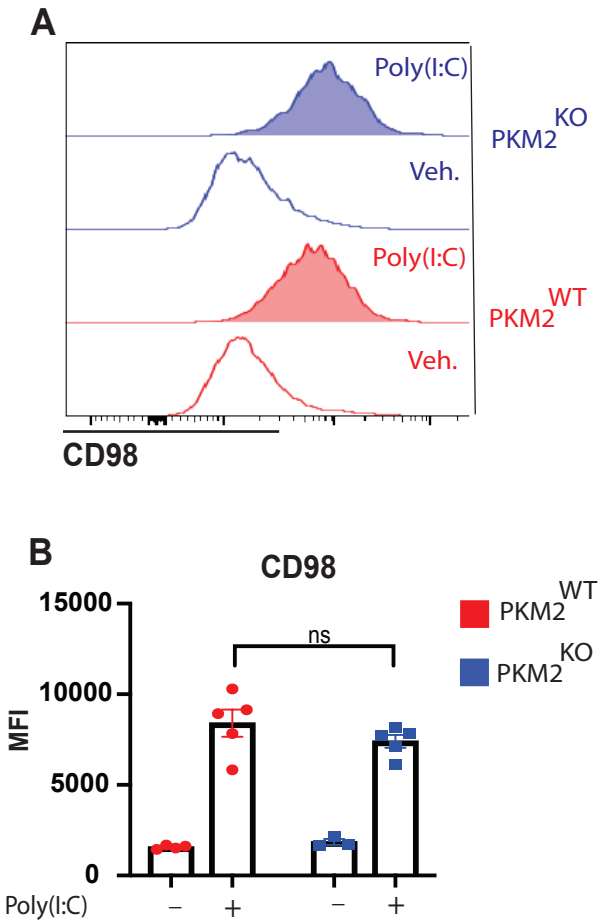

Figure 3. 9. Deletion of PKM2 does not affect poly(I:C) induced expression of CD98 on splenic NK cells *in vivo*

Mice from *Ncr1*$^{Cre/+}$ (PKM^{WT}) or *Ncr1*$^{Cre/+}$*Pkm2*$^{fl/fl}$ (PKM2^{KO}) were administered saline (-) or 200ug of poly(I:C)(+) by i.p. injection and spleens harvested 24 hours post treatment. Splenocytes were isolated and NK1.1^{+}NKp46^{+}CD3^{-} cells were analysed by flow cytometry for CD98 expression. (A) Data are representative histograms of CD98 expression from NK cells of Ncr1$^{Cre/+}$(PKM2^{WT}) or *Ncr1*$^{Cre/+}$*Pkm2*$^{fl/fl}$ (PKM2^{KO}) mice treated with saline(-) or poly(I:C)(+) . (B) Data are mean +/- SEM of CD98 MFI from 4 mice (-) or 5 mice (poly(I:C). Each data point represents one individual animal. Data are from one experiment. Data were analysed using two-way ANOVA. ns: non-significant

3.7. Deletion of PKM2 in splenic NK cells does not affect poly(I:C) induced proliferation *in vivo*

PKM2 is a key glycolytic enzyme and is involved in the regulation of biomass production. Therefore, it was investigated whether PKM2 deletion would affect the proliferative cycle of NK cells. This was evaluated based on the incorporation of the thymidine analogue bromodeoxyuridine (BrDU). This thymidine analogue is incorporated into the DNA of proliferating cells.

$PKM2^{WT}$ or $PKM2^{KO}$ mice were injected with 200µg of poly(I:C) intraperitoneally. Then 20 hours later they were injected with 2 mg of bromodeoxyuridine (BrDU) intraperitoneally. At the 24 hour post-poly(I:C) timepoint, mice were euthanised and spleens were harvested.

NK cells were then identified by flow cytometry (NK1.1, NKp46) and stained intracellularly with an antibody specific for BrDU. $PKM2^{WT}$ mice injected with poly(I:C) showed an increase in BrDU incorporation relative to saline controls **(Fig. 3.10 A,B).** This indicated that poly(I:C) was inducing NK cell proliferation *in vivo.*

Indeed when the frequency of BrDU positive cells was compared between $PKM2^{WT}$ and $PKM2^{KO}$ there was no difference **(Fig. 3.10 A,B).**

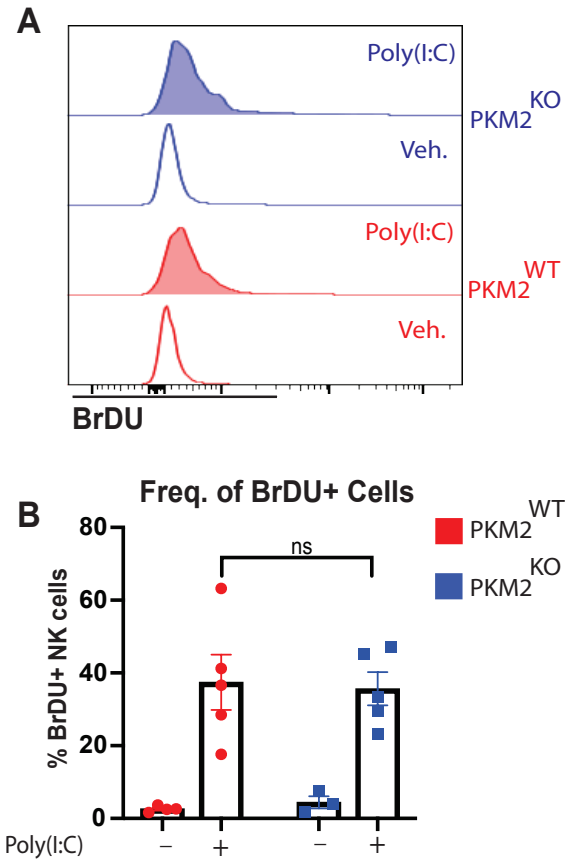

Figure 3. 10. Deletion of PKM2 in splenic NK cells does not affect poly(I:C) induced proliferation *in vivo* as measured by BrDU incorporation

Ncr1$^{Cre/+}$ or *Ncr1*$^{Cre/+}$*Pkm2*$^{fl/fl}$ mice were administered saline (-) or 200µg of poly(I:C) (+) by i.p. injection. 20 hours later mice were administered 2mg of BrDU i.p. Spleens were then harvested 4 hours later (24 hours post poly(I:C) treatment). Splenocytes were isolated and NK1.1^{+}NKp46^{+}CD3^{-} cells were analysed by flow cytometry for BrDU incorporation using the BD BrDU APC kit. (A) Data are representative histograms of BrDU incorporation in NK cells of *Ncr1*$^{Cre/+}$ (PKM2^{WT}) or *Ncr1*$^{Cre/+}$*Pkm2*$^{fl/fl}$ (PKM2^{KO}) mice . (B) pooled data of BrDU positive NK cells from 4 mice (-) or 5 mice (poly(I:C)). Each data point represents one individual animal. Data are from one experiment. Data were analysed using two-way ANOVA. ns: non-significant

3.8. Splenic PKM2^{WT} and PKM2^{KO} NK cells respond similarly to MCMV infection 4 days post infection

Poly(I:C) is an inducer of NK cell activation *in vivo.* However, it is not a true virus. Therefore, it was next investigated whether directly infecting mice with a virus would reveal a phenotype between PKM2^{WT} and PKM2^{KO} NK cells. The virus utilised was murine cytomegalovirus (MCMV). C57Bl/6 mice have innate resistance to this virus, due to their ability to recognise a specific viral epitope m157 on the surface of infected cells. This resistance is mainly mediated by Ly49H^{+} NK cells which is a receptor that recognises the viral epitope m157 [140].

A stock of this virus was supplied by the Brown lab at the University of Virginia. The Brown lab has optimised this viral stock at a viral load of 1 x 10^5 PFU per mouse. This viral load is readily detectable in the spleen of mice at 4 days post infection, and induces proliferation of Ly49H positive cells. Therefore a similar experimental setup was used in this study. Mice were injected with 1 x 10^5 PFU of MCMV (or saline) intraperitoneally, and spleens were harvested 4 days post infection.

MCMV infected mice appeared to have a small but not significant increase in spleen weight when compared to the saline treated controls at 4 days post infection. When spleens of mice with PKM2^{WT} and PKM2^{KO} NK cells were compared, there was found to be no significant difference between genotype **(Fig. 3.11 A)** .

Similarly, the frequency and number of splenic NK cells was also assessed **(Fig. 3.11 B C)**. There was no significant difference between the two genotypes infected with virus.

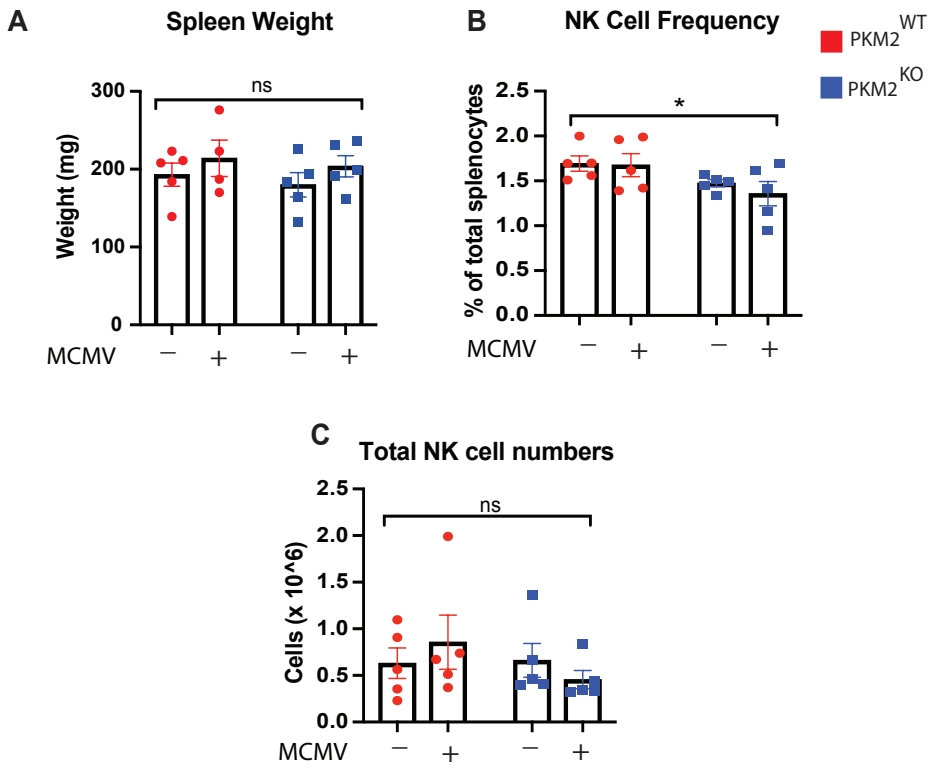

Figure 3. 11. Spleen weight and NK cell frequency are comparable between PKM2 ^{WT} and PKM2 ^{KO} NK cells

Mice from *Ncr1*$^{Cre/+}$ (PKM2 ^{WT}) or *Ncr1*$^{Cre/+}$*Pkm2*$^{fl/fl}$ (PKM2 ^{KO}) were administered saline (-) of 1 x 10^5 PFU of salivary passaged MCMV (+). 4 days later mice were injected with 2mg of BrDU i.p. Mice were then sacrificed 4 hours later and spleens were harvested. (A) spleens were weighed and data is displayed in mg (B) Splenocytes were isolated and NK1.1$^+$NKp46$^+$CD3$^-$ cells were identified and expressed as a percentage of total living splenocytes (C) total splenic NK cell number was identified using NK cell frequency and total splenocyte number. Data are n=5 animals per group. Each data point represents one individual animal. Data are representative of two independent experiments. Data were analysed using two-way ANOVA. ns: non-significant

3.9. Splenic PKM2^{WT} and PKM2^{KO} NK cells express similar levels of CD69 after MCMV infection

As there were no significant effects on NK cell number or frequency after MCMV infection, it was next confirmed that the NK cells were being activated in response to virus. As previously mentioned, CD69 is a classic marker of NK cell activation. Therefore, the expression of this marker was assessed on NK cells 4 days post MCMV infection. There was a significant increase in the expression of CD69 relative to saline controls on both PKM2^{WT} and PKM2^{KO} NK cells **(Fig. 3.12 A)**. This indicated that there was an NK cells were responding to the infection. When PKM2^{WT} and PKM2^{KO} levels of CD69 expression were compared, there was a small but significant increase between the genotypes (**Fig 3.12 B)**. However, this was not observed in the experimental repeat. Therefore, it remains inconclusive as to whether there is a difference in activation between PKM2^{WT} and PKM2^{KO} NK cells after MCMV infection.

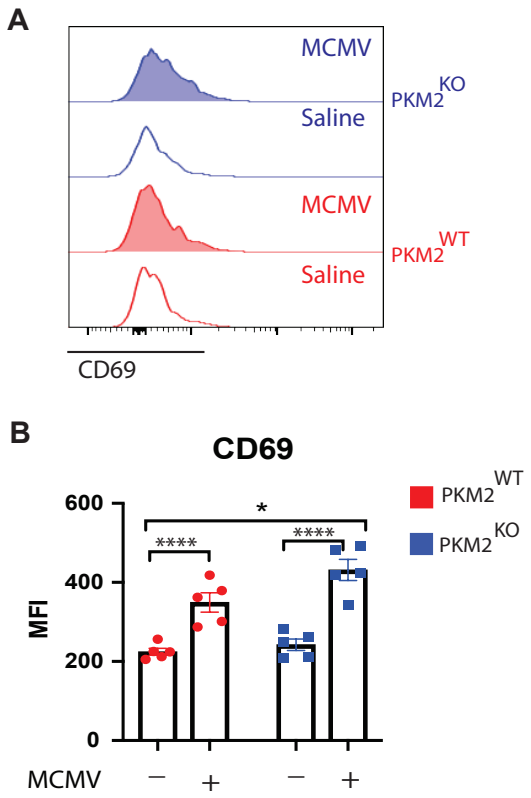

Figure 3. 12. CD69 expression may be comparable between PKM2 ^{WT} and PKM2 ^{KO} NK cells

Mice from *Ncr1*$^{Cre/+}$ (PKM2 WT) or *Ncr1*^{Cre}*Pkm2*$^{fl/fl}$ (PKM2 KO) were administered saline (-) or 1 x 10^5 PFU of salivary passaged MCMV (+). 4 days later mice were injected with 2mg of BrDU i.p. Mice were then sacrificed 4 hours later and spleens were harvested. (A) Representative histogram of saline and MCMV treated NK cells (NK1.1$^+$CD3$^-$) for CD69 expression in both PKM2 ^{WT} and PKM2 ^{KO} NK cells as measured by flow cytometry (B) Pooled data of CD69 expression on NK cells for both saline(-) and MCMV(+) treated PKM2 ^{WT} and PKM2 ^{KO} mice. Data are n=5 animals per group. Each data point represents one individual animal. Data were analysed using two-way ANOVA with Sidak post test. *p< 0.05, ****p< 0.001 ns: non-significant

3.10. PKM2^{WT} and PKM2^{KO} splenic NK cells demonstrate a similar frequency of IFNγ production post-MCMV infection

Next, it was assessed whether MCMV infection induced the expression of the proinflammatory cytokine IFNγ on NK cells. Four days post MCMV infection, there was a significant increase in the frequency of IFNγ positive NK cells relative to saline controls (**Fig. 3.13 A**). When the frequency of IFNγ production was compared between PKM2 ^{WT} and PKM2^{KO} NK cells, there was no significant difference (**Fig. 3.13 B**). This was also observed to be highly reproducible in the experimental repeat.

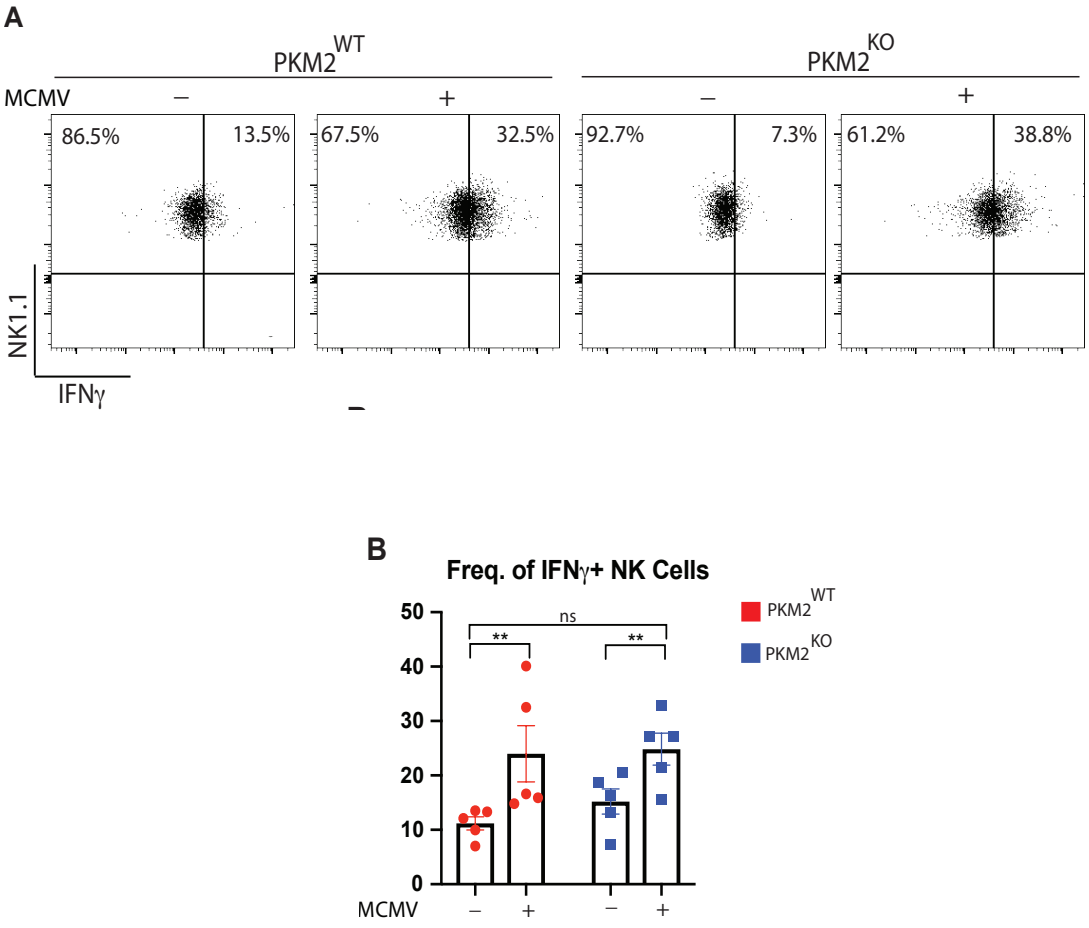

Figure 3. 13. Frequency of IFNγ positive NK cells is similar between PKM2 ^{WT} and PKM2 ^{KO} NK cells

Ncr1$^{Cre/+}$ (PKM2^{WT}) or *Ncr1*$^{Cre/+}$*Pkm2*$^{fl/fl}$ (PKM2^{KO}) were administered saline (-) of 1 x 10^5 PFU of salivary passaged MCMV (+). 4 days later mice were injected with 2mg of BrDU i.p. Mice were then sacrificed 4 hours later and spleens were harvested. (A) Representative dot plot of saline and MCMV treated NK cells (NK1.1$^+$ CD3$^-$) for IFNγ expression in both PKM2 ^{WT} and PKM2 ^{KO} NK cells as measured by flow cytometry (B) Pooled data of frequency of IFNγ positive NK cells for both saline(-) and MCMV(+) treated PKM2 ^{WT} and PKM2 ^{KO} mice. Data are n=5 animals per group. Each data point represents one individual animal. Data were analysed using two-way ANOVA. **p< 0.001 ns: non-significant

3.11. Frequency of Ly49H^{+} cells is comparable between PKM2^{WT} and PKM2^{KO} mice infected with MCMV

MCMV is known at later timepoints to induce the proliferation of Ly49H positive NK cells. Therefore, the frequency of Ly49H positive NK cells in response to MCMV treatment was assessed. This was analysed by flow cytometry and it was found that the frequency of Ly49H positive cells was normal between saline and MCMV treated mice (**Fig. 3.14 A)**. There is generally an association between MCMV infection and increased Ly49H positive NK cell frequency, however, splenic NK cells do not normally show significant expansion of Ly49H positive cells between 3-5 days post infection [141, 142]. However, studies show that splenic Ly49H positive cells begin to incorporate BrDU at 3 days post infection [142].

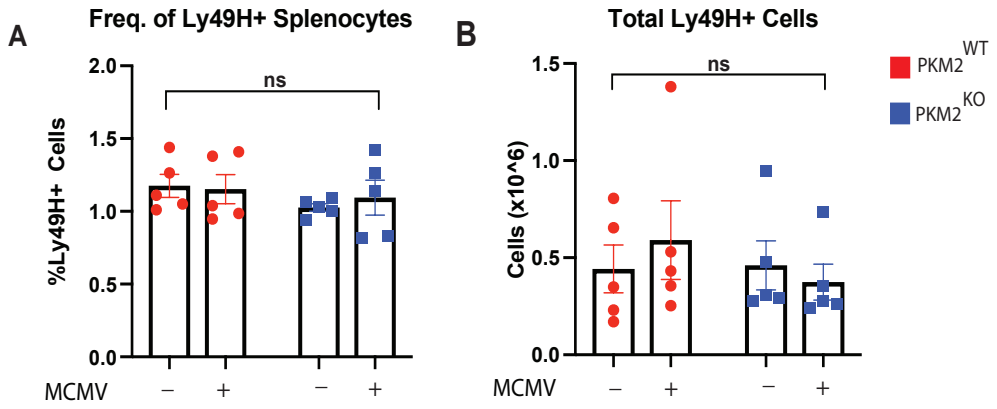

Figure 3. 14. Frequency and total number of Ly49H^{+} cells are comparable between PKM2 ^{WT} and PKM2 ^{KO} NK cells

Mice from *Ncr1*$^{Cre/+}$ (PKM2^{WT}) ^{or} *Ncr1*$^{Cre/+}$*Pkm2*$^{fl/fl}$ (PKM2^{KO}) were administered saline (-) or 1 x 10^5 PFU of salivary passaged MCMV (+). 4 days later mice were injected with 2mg of BrDU i.p. Mice were then sacrificed 4 hours later and spleens were harvested. (A) Pooled data of frequency of Ly49H positive cells expressed as a percentage of total splenocytes for both saline(-) and MCMV(+) treated PKM2 WT and PKM2 KO mice. (B) Pooled data of total Ly49H positive cells expressed calculated using total splenocyte numbers. Data are n=5 animals per group. Each data point represents one individual animal. Data are representative of two individual experiments. Data were analysed using two-way ANOVA. ns: non-significant

3.12. PKM2^{WT} and PKM2^{KO} Ly49H^{+} cells incorporate the same amount of BrDU after MCMV infection

There was no significant differences between genotype in the percentage of Ly49H^{+} cells after MCMV infection. However, it was also investigated as to whether these cells were undergoing active proliferation. In order to investigate this, PKM2 ^{WT} and PKM2 ^{KO} mice with either saline or MCMV (1x10^{5} PFU) for 4 days. On day 4 mice were injected with 2mg of BrDU I.P and spleens were harvested 4 hours later. Mice treated with MCMV demonstrated a higher percentage of Ly49H^{+} cells incorporating BrDU, indicating that these cells are actively undergoing DNA replication (**Fig. 3.15).** However, when assessed the Ly49H^{+} BrDU incorporation was compared between the two genotypes, there was no significant difference, indicating that they were undergoing similar levels of proliferation.

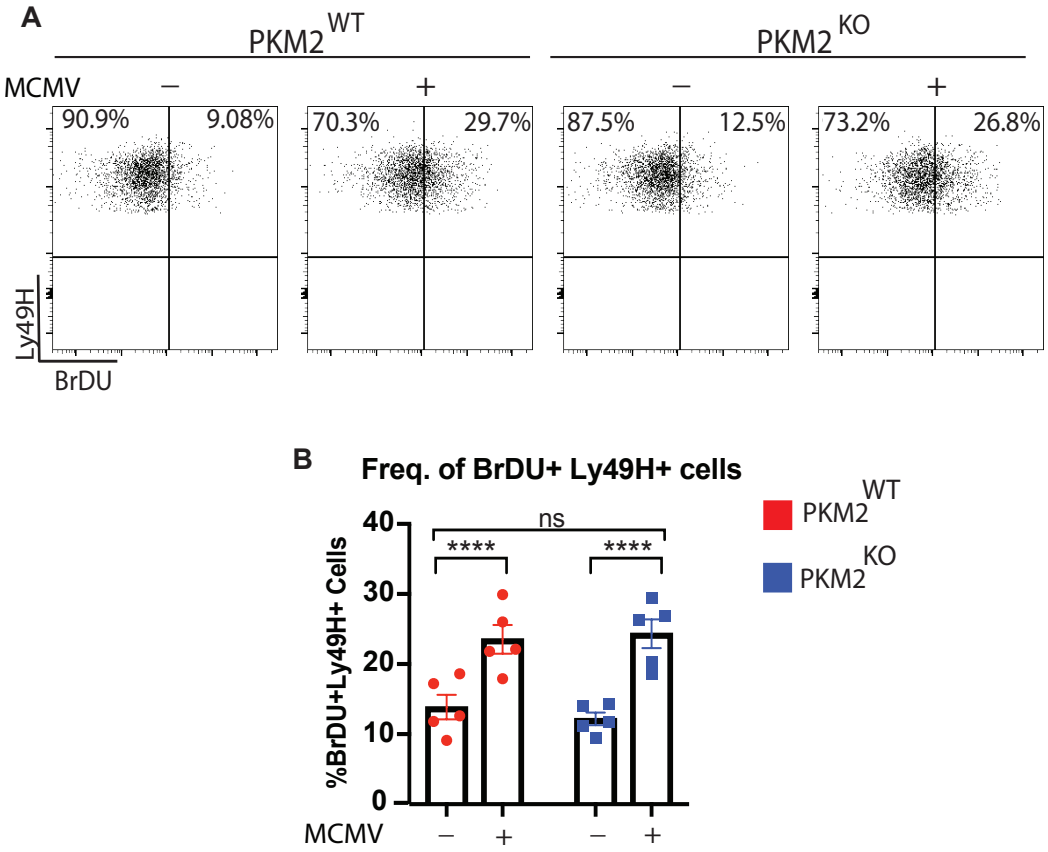

Figure 3. 15. Freq. of BrDU^{+} Ly49H^{+} cells are comparable between PKM2^{WT} and PKM2^{KO} NK cells

Ncr1$^{Cre/+}$(PKM2^{WT}) or *Ncr1*$^{Cre/+}$*Pkm2*$^{fl/fl}$ (PKM2^{KO}) mice were administered saline (-) of 1 x 10^{5} PFU of salivary passaged MCMV (+). 4 days later mice were injected with 2mg of BrDU i.p. Mice were then sacrificed 4 hours later and spleens were harvested. (A) Representative histograms for BrDu^{+}Ly49H^{+} cells for both saline(-) and MCMV(+) treated PKM2 ^{WT} and PKM2 ^{KO} mice. (B) Pooled data of total BrDU^{+} Ly49H^{+} cells relative to FMO control. Data are n=5 animals per group. Each data point represents one individual animal. Data are representative of two individual experiments. Data were analysed using two-way ANOVA. ****p<0.0001 ns: non-significant

3.13. Serum cytokines are comparable between mice with PKM2^{WT} and PKM2^{KO} NK cells 4 days post MCMV infection

Previous data in this chapter assessed the direct effect of MCMV on NK cells. Next it was investigated whether there were any differences in the systemic inflammatory response to MCMV between the two genotypes. This was evaluated based on the level of four serum cytokines. The cytokines that were evaluated were IFNγ, TNF, IL-6, and IL-10. Serum was obtained through cardiac puncture 4 days post MCMV infection (1 x 10^5 PFU).

There was a significant elevation of some serum cytokines in response to MCMV infection (IFNγ and TNF) (**Fig. 3.16 A, C)**, and non-significant but trending increases in IL-10 and IL-6 (**Fig. 3.16 B, D)** production relative to saline controls. However, when the levels of serum cytokines were compared between PKM2^{WT} and PKM2^{KO} NK mice, there were no significant differences (**Fig. 3.16 A – D)**.

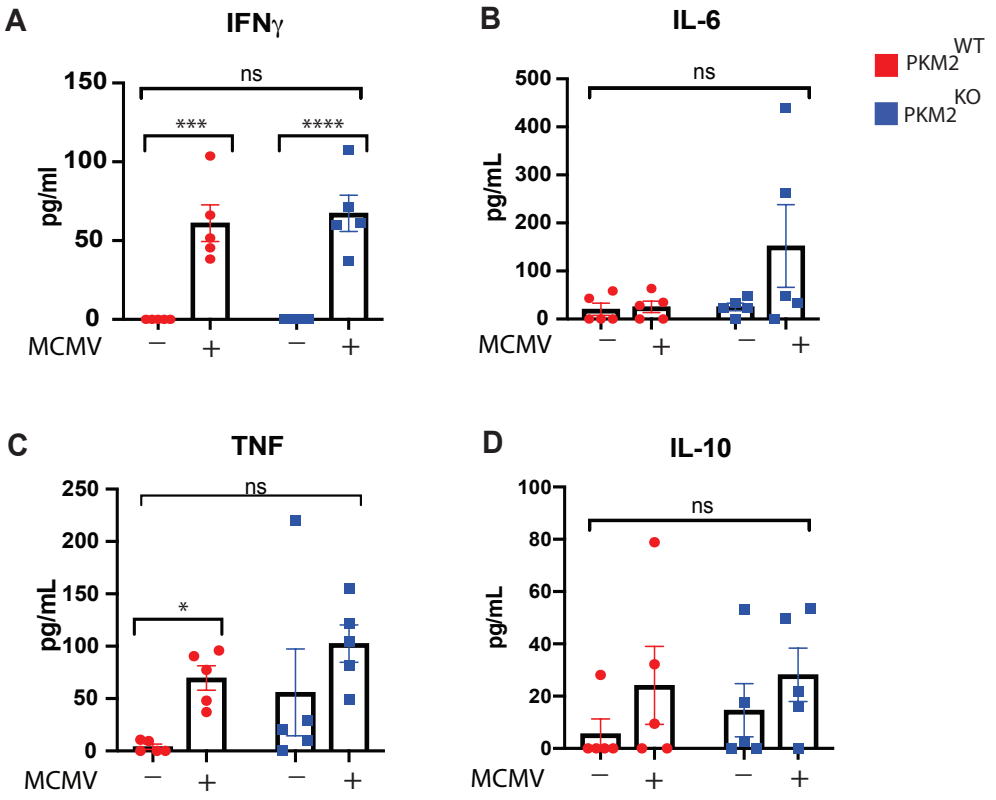

Figure 3. 16. There is no significant difference in serum cytokine levels (IFN, TNF, IL-10 and IL-6) between mice with PKM2^{WT} or PKM2^{KO} NK cells infected with MCMV

Ncr1$^{Cre/+}$ (PKM2^{WT}) ^{or} *Ncr1*$^{Cre/+}$*Pkm2*$^{fl/fl}$ (PKM2^{KO}) mice were administered saline (-) or 1 x 10^5 PFU of salivary passaged MCMV (+). 4 days later mice were injected with 2mg of BrDU i.p. Mice were then sacrificed 4 hours later and spleens were harvested. Serum was also isolated via cardiac puncture. Serum cytokines were then analysed using BD cytometric bead array technology (A) serum concentration (pg/mL) of IFNγ from mice with PKM2 ^{WT} and PKM2 ^{KO} NK cells in response to 4 day MCMV infection (+) or saline control (-). (B) serum concentration (pg/mL) of IL-6 from mice with PKM2 ^{WT} and PKM2 ^{KO} NK cells in response to 4 day MCMV infection (+) or saline control (-). (C) serum concentration pg/mL) of TNF from mice with PKM2 ^{WT} and PKM2 ^{KO} NK cells in response to 4 day MCMV infection (+) or saline control (-) (D) serum concentration (pg/mL) of IL-10 from mice with PKM2 ^{WT} and PKM2 ^{KO} NK cells in response to 4 day MCMV infection (+) or saline control (-) Data are n=5 animals per group. Each data point represents one individual animal. Data are representative of two individual experiments. Data were analysed using two-way ANOVA.*p< 0.05 ***p<0.001 ****p<0.0001 ns: non-significant

3.14. Relative splenic viral load of MCMV was comparable between mice with PKM2^{WT} or PKM2^{KO} NK cells

It was next investigated whether there was any difference in the viral load between the two genotypes. The presence of MCMV DNA was confirmed in the spleen 4 days post-infection using qPCR with a primer specific for the MCMV-IE region that has previously been published [143]. The data confirm that the spleen was infected with MCMV as there was a significant increase in viral burden relative to saline controls (**Fig. 3.17)**. However, when the relative viral load was compared between the two genotypes, there was no difference. This is consistent with the observation that the NK cells from these mice respond comparably at 4 days post infection.

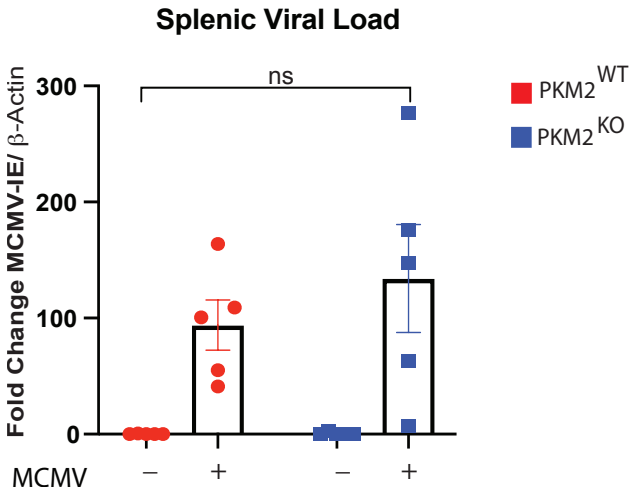

Figure 3. 17. There is no difference in the relative viral load of mice with PKM2 ^{WT} and PKM2 ^{KO} NK cells 4 days post MCMV infection

Ncr1$^{Cre/+}$ (PKM2^{WT}) ^{or} *Ncr1*$^{Cre/+}$*Pkm2*$^{fl/fl}$ (PKM2^{KO}) mice were administered saline (-) of 1 x 10^5 PFU of salivary passaged MCMV (+). 4 days later mice were injected with 2mg of BrDU i.p. Mice were then sacrificed 4 hours later and spleens were harvested. A small section of splenic tissue was reserved for DNA extraction for qPCR analysis. DNA was isolated and normalized to 100ng/qPCR sample. qPCR was then conducted with an MCMV-IE specific primer. Data was analysed via the ΔΔCt method and normalized to corresponding ΔΔCt values for β-Actin. Data are n=5 animals per group. Each data point represents one individual animal. Data are representative of two individual experiments. Data were analysed using two-way ANOVA. (ns: non-significant)

Discussion

The data here have extensively characterised the effect of PKM2 deletion in NK cells *in vivo.* These data are important as there are numerous publications showing that inhibition of NK cell glycolysis is detrimental to function *in vitro*, but limited studies on NK cell glycolysis *in vivo* [52, 103, 104]. Indeed, one such *in vivo* study from Megan Cooper's lab has detailed the requirement for NK cell glycolysis to respond to MCMV using pharmacological inhibitors. Therefore, it was hypothesised that deletion of a glycolytic enzyme, *Pkm2,* would be detrimental to NK cell functional responses *in vivo*. However, this was not the case in our experiments.

The simplest explanation for this could be that PKM2 is not required for NK cell function. However, there are numerous reasons why this is unlikely. Firstly, the data presented in this chapter show that PKM2 is significantly induced in NK cells in response to Poly(I:C) treatment *in vivo.* This is indicative that it is required by activated NK cells. Secondly, PKM2 has been shown to be a crucial regulator of glycolysis and function in other immune cells such as T cells [121]. Although, metabolism of T cells and NK cells is not directly correlated, there are likely to be similarities as they are both lymphocytes. However, the fact remains that we observed no impairment of NK cell function with *in vivo* activation. Therefore, it is necessary to consider other explanations both biological and technical, for the lack of phenotype with PKM2 deletion in NK cells.

Pharmacological inhibitors and genetic knock outs can have two very different outcomes due to genetic compensation, a phenomenon whereby loss a particular gene can be functionally compensated by an expression of a different gene [144]. Indeed, there are numerous examples of this occurring. For example, knock outs for HDAC1

show considerable upregulation of HDAC2 [145]. A similar phenomenon might in part explain the lack of phenotype observed with PKM2 deletion of NK cell *in vivo* function. Genetic compensation may be mediated by the alternate *Pkm* isoform, *Pkm1*. This possibility will be further investigated in chapter 4.

The data in this chapter showed that *Pkm2* was efficiently deleted using an *Ncr1*^{Cre} system. This Cre system requires activation of the *Ncr1* promoter which will happen anytime the NKp46 protein is expressed. This in itself is an experimental limitation as NKp46 is not expressed during early NK cell development in the bone marrow, and is only acquired during the "immature" NK cell stage [138]. Therefore, it is possible that PKM2 may be required early on in NK cell development, although this could not be tested using the *Ncr1*^{Cre} system. A possible solution to this would be to use a *Vav*^{Cre} system which would delete *Pkm2* earlier, but may also have negative effects on other developing lymphocytes.

The lack of phenotype in response to PKM2 deletion may also be explained by experimental caveats. This *in vivo* study used two methods of PKM2 activation, poly(I:C) and MCMV. With regards to the poly(I:C) based investigation, poly(I:C) is a viral analogue that is known to activate NK cells through MDA-5 and TLR3 [136]. During this study activation of NK cells by poly(I:C) was assessed by CD69, CD98 and IFNγ expression. However, poly(I:C) is not actually a virus and therefore there is no true effector output in this study i.e. it is not possible to assess viral clearance, and only NK cell activation markers/cytokine production can be assessed.

Indeed, this is the main reason why MCMV was chosen to activate NK cells *in vivo*. This is due to the fact that MCMV viral replication is mainly controlled by NK cells in MCMV infected C57Bl/6 mice through cytotoxicity. However, there was also no observable

phenotype in this model. A caveat in this is that these experiments were carried out during the early MCMV response at 4 days post infection. Early responses to MCMV are generally cytokine mediated, resulting from increased IL-12 and IL-18 and may not be representative of NK cell cytotoxicity [68]. Indeed, the fact that the virus was still readily detectable in the spleens of these mice indicates that the NK cells have not fully responded to this virus. Future studies should perhaps focus on the later responses of NK cells to MCMV *in vivo,* in particular on NK cell viral clearance at later timepoints.

We also assessed proliferation as glycolysis is one of the main pathways that fuels biomass production through the pentose phosphate pathway (required for nucleotide synthesis for DNA replication). Glycolysis is also required for the production of triglycerides through glycerol-3-phosphate synthesis. Similarly, glycolysis also generates serine from 3-phosphoglycerate. For this reason, it was hypothesised that genetic perturbation of glycolysis through PKM2 deletion would affect cellular proliferation. However, this did not appear to be the case, as $PKM2^{WT}$ and $PKM2^{KO}$ Ly49H positive cells incorporated the same amount of BrDU in response to poly(I:C) and MCMV.

A limitation of this *in vivo* study is that it was not possible to assess the level of glycolytic metabolites in these NK cells. This was due to limitations in the number of recoverable cells for mass spectrometry analysis. Therefore, in order to assess the metabolic phenotype of activated $PKM2^{WT}$ and $PKM2^{KO}$ NK cells, it was decided to employ an *in vitro* approach, which will be further described in chapter 4.

Chapter 4: PKM2 is not required NK cell transcriptional regulation

Introduction

Chapter 3 uncovered that PKM2 was not required for splenic NK cell responses to Poly(I:C) and MCMV *in vivo.* This result was surprising as NK cell glycolysis has previously been shown to be important in the control of MCMV *in vivo* by the Cooper lab [135]. Therefore, this chapter conducts precise analysis *in vitro* to uncover whether the glycolytic enzyme, PKM2, is required for metabolic and functional NK cell responses *in vitro*.

Murine splenic NK cells encounter a wide range of stimuli during an immune response. While they are important for the control of early transformations and viral infections, they also function in tandem with the adaptive immune system. One of the key adaptive cytokines produced by effector T cells is IL-2. NK cells readily respond to this through the high affinity IL-2 receptor CD25, which can be induced on NK cells by IL-12 or receptor ligation [52, 104]. IL-2 plus IL-12 stimulation has been previously shown to induce robust metabolic changes in NK cells, including the induction of elevated levels of glycolysis [52].

PKM2 is a key glycolytic enzyme and critically regulates glycolytic flux. It has been shown that PKM2 expression gives a growth advantage to cancer cells. This is because the inactive form is thought to slow the overall rate of glycolysis, and to siphon intermediates to other pathways, such as the pentose phosphate pathway, for biosynthesis (**Fig. 4**) [146]. Indeed, for this reason the inactive form of PKM2 is often associated with proliferating cells in tumours [147]. Using an *in vitro* culture stimulus of IL-2/12, this chapter will investigate whether PKM2 is important for regulating NK cell metabolism.

Aside from a direct metabolic role in glycolysis, previous studies by the O'Neill lab have also implicated PKM2 in controlling transcription of key glycolytic enzymes such as *Ldha* in macrophages [119]. Similarly, PKM2 has also been shown to function as a protein kinase, phosphorylating targets such as STAT3 [131]. Therefore, PKM2 can also function as a signalling molecule. Cells can possess both active tetrameric and inactive monomeric/dimeric PKM2 at once [119]. Therefore, it is important to consider that there are two arms of PKM2 function, a glycolytic regulator that controls biosynthesis, and a transcriptional regulator. This chapter will focus on discovering if PKM2 is also a key regulator of NK cell metabolism and transcription.

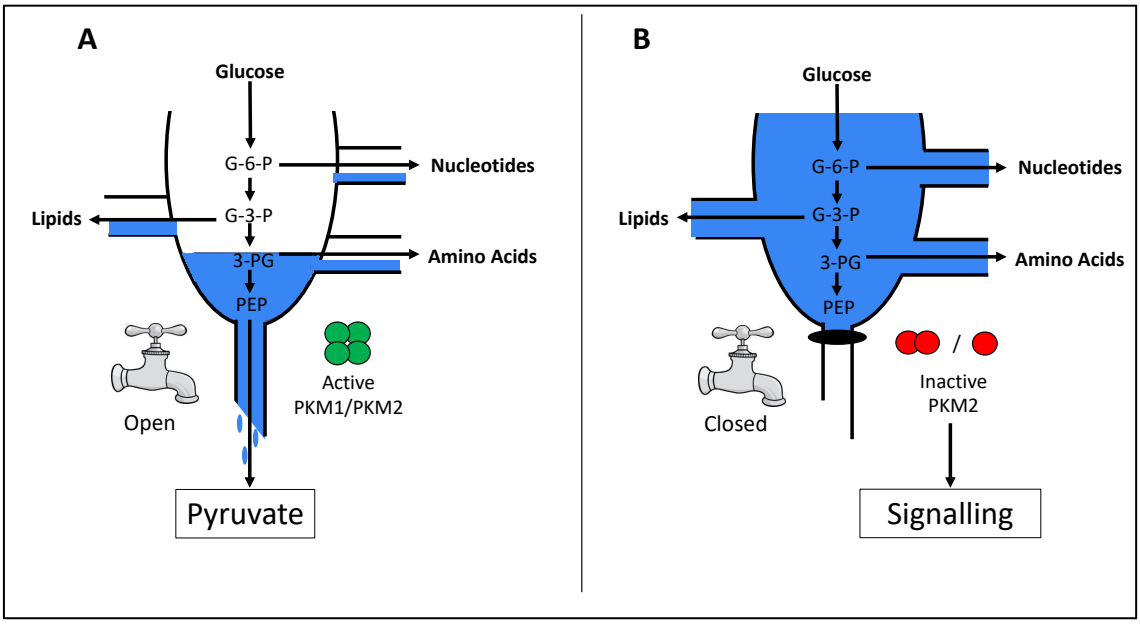

Figure 4. PKM2 regulates glycolytic flux, biosynthesis and has non-canonical functions A) PKM2 can exist as an active tetramer (similar to PKM1) which is highly active and efficient at generating pyruvate. This allows flow through glycolysis and does not allow for accumulation of upstream metabolites. (B) PKM2 can also exist as inactive monomers/dimers. These oligomers are relatively inactive and inefficient at producing pyruvate however they can produce pyruvate at high concentrations of PEP. Expression of these inactive oligomers allows for accumulation of upstream metabolites into pathways for the synthesis of nucleotides, lipids and amino acids, Inactive monomeric/dimeric PKM2 can also function as a signalling molecule. Both conformations can be present simultaneously in cells.

4.1 *Pkm2* expression is increased in IL-2/12 stimulated NK cells *in vitro*

Previously, the Finlay/Gardiner labs have used 6 day IL-15 cultured splenic NK cells for detailed metabolic and functional analysis *in vitro*. This allows for NK cell expansion and priming without overt NK cell activation [52]. IL-15 is a cytokine required for dendritic cell-mediated NK cell priming *in vivo* [57, 148, 149]. Splenocytes were cultured in low dose IL-15 (15ng/mL) for 6 days (hereafter termed "cultured NK cells"), purified using magnetic bead separation and stimulated for up to 48 hours with IL-2 and IL-12. Over the course of 48 hours there was a time dependent increase in both PKM2 protein and *Pkm2* mRNA expression **(Fig 4.1)**.

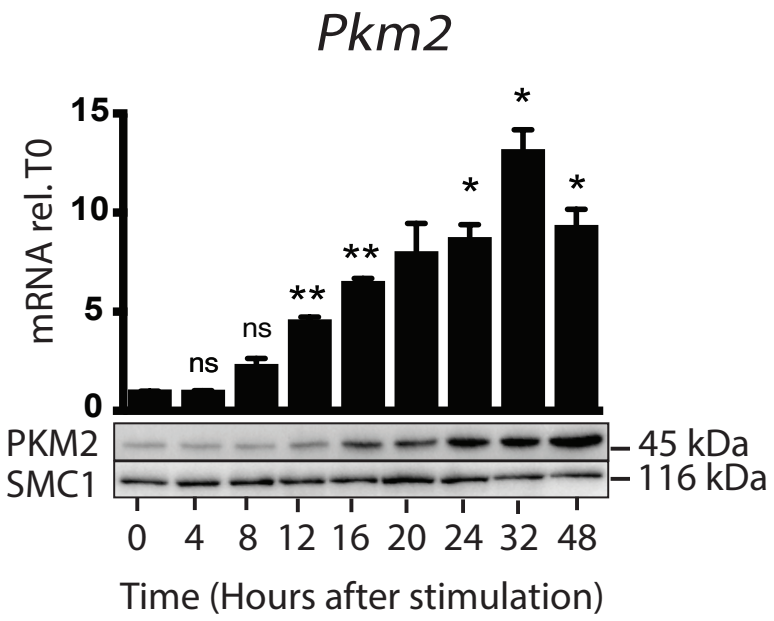

Figure 4. 1. IL-2/12 stimulation of splenic expanded NK cells induces Pkm2 mRNA and PKM2 protein

Splenocytes were expanded for 6 days in IL-15 (15ng/mL). On day 4 cultures were supplemented with IL-15. On day 6 NK cells were MACS purified and stimulated with IL-2 (330U/mL) and IL-12 (10ng/mL) for 48 hours. Cells were then lysed for RNA and protein (A) RT-PCR pooled data of PKM2 expression in IL-2/12 stimulated cells at different timepoints normalized to *Rplp0.* (B) Representative western blot of IL-2/12 stimulated NK cells at different timepoints. SMC1 was used as a loading control. Western blot is representative of n=3 experiments. mRNA is pooled data of three individual experiments *p< 0.05 **p < 0.01 (one-way ANOVA).

4.2 PKM2 expression is dependent on metabolic regulators mTORC1 and c-Myc

Previous data from the Finlay/Gardiner lab has demonstrated that the IL-2/12 stimulation of murine NK cells cause profound increases in glycolysis after 18 hours relative to unstimulated cells. They showed that this glycolytic switch is dependent on both the key metabolic regulator mTORC1 and c-Myc through transcriptional and translational control of key glycolytic machinery [52, 109].

As PKM2 is a glycolytic enzyme, it was investigated whether IL-2/12 induction of *Pkm2* mRNA and PKM2 protein was also dependent on mTORC1 activation. To test this hypothesis, the specific mTORC1 inhibitor rapamycin was used. Murine NK cells were activated with IL-2/12 for 18 hours, in the presence or absence of rapamycin and PKM2 expression was evaluated by both qPCR and western blot. Efficacy of rapamycin was initially confirmed by the decrease in phosphorylated S6 ribosomal protein, a downstream target of mTORC1 **(Fig. 4.2 B)**. In the presence of rapamycin, IL-2/12-induced PKM2 mRNA and protein expression was significantly blunted (**Fig. 4.2 A B)** . This indicated that mTORC1 activation is required for normal PKM2 expression.

The Finlay lab also published that the transcription factor c-Myc plays an important role in the regulation of murine NK cell metabolism. Therefore, it was investigated whether this transcription factor is also required for the expression of PKM2 using NK cells lacking c-Myc. This work was done in collaboration with Roisin Loftus a former Ph.D student in the lab. Experimentally, this was achieved using NK cells from a tamoxifen^{Cre} x cMyc$^{fl/fl}$ mouse. Murine splenocytes were treated for 4 days with tamoxifen and low dose IL-15 and tamoxifen then purified and stimulated with IL-2/12 to induce excision of the cMyc gene. Lysates were then analysed by western blotting. Cultured, IL-2/12 activated NK

cells from these mice showed reduced PKM2 protein expression, indicating that c-Myc is required for normal PKM2 expression **(Fig. 4.2 C).**

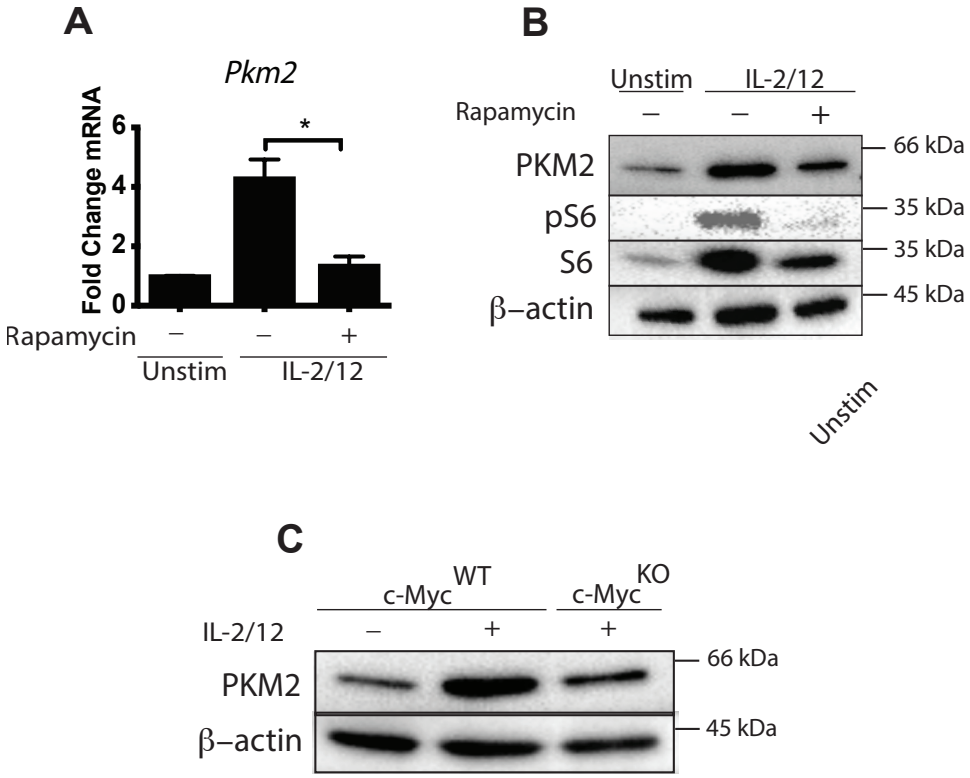

Figure 4.2. PKM2 mRNA and protein expression are dependent on the serine/threonine kinase mTORC1

Splenocytes were expanded for 6 days in IL-15 and were MACS purified and stimulated with IL-2 (20ng/mL) and IL-12 (10ng/mL) for 18 hours +/- rapamycin. (A) RT-PCR pooled data of PKM2 expression in IL-2/12 stimulated cells +/- rapamycin normalized to RPLP0. (B) Representative western blot of PKM2 expression in IL-2/12 stimulated NK cells +/- rapamycin at 18 hours post- stimulation. Western blot is representative of n=3 experiments (C) NK cells were expanded for 3 days in IL-15 (10ng/mL) and 4-hydroxytamoxifen (0.6 μM) and then activated with IL-2/12 (330U/10ng per mL) or left unstimulated (IL-15 5ng/mL). After 18 hours, cells were lysed at 10 x 10^6 per mL and analysed by western blot. Myc deletion blot is representative of 2 experiments. mRNA is pooled data of three individual experiments *p< 0.05 **p < 0.01 (one-way ANOVA).

4.3. PKM2^{WT} and PKM2^{KO} NK cells expand normally in IL-15 over 6 days

The impact of PKM2 deletion in splenic NK cells *in vivo* was previously assessed in chapter 3. However, it can be technically difficult to assess NK cell metabolic changes *in vivo.* Therefore, we next moved to an *in vitro* system. PKM2^{WT} and PKM2^{KO} NK cells were expanded using low dose IL-15 for 6 days. This generated the NK cell numbers necessary to conduct metabolic assays.

This culture system induces proliferation of NK cells over the course of 6 days. As PKM2 has been previously implicated as a regulator of proliferation in cancer [150], it was next confirmed that there was no proliferative/expansion defect in NK cells from the *Ncr1$^{cre/+}$ Pkm$^{fl/fl}$* (*Pkm2^{KO}*) mice. As demonstrated in figure 4.3 (A), the yield of PKM2^{KO} NK cells obtained after 6 days in culture was comparable to that of the PKM2^{WT} NK cells. Indeed, after magnetic purification, roughly the same number of NK1.1^{+}NKp46^{+} cells were obtained.

It was also confirmed that PKM2 was also deleted in these cultured cells. When RNA sequencing was performed on purified cultured NK cells, *Pkm* was one of the most differentially expressed genes between the two genotypes. When the levels of transcript for *Pkm2* were assessed, it was confirmed that PKM2 was indeed deleted from cultured PKM2^{KO} NK cells. (**Fig. 4.3 B)**.

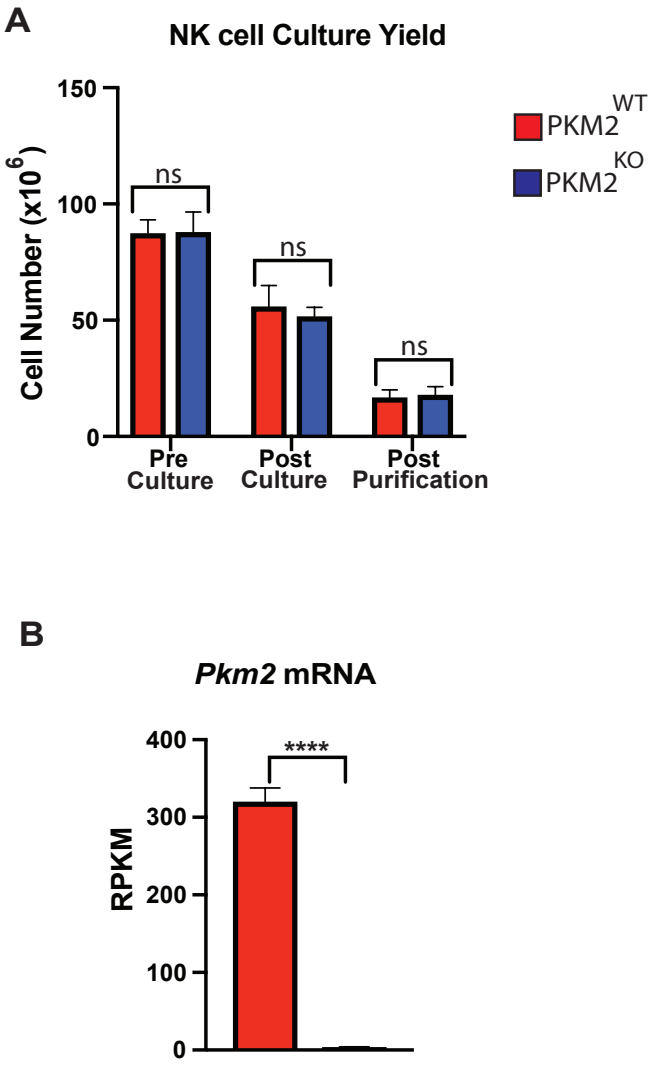

Figure 4.3. PKM2^{KO} NK cells expand normally in IL-15 culture and efficiently delete PKM2

Splenocytes were isolated and NK cells were identified by flow cytometry as being NK1.1^{+}NKp46^{+}CD3^{-}. NK cell numbers were then determined using frequency, and total splenocyte numbers**.** Splenocytes were then expanded for 6 days in IL-15 (15ng/mL). On day 4 cultures were further supplemented with IL-15 (15ng/mL). After 6 days NK cell frequency was determined by flow cytometry and total NK cell numbers were calculated. On day 6 splenocytes were MACS purified analysed again by flow cytometry. (A) NK cell yield from IL-15 expanded splenocytes after 6 days in IL-15 (15ng/mL) for both PKM2^{WT} or PKM2^{KO} NK cells. Data are from 5 independent experiments (B) Splenocytes from PKM2^{WT} and PKM2^{KO} NK cells were expanded for 6 days in IL-15. NK cells were then MACS purified and RNA isolated. RNA was sequenced using HiSeq. The expression of PKM2 is displayed as RPKM (reads per kilo base of transcript per million mapped reads. Data are from 3 independent experiments. ns- non-significant, *p< 0.05 **p < 0.01 ****p<0.0001 ((A) two-way ANOVA with Sidak's post-test (B) student t test).

4.4. IL-2/12-activated cultured PKM2^{KO} NK cells show efficient *Pkm2* deletion

The Cre recombinase system generally results in deletion of genetic sequences contained within two floxed sequences. It was verified in chapter 3 that this Cre system was capable of deleting the *Pkm2* gene. Next, it was also confirmed that this was true on an mRNA and protein level. *Ncr1*^{Cre} (PKM2^{WT}) or *Ncr1*^{Cre}*Pkm2*$^{fl/fl}$ (PKM2^{KO}) NK cells were activated with IL-2/12 or left unstimulated (5ng/mL of IL-15) for 18 hours and mRNA and protein were isolated. As measured by real-time PCR and western blot, *Pkm2* was efficiently deleted in cultured *Pkm2*^{KO} NK cells (**Fig. 4.4 A B).**

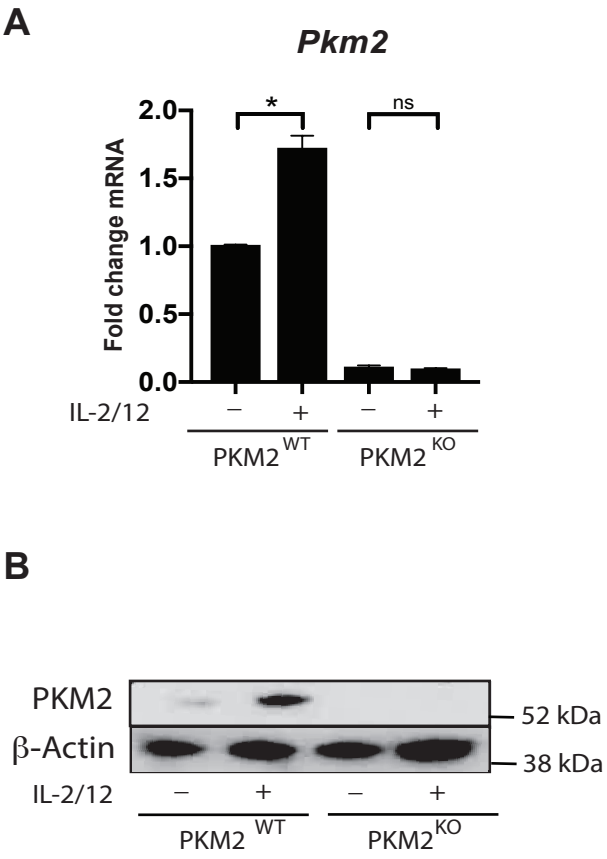

Figure 4.4. Cultured, IL-2/12 activated PKM2^{KO} NK cells do not express *Pkm2* mRNA/protein

Splenocytes from Ncr1$^{cre/+}$ (PKM2^{WT}) or *Ncr1*$^{Cre/+}$*Pkm2*$^{fl/fl}$ (PKM2^{KO}) mice were expanded for 6 days in IL-15 (15ng/mL).On day 4 cultures were further supplemented with IL-15 (15ng/mL). On day 6 splenocytes were MACS purified and seeded at 2 x 10^6 NK cells per mL. NK cells were treated with either low dose IL-15 (5 ng/mL) or IL-2/12 (330U/10ng per mL) for 18 hours. (A) mRNA was isolated and cDNA generated using reverse transcription. RT-qPCR analysis of the expression *Pkm2* was carried out and normalised to the control gene HPRT. (B) cells were lysed at 10 x 10^6 per mL and analysed by western blot PKM2 expression. Loading control was actin. Data are mean +/- S.E.M. Bar graphs are pooled data of 4 individual experiments. Western blot is representative of 3 individual experiments. Data were analysed by two-way ANOVA with a Sidak post-test (ns: non-significant, *p<0.05, ** p<0.01)

4.5. Normal IFNγ and Granzyme production in IL-2/12 stimulated PKM2^{KO} NK cells

The Finlay/Gardiner labs have previously published that murine NK cells stimulated with IL-2/12 rapidly increased their rates of glycolysis within 18 hours. This upregulation of glycolysis was required to sustain normal IFNγ production by NK cells. Therefore, as PKM2 is a key glycolytic enzyme, it was investigated whether deletion of PKM2 would affect IL-2/12-induced IFNγ production.

After 20 hours of IL-2/12 stimulation, the percentage of IFNγ positive cells was comparable between both PKM2^{WT} and PKM2^{KO} cells **(Fig. 4.5)**. This indicates that PKM2 is not required for IL-2/12 induced iFNγ production cultured NK cells.

Similarly, the Finlay/Gardiner labs also observed that expression of the key cytotoxic molecule granzyme B was dependent on fuelling of NK cell glycolysis. Seeing as pyruvate kinase is poised to regulate glycolysis, it was also investigated whether expression of granzyme B was altered in PKM2 null cells. Cultured, IL-2/12 activated NK cells were stained for granzyme B and analysed by flow cytometry. IL-2/12 stimulation normally induces an upregulation of granzyme B protein relative to unstimulated cells. Indeed, the induction of granzyme B protein was comparable between both PKM2 WT and PKM2 KO cells indicating that the enzyme PKM2 is not required for normal IL-2/12 induced granzyme B expression (**Fig. 4.6)** .

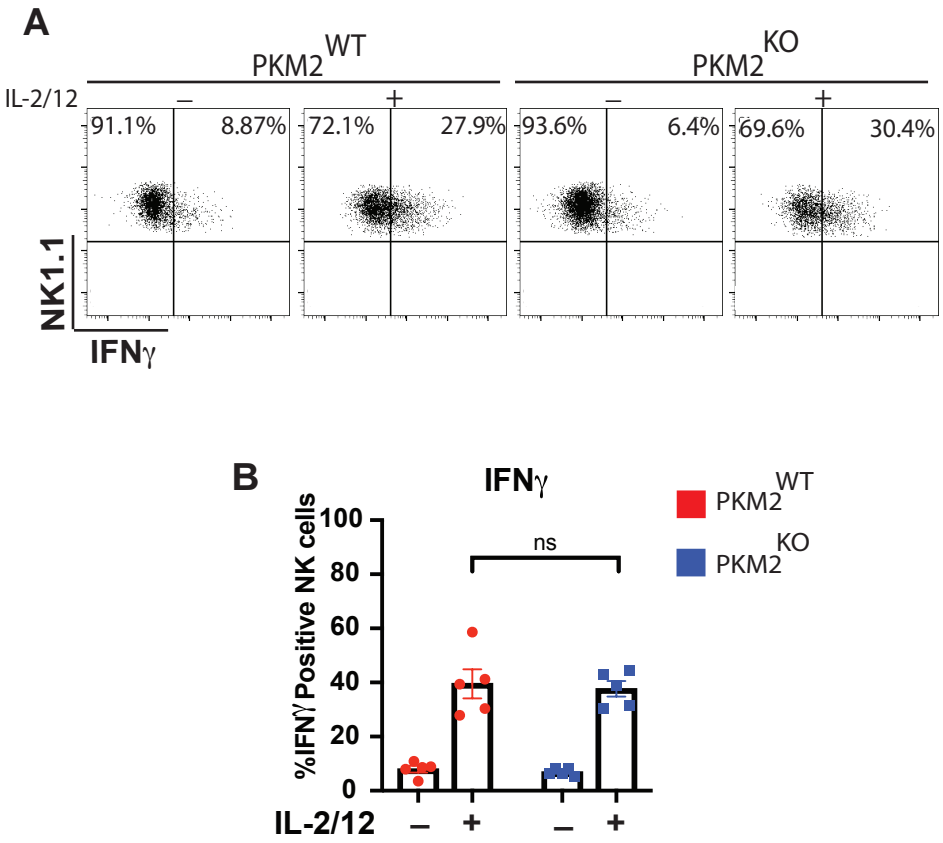

Figure 4. 5. IL-2/12 activated PKM2^{KO} NK cells have a normal IFNγ positive frequency

Splenocytes from Ncr1$^{cre/+}$ (PKM2^{WT}) or *Ncr1*$^{Cre/+}$*Pkm2*$^{fl/fl}$ (PKM2^{KO}) mice were expanded for 6 days in IL-15 (15ng/mL). On day 4 cultures were further supplemented with IL-15 (15ng/mL). On day 6 splenocytes were MACS purified and seeded at 2 x 10^6 NK cells per mL. NK cells were treated with either low dose IL-15 (5 ng/mL) or IL-2/12 (330U/10ng per mL) for 16 hours. After 16 hours, cells were treated with BD GolgiPlug (Brefeldin A). 4 hours later cells, were stained extracellularly and gated on NK1.1$^+$NKp46$^+$CD3$^-$. Cells were then fixed in BD Cytofix/Cytoperm and stained intracellularly for IFNγ. Cells were run on a BD LSR II or BD Fortessa and assessed for expression of IFNγ. Data are mean +/- S.E.M. (A) Representative dot plot of IFNγ positive cells. B) Pooled data of IFNγ expression for 5 individual experiments. Data were analysed by two-way ANOVA with a Sidak post-test (ns: non-significant)

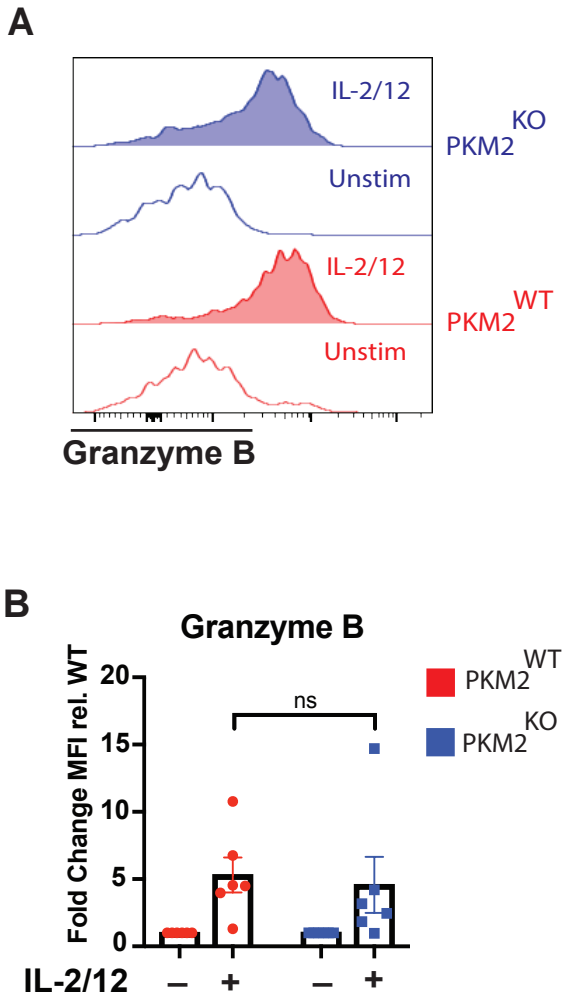

Figure 4. 6. IL-2/12 activated PKM2^{KO} NK cells express normal levels of granzyme B

Splenocytes from Ncr1$^{cre/+}$ (PKM2^{WT}) or *Ncr1*$^{Cre/+}$*Pkm2*$^{fl/fl}$ (PKM2^{KO}) mice were expanded for 6 days in IL-15 (15ng/mL). On day 4, cultures were supplemented with IL-15 (15ng/mL). On day 6 splenocytes were MACS purified and seeded at 2 x 10^6 NK cells per mL. NK cells were treated with either low dose IL-15 (5 ng/mL) or IL-2/12 (330U/10ng per mL) for 16 hours. After 16 hours, cells were treated with BD GolgiPlug (Brefeldin A). 4 hours later cells, were stained extracellularly and gated on NK1.1$^+$NKp46$^+$CD3$^-$. Cells were then fixed in BD Cytofix/Cytoperm and stained intracellularly for granzyme b. Cells were run on a BD LSR II or BD Fortessa and assessed for expression of granzyme b. Data are mean +/- S.E.M. A) Representative histogram of granzyme b expression. B) Pooled data of granzyme expression for 5 individual experiments. Data were analysed by two-way ANOVA with a Sidak post-test (ns: non-significant)

4.6. Secreted cytokine production is not significantly affected by PKM2 deletion in NK cells

Although there was no difference in IFNγ or granzyme B production as measured by intracellular flow cytometry staining, it was possible that there could be an effect on the secretion of other pro-inflammatory cytokines. This is specifically pertinent, as in macrophages, loss of PKM2 resulted in decreased production of IL-1β production and increased IL-10 secretion [119]. Therefore, in order to assess whether this might be relevant in NK cells, cytometric bead array technology was used. This is a flow cytometry based assay that allow for precise measurements of certain secreted factors relative to a standard curve. This facilitates the measurement of cytokine secretion over the course of 18 hour IL-2/12 stimulation.

Using a panel of markers, the production of TNF, IFNγ, IL-10, MIP1α, and MIP1β was measured . All of these cytokines appeared to be induced with IL-2/12 stimulation of $PKM2^{WT}$ NK cells. The levels of these cytokines also appeared to be normal and comparable in $PKM2^{KO}$ NK cells **(Fig. 4.7)**. This indicates that PKM2 is not required for expression of certain pro-inflammatory cytokines and chemokines in response to IL-2/12 stimulation.

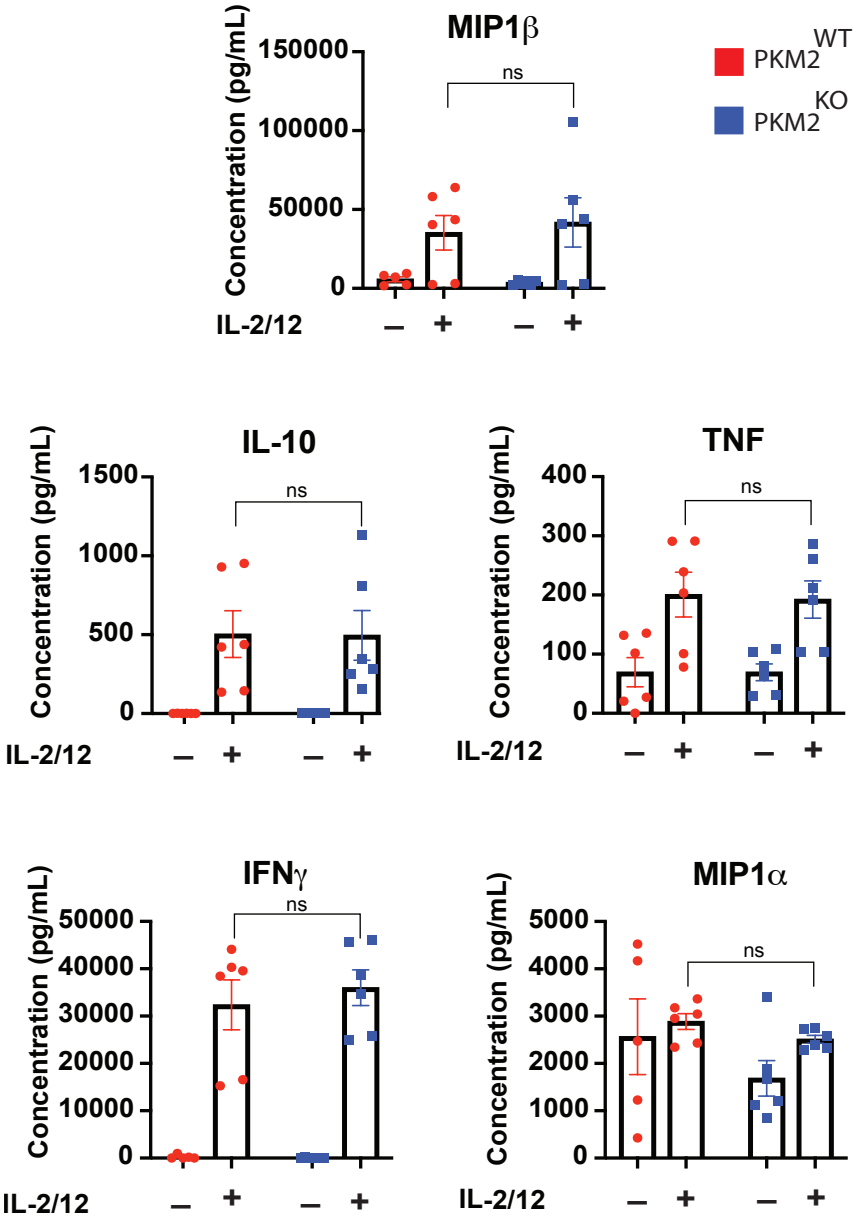

Figure 4. 7. IL-2/12 activated PKM2^{KO} NK cells secrete normal levels of select cytokines

Splenocytes from Ncr1$^{cre/+}$ (PKM2^{WT}) or *Ncr1*$^{Cre/+}$*Pkm2*$^{fl/fl}$ (PKM2^{KO}) mice were expanded for 6 days in IL-15 (15ng/mL). On day 4, cultures were further supplemented with IL-15 (15ng/mL). On day 6 splenocytes were MACS purified and seeded at 2 x 10^6 NK cells per mL. NK cells were treated with either low dose IL-15 (5 ng/mL) or IL-2/12 (330U/10ng per mL) for 18 hours. After 18 hours, cells were centrifuged and supernatants taken and frozen. Supernatants were later stained using BD cytokine bead array technology . Samples were run on a BD LSR II or BD Fortessa and assessed for cytokine levels relative to internal standards. Graphs are pooled data of 6 biological replicates. Data are mean +/- S.E.M Data were analysed by two-way ANOVA with a Sidak post-test (ns: non-significant)

4.7. PKM2 is not required for IL-2/12-induced glycolysis and OxPhos

Pyruvate kinase is a key enzyme required in the regulation of glycolytic flux. In macrophages, PKM2 is required for the upregulation of key glycolytic genes [119]. Therefore, it was next assessed whether PKM2 was required for the upregulation of glycolysis that is associated with IL-2/12 activation of cultured NK cells. NK cell glycolysis was assessed using seahorse extracellular flux analysis.

Cultured NK cells were activated for 18 hours with IL-2/12 (or left unstimulated) and then transferred to a seahorse plate supplemented with replete cell culture medium complete with low dose IL-15 (unstimulated) or IL-2/12. As demonstrated by figure 4.8, there was no significant difference in the extracellular acidification rate of $PKM2^{WT}$ or $PKM2^{KO}$ NK cells. This indicated that PKM2 was not required for NK cell glycolysis or to sustain cellular lactate production after 18 hours of IL-2/12 stimulation (**Fig. 4.8)** .

Next, it was investigated whether PKM2 deletion would affect the rate of OxPhos within IL-2/12 activated NK cells. Interestingly, after 18 hours of IL-2/12 stimulation there was no significant effect on NK cell basal oxidative phosphorylation in $PKM2^{KO}$ NK cells. The rate of maximum respiration can also be measured using seahorse by subtracting the rate of oxygen consumption after antimycin A/rotenone treatment, from the maximum rate after treatment with uncoupler FCCP. When the rate of maximum respiration was assessed, there appeared to be no defect in $PKM2^{KO}$ NK cells relative to $PKM2^{WT}$ controls. (**Fig. 4.9)**.

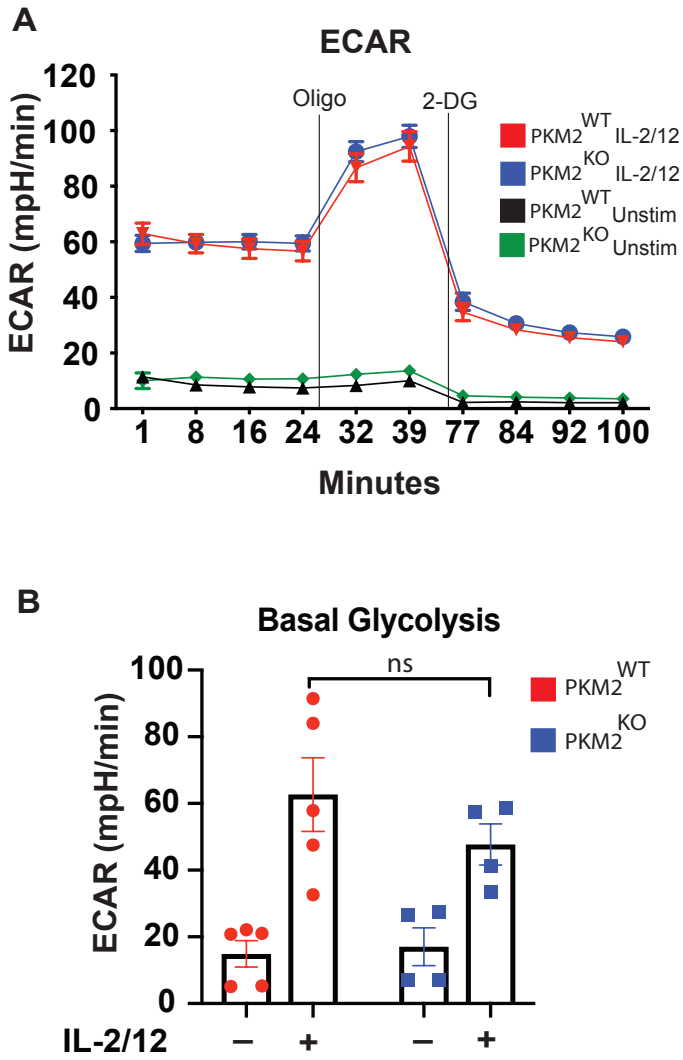

Figure 4. 8. IL-2/12 activated PKM2^{KO} NK cells have a normal extracellular acidification rate

Splenocytes from Ncr1$^{cre/+}$ or *Ncr1*$^{Cre/+}$*Pkm2*$^{fl/fl}$ mice were expanded for 6 days in IL-15 (15ng/mL). On day 4 cultures were further supplemented with IL-15 (15ng/mL). On day 6 splenocytes were MACS purified and seeded at 2 x 10^6 NK cells per mL. NK cells were treated with either low dose IL-15 (5 ng/mL) or IL-2/12 (330U/10ng per mL) for 18 hours. After 18 hours, cells were changed into replete seahorse media plus cytokines at a concentration of 200,000 cells per well. Cells were analysed on a Seahorse 96e extracellular flux analyser. (A) Representative seahorse plot of extracellular acidification rate (B) Pooled data of 5 individual experiments for PKM2 ^{WT} and 4 experiments for PKM2 ^{KO} NK cells. Data are mean +/- S.E.M. Data were analysed by two-way ANOVA with a Sidak post-test (ns: non-significant)

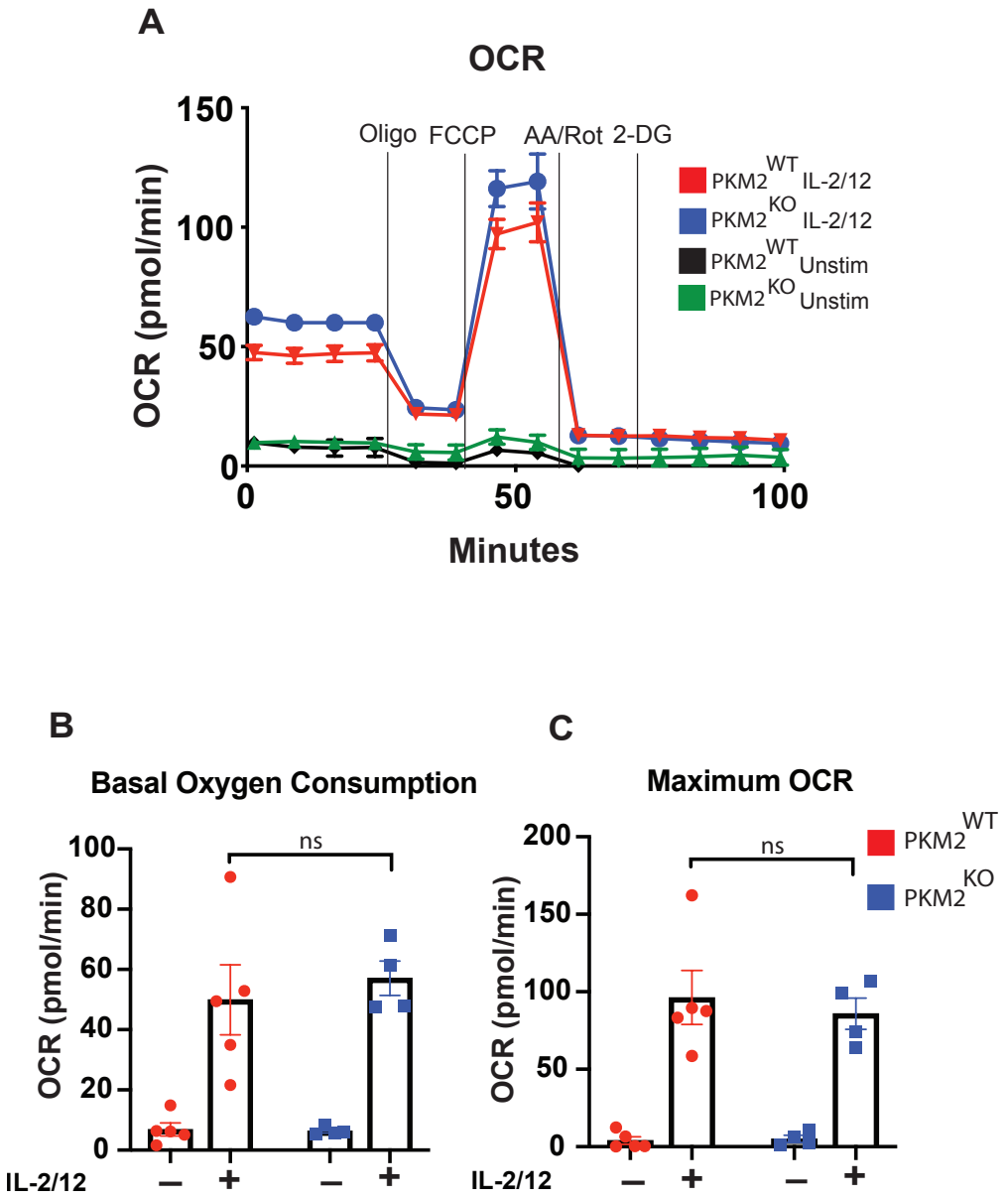

Figure 4. 9. IL-2/12 activated PKM2^{KO} NK cells have a normal oxygen consumption rate

Splenocytes from *Ncr1*$^{cre/+}$ (PKM2^{WT}) or *Ncr1*$^{Cre/+}$*Pkm2*$^{fl/fl}$ (PKM2^{KO}) mice were expanded for 6 days in IL-15 (15ng/mL). On day 4 cultures were further supplemented with IL-15 (15ng/mL). On day 6 splenocytes were MACS purified and seeded at 2 x 10^6 NK cells per mL. NK cells were treated with either low dose IL-15 (5 ng/mL) or IL-2/12 (330U/10ng per mL) for 18 hours. After 18 hours, cells were changed into replete seahorse media plus cytokines at a concentration of 200,000 cells per well. Cells were analysed on a Seahorse 96e extracellular flux analyser. (A) Representative seahorse plot of extracellular acidification rate (B) Pooled data of 5 individual experiments for PKM2^{WT} and 4 experiments for PKM2^{KO}. Data are mean +/- S.E.M. Data were analysed by two-way ANOVA with a Sidak post-test (ns: non-significant)

4.8. Levels of glycolytic metabolites are comparable between PKM2^{WT} and PKM2^{KO} cultured NK cells

The data showed that there were no significant changes in glycolysis or OxPhos between PKM2^{WT} or PKM2^{KO} cultured NK cells that were activated with IL-2/12 for 18 hours. In order to validate this finding , metabolomics analysis was carried out. This would allow the relative measurement of glycolytic and TCA metabolites from both IL-2/12 stimulated PKM2^{WT} and PKM2^{KO} cultured NK cells. It would also provide more information than Seahorse, assessing metabolites such as amino acids and pentose phosphate intermediates. This work was carried out in collaboration with Dr. Erika Palmieri.

The glycolytic intermediates were first investigated. These included fructose-6-phosphate, glycerol-3-phosphate, glyceraldehyde-3-phosphate, 3-phosphoglycerate, phosphoenolpyruvate or pyruvate. Consistent with the Seahorse data for ECAR, there were no significant differences in the levels of these metabolites between PKM2^{WT} and PKM2^{KO} NK cells. This confirmed that PKM2 is not required for glycolysis in IL-2/12 stimulated cultured NK cells after 18 hours (**Fig. 4.10)**.

The levels of metabolites in the pentose phosphate pathway were also assessed. The pentose phosphate pathway is an important source of 5-carbon sugars for nucleotide synthesis, and it is primarily fuelled by glucose. The metabolites assessed were glucose-6phosphate, 6-phosphogluconate, sedoheptulose-7-phosphate, ribulose-5-phosphate, ribose-5-5phosphate and erythrose-5-phosphate. Interestingly the level of glucose-6-phosphate was lower in PKM2^{KO} NK cells than their PKM2^{WT} NK cells. However, when metabolites downstream from glucose-6-phosphate in the pentose phosphate pathway were analysed (such as 6-phosphogluconate), there were no significant differences. It is

possible that although the glucose-6-phosphate is lower, it is not low enough to affect the level of the other intermediates at this specific timepoint (**Fig. 4.11)**.

The levels of TCA metabolites were also measured. Similarly to glycolysis, there was no significant difference between genotype in the level of TCA metabolites. These included citrate/isocitrate, cis-aconitate, 2-oxoglutarate, succinate, fumarate and malate. This is in line with the data from Seahorse showing normal levels of OxPhos in IL-2/12 activated cultured $PKM2^{KO}$ NK cells (**Fig. 4.12)**.

The next metabolites assessed by metabolomics were amino acids, Interestingly, there were some differences between $PKM2^{WT}$ and $PKM2^{KO}$ NK cells in regards to amino acids. Specifically, the levels of arginine, glutamine and glutamate were all significantly increased in $PKM2^{KO}$ NK cells **(Fig. 4.13)**.

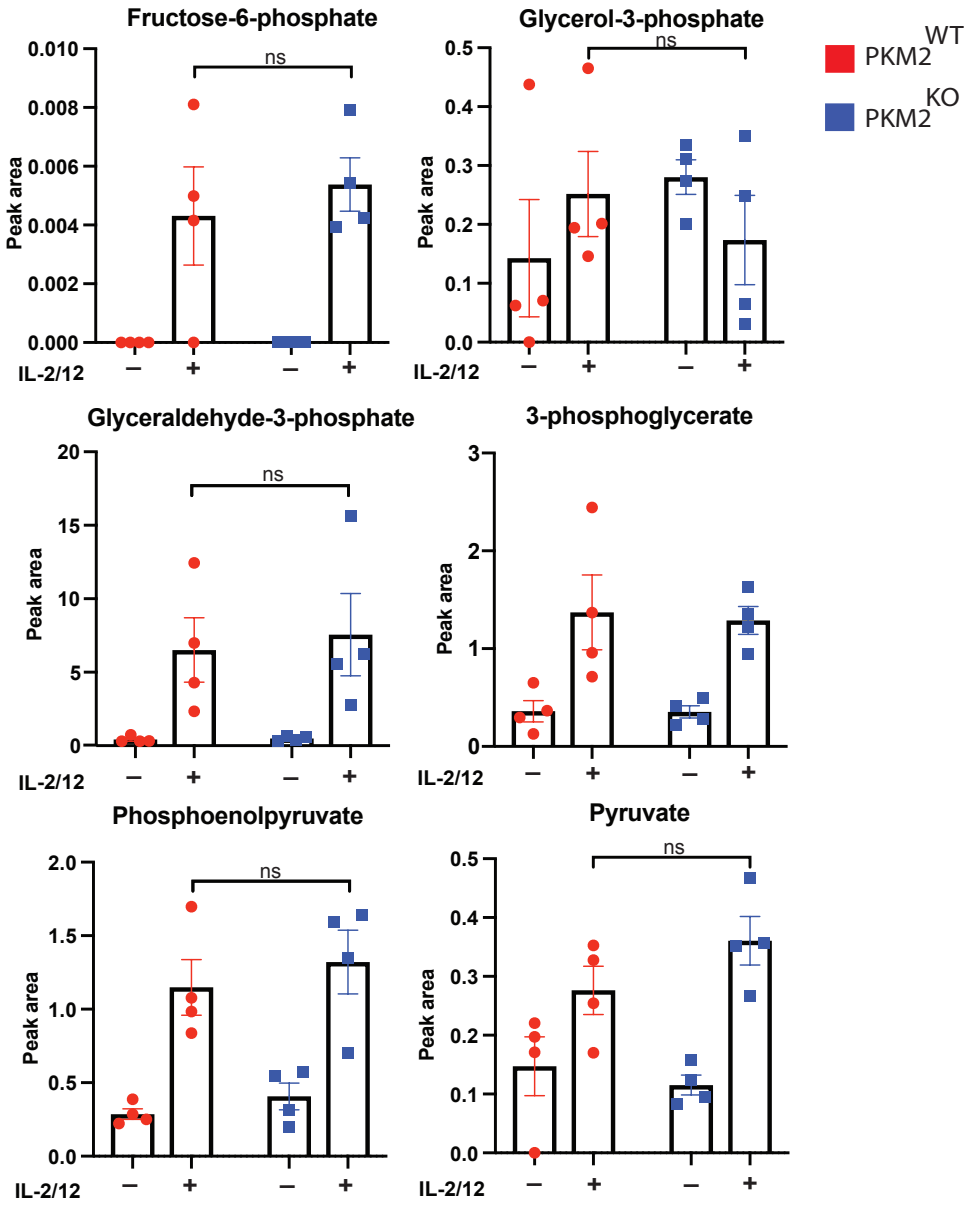

Figure 4. 10. Relative levels of glycolytic intermediates appear to be normal between PKM2^{WT} and PKM2^{KO} cultured NK cells

Splenocytes from Ncr1$^{cre/+}$ (PKM2^{WT}) or *Ncr1*$^{Cre/+}$*Pkm2*$^{fl/fl}$ (PKM2^{KO}) mice were expanded for 6 days in IL-15 (15ng/mL). On day 4 cultures were further supplemented with IL-15. On day 6 splenocytes were MACS purified and seeded at 2 x 10^6 NK cells per mL. NK cells were treated with either low dose IL-15 (5 ng/mL) or IL-2/12 (330U/10ng per mL) for 18 hours. After which cells were harvested, washed in NaCl buffer and metabolites were extracted using 90% methanol. Samples were dried using a RotEvap and then run on LC/MS. Data are displayed as peak area of each metabolite normalized to protein content. Graphs are pooled data of 4 individual experiment. Data are +/- S.E.M. Data were analysed by two-way ANOVA with Sidak's post-test (ns= non-significant).

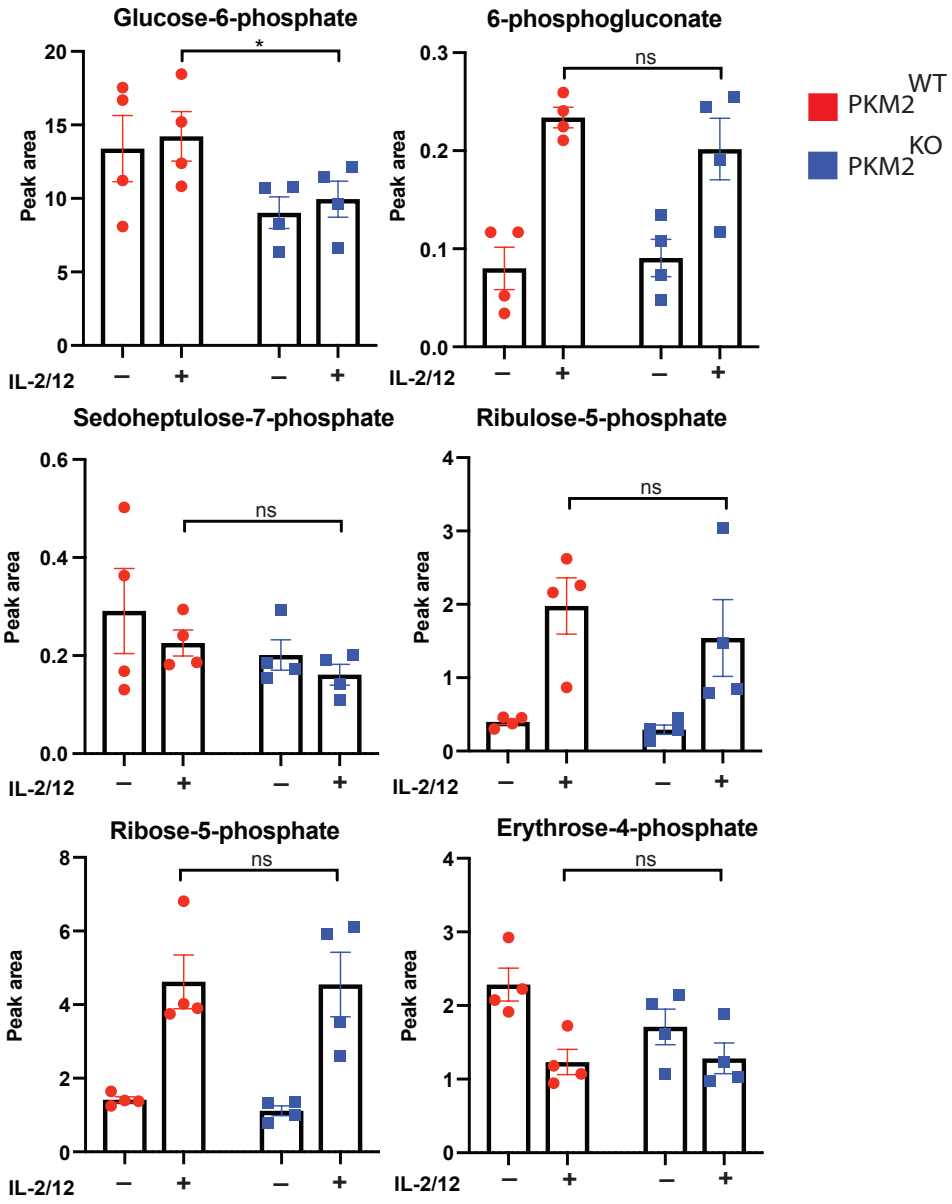

Figure 4. 11. Glucose-6-phosphate levels are lower in PKM2^{KO} cells relative to PKM2^{WT} cultured NK cells

Splenocytes from Ncr1$^{cre/+}$ (PKM2^{WT}) or *Ncr1*$^{Cre/+}$*Pkm2*$^{fl/fl}$ (PKM2^{KO}) mice were expanded for 6 days in IL-15 (15ng/mL). On day 4 cultures were further supplemented with IL-15. On day 6 splenocytes were MACS purified and seeded at 2 x 10^6 NK cells per mL. NK cells were treated with either low dose IL-15 (5 ng/mL) or IL-2/12 (330U/10ng per mL) for 18 hours. After which cells were harvested, washed in NaCl buffer and metabolites were extracted using 90% methanol. Samples were dried using a RotEvap and then run on LC/MS. Data are displayed as peak ae of each metabolite normalized to protein content. Graphs are pooled data of 4 individual experiment. Data are +/- S.E.M. Data were analysed by two-way ANOVA with Sidak's post-test (ns= non-significant).

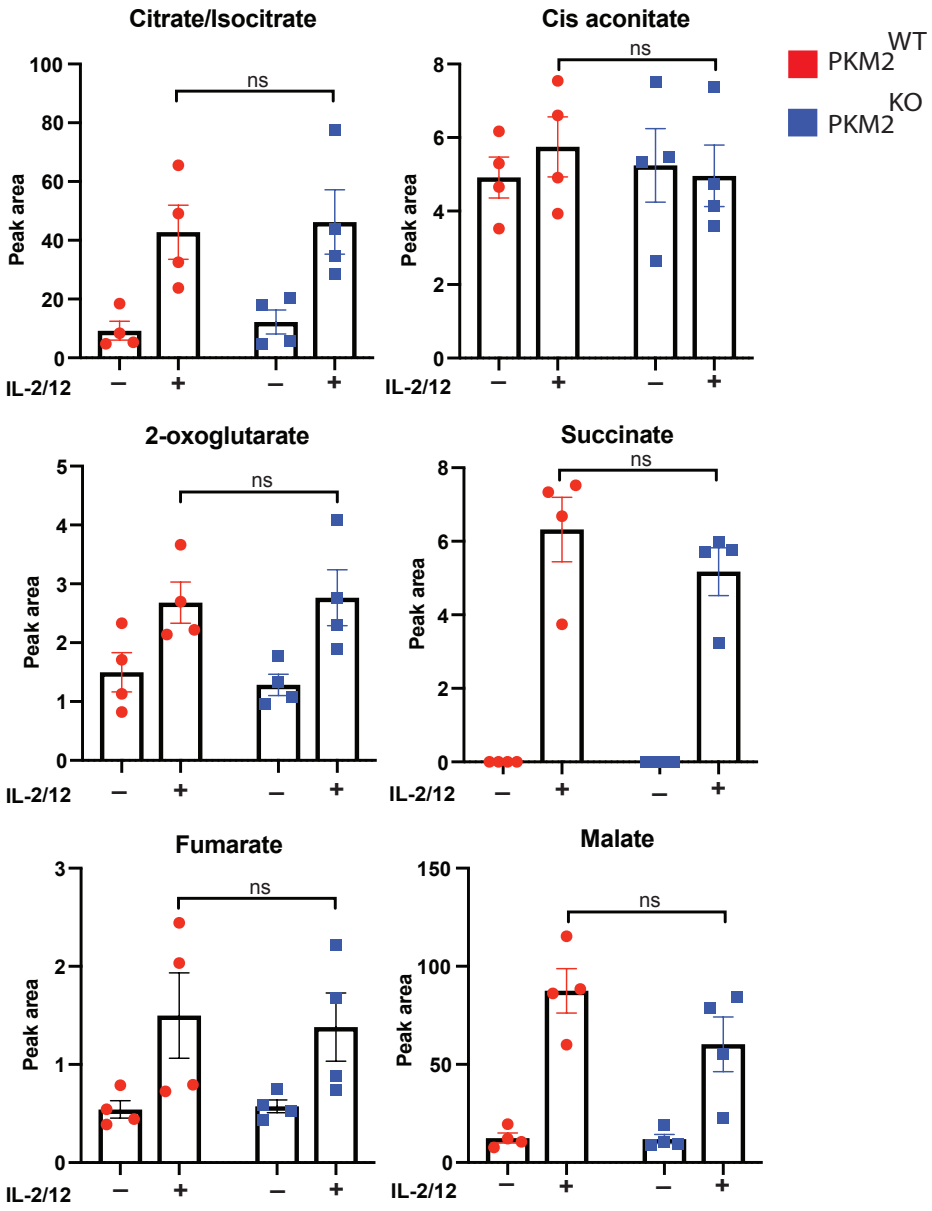

Figure 4.12. TCA intermediate levels are normal between PKM2^{WT} and PKM2^{KO} cultured NK cells

Splenocytes from Ncr1$^{cre/+}$ (PKM2^{WT}) or *Ncr1*$^{Cre/+}$*Pkm2*$^{fl/fl}$ (PKM2^{KO}) mice were expanded for 6 days in IL-15 (15ng/mL). On day 4 cultures were further supplemented with IL-15. On day 6 splenocytes were MACS purified and seeded at 2 x 10^6 NK cells per mL. NK cells were treated with either low does IL-15 (5ng/mL) or IL-2/12 (330U/10ng per mL) for 18 hours. After which cells were harvested, washed in NaCl buffer and metabolites were extracted using 90% methanol. Samples were dried using a RotEvap and then run on LC/MS. Data are displayed as peak ae of each metabolite normalized to protein content. Graphs are pooled data of 4 individual experiment. Data are +/- S.E.M. Data were analysed by two-way ANOVA with Sidak's post-test (ns= non-significant).

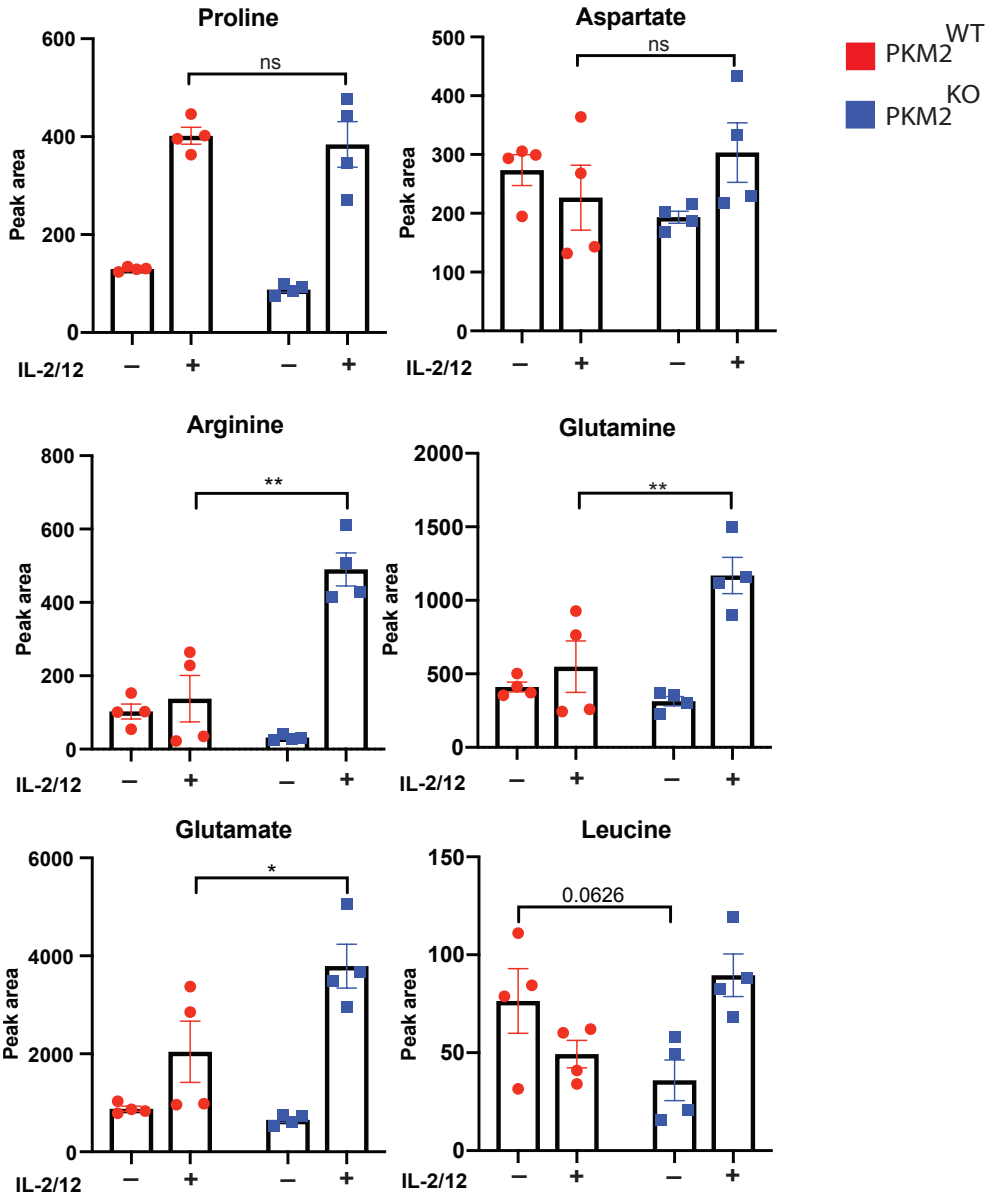

Figure 4. 13. Amino acid levels differ between PKM2^{WT} and PKM2^{KO} cultured NK cells

Splenocytes from Ncr1$^{cre/+}$ (PKM2^{WT}) or *Ncr1*$^{Cre/+}$*Pkm2*$^{fl/fl}$ (PKM2^{KO}) mice were expanded for 6 days in IL-15 (15ng/mL). On day 4 cultures were further supplemented with IL-15. On day 6 splenocytes were MACS purified and seeded at 2 x 10^6 NK cells per mL. NK cells were treated with either low dose IL-15 (5ng/mL) or IL-2/12 (330U/10ng per mL) for 18 hours. After which cells were harvested, washed in NaCl buffer and metabolites were extracted using 90% methanol. Samples were dried using a RotEvap and then run on LC/MS. Data are displayed as peak area of each metabolite normalized to protein content. Graphs are pooled data of 4 individual experiment. Data are +/- S.E.M. Data were analysed by two-way ANOVA with Sidak's post-test (ns= non-significant).

4.9. IL-2/12 stimulated PKM2^{KO} NK cells have normal levels of pyruvate kinase activity

Although there were significant metabolite differences between PKM2^{WT} and PKM2^{KO} NK cells in pathways such as amino acids, the overwhelming majority of the metabolites assessed were normal. More specifically, the metabolites involved in glycolysis and TCA cycle showed no overt differences. Pyruvate kinase is a key step in glycolysis, generating pyruvate, which is an important fuel for the TCA cycle and to fuel the citrate malate shuttle. This is the main reason that it was initially hypothesised that there would differences in metabolite levels between glycolysis and the TCA cycle.

Indeed, it appeared that PKM2^{KO} NK cells were still capable of producing pyruvate. It was possible that a different enzyme was compensating for the loss of PKM2.

To initially assess this, pyruvate kinase activity was measured using a biochemical kit that utilises pyruvate oxidase. When pyruvate is present, this enzyme will oxidise it producing a red colour which can be measured by fluorescence. Using this assay it was determined that IL-2/12 stimulated PKM2^{KO} NK cells maintain the same level of pyruvate kinase activity as PKM2^{WT} NK cells **(Fig. 4.14)**.

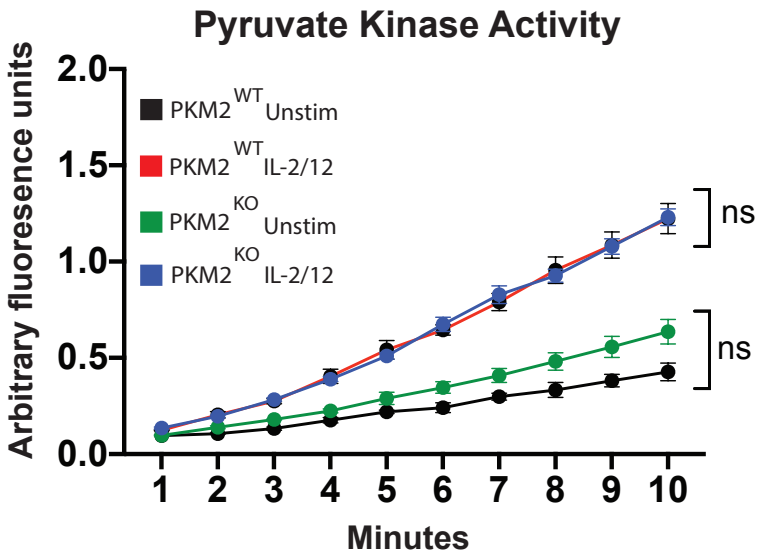

Figure 4. 14. Overall pyruvate kinase activity is similar between PKM2^{WT} and PKM2^{KO} cultured NK cells

Splenocytes from Ncr1$^{cre/+}$ (PKM2^{WT}) or *Ncr1*$^{Cre/+}$*Pkm2*$^{fl/fl}$ (PKM2^{WT}) mice were expanded for 6 days in IL-15 (15ng/mL). On day 4 cultures were further supplemented with IL-15 On day 6 splenocytes were MACS purified and seeded at 2 x 10^6 NK cells per mL. NK cells were treated with either low dose IL-15 (5ng/mL) or IL-2/12 (330U/10ng per mL) for 18 hours. After 18 hours, cells were centrifuged and washed. Cells were then prepared as per manufactures instructions. Assay was performed using 50,000 cells per well. Data are pooled data of 5 biological replicates with 3 technical replicates each. of Data are mean +/- S.E.M. Data were analysed by two-way ANOVA with a Sidak post-test (ns: non-significant)

4.10. RNAseq analysis reveals that PKM2^{KO} NK cells express higher levels of PKM1 relative to PKM2^{WT} NK cells

PKM2^{WT} and PKM2^{KO} NK cells maintained the same level of pyruvate kinase activity. Therefore, it was predicted that these cells must be expressing an alternate *Pkm* isoform. To test this, RNA sequencing was carried out on IL-2/12 activated cultured PKM2^{WT} and PKM2^{KO} NK cells, and the levels of the alternate transcript (*Pkm1*) were assessed. The data show that PKM2^{WT} NK cells express very little PKM1. However, the PKM2^{KO} NK cells show a significant upregulation of PKM1 (**Fig. 4.15 A**), suggesting that this enzyme is responsible for the maintenance of pyruvate kinase activity observed in the previous figure. PKM1 protein expression was confirmed to be elevated in PKM2^{KO} NK cells by western blot (**Fig. 4.15 B**).

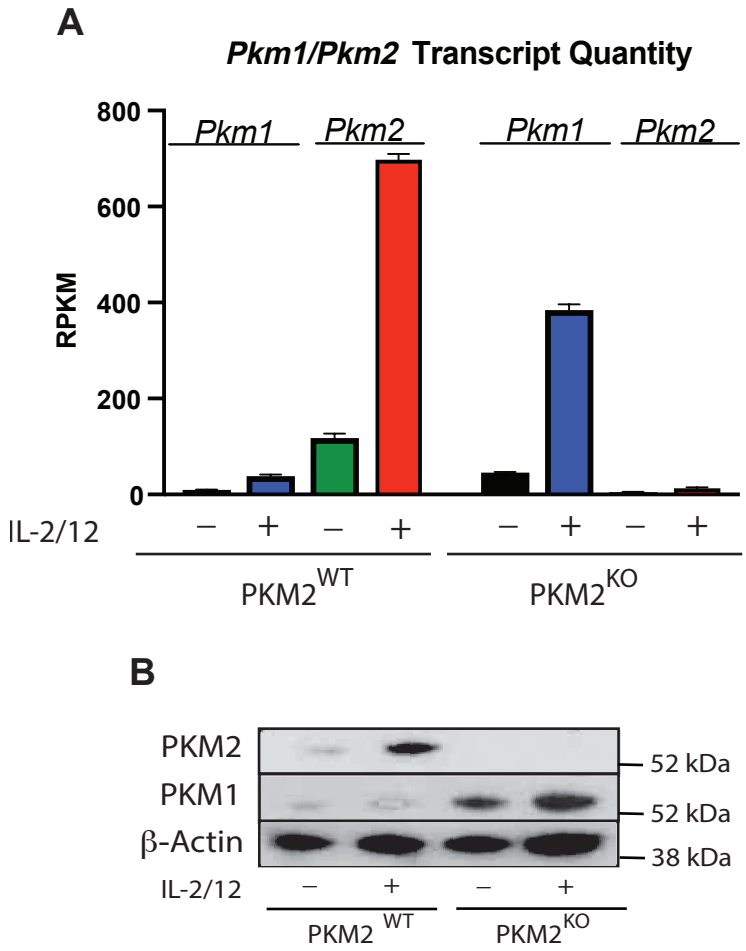

Figure 4.15. PKM1 is expressed in IL-2/12 activated PKM2^{KO} NK cells, although not at the same level of PKM2 transcript in the PKM2^{WT} cells

Splenocytes from Ncr1$^{cre/+}$(PKM2^{WT}) or *Ncr1*$^{Cre/+}$*Pkm2*$^{fl/fl}$ (PKM2^{WT}) mice were expanded for 6 days in IL-15 (15ng/mL). On day 4, cultures were further supplemented with IL-15 (15ng/mL). On day 6 splenocytes were MACS purified and seeded at 2 x 10^6 NK cells per mL. NK cells were treated with either low dose IL-15 (5ng/mL) or IL-2/12 (330U/10ng per mL) for 18 hours. After 18 hours, cells were centrifuged and lysed for RNA and protein. (A) RNA was analysed by HiSeq RNA sequencing (B) Cells were lysed at 10 x 10^6 per mL and analysed by western blot for PKM1 and PKM2 expression. Loading control was actin. RNA seq data are pooled data of 3 biological replicates. Western blot is representative of 3 independent experiments. Representative blot for PKM2 and Actin also appears in figure 4.4. Data are mean +/- S.E.M.

4.11. PKM2^{WT} and PKM2^{KO} NK cells have similar transcriptomes.

In order to assess the transcriptional effects of *Pkm2* deletion, we performed RNA sequencing analysis. The conditions chosen were PKM2^{WT} and PKM2^{KO} NK cells activated with IL-2/12 for 18 hours or left unstimulated (low dose IL-15 as a survival factor). Unstimulated NK cells, are typically metabolically quiescent and generally have no cytokine readout. Therefore, it was predicted that transcriptomics would be an interesting way to assess the importance of PKM2 in these cells.

However, when RNA sequencing was analysed using Partek software, there were only 27 observed significantly altered genes with a fold change cutoff of 1.5. Similarly, when KEGG pathway analysis was carried out using Metascape there were no enriched pathways for these differentially expressed genes. This would indicate that PKM2 expression is not required for maintenance of any specific transcriptional program in unstimulated cultured NK cells and is consistent with the fact that PKM2 expression is very low in unstimulated NK cells.

When IL-2/12 stimulated PKM2^{WT} and PKM2^{KO} NK cells were sequenced, there were some significantly altered genes at a threshold fold change of 1.5. Excluding *Pkm* as a significantly altered gene, there were 131 differentially expressed genes between IL-2/12 activated PKM2^{WT} and PKM2^{KO} NK cells . Of these genes, 51 were decreased in expression in PKM2^{KO} NK cells relative to PKM2^{WT} NK cells. 80 genes were significantly increased in expression in PKM2^{KO} NK cells relative to PKM2^{WT} NK cells.

When pathway enrichment analysis was performed using Metascape, (filtering on Reactome gene sets and KEGG pathways) there were three significantly altered pathways. These pathways were cytokine – cytokine receptor interaction, collagen degradation and arachidonic acid metabolism **(Table 4.1)**. Although these pathways

came back as significantly enriched, it is noteworthy that each of these only have 6/270, 3/55 and 3/89 hits in their respective pathways. This may have some significance, however, these alterations may not have functional implications.

	Category	Term	Description	LogP	# of Genes	Genes
Summary	**KEGG Pathway**	**mmu04060**	**Cytokine-cytokine receptor interaction**	**-2.63624**	**6/270**	**Amh,Flt1, Il13ra1, Tnfrsf11b, Ccl27a, Il19**
1	KEGG Pathway	mmu04060	Cytokine-cytokine receptor interaction	-2.63624	6/270	Amh,Flt1 Il13ra1, Tnfrsf11b, Ccl27a, Il19
Summary	**Reactome Gene Sets**	**R-MMU-1442490**	**Collagen degradation**	**-2.58526**	**3/55**	**Col13a1, Col18a1, Mmp13, Icam4**
1	Reactome Gene Sets	R-MMU-1442490	Collagen degradation	-2.58526	3/55	Col13a1, Col18a1, Mmp13
2	Reactome Gene Sets	R-MMU-21608	Integrin cell surface interactions	-2.27198	3/71	Col13a1, Col18a1, Icam4
3	Reactome Gene Sets	R-MMU-1474290	Collagen formation	-2.11349	3/81	Col13a1, Col18a1, Mmp13
Summary	**KEGG Pathway**	**mmu00590**	**Arachidonic acid metabolism**	**-2.00169**	**3/89**	**Cyp4a12b Ggt1, Ptgis**
1	KEGG Pathway	mmu00590	Arachidonic acid metabolism	-2.00169	3/89	Cyp4a12b, Ggt1, Ptgis

Table 4. 1. Enrichment analysis for differentially expressed genes between $PKM2^{WT}$ and $PKM2^{KO}$ IL-2/12 stimulated cells

Splenocytes from $Ncr1^{cre/+}$ or $Ncr1^{Cre/+}Pkm2^{fl/fl}$ mice were expanded for 6 days in IL-15 (15ng/mL). On day 6 splenocytes were MACS purified and seeded at 2 x 10^6 NK cells per mL. NK cells were treated with IL-2/12 (330U/10ng per mL) for 18 hours. After 18 hours, cells were centrifuged, lysed and RNA was extracted. RNA was analysed by HiSeq RNA sequencing. Data was initially analysed using Partek with F.C 1.5 of $PKM2^{KO}$ rel. $PKM2^{WT}$ and then sorted by fold change on DEG with a p value of less than 0.05. Data was then analysed for enrichment of pathways using Metascape. Data were filtered on canonical pathways for KEGG and reactome gene sets.

4.12. There is no significant alteration of key HIF1α target genes in PKM2^{KO} NK cells

As previously mentioned PKM2 has been shown to be a key regulator of the HIF1α pathway in activated macrophages [119]. Although the HIF1α pathway did not come up as altered within the Metascape pathway analysis, it was manually assessed whether there were any alternations in key HIF1α target genes. The levels of 5 key HIF1α target genes were compared between PKM2^{WT} and PKM2^{KO} NK cells. The genes assessed were *Eno1, Gapdh, Ldha, Pgk1,* and *Tfrc*. The RPKM (reads per kilobase or transcript per million mapped reads) of these genes between both PKM2^{WT} and PKM2^{KO} cells for unstimulated and IL-2/12 stimulated conditions were found to be comparable (**Fig. 4.16)**.

Similarly, as PKM2 has been previously shown to regulate STAT5 activation, the levels of key STAT5 target genes were also assessed. As demonstrated in figure 4.17, there was no significant difference in STAT5 target gene expression between the two genotypes.

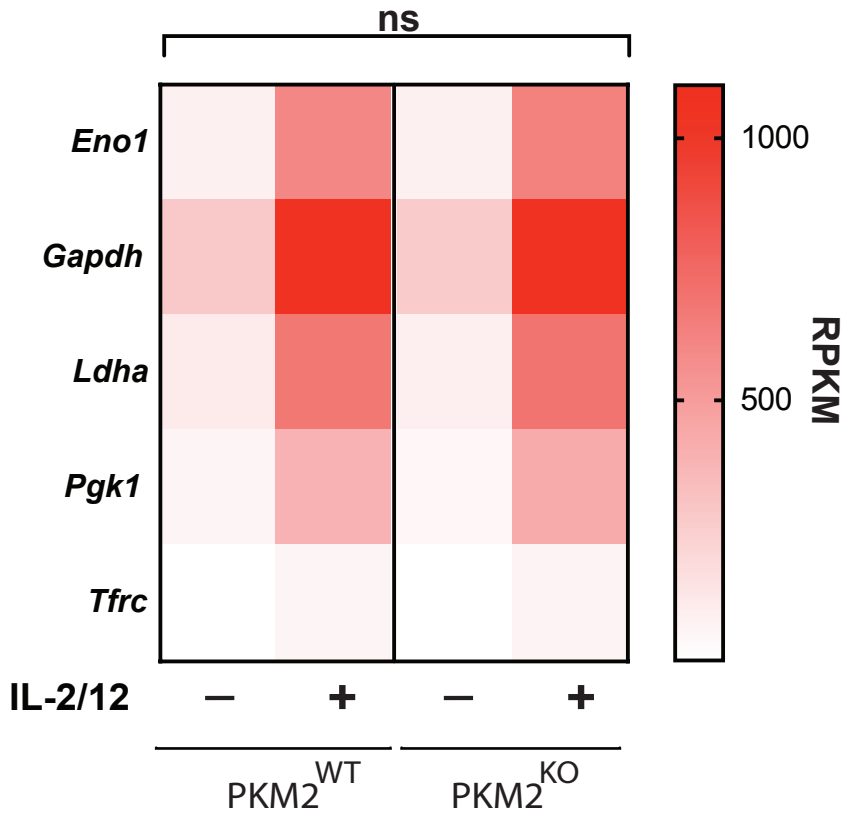

Figure 4. 16. Expression of key HIF1α genes are not changed in PKM2^{KO} NK cells

Splenocytes from Ncr1$^{cre/+}$ (PKM2^{WT}) or *Ncr1*$^{Cre/+}$*Pkm2*$^{fl/fl}$ (PKM2^{KO}) mice were expanded for 6 days in IL-15 (15ng/mL). On day 6 splenocytes were MACS purified and seeded at 2 x 10^6 NK cells per mL. NK cells were treated with either low dose IL-15 (5ng/mL) or IL-2/12 (330U/10ng per mL) for 18 hours. After 18 hours, cells were centrifuged, lysed and RNA was extracted. RNA was analysed by HiSeq RNA sequencing. RPKM were then compared for HIF1α target genes. Data are pooled data of 3 individual animals. Data were analysed using two way ANOVA with Sidaks post-test.

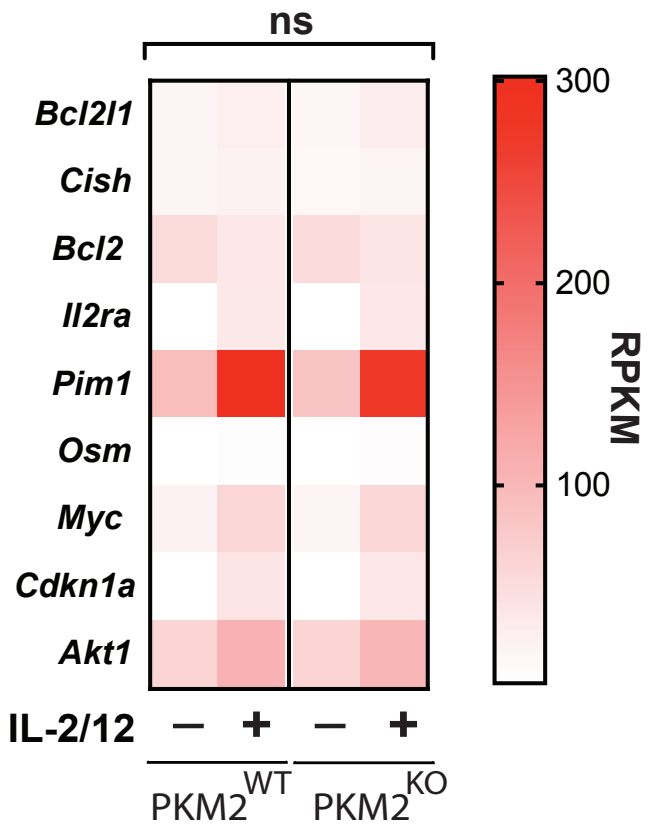

Figure 4. 17. Expression of key STAT5 genes are not changed in PKM2^{KO} NK cells

Splenocytes from Ncr1$^{cre/+}$ (PKM2^{WT}) or *Ncr1*$^{Cre/+}$*Pkm2*$^{fl/fl}$ (PKM2^{KO}) mice were expanded for 6 days in IL-15 (15ng/mL). On day 6 splenocytes were MACS purified and seeded at 2 x 10^6 NK cells per mL. NK cells were treated with either low dose IL-15 (5ng/mL) or IL-2/12 (330U/10ng per mL) for 18 hours. After 18 hours, cells were centrifuged, lysed and RNA was extracted. RNA was analysed by HiSeq RNA sequencing. RPKM were then compared for STAT5 target genes. Data are pooled data of 3 individual animals. Data were analysed using two way ANOVA with Sidaks post-test.

Discussion

The data presented in this chapter characterised the effect of *Pkm2* deletion on cultured NK cell *in vitro,* assessing both metabolic and functional parameters. Interestingly, when $PKM2^{KO}$ NK cells were metabolically and functionally analysed there were no defects. It appears that this is due to enzymatic compensation by the alternate *Pkm* isoform, *Pkm1.* Data presented in other studies have shown two distinct roles for *Pkm2:* control of metabolism and control of transcription. The metabolic role refers to its part in pyruvate generation and regulation of glycolysis [146]. The transcriptional role, refers to its part as a signalling molecule and transcriptional co-activator as it has been shown to regulate HIF1α and STAT3 signalling [126]. In this present study, we assessed both the metabolic and transcriptional roles of PKM2. It is clear from RNA sequencing data that there is no role for *Pkm2* in controlling NK cell transcription.

Pkm1 appears to metabolically compensate as $Pkm2^{KO}$ NK cells can maintain glycolysis and pyruvate kinase activity. However, transcriptionally, it is not possible for the *Pkm1* isoform to compensate. Indeed, there was no significant difference in HIF1α target gene expression between $PKM2^{WT}$ and $PKM2^{KO}$ NK cells. Seeing as only PKM2 can be present in the monomeric/dimeric form, and PKM1 is only present as a tetramer, it is unlikely that the compensatory expression of PKM1 is leading to a normal phenotype, and it is more likely that PKM2 is not required for transcription of these genes in NK cells.

With regards to the metabolic role for PKM2 in the final step of glycolysis, the compensatory increase in PKM1 expression is able to maintain pyruvate production with PKM2 deletion.

The previously published literature shows that *Pkm1* has higher enzymatic activity than *Pkm2* [151]. This is due to the fact that PKM1 is constitutively active. Therefore, it is intuitive to expect that in this NK cell system where PKM1 is highly expressed, that these cells would have a higher level of overall pyruvate kinase activity. In fact, the data presented here show that the PKM1 expressing NK cells match their overall pyruvate kinase activity to that of $PKM2^{WT}$ NK cells (Fig. 4.14). These data may be explained by looking at the expression levels of both isoforms. Although the $PKM2^{KO}$ NK cells only express PKM1 (the more active isoform), the amount of total *Pkm* transcript that they express is lower than that of $PKM2^{WT}$ cells (Figure 4.15). It is interesting to speculate that this reduced total level of *Pkm* is an attempt by the cells to regulate their overall pyruvate kinase activity. This supports the concept that regulation of pyruvate kinase activity may be important for NK cell function. This hypothesis will be explored in chapter 5 when pyruvate kinase activity will pharmacologically manipulated.

Although there was very little functional implications of PKM2 deletion, one striking observation was that there was increased levels of amino acids. These amino acids included arginine, glutamine and glutamate. It Is interesting to question whether this is due to alterations in amino acid uptake or reduced cellular utilisation of these amino acids. This could be tested by measuring supernatant levels after stimulation. If uptake is increased in $PKM2^{KO}$ relative to $PKM2^{WT}$ NK cells, it would hint that they are elevated due to increased uptake from the media. If this is the case, it is interesting to question why they might be elevated. Increased glutamine and glutamate uptake are associated

with increased fuelling of the TCA cycle, however based on the other data presented in this study, this is not the case. Succinate, citrate and malate levels were all normal in $PKM2^{KO}$ NK cells. Glutamine and glutamate are also required for glutathione synthesis. Glutathione is a key antioxidant molecule that protects against reactive oxygen species [152]. Therefore in futures studies it would be interesting to investigate whether PKM2 deletion affects the redox balance in activated NK cells.

Although the data presented in this chapter comprehensively analysed the transcriptional and metabolic landscape of cytokine activated NK cells, it is interesting to hypothesise that PKM2 may be required for other aspects of NK cell regulation. Specifically, PKM2 could be required for NK cell function in response to receptor ligation, such as NK1.1. A previous study by the Kaech lab at Yale demonstrated that the substrate of pyruvate kinase, phosphoenolpyruvate (PEP), is required for calcium signalling in T cells [115]. This is intriguing as receptor ligation of NK cells also often leads to calcium mediated signalling. Indeed, NK1.1 ligation is accompanied by metabolic reprogramming and Syk mediated calcium signalling [103, 153]. T cells activated with anti CD3/CD28 have impaired calcium signalling when PEP (PKM substrate) is reduced. Therefore it could be possible that PKM2 may affect the overall PEP levels, anf future lines of investigation may assess whether NK receptor mediated activation is impaired in $PKM2^{KO}$ NK cells.

Chapter 5: Pharmacological activation of PKM2 is detrimental to NK cell metabolic and functional responses *in vitro*

Introduction

Chapter 3 and 4 demonstrated that PKM2 is not required for NK cell function *in vivo,* or *in vitro.* This was due to metabolic compensation by expression of the alternate *Pkm* isoform, *Pkm1.* Therefore, it was next investigated whether the role of PKM2 in NK cells could be investigated pharmacologically. A pharmacological activator of PKM2 called TEPP-46 exists, and cause tetramerisation/activation of PKM2 (**Fig. 5.1).** This drug has been used extensively by other groups and has been shown to increase the pool of active PKM2 [133]. Therefore to overcome the limitations of the genetic model, this chapter will study the effects of PKM2 manipulation by TEPP-46 in activated NK cells *in vitro.*

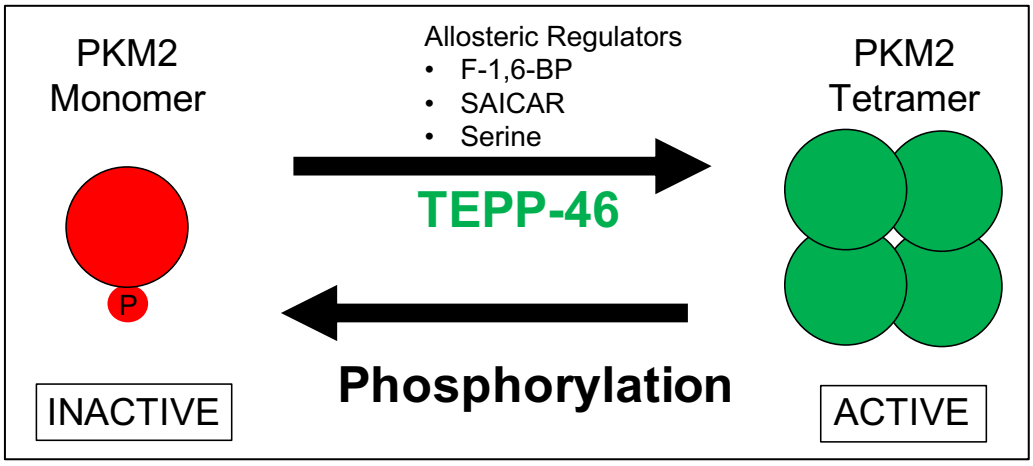

Fig. 5.1: PKM2 can be pharmacologically activated using TEPP-46: PKM2 exists as inactive monomers/dimers and active tetramers. Phosphorylation leads to PKM2 inactivation. Endogenous activators of PKM2 include fructose-1,6-bisphosphate (F-1,6-BP), phosphoribosylaminoimidazolesuccinocarboxamide (SAICAR), and serine. PKM2 can also be pharmacologically activated/tetramerized by a drug called TEPP-46.

5.1. PKM2 activity in NK cells is limited and can be increased using pharmacological activator TEPP-46

The data from chapter 4 demonstrated that $PKM2^{KO}$ cultured NK cells have no overt phenotype in response to IL-2/12 stimulation. This appears to be due to metabolic compensation by PKM1. Therefore, it was next investigated whether PKM2 activity could be manipulated pharmacologically. There is a commercially available PKM2 activator called TEPP-46, which has been utilised extensively in the field. Cultured NK cells were activated 17 hours with IL-2 and IL-12 (to induce PKM2), and then TEPP-46 was added for one hour. A pyruvate kinase assay was then carried out. Normally IL-2/12 activated NK cells show increased pyruvate kinase activity relative to unstimulated. Treatment with TEPP-46 caused an additional increase in pyruvate kinase activity, indicating that the drug is effective in causing activation of PKM2 (**Fig 5.1).** This data also demonstrated that monomeric, inactive PKM2, exists in 18 hour cytokine stimulated NK cells.

Pyruvate kinase is traditionally known as a key regulatory step in glycolysis [154]. Therefore, the impact of TEPP-46-mediated activation of PKM2 on the rate of glycolysis was also assessed. Using the same experimental conditions as above (17 hours of IL-2/12 + 1 hour TEPP-46/vehicle treatment), the extracellular acidification rate was assessed using a Seahorse flux analyser. Interestingly, the basal rate of glycolysis was increased with TEPP-46 treatment, although there was no effect on the glycolytic capacity **(Fig. 5.2 B,C).** When the level of oxygen consumption was assessed, there was no significant effect on either the basal or maximum rate. **(Fig. 5.3 B,C).** These data indicate that TEPP-46 increases PKM2 activity as predicted, and that PKM2 is a limiting enzyme in NK cell glycolysis.

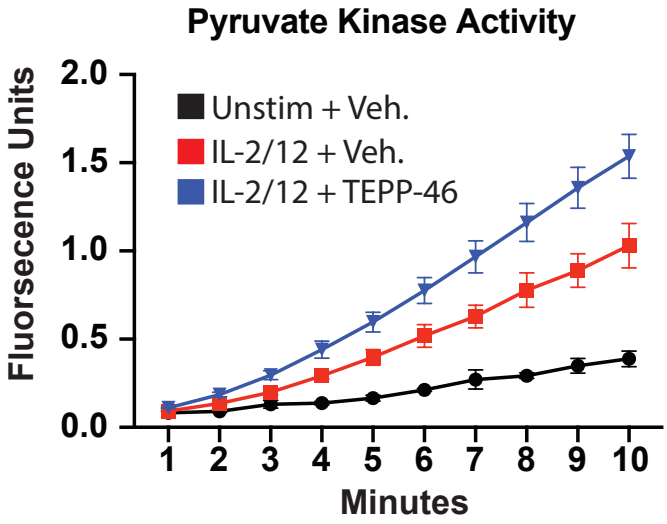

Figure 5. 1. Acute TEPP-46 treatment of IL-2/12 activated cultured NK cells increased pyruvate kinase activity

Splenocytes wild-type C57Bl/6 mice were expanded for 6 days in IL-15 (15ng/mL). On day 6 splenocytes were MACS purified and seeded at 2 x 10^6 NK cells per mL. NK cells were treated with either low dose IL-15 (5ng/mL) or IL-2/12 (330U/10ng per mL) for 17 hours. After 17 hours, the IL-2/12 fraction of cells was split and treated with either vehicle (DMSO- 0.1%) or TEPP-46 (50 μM). Unstimulated cells also had DMSO added (0.1%). After 1 hour, cells were washed. Cells were then prepared as per pyruvate kinase assay kit manufacturer's instructions. Assay was performed using 50,000 cells per well. Data are pooled data of 2 biological replicates with at least 2 technical replicates each.

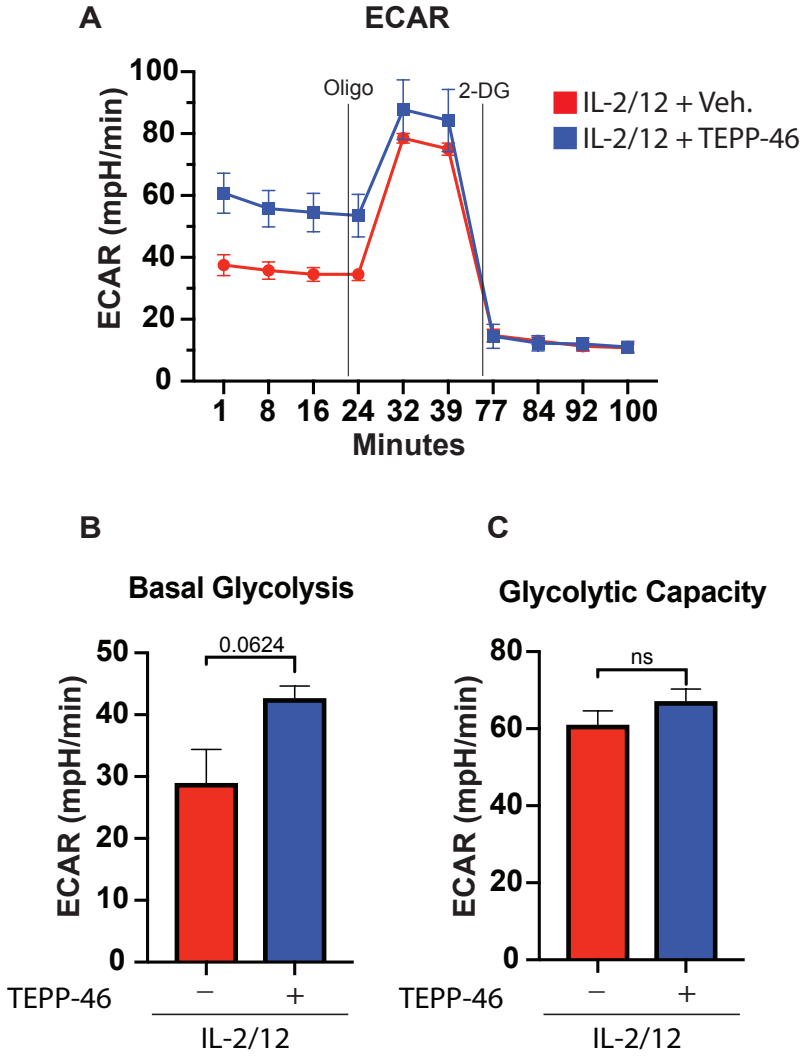

Figure 5. 2. Acute TEPP-46 treatment of IL-2/12 activated cultured NK cells increased basal glycolysis

Splenocytes from wild-type C57Bl/6 mice were expanded for 6 days in IL-15 (15ng/mL). On day 6 splenocytes were MACS purified and seeded at 2 x 10^6 NK cells per mL. NK cells were treated with IL-2/12 (330U/10 ng per mL) for 17 hours. After 17 hours, the IL-2/12 fraction of cells was split and treated with either vehicle (DMSO- 0.1%) or TEPP-46 (50 μM). Cells were changed into replete Seahorse medium at a concentration of 750,000 cells per well and analysed on a Seahorse 24 well extracellular flux analyser. (A) Representative seahorse plot of extracellular acidification rate with IL-2/12 + DMSO (Veh.) or IL-2/12 (TEPP-46 50 μM 1 hr) (B) Pooled data of 3 individual experiments for basal glycolysis of IL-2/12 + DMSO (Veh.) or IL-2/12 (TEPP-46 50 μM 1 hr) treated cells. (C) Pooled data of 3 individual experiments for glycolytic capacity of IL-2/12 + DMSO (Veh.) or IL-2/12 (TEPP-46 50 μM 1 hr) treated cells. Data are from 3 independent experiments and are represented as mean +/- S.E.M. Data were analysed by a paired student t test (ns: non-significant)

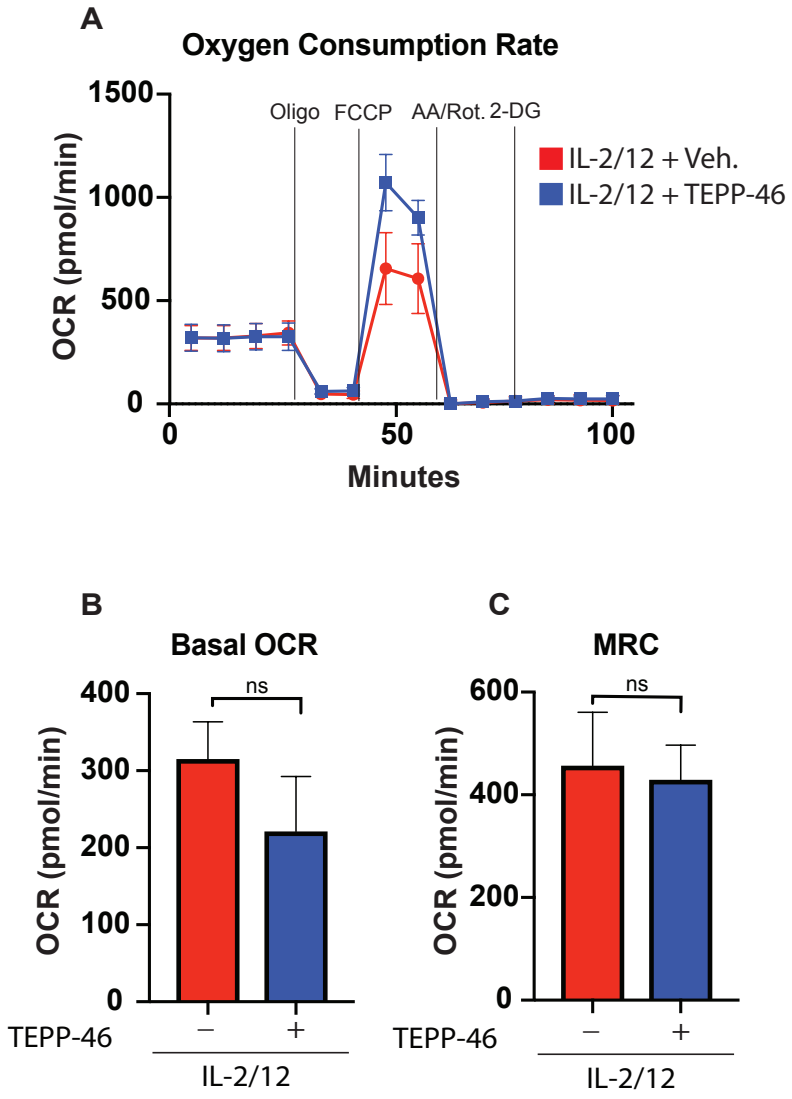

Figure 5. 3. Acute TEPP-46 treatment of IL-2/12 activated cultured NK cells does not affect oxygen consumption rates

Splenocytes from wild-type C57Bl/6 mice were expanded for 6 days in IL-15 (15ng/mL). On day 6 splenocytes were MACS purified and seeded at 2 x 10^6 NK cells per mL. NK cells were treated with IL-2/12 (330U/10ng per mL) for 17 hours. After 17 hours, the IL-2/12 fraction of cells was split and treated with either vehicle (DMSO- 0.1%) or TEPP-46 (50 μM). Cells were changed into replete Seahorse medium at a concentration of 750,000 cells pew well and analysed on a Seahorse 24 well extracellular flux analyser. (A) Representative seahorse plot of Oxygen Consumption rate with IL-2/12 + DMSO (Veh.) or IL-2/12 (TEPP-46 50 μM 1 hr) (B) Pooled data of 3 individual experiments for basal oxygen consumption rate of IL-2/12 + DMSO (Veh.) or IL-2/12 (TEPP-46 50 μM 1 hr) treated cells. (C) Pooled data of 3 individual experiments for maximum respiratory capacity of IL-2/12 + DMSO (Veh.) or IL-2/12 (TEPP-46 50 μM 1 hr) treated cells. Data are from 3 independent experiments and are represented as mean +/- S.E.M. Data were analysed by a paired student t test (ns: non-significant)

5.2. Prolonged PKM2 activation of IL-2/12-stimulated NK cells impairs blastogenesis

The increased PK activity and glycolysis observed in IL-2/12 activated cells treated with TEPP-46 confirmed that activated NK cells express some inactive, monomeric PKM2. Glycolysis is an important arm of metabolism for NK cells as it breaks down glucose and fuels the citrate malate shuttle, which is required for NK cell function [86]. Therefore, it seemed logical to question why NK cells would express an inactive form of a glycolytic enzyme.

In order to examine whether PKM2 was required for NK cell activation, cultured NK cells were simultaneously treated with IL-2/12 and TEPP-46, for the full 18 hour stimulation. This differs from the previous experiment where the NK cells were already activated with IL-2/12 and then acutely treated with TEPP-46 for 1 hour.

As this is a long term treatment with a drug, it was first tested whether there was any negative effect on NK cell viability. Purified cultured NK cells were activated for 18 hours with IL-2/12 in the presence or absence of TEPP-46 (50 μM) or vehicle (0.1% DMSO). The cells were then harvested and stained with propidium iodide and an antibody specific for Annexin V. Propidium Iodide is a DNA dye that will only stain permeabilized cells, and Annexin V is a marker that is expressed on the surface of cells undergoing apoptosis. Therefore this is an effective method to visualize cell death or cells undergoing apoptosis respectively.

When the percentage of dead NK cells and the percentage of cells undergoing apoptosis were analysed, there was no significant difference between cells treated with or without TEPP-46 **(Fig. 5.4)**. This indicates that this drug is suitable to use for this 18 hour timepoint.

The effect of TEPP-46 on IL-2/12 induced blastogenesis (increase in cell size) was next investigated. Activation of cultured NK cells with IL-2/12 usually results in the increase of forward scatter as measured by flow cytometry which is indicative of blastogenesis,. Interestingly, IL-2/12 activated cells treated with TEPP-46 had reduced forward scatter. This suggests that PKM2 activation may have a negative effect on NK cell growth and blastogenesis (**Fig 5.5)** .

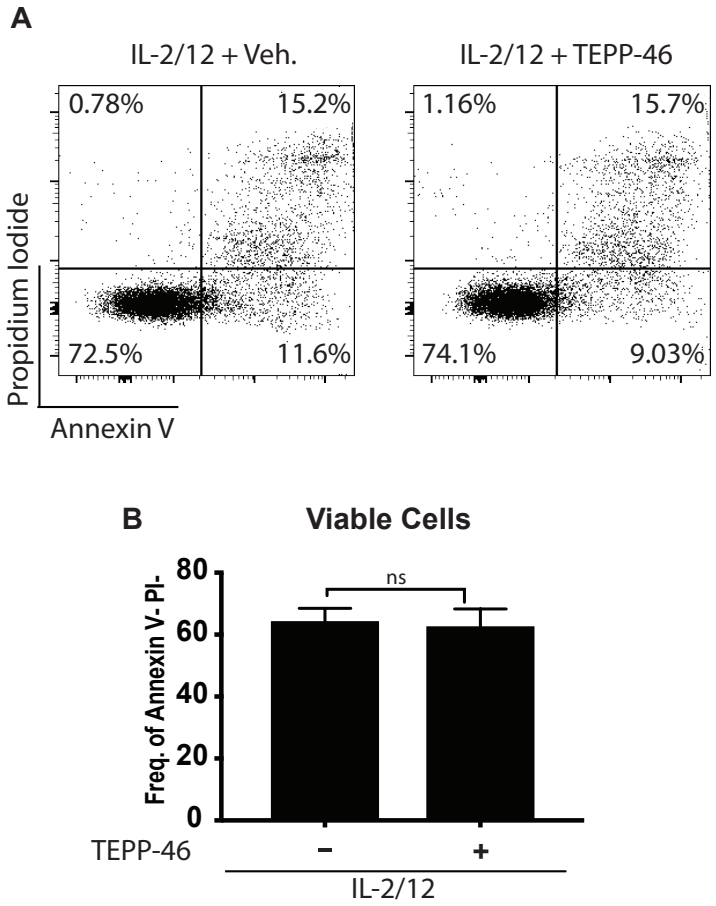

Figure 5.4. TEPP-46 treatment of IL-2/12 activated cultured NK cells does not significantly affect viability

Splenocytes from wild-type C57Bl/6 mice were expanded for 6 days in IL-15 (15ng/mL). On day 6 splenocytes were MACS purified and seeded at 2 x 10^6 NK cells per mL. NK cells were treated with either low dose IL-2/12 (330U/10ng per mL) +/- TEPP-46 (50 μM) or vehicle (DMSO – 0.1%) for 18 hours. Cells were then isolated and stained for propidium iodide or Annexin V (A) Representative dot plot of staining for propidium iodide or Annexin V for IL-2/12 activated cells +/- TEPP-46 (B) Pooled data of 3 individual experiments of propidium iodide or Annexin V staining for IL-2/12 activated cells +/- TEPP-46 after 18 hours Data are from 3 independent experiments and are represented as mean +/- S.E.M. Data were analysed by a paired student t-test. (ns: non-significant)

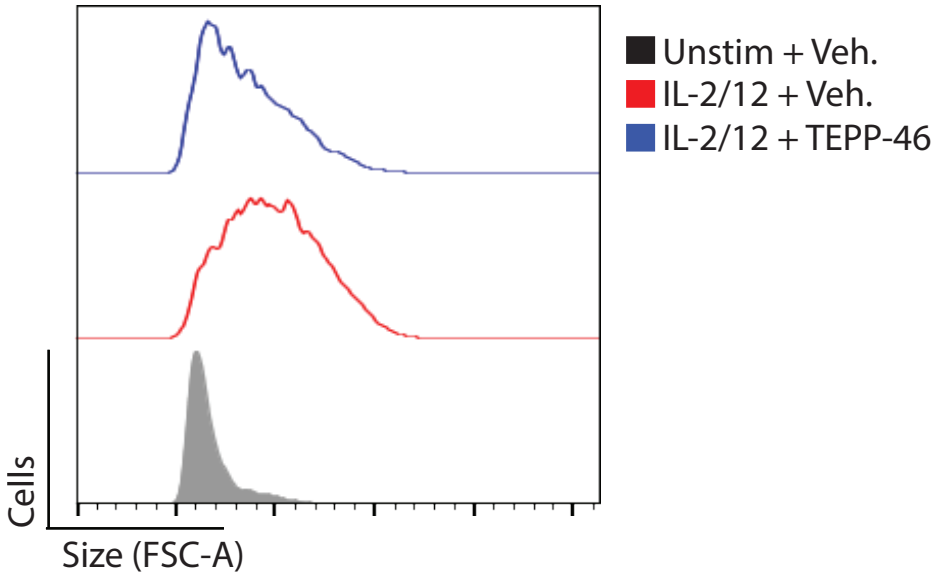

Figure 5. 5. TEPP-46 treatment of IL-2/12 activated cultured NK cells prevents normal blastogenesis

Splenocytes from wild-type C57Bl/6 mice were expanded for 6 days in IL-15 (15ng/mL). On day 6 splenocytes were MACS purified and seeded at 2 x 10^6 NK cells per mL. NK cells were treated with either low dose IL-15 (5ng/mL Unstimulated) or IL-2/12 (330U/10ng per mL) +/- TEPP-46 (50 μM) or vehicle (DMSO – 0.1%) for 18 hours. NK cells were then harvested, treated with BD FC block and stained for flow cytometry. NK cells were identified as being NKp46$^+$, NK1.1$^+$ and CD3.Histograms were then generated for forward scatter using Flow Jo. Data are a representative histogram from 5 independent experiments.

5.3. TEPP-46 treatment of NK cells inhibits IL-2/12-induced effector molecule production

The O'Neill lab has previously published that PKM2 activation with TEPP-46 in murine macrophages, inhibits pro-inflammatory cytokine production [119]. Therefore, the frequency of IFNγ expressing cultured NK cells treated with IL-2/12 +/- TEPP-46 after 20 hours was assessed. IL-2/12-activated NK cells show a significant increase in IFNγ production relative to unstimulated cells. However, in the presence of TEPP-46 this increase in IFNγ was significantly blunted **(Fig. 5.6).** Therefore, PKM2 activation inhibits IFNγ production in cytokine stimulated NK cells.

Granzyme B is a key cytotoxic molecule expressed by NK cells. The effect of PKM2 activation on the expression of this enzyme was next assessed. Cultured NK cells were activated with IL-2/12 in the presence or absence of TEPP-46 for 20 hours. Normally, IL-2/12 activated cultured NK cells significantly increase granzyme B production relative to unstimulated cells. In the presence of TEPP-46 IL-2/12-activated cultured NK cells had significantly reduced granzyme B expression (**Fig. 5.7).** Therefore, PKM2 activation inhibits granzyme B expression in cytokine stimulated NK cells.

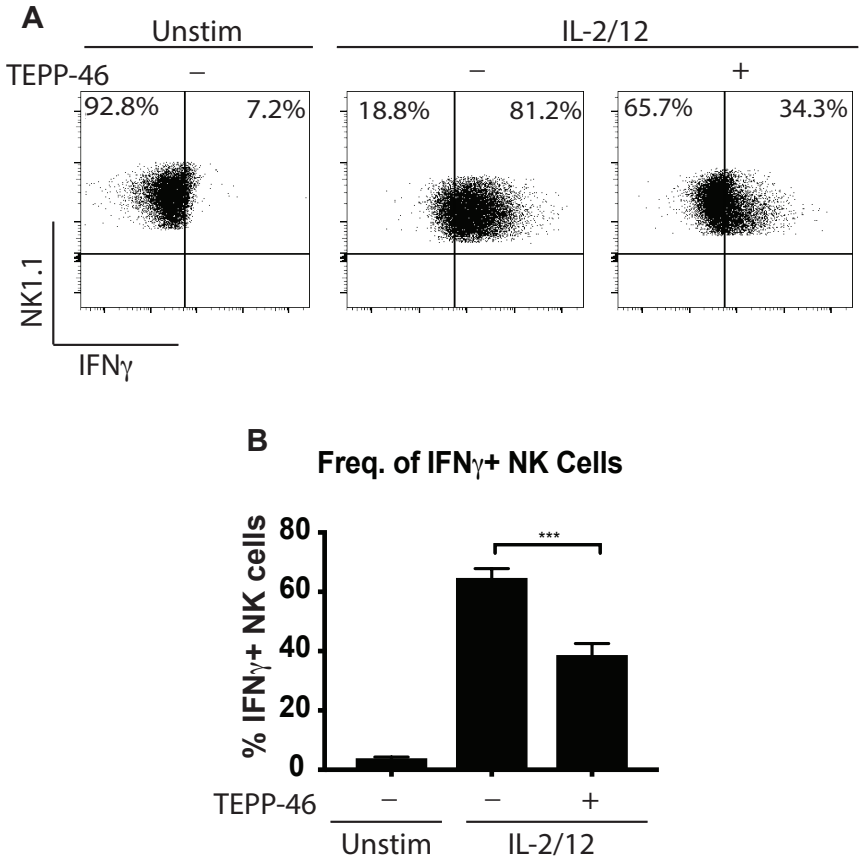

Figure 5.6. Long term TEPP-46 treatment of IL-2/12 activated cultured NK cells prevents normal IFNγ production

Splenocytes from wild-type C57Bl/6 mice were expanded for 6 days in IL-15 (15ng/mL). On day 6 splenocytes were MACS purified and seeded at 2 x 10^6 NK cells per mL. NK cells were treated with either low dose IL-15 (5ng/mL Unstimulated) or IL-2/12 (330U/10ng per mL) +/- TEPP-46 (50 μM) or vehicle (DMSO – 0.1%) for 20 hours. NK cells were treated with BD GolgiPlug (Brefeldin A) for 4 hours prior to flow cytometry staining. NK cells were then harvested, treated with BD FC block and stained for flow cytometry. NK cells were identified as being NKp46$^+$, NK1.1$^+$ and CD3$^-$. (A) Representative dot plot of IFNγ positive NK cells as measured by flow cytometry. (B) Pooled data of frequency of IFNγ positive NK cells 20 hours post IL-2/12 +/- TEPP-46 treatment. Data are pooled from 7 individual experiments. Data are represented as mean +/- S.E.M. Data were analysed using a one way ANOVA with Tukeys post test (***$p < 0.001$)

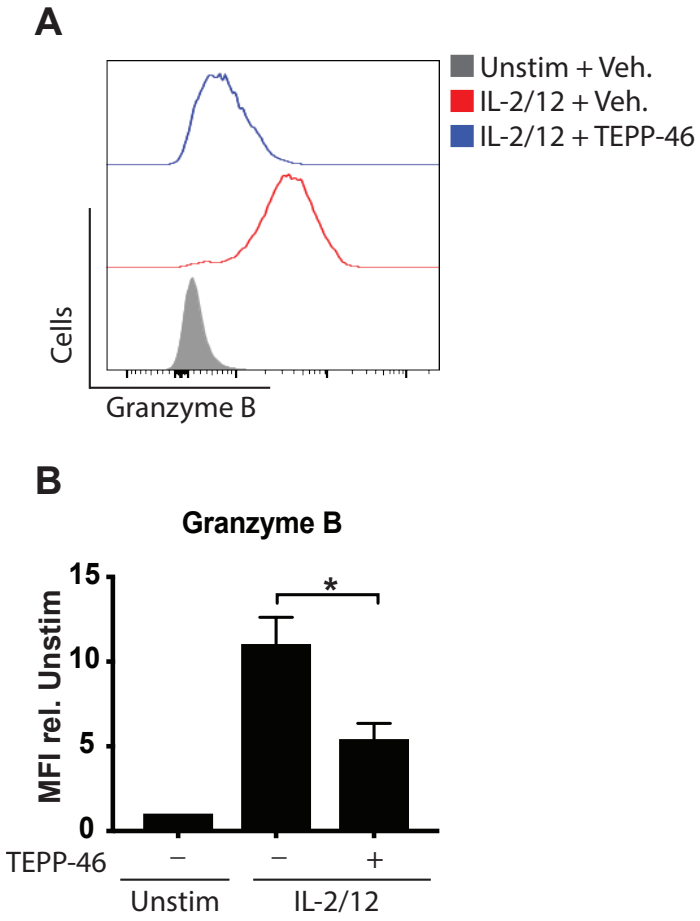

Figure 5.7. Long term TEPP-46 treatment of IL-2/12 activated cultured NK cells prevented normal Granzyme B production

Splenocytes from wild-type C57Bl/6 mice were expanded for 6 days in IL-15 (15ng/mL). On day 6 splenocytes were MACS purified and seeded at 2 x 10^6 NK cells per mL. NK cells were treated with either low dose IL-15 (3.33 ng/mL Unstimulated) or IL-2/12 (330U/10ng per mL) +/- TEPP-46 (50 μM) or vehicle (DMSO – 0.1%) for 20 hours. NK cells were treated with BD GolgiPlug (Brefeldin A) 4 hours prior to flow cytometry staining. NK cells were then harvested, treated with BD FC block and stained for flow cytometry. NK cells were identified as being NKp46$^+$, NK1.1$^+$ and CD3$^-$. Granzyme B MFI of these cells was then determined. (A) Representative histogram of granzyme B expression by NK cells as measured by flow cytometry. (B) Pooled data of granzyme B MFI rel. to unstim by NK cells 20 hours post IL-2/12 +/- TEPP-46 treatment. Data are pooled from 6 individual experiments. Data are represented as mean +/- S.E.M. Data were analysed using a one way ANOVA with Tukeys post-test (*$p < 0.05$)

5.4. TEPP-46 treatment of NK cells inhibits IL-2/12-induced cytokine production

The frequency of cells expressing granzyme B and IFNγ were reduced in IL-12/12 activated cultured NK cells treated with TEPP-46. In order to investigate if TEPP-46 caused a global decreases in cytokine and chemokine production, we investigated the cumulative production of IFNγ , TNF, IL-10, MIP-1α and MIP-1β over the course of 20 hours using cytometric bead array technology. All cytokines and chemokines analysed were produced in response to IL2/12 stimulation. TEPP-46 inhibited the production of the cytokines TNF, IFNγ and IL-10, but had no significant effect on MIP-1α and MIP-1β chemokine production (**Fig. 5.8 D,E)** suggesting that there may be a specific defect in pro-inflammatory cytokine production with prolonged PKM2 activation.

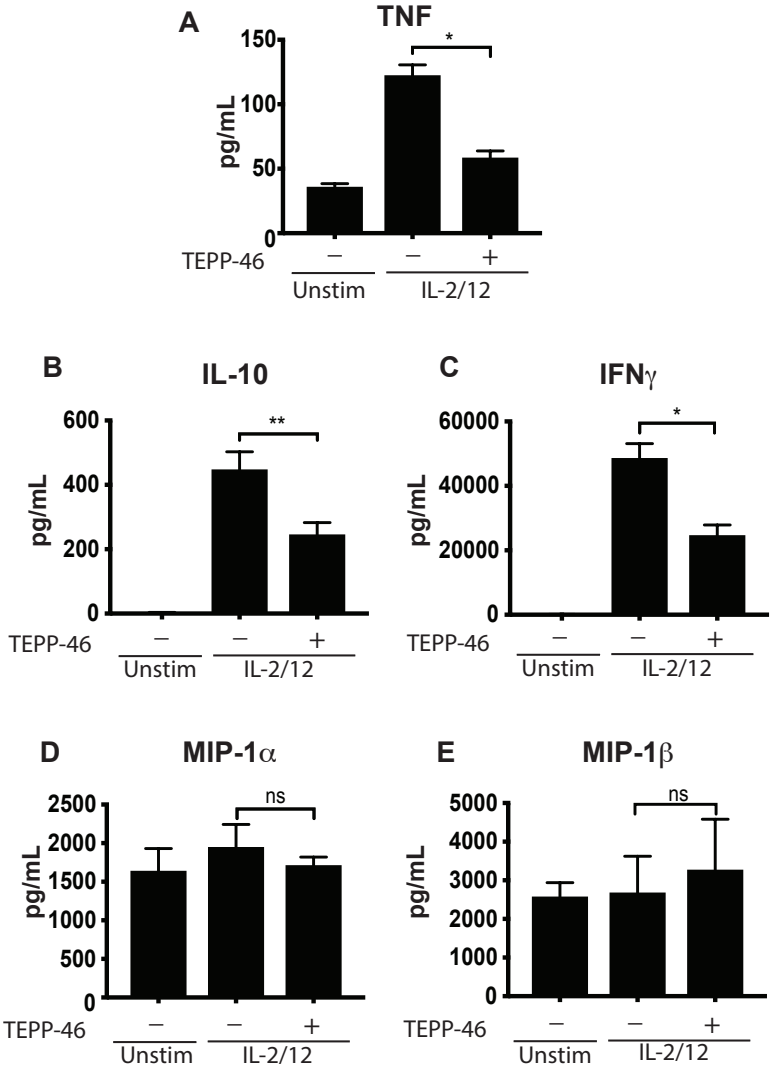

Figure 5. 8. IL-2/12-activated NK cells treated with TEPP-46 showed reduced cytokine production

Splenocytes from wild-type C57Bl/6 mice were expanded for 6 days in IL-15 (15ng/mL). On day 6 splenocytes were MACS purified and seeded at 2 x 10^6 NK cells per mL. NK cells were treated with either low dose IL-15 (5ng/mL) or IL-2/12 (330U/10ng per mL) +/- TEPP-46 (50 μM) or vehicle (DMSO – 0.1%) for 18 hours. After 18 hours, cells were centrifuged and supernatants taken and frozen. Supernatants were later stained using BD cytokine bead array technology. Samples were run on a BD LSR II or BD Fortessa and assessed for cytokine levels relative to internal standards. Graphs are pooled data of 4 biological replicates. Data are mean +/- S.E.M Data were analysed by one-way ANOVA with a Tukey post-test (*$p < 0.05$, p** < 0.01, ns: non-significant)

5.5. Elevated pyruvate kinase activity was maintained after 18 hours of TEPP-46 treatment

It was previously shown that acute TEPP-46 treatment elevated pyruvate kinase activity in 17 hour IL-2/12-activated NK cells. However, it was not clear whether this elevated PK activity would be maintained throughout the 18 hour period of IL-2/12 stimulation. In fact, pyruvate kinase activity remained elevated 18 hours after treatment with IL-2/12 plus TEPP-46 demonstrating sustained PKM2 activation/tetramerisation (**Fig. 5.9).** Considering that TEPP-46 could sustain PKM2 activation, further metabolic analysis of these 18 hour cytokine-stimulated NK cells was next performed.

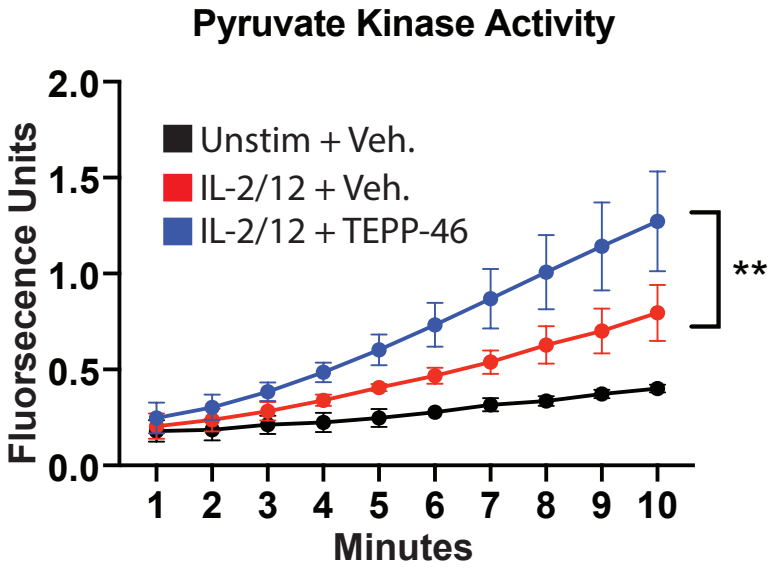

Figure 5. 9. TEPP-46 is stable and maintains pyruvate kinase activity 18 hours post treatment

Splenocytes from wild-type C57Bl/6 mice were expanded for 6 days in IL-15 (15ng/mL). On day 6 splenocytes were MACS purified and seeded at 2 x 10^6 NK cells per mL. NK cells were treated with either low dose IL-15 (5ng/mL Unstimulated) or IL-2/12 (330U/10ng per mL) +/- TEPP-46 (50 μM) or vehicle (DMSO – 0.1%) for 18 hours. After 18 hours, cells were centrifuged and washed. Cells were then prepared as per manufactures instructions. Assay was performed using 50,000 lysed cells per well. Data are pooled data of 3 biological replicates with at least 2 technical replicates each. Data are mean +/- S.E.M. Data were analysed by one-way ANOVA with Tukey post-test ($p^{**} < 0.01$)

5.6. TEPP-46 treatment of NK cells inhibits IL-2/12-induced glycolytic capacity

Considering that TEPP-46 treated cells were smaller after 18 hours stimulation, and metabolism is required to fuel biosynthesis, it next assessed whether TEPP-46 altered NK cell metabolic reprogramming. Cultured NK cells were activated with IL-2/12 with or without TEPP-46 for 18 hours and glycolysis and OxPhos were measured using the seahorse extracellular flux analyser. Interestingly, TEPP-46 did not affect basal NK cell glycolysis but did reduce the glycolytic capacity of the cells, which is indicative of the glycolytic machinery available (**Fig. 5.10)**. Therefore, this data suggests that TEPP-46 may be impacting upon the metabolic machinery of the NK cells.

The effect of PKM2 activation on the level of NK cell OxPhos after 18 hours was also assessed. Surprisingly, although the rate of basal glycolysis was normal, there was a significant reduction in OxPhos levels in TEPP-46 treated cells (**Fig. 5.11 B).** This also supported the idea that TEPP-46 treatment was somehow leading to alterations in metabolic reprogramming. The maximum respiratory capacity (that is the maximum level of OxPhos) was also assessed. There was a significant decrease in the maximum respiratory capacity of TEPP-46 treated NK cells when compared with vehicle controls **(Fig. 5.11 C)**. This also supported the idea that TEPP-46 treatment was somehow leading to alterations in metabolic reprogramming.

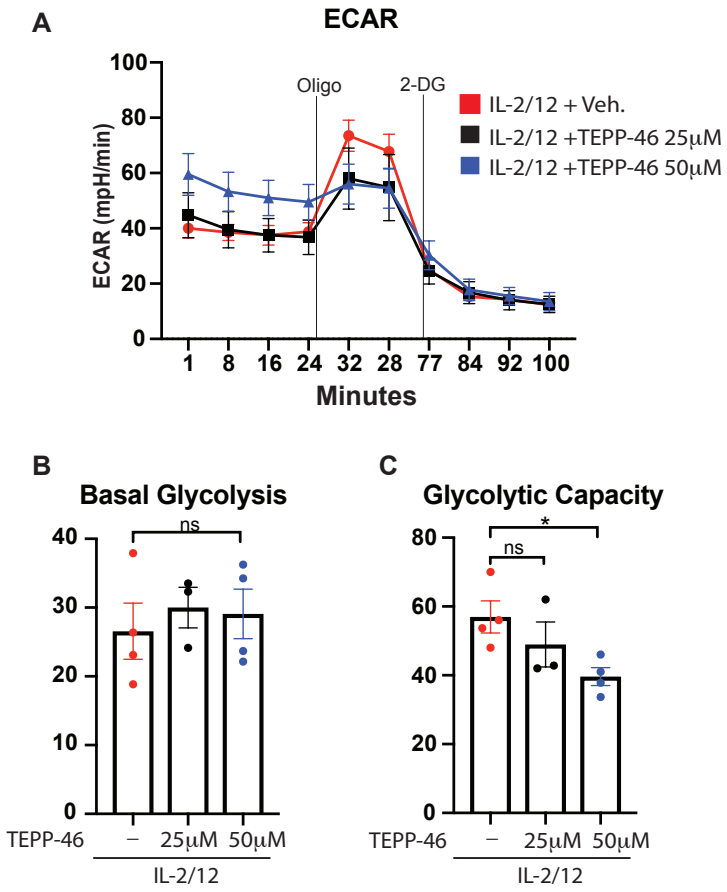

Figure 5.10. TEPP-46 treatment maintains normal levels of basal glycolysis but inhibits glycolytic capacity in IL-2/12 activated NK cells

Splenocytes from wild-type C57Bl/6 mice were expanded for 6 days in IL-15 (15ng/mL). On day 6 splenocytes were MACS purified and seeded at 2 x 10^6 NK cells per mL. NK cells were treated with IL-2/12 (330U/10ng per mL) +/- TEPP-46 (25 or 50 μM) or vehicle (DMSO – 0.1%) for 18 hours. After 18 hours, cells were changed into replete seahorse media plus cytokines at a concentration of 750,000 cells per well. Cells were analysed on a Seahorse 24 well extracellular flux analyser. (A) Representative seahorse plot of extracellular acidification rate (B) Pooled data for basal glycolysis from 3 (25 μM TEPP-46) or 4 (50 μM TEPP-46) individual experiments (C) Pooled data for glycolytic capacity from 3 (25 μM TEPP-46) or 4 (50 μM TEPP-46) individual experiments. Data are mean +/- S.E.M. Data were analysed by one-way ANOVA with a Tukey post-test (*$p < 0.05$, ns: non-significant)

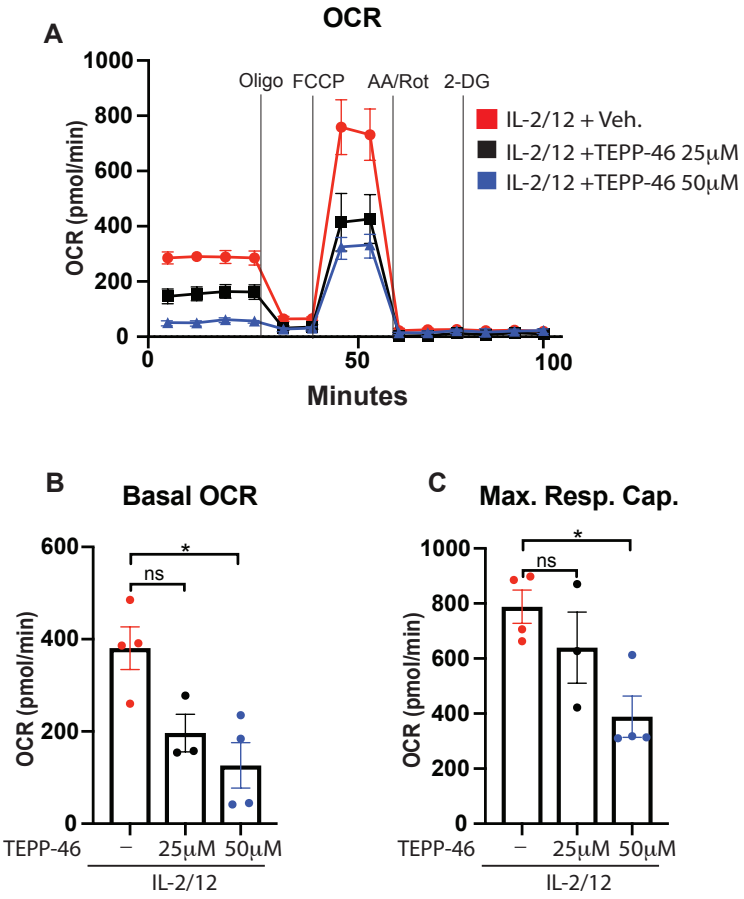

Figure 5. 11. 18 hour TEPP-46 treatment dramatically inhibits NK cell OxPhos

Splenocytes from wild-type C57Bl/6 mice were expanded for 6 days in IL-15 (15ng/mL). On day 6 splenocytes were MACS purified and seeded at 2 x 10^6 NK cells per mL. NK cells were treated with IL-2/12 (330U/10ng per mL) +/- TEPP-46 (25 or 50 μM) or vehicle (DMSO – 0.1%) for 18 hours. After 18 hours, cells were changed into replete seahorse media plus cytokines at a concentration of 750,000 cells per well. Cells were analysed on a Seahorse 24 well extracellular flux analyser. (A) Representative seahorse plot of oxygen consumption rate (B) Pooled data for basal OxPhos from 3 (25 μM TEPP-46) or 4 (50 μM TEPP-46) individual experiments (C) Pooled data for maximum respiratory rate from 3 (25 μM TEPP-46) or 4 (50 μM TEPP-46) individual experiments. Data are mean +/- S.E.M. Data were analysed by one-way ANOVA with a Tukey post-test (*p < 0.05, ns: non-significant)

5.7. Alterations in the levels of TCA cycle intermediates in NK cells following TEPP-46 treatment

To further explore metabolic pathways in TEPP-46 treated NK cells, untargeted metabolomics (GC/MS-TOF) analysis was carried out. Metabolic analysis was performed on unstimulated NK cells and NK cells stimulated with IL-2/12 in the presence or absence of TEPP-46 for 18 hours. Samples were outsourced to West Coast Metabolomics at UC Davis. Significantly altered metabolites are shown in **table 5.1**. In total, there were 24 significantly altered metabolites - 9 metabolites were increased and 15 metabolites were decreased with TEPP-46 treatment.

In order to interpret these data, over representation analysis to show the enrichment of the metabolites within biochemical pathways was carried out using the free online tool from the Wishart group, MetaboAnalyst [155]. This analysis tests whether a group of metabolites are represented more in specific metabolic pathways than they would be by chance. This was calculated using hypergeometric distribution relative to known mouse metabolite databases. Indeed, when this analysis was carried out, it was revealed that a number of pathways were enriched for. This can be visualised in table 5.2, as well as in the PCA plot **Fig 5.12.**

The most significantly enriched pathway was alanine, aspartate and glutamate metabolism. Consistent with the previous data obtained by Seahorse that there was lower OxPhos in TEPP-46 treated NK cells, the enrichment analysis also revealed that there was alterations in the TCA cycle. Although NK cell OxPhos is mainly fuelled by the Citrate Malate shuttle, it is thought that low levels of succinate, fumarate and malate may be needed to supplement early OxPhos. This indicates that increased pyruvate

kinase activity may prevent accumulation of substrates for OxPhos in IL-2/12 activated NK cells.

Metabolite Name	pValue	Fold Change (IL-2/12-TEPP-46: Vehicle)
Glutamine	0.03965591	0.229160568
Octadecylglycerol	0.00031151	0.39561214
Hexadecylglycerol	0.00094647	0.42300017
Aminomalonate	0.01449395	0.43646335
Zymosterol	0.00010311	0.52178691
Glutamic acid	0.03929801	0.60345881
N-carbamoylaspartate	0.03107503	0.63284945
4-aminobutyric acid	0.03928674	0.67869836
Succinic acid	0.00931608	0.68234348
Fumaric acid	0.00595528	0.69121338
Malic acid	0.00239731	0.71186892
Threitol	0.0105314	0.77470976
Ribitol	0.00446091	0.79236309
Cholesterol	0.03926424	0.84851883
3-aminoisobutyric acid	0.03762422	0.8616086
Glycine	0.02200827	1.19661062
Oxoproline	0.01997289	1.295114
N-acetylmannosamine	0.01907578	1.41837645
Linoleic acid	0.04286878	1.485887972
Lanosterol	0.01406469	1.51923077
Hydroxylamine	0.0401458	1.550269171
Pantothenic acid	0.00060344	1.62792512
1-hexadecanol	5.21E-05	1.82507772
Octadecanol	0.00017485	4.89549962

Table 5. 1 List of significantly altered metabolites between IL-2/12 + Vehicle and IL-2/12 + TEPP-46 (50μM)

Splenocytes from wild-type C57Bl/6 mice were expanded for 6 days in IL-15 (15ng/mL). On day 6 splenocytes were MACS purified and seeded at 2 x 10^6 NK cells per mL. NK cells were treated with IL-2/12 (330U/10ng per mL) +/- TEPP-46 (50 μM) or vehicle (DMSO – 0.1%) for 18 hours. After which, cells were washed twice in ice cold PBS and pellets were snap frozen in liquid nitrogen. Metabolites were later extracted by West Coast metabolomics and analysed using GC/MS-TOF mass spectrometry. Metabolites were normalized to the mean of the total ion chromatogram (mTIC). Peak areas were then calculated as a measure of intensity for each metabolite. Data were generated above through a student t test of significantly altered metabolite levels between IL-2/12 vehicle and IL-2/12 TEPP-46. Fold change of less than 1 indicates metabolite is reduced with TEPP-46. Fold change of greater than 1 indicates metabolite is increased with TEPP-46 treatment. Data were generated using n=5 mice per group. The cutoff p value was $p<0.05$

Pathway	Total	Hits	p Value
Alanine, aspartate and glutamate metabolism	24	6	7.57E-07
Nitrogen metabolism	9	3	0.00025726
D-Glutamine and D-glutamate metabolism	5	2	0.0022381
Arginine and proline metabolism	44	4	0.0039364
Butanoate metabolism	22	3	0.0041354
Glutathione metabolism	26	3	0.0067055
Steroid biosynthesis	35	3	0.015415
Pyrimidine metabolism	41	3	0.023634
Citrate cycle (TCA cycle)	20	2	0.036931

Table 5. 2 List of significantly enriched metabolic pathways for altered metabolites between IL-2/12 + Vehicle and IL-2/12 + TEPP-46 (50μM)

Splenocytes from wild-type C57Bl/6 mice were expanded for 6 days in IL-15 (15ng/mL). On day 6 splenocytes were MACS purified and seeded at 2 x 10^6 NK cells per mL. NK cells were treated with IL-2/12 (330U/10ng per mL) +/- TEPP-46 (50 μM) or vehicle (DMSO – 0.1%) for 18 hours. After which, cells were washed twice in ice cold PBS and pellets were snap frozen in liquid nitrogen. Metabolites were later extracted by West Coast metabolomics and analysed using GC/MS-TOF mass spectrometry. Metabolites were normalized to the mean of the total ion chromatogram (mTIC). Peak areas were then calculated as a measure of intensity for each metabolite. Data were generated above through a student t test of significantly altered metabolite levels between IL-2/12 vehicle and IL-2/12 TEPP-46. Data were generated using n=5 mice per group. The cutoff p value was $p<0.05$. Data were then entered into Metaboanalyst and assessed for enrichment of defined mouse metabolic pathways

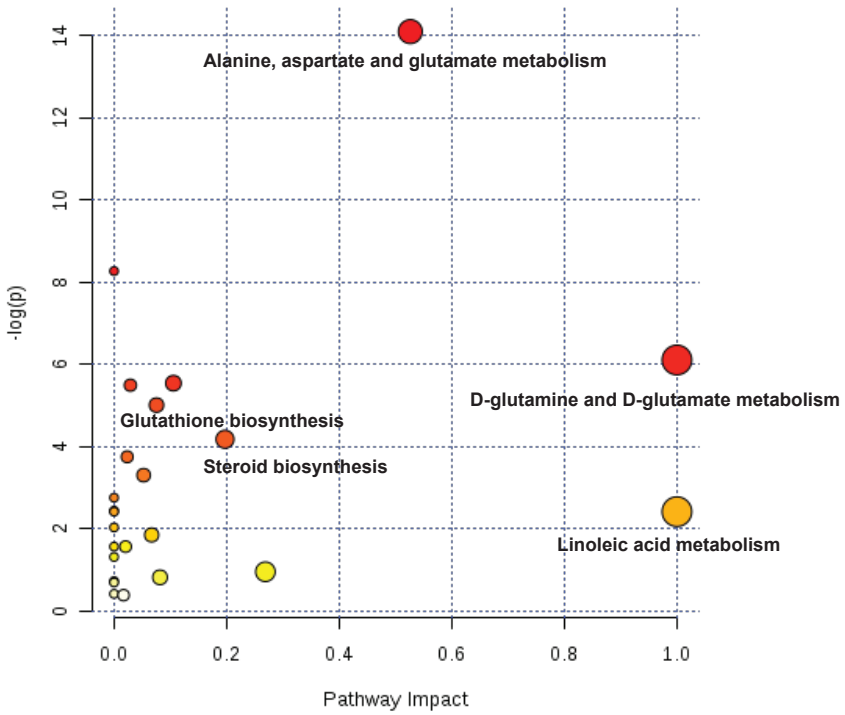

Figure 5. 12. Metabolic pathway enrichment analysis comparing IL-2/12 + Vehicle and IL-2/12 + TEPP-46 (50μM):

Splenocytes from wild-type C57Bl/6 mice were expanded for 6 days in IL-15 (15ng/mL). On day 6 splenocytes were MACS purified and seeded at 2 x 10^6 NK cells per mL. NK cells were treated with low dose IL-15 (Unstimulated) (5ng/mL) IL-2/12 (330U/10ng per mL) +/- TEPP-46 (50 μM) or vehicle (DMSO – 0.1%) for 18 hours. After which, cells were washed twice in ice cold PBS and pellets were snap frozen in liquid nitrogen. Metabolites were later extracted by West Coast metabolomics and analysed using GC/MS-TOF mass spectrometry. Metabolites were normalized to the mean of the total ion chromatogram (mTIC). Peak areas were then calculated as a measure of intensity for each metabolite. Data were generated above through a student t test of significantly altered metabolite levels between IL-2/12 vehicle and IL-2/12 TEPP-46. Data were then entered into metaboanalyst and a chart was generated comparing the p value of enriched pathways vs the pathway impact (which is representative of the centrality of the changed metabolites within the pathways). Data were generated using n=5 mice per group. The cutoff p value was $p<0.05$

5.8. Glycolytic intermediates are normal in IL-2/12 + TEPP-46 treated NK cells

Next the metabolic intermediates of glycolysis were analysed. While there was a significant increase in the level of glycolytic intermediates in IL-2/12 stimulated NK cells, there was no difference with TEPP-46 treatment. This indicates that the glucose fuelling of this pathway was functional (**Fig. 5.13**). Therefore the decreased glycolytic capacity observed in the Seahorse may hint at a defect in the expression of glycolytic machinery as opposed to fuelling.

Similarly, It was observed that the levels of key pentose phosphate pathway metabolites (an off-shoot of glycolysis) ribose-5-phosphate and ribulose-5-phosphate were normal in IL-2/12 TEPP-46 treated cells relative to IL-2/12 vehicle only (**Fig. 5.14)**. This similarly supports the idea that glucose fuelling was normal.

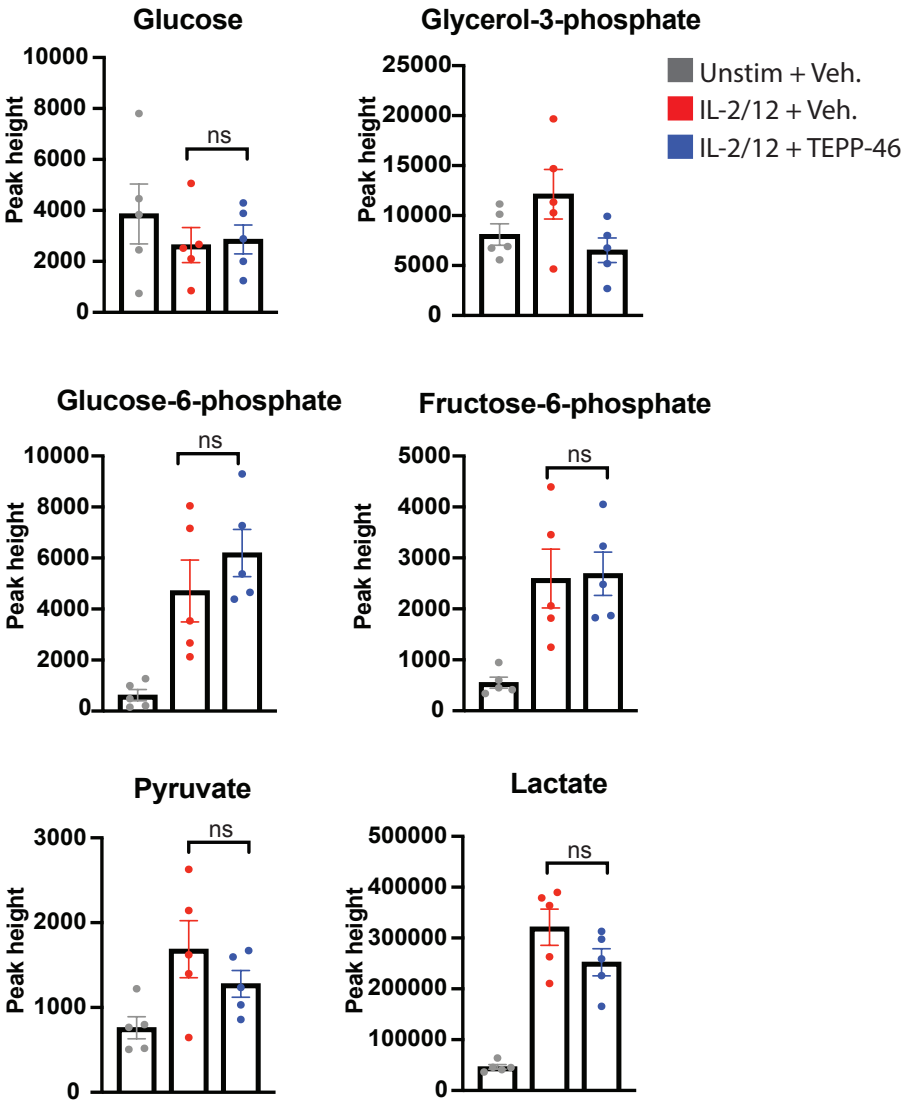

Figure 5. 13. Fuelling of glycolysis is maintained in IL-2/12-activated cultured NK cells

Splenocytes from wild-type C57Bl/6 mice were expanded for 6 days in IL-15 (15ng/mL). On day 6 splenocytes were MACS purified and seeded at 2 x 10^6 NK cells per mL. NK cells were treated with low dose IL-15 (Unstimulated) (5ng/mL IL-15) IL-2/12 (330U/10ng per mL) +/- TEPP-46 (50 μM) or vehicle (DMSO – 0.1%) for 18 hours. After which, cells were washed twice in ice cold PBS and pellets were snap frozen in liquid nitrogen. Metabolites were later extracted by West Coast metabolomics and analysed using GC/MS-TOF mass spectrometry. Metabolites were normalized to the mean of the total ion chromatogram (mTIC). Peak areas were then calculated as a measure of intensity for each metabolite. Data were then grouped into glycolysis associated metabolites and analysed using one-way ANOVA with Tukey's post-test. (ns: non-significant)

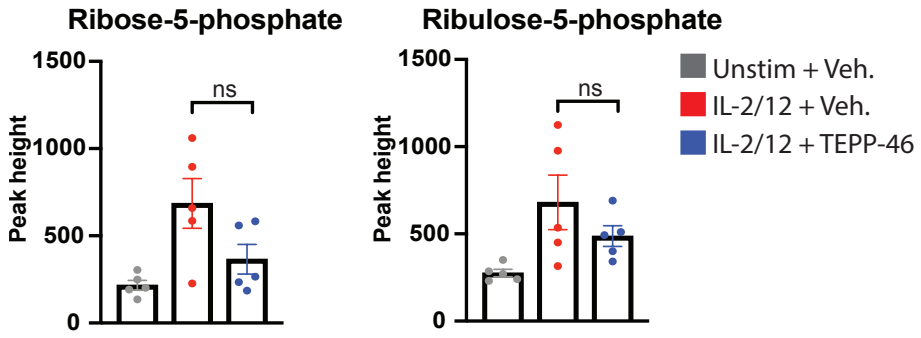

Figure 5. 14. Levels of key pentose phosphate intermediates are maintained in IL-2/12-activated cultured NK cells

Splenocytes from wild-type C57Bl/6 mice were expanded for 6 days in IL-15 (15ng/mL). On day 6 splenocytes were MACS purified and seeded at 2 x 10^6 NK cells per mL. NK cells were treated with low dose IL-15 (Unstimulated) (5ng/mL) IL-2/12 (330U/10ng per mL) +/- TEPP-46 (50 μM) or vehicle (DMSO – 0.1%) for 18 hours. After which, cells were washed twice in ice cold PBS and pellets were snap frozen in liquid nitrogen. Metabolites were later extracted by West Coast metabolomics and analysed using GC/MS-TOF mass spectrometry. Metabolites were normalized to the mean of the total ion chromatogram (mTIC). Peak areas were then calculated as a measure of intensity for each metabolite. Data were then grouped into pentose phosphate pathway associated metabolites and analysed using one-way ANOVA with Tukey's post-test. (ns: non-significant)

5.9. Reduced TCA intermediates in TEPP-46-treated IL-2/12-activated NK cells

As the enrichment analysis revealed significance of the TCA cycle, it was next investigated which metabolites in this pathway were altered. The levels of citrate were normal (**Fig. 5.15).** The Finlay lab has previously demonstrated that citrate synthesis is mainly fuelled by glucose [86]. This supports the idea that glucose metabolism was normal. However, It was observed that the levels of succinate, fumarate and malate were lower in TEPP-46 treated cells than vehicle controls. Interestingly, the Finlay lab has also shown that the levels of fumarate and succinate are mainly maintained by glutamine metabolism [109].

In support of this, the levels of both glutamine and glutamate were significantly lower in IL-2/12 activated NK cells treated with TEPP-46 (**Fig. 5.16)**. In contrast, the levels of the other amino acids analysed were normal, with the exception of glycine. There was a significant increase in the levels of cellular glycine which has a major role in the synthesis of antioxidant molecules such as glutathione and nucleic acids [156].

Generally, these metabolomics data indicate that glycolysis is maintained in cultured IL-2/12 activated NK cells in the presence of TEPP-46, but there are specific defects the glutamine fuelling of the TCA cycle.

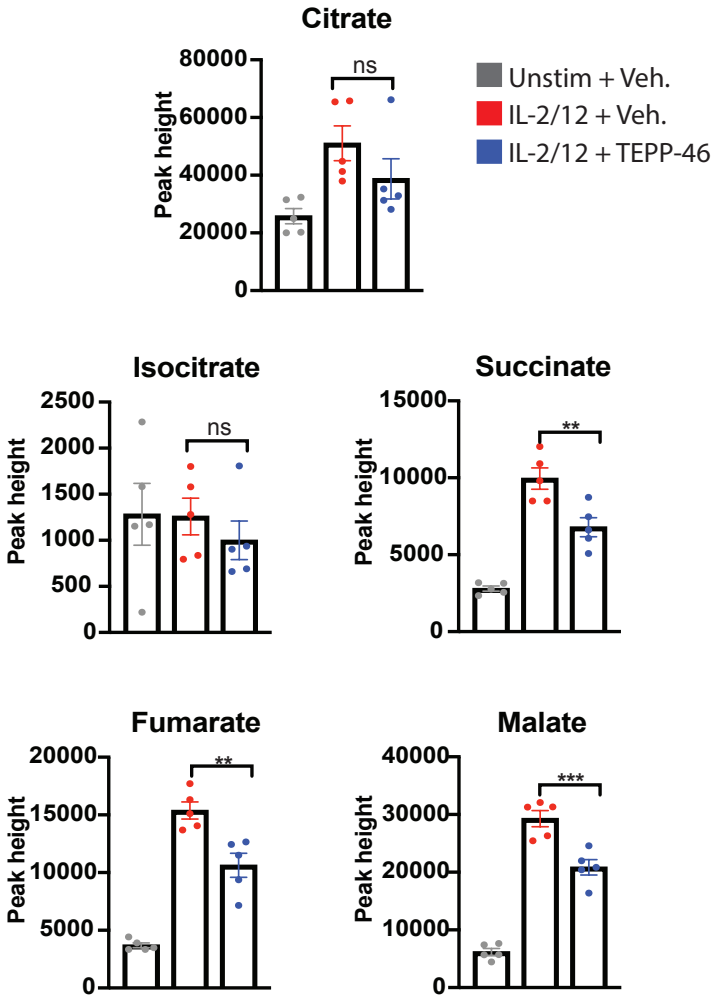

Figure 5. 15. Fuelling of the TCA pathway is altered in IL-2/12-activated cultured NK cells

Splenocytes from wild-type C57Bl/6 mice were expanded for 6 days in IL-15 (15ng/mL). On day 6 splenocytes were MACS purified and seeded at 2 x 10^6 NK cells per mL. NK cells were treated with low dose IL-15 (Unstimulated) (5ng/mL) IL-2/12 (330U/10ng per mL) +/- TEPP-46 (50 μM) or vehicle (DMSO – 0.1%) for 18 hours. After which, cells were washed twice in ice cold PBS and pellets were snap frozen in liquid nitrogen. Metabolites were later extracted by West Coast metabolomics and analysed using GC/MS-TOF mass spectrometry. Metabolites were normalized to the mean of the total ion chromatogram (mTIC). Peak areas were then calculated as a measure of intensity for each metabolite. Data were then grouped into TCA-associated metabolites and analysed using one-way ANOVA with Tukey's post-test. (ns: non-significant)

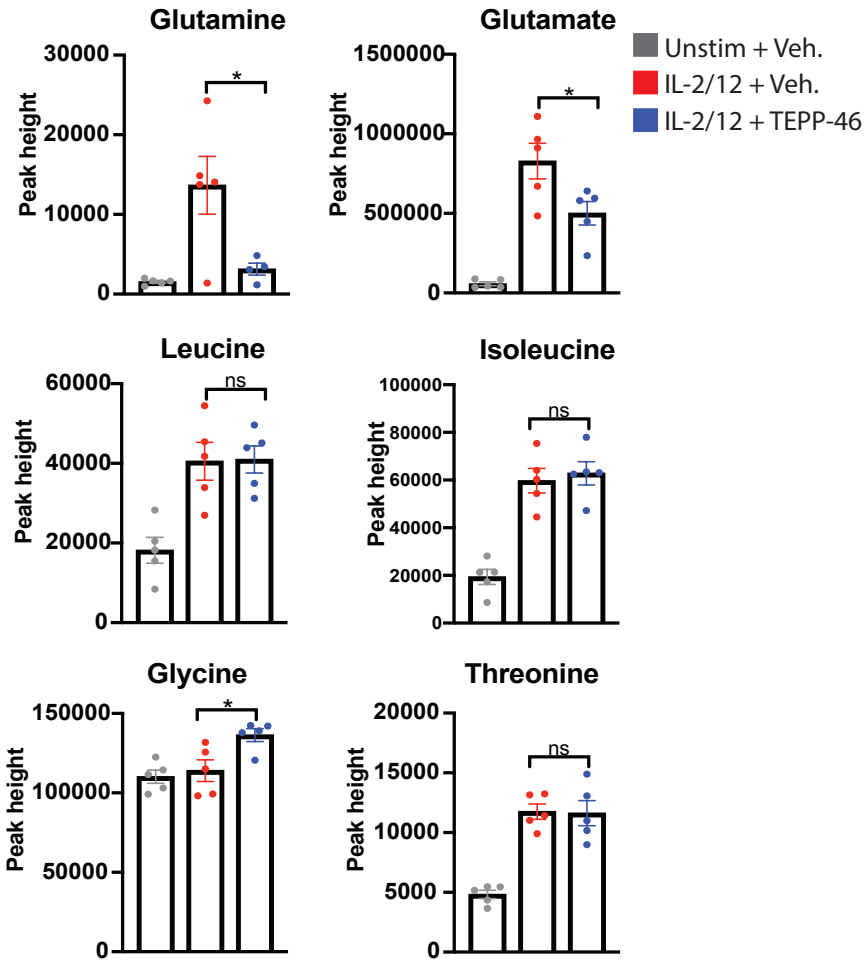

Figure 5. 16. Levels of key amino acids were altered in IL-2/12-activated cultured NK cells

Splenocytes from wild-type C57Bl/6 mice were expanded for 6 days in IL-15 (15ng/mL). On day 6 splenocytes were MACS purified and seeded at 2 x 10^6 NK cells per mL. NK cells were treated with low dose IL-15 (Unstimulated) (5ng/mL IL-15) IL-2/12 (330U/10ng per mL) +/- TEPP-46 (50 μM) or vehicle (DMSO – 0.1%) for 18 hours. After which, cells were washed twice in ice cold PBS and pellets were snap frozen in liquid nitrogen. Metabolites were later extracted by West Coast metabolomics and analysed using GC/MS-TOF mass spectrometry. Metabolites were normalized to the mean of the total ion chromatogram (mTIC). Peak areas were then calculated as a measure of intensity for each metabolite. Data were then grouped into amino acid-associated metabolites. One outlier was omitted from glutamine using a Grubbs test (α = 0.05). Data were then analysed using one-way ANOVA with Tukey's post-test. (ns: non-significant)

5.10. Reduced cMyc expression in TEPP-46 treated NK cells

The data show dysregulated glutamine metabolism in cultured IL-2/12 activated NK cells treated with TEPP-46. Whether low intracellular glutamine was a result of increased utilisation, or as a result of reduced glutamine uptake was investigated. In order to test this, supernatants were taken from cultured NK cells treated with IL-2/12 +/- TEPP-46 or Vehicle for 18 hours and analysed using a YSI bioanalyser. This machine consists of an enzymatically loaded electrode, that will generate an electrical signal when glutamine is processed through distinct enzymatic reactions. This is calibrated to give exact millimolar concentrations of glutamine. The data showed that NK cells treated with IL-2/12 + TEPP-46 (50 μM) had impaired glutamine uptake when compared to controls **(Fig. 5.17 A)**. Therefore, the data suggest that decreased intracellular glutamine levels were as a result of reduced glutamine uptake.

The Finlay lab has previously published that glutamine is important for the expression of the transcription factor c-Myc. cMyc was shown to be dramatically downregulated in low glutamine conditions [109]. Indeed, IL-2/12 + TEPP-46 treated NK cells had reduced cMyc protein expression when compared to vehicle treated controls **(Fig, 5.17 B)**

This indicates that PKM2 activation with TEPP-46 leads to reduced cMyc expression in IL-2/12 cultured NK cells.

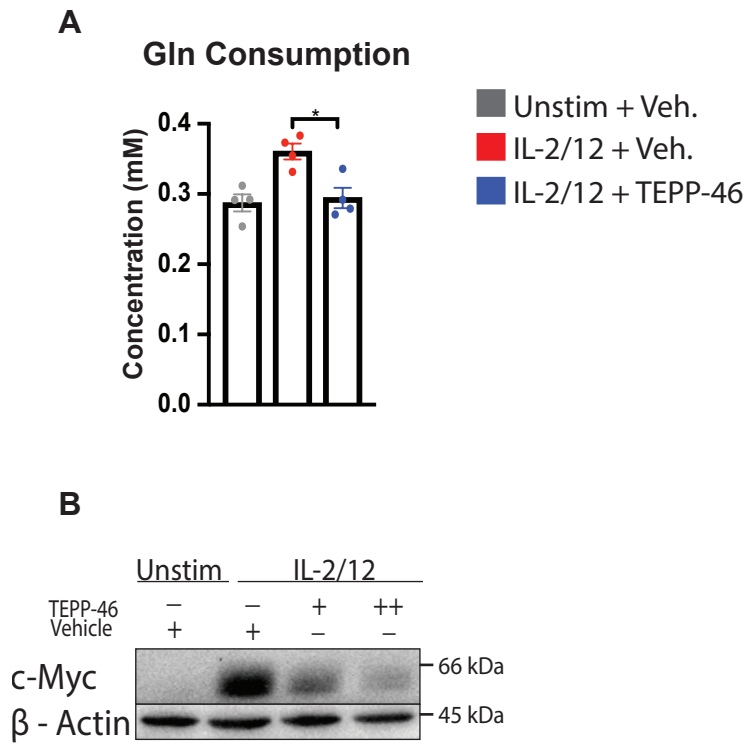

Figure 5. 17. TEPP-46 of IL-2/12 activated cultured NK cells prevents normal glutamine uptake and cMyc protein expression after 18 hours

Splenocytes from wild-type C57Bl/6 mice were expanded for 6 days in IL-15 (15ng/mL). On day 6 splenocytes were MACS purified and seeded at 2 x 10^6 NK cells per mL. NK cells were treated with low dose IL-15 (Unstimulated) (5ng/mL) or IL-2/12 (330U/ 10ng per mL) +/- TEPP-46 (50 μM) or vehicle (DMSO – 0.1%) for 18 hours. (A) Supernatants were then harvested and snap frozen. Supernatatants were then sent for analysis by YSI Bioanalyser. Glutamine consumption was calculated by subtracting the concentration of glutamine in media from a blank "no cell" media control subjected to the same analysis. (B) Cells were lysed at 10 x 10^6 per mL and analysed by western blot for cMyc expression. Loading control was actin. Data for glutamine consumption are from 4 independent experiments with 3 technical replicates each. Western blot is representative of 3 individual experiments. Data were analysed using one-way ANOVA with Tukey's post-test. (*$p<0.05$)

5.11. TEPP-46 mediated PKM2 activation has a modest impact on the NK cell transcriptome

Given the impact of PKM2 activation on cMyc expression, it was next investigated whether TEPP-46 affected the NK cell transcriptome. RNA sequencing analysis was conducted on cultured NK cells treated with either IL-2/12 + Vehicle or IL-2/12 + TEPP-46. Partek genomics suite was then used to compare significantly altered genes by fold change and p value. cMyc is generally known as a transcriptional "enhancer" so therefore the fold threshold cutoff at 1.2 was set at in order to see any possible alterations in Myc genes.

Interestingly, some key Myc target genes were significantly altered with TEPP-46 treatment of IL-2/12 activated cultured NK cells. The level of *Slc7a5* a key amino acid transporter was significantly decreased, along with *Pfkm* and *Shmt2*, which have also been shown to be cMyc targets [157, 158]. There was also a significant increase in expression of the apoptosis related gene, *Bcl2,* which is normally repressed by cMyc [159]. This indicates that the decreased cMyc expression in IL-2/12 activated NK cells may have a knock on effect on the cells transcriptional landscape. Interestingly, the reduced expression of Pfkm, a glycolytic gene, may help explain the reduced glycolytic capacity in IL-2/12 activated NK cells treated with TEPP-46.

Along with these potential cMyc targets, there was also significant alterations in 125 different genes**.** In order to evaluate whether there was any overrepresentation of these genes in biological pathways, gene enrichment analysis was carried out using MetaScape. Pathways that were enriched for included ''Nucleoside biosynthetic processes', 'Carbon Metabolism' and interestingly, 'Regulation of mitochondrial translation'. This observation of reduced mitochondrial translation may also be a

contributing factor to the reduced OxPhos observed after IL-2/12 + TEPP-46 overnight treatment. However, overall, 125 gene changes is quite low. Indeed, at a fold change cutoff of 1.5, there were only 24 significantly altered genes. Therefore, it may be surmised that alterations in PKM2 activity do not vastly alter the transcriptional landscape of NK cells.

Category	Term	Description	LogP	# of Genes	Genes
GO Biological Processes	GO:0044283	**Small molecule biosynthetic process**	-8.83402	20/652	Aprt,Coq7,Fdft1,Galk1, Hsd17b7,Fabp5,Lipg,Mvk, Nme2,Pcx,Pfkm, Spr,Upp1,Asns, Pmvk,Shmt2,Atic,Mvd, Phgdh,Dnph1,Atp1b1, Pmm1,Sult2b1,Enpp4, Ahcy,Pcyt2,Gpt2
Reactome Gene Sets	R-MMU-191273	**Cholesterol biosynthesis**	-8.10722	6/26	Fdft1,Hsd17b7,Mvk,Pmvk, Acat2,Mvd,Sult2b1,Spr,Fa bp5,Pcx,Pcyt2,Galk1, Bpnt,Afp, Bcl2,Lipg,Phgdh,Ahcy,Aacs
GO Biological Processes	GO:0009116	**Nucleoside metabolic process**	-4.86486	6/88	Aprt,Nme2,Upp1,Atic, Enpp4,Ahcy, Dnph1,Galk1,Pfkm,Pde4b, Pde8a, Shmt2,Acat2,Lsm7,Pabpc4
GO Biological Processes	GO:0008626	**Granzyme-mediated apoptotic signaling**	-4.49476	3/11	Gzmd,Gzme,Gzmf, Bcl2,Satb1
KEGG Pathway	mmu01200	**Carbon metabolism**	-4.14336	6/118	Pcx,Pfkm,Shmt2,Gpt2, Acat2, Phgdh,Spr,Asns,Nars,Mars Ahcy,Galk1,Fabp5,Lipg, Atic,Aacs,Slc7a5
GO Biological Processes	GO:0070129	**Regulation of mitochondrial translation**	-3.32536	3/26	Rcc1l,Shmt2,Mtg1, Trmt10a
GO Biological Processes	GO:0042558	**Pteridine-containing compound metabolic process**	-3.01653	3/33	Spr,Shmt2,Atic
KEGG Pathway	mmu00051	**Fructose and mannose metabolism**	-2.94123	3/35	Pfkfb1,Pfkm,Pmm1,Galk1, Fabp5,Pcx

Table 5. 3 TEPP-46 treatment of IL-2/12 activated cultured NK cells resulted in altered expression of 125 genes after 18 hours

125 differentially expressed genes were initially identified using Partek analysis at a fold change cutoff of 1.2. Data was then analysed for enrichment of pathways using Metascape. Data were filtered on canonical pathways for KEGG, Reactome gene sets an GO biological processes**.**

5.12. TEPP-46 treatment results in decreased protein expression of key mitochondrial electron transport chain protein ATP5B

It was observed through RNA sequencing that there was pathway enrichment with IL-2/12 + TEPP-46 treatment for genes involved in the regulation of mitochondrial translation. As one of the main metabolic phenotypes we observed with TEPP-46 treatment of IL-2/12 activated NK cells (relative to IL-2/12 + Vehicle controls) was reduced oxygen consumption rate, it was next assessed as to whether there was any alteration in the expression of mitochondrial components. The protein chosen to test this was the mitochondrial electron transport chain ATP Synthase subunit 5B (ATP5B). This is a key subunit of ATP synthase that is involved in the generation of ATP. The level of this ATP5B protein was assessed using flow cytometry. Cultured NK cells were activated with IL-2/12 +/- TEPP-46 or Vehicle for 18 hours. Interestingly, the levels of ATP5B protein were reduced in TEPP-46 treated cells relative to vehicle control treated cells (**Fig. 5.18)**. This may indicate that cells treated with TEPP-46 displayed reduced OxPhos as a result of mitochondrial dysfunction.

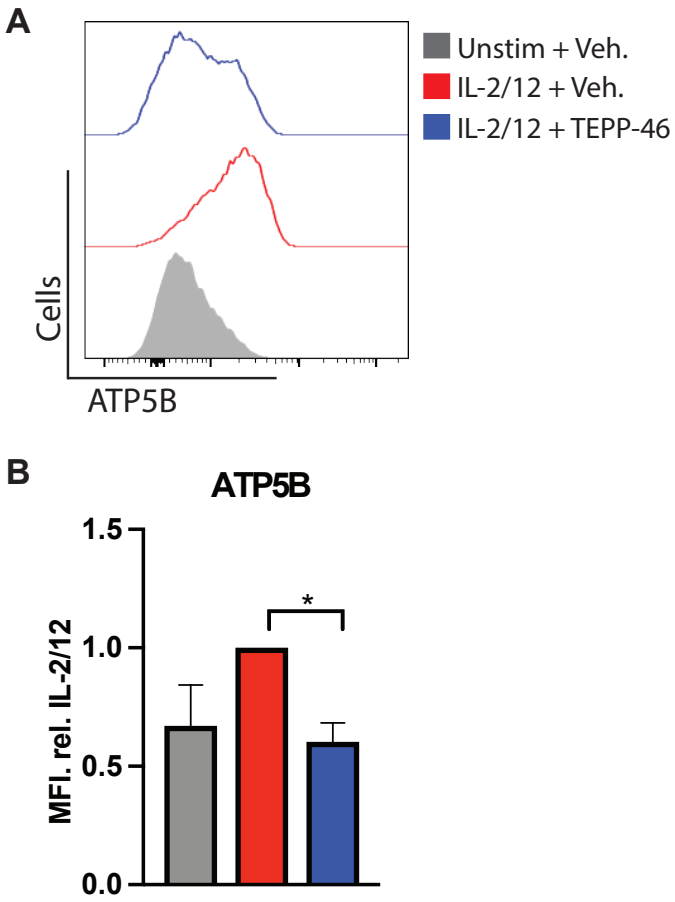

Figure 5. 18. TEPP-46 treatment of IL-2/12 stimulated NK cells results in reduced expression of key mitochondrial subunit ATP5B

Splenocytes from wild-type C57Bl/6 mice were expanded for 6 days in IL-15 (15ng/mL). On day 6 splenocytes were MACS purified and seeded at 2 x 10^6 NK cells per mL. NK cells were treated with low dose IL-15 (Unstimulated) (5ng/mL) or IL-2/12 (330U/ 10ng per mL) +/- TEPP-46 (50 μM) or vehicle (DMSO – 0.1%) for 18 hours. NK cells were then stained for flow cytometry and identified as $NK1.1^+NKp46^+CD3^-$ cells. The level of ATP5B expression was then assessed by MFI (A) Representative histogram of ATP5B expression in NK cells treated with low dose IL-15 (5ng/mL), IL-2/12 (330 U/10ng per mL) +/- TEPP-46 (50 μM) or vehicle (DMSO – 0.1%) for 18 hours (B) pooled data for ATP5B expression in NK cells from 3 individual expression. Data are displayed as S.E.M and are normalized to IL-2/12. Data were analysed using one-way ANOVA with Tukey's post-test. (*$p<0.05$)

5.13. TEPP-46 treatment increases reactive oxygen species production.

The RNAseq data revealed that two of the most significantly upregulated genes in IL-2/12 activated cells treated with TEPP-46 were members of the metallothionein family, *Mt1* and *Mt2* (**Fig. 5.19)**. These two genes were also increased in LPS activated BMDM treated with a similar PKM2 activating compound DASA-58 [119]. Metallothioneins are a set of zinc responsive proteins that have antioxidant properties [160]. Indeed, the expression levels of metallothionein have been shown to increase several times in response to reactive oxygen species (ROS) [161, 162]. Indeed, when. cultured NK cells were activated with IL-2/12 plus TEPP-46 there were increased levels of ROS compared to vehicle controls, as measured using the flow cytometric ROS probe DCFDA **(Fig. 5.20).**

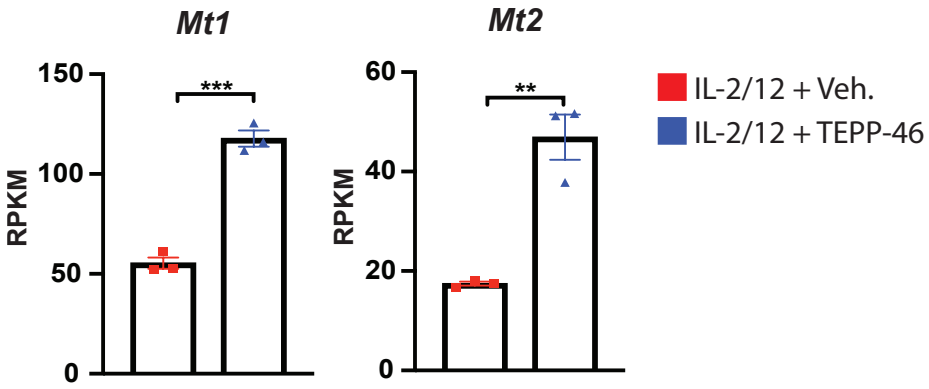

Figure 5.19. TEPP-46 treatment of IL-2/12 stimulated NK cells results in increased expression of metallothionein genes

Splenocytes from wild-type C57Bl/6 mice were expanded for 6 days in IL-15 (15ng/mL). On day 6 splenocytes were MACS purified and seeded at 2 x 10^6 NK cells per mL. NK cells were treated with IL-2/12 (330U/ 10ng per mL) +/- TEPP-46 (50 μM) or vehicle (DMSO – 0.1%) for 18 hours. After 18 hours, cells were centrifuged, lysed and RNA was extracted. RNA was analysed by HiSeq RNA sequencing. Data was initially analysed using Partek with F.C 1.2 and then sorted by fold change on DEG with a p value of less than 0.05. Metallothioneins were identified as being significantly upregulated, Data are displayed as reads per kilobase of transcript, per million mapped reads (RPKM). Data were obtained from 3 biological replicates and are displayed as S.E.M. Data were analysed by an unpaired student t test (**p<0.01, ***p<0.001)

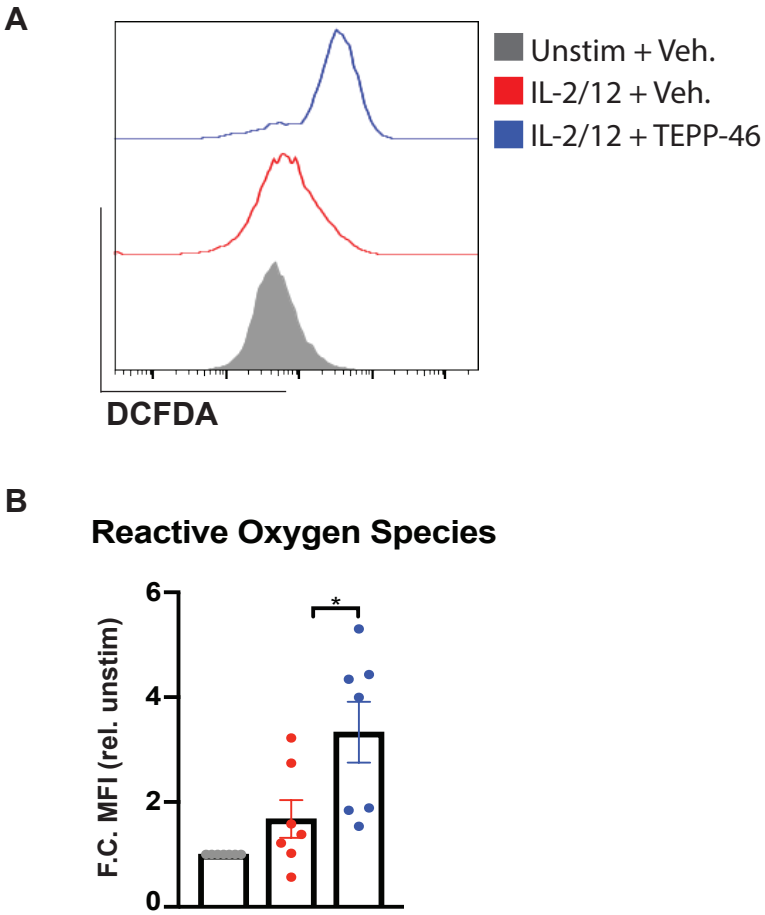

Figure 5. 20. TEPP-46 treatment of IL-2/12 stimulated NK cells results in increased levels of reactive oxygen species

Splenocytes from wild-type C57Bl/6 mice were expanded for 6 days in IL-15 (15ng/mL). On day 6 splenocytes were MACS purified and seeded at 2 x 10^6 NK cells per mL. NK cells were treated with low dose IL-15 (Unstimulated) (5ng/mL) or IL-2/12 (330U/ 10ng per mL) +/- TEPP-46 (50 μM) or vehicle (DMSO – 0.1%) for 18 hours. NK cells were then stained for flow cytometry and identified as $NK1.1^+NKp46^+CD3^-$ cells. The level of ROS was then assessed by DCFDA staining (A) Representative histogram of DCFDA staining in NK cells treated with low does IL-15 (5ng/mL), IL-2/12 (330 U/10ng per mL) +/- TEPP-46 (50 μM) or vehicle (DMSO – 0.1%) for 18 hours (B) pooled data for DCFDA MFI in NK cells from 7 individual experiments. Data are displayed as S.E.M and are normalized to unstimulated. Data were analysed using one-way ANOVA with Tukey's post-test. (*$p<0.05$)

5.14. Partial rescue of cMyc expression but not IFNγ production with antioxidant treatment

TEPP-46 treatment of IL-2/12 activated NK cells increased levels of intracellular ROS. Next it was investigated whether TEPP-46-induced ROS was responsible the signalling and functional changes in these NK cells. In order to test this, mitochondrial reactive oxygen species scavenger mitoquinol was utilised. As there was a profound defect in cMyc expression in IL-2/12 activated NK cells treated with TEPP-46, it was investigated whether MitoQ could rescue reduced Myc. IL-2/12 activated NK cells were treated with or without TEPP-46 and MitoQ. MitoQ had a small, but statistically insignificant effect on TEPP-induced mitochondrial ROS when used at concentrations recommended in the literature (**Fig. 5.21 A)**. As mitoQ only resulted in a slight reduction in ROS, It is tempting to hypothesize that higher concentrations or use of other antioxidants such as N-acetylcysteine may provide better protection against ROS.

However, the small protection provided by MitoQ did result in increased expression of cMyc in IL-2/12 TEPP-46 treated cells relative to TEPP-46 alone (**Fig. 5.22. A)** . This indicates that ROS may negatively impact cMyc expression in NK cells. As MitoQ could partially rescue cMyc expression, the level of IFNγ production by these cells was also assessed (**Fig. 5.22 B)**. Interestingly, the addition of MitoQ was not sufficient to rescue the percentage of cells that are expressing IFNγ. However, this may be due to the inefficacy of the MitoQ to completely scavenge ROS produced by TEPP-46 treated NK cells. Alternate antioxidants such as NAC may provide more protection.

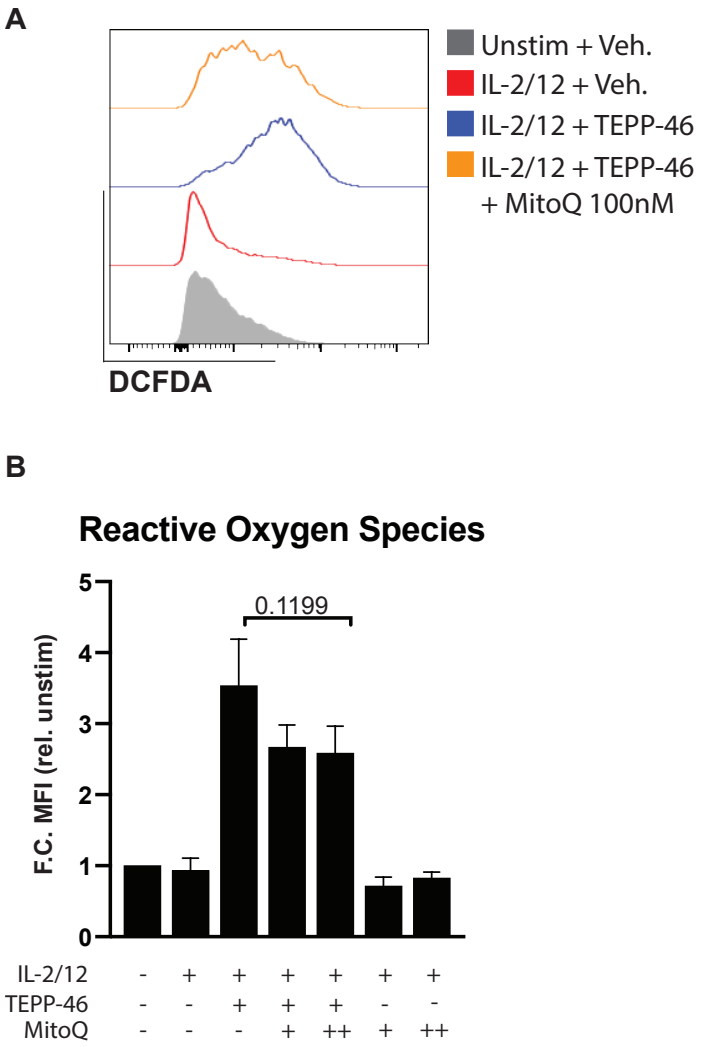

Figure 5.21. Mitochondrial ROS scavenger MitoQ only partially reduces TEPP-46 induced ROS in IL-2/12 activated NK cells

Splenocytes from wild-type C57Bl/6 mice were expanded for 6 days in IL-15 (15ng/mL). On day 6 splenocytes were MACS purified and seeded at 2 x 10^6 NK cells per mL. NK cells were treated with low dose IL-15 (Unstimulated) (5ng/mL IL-15) or IL-2/12 (330U/ 10ng per mL). IL-2/12 activated cells were additionally treated +/- TEPP-46 (50 μM) alone or MitoQ 50nM (+) or 100nM (++) alone for 18 hours. TEPP-46 treated cells were additionally also treated with MitoQ 50nM (+) or 100nM (++). All conditions were vehicle controlled. NK cells were stained for flow cytometry. NK cells were identified as $NK1.1^+NKp46^+CD3^-$ cells. The level of ROS was then assessed by DCFDA staining (A) Representative histogram of DCFDA staining in NK cells treated with low does IL-15 (5ng/mL), IL-2/12 (330 U/10ng per mL) +/- TEPP-46 (50 μM) or IL-2/12 + TEPP-46 (50 μM) + MitoQ (100nM) for 18 hours (B) pooled data for DCFDA MFI in NK cells from 3 individual experiments. Data are displayed as S.E.M and are normalized to unstimulated. Data were analysed using one-way ANOVA with Tukey's post-test. (*$p<0.05$)

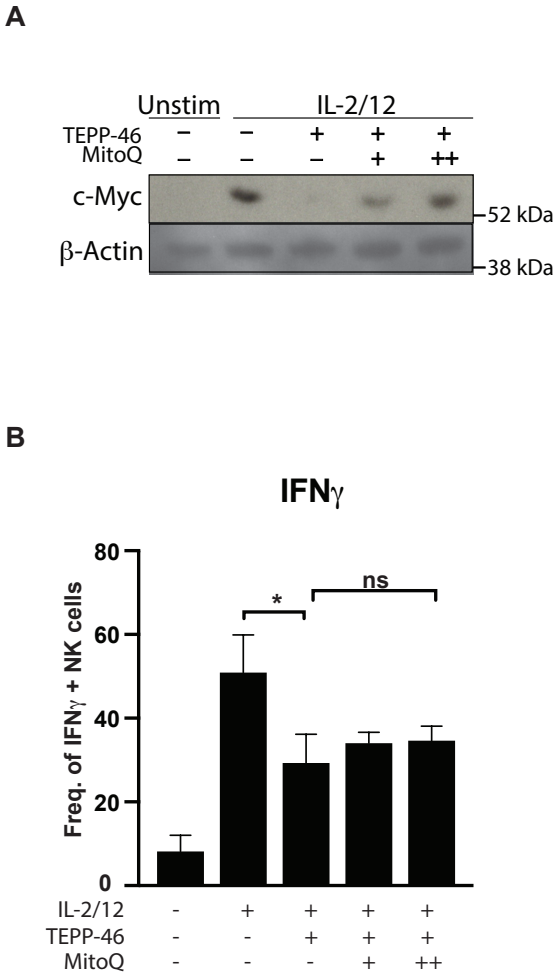

Figure 5. 22. Mitochondrial ROS scavenger MitoQ does not rescue IFNγ production in TEPP-46-treated NK cells

Splenocytes from wild-type C57Bl/6 mice were expanded for 6 days in IL-15 (15ng/mL). On day 6 splenocytes were MACS purified and seeded at 2 x 10^6 NK cells per mL. NK cells were treated with low dose IL-15 (5ng/mL) or IL-2/12 (330U/ 10ng per mL). IL-2/12 activated cells were additionally treated +/- TEPP-46 (50 μM) alone or MitoQ 50nM (+) or 100nM (++) alone for 18 hours. TEPP-46 treated cells were additionally also treated with MitoQ 50nM (+) or 100nM (++). All conditions were vehicle controlled. After 16 hours cells were treated with BD GolgiPlug (Brefeldin A). At the 20 hour timepoint NK cells were stained for flow cytometry. NK cells were identified as $NK1.1^+NKp46^+CD3^-$ cells. Cells were fixed and permeabilised with BD Cytofix/Cytoperm. Cells were run on a LSR II or BD Fortessa flow cytometer (A) Representative western blot cMyc expression with TEPP-46 and mitoQ treatment of IL-2/12 activated NK cells after 18 hours. Loading control was actin (B) Pooled data for of IFNγ positive NK cells in IL-2/12 activated NK cells treated with TEPP-46/MitoQ. Western Blot is representative of 3 experiment. Pooled flow cytometry data is from 3 experiments. Data are displayed as S.E.M. Data were analysed using one-way ANOVA with Tukey's post-test. (*p<0.05

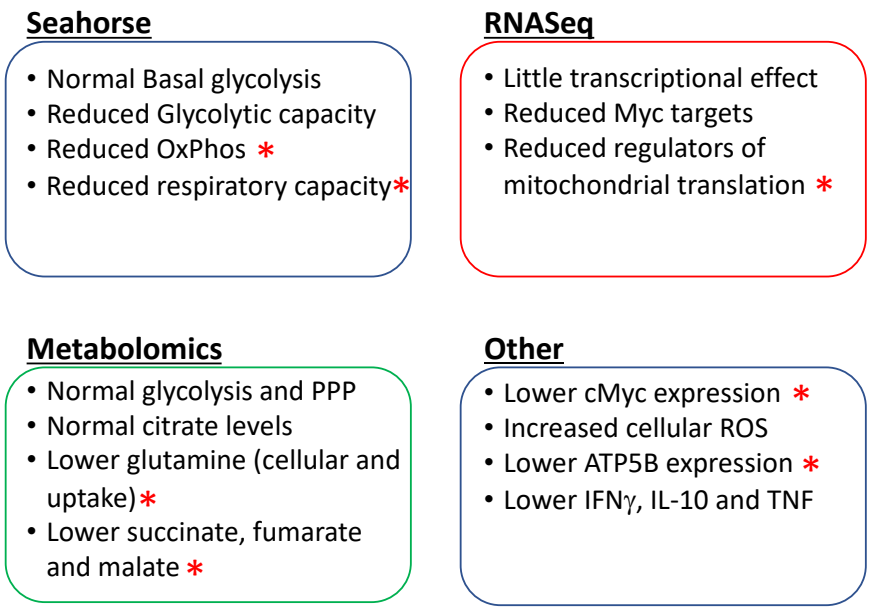

Figure 5. 23. Summary of changes induced by PKM2 activation in IL-2/12 stimulated NK cells

Table shows main findings of metabolic and functional data obtained in this chapter. Points represent changed parameters in response to TEPP-46 treatment of IL-2/12 activated NK cells relative to IL-2/12 activated cells treated with vehicle control. *denotes data that are consistent with reduced OxPhos levels

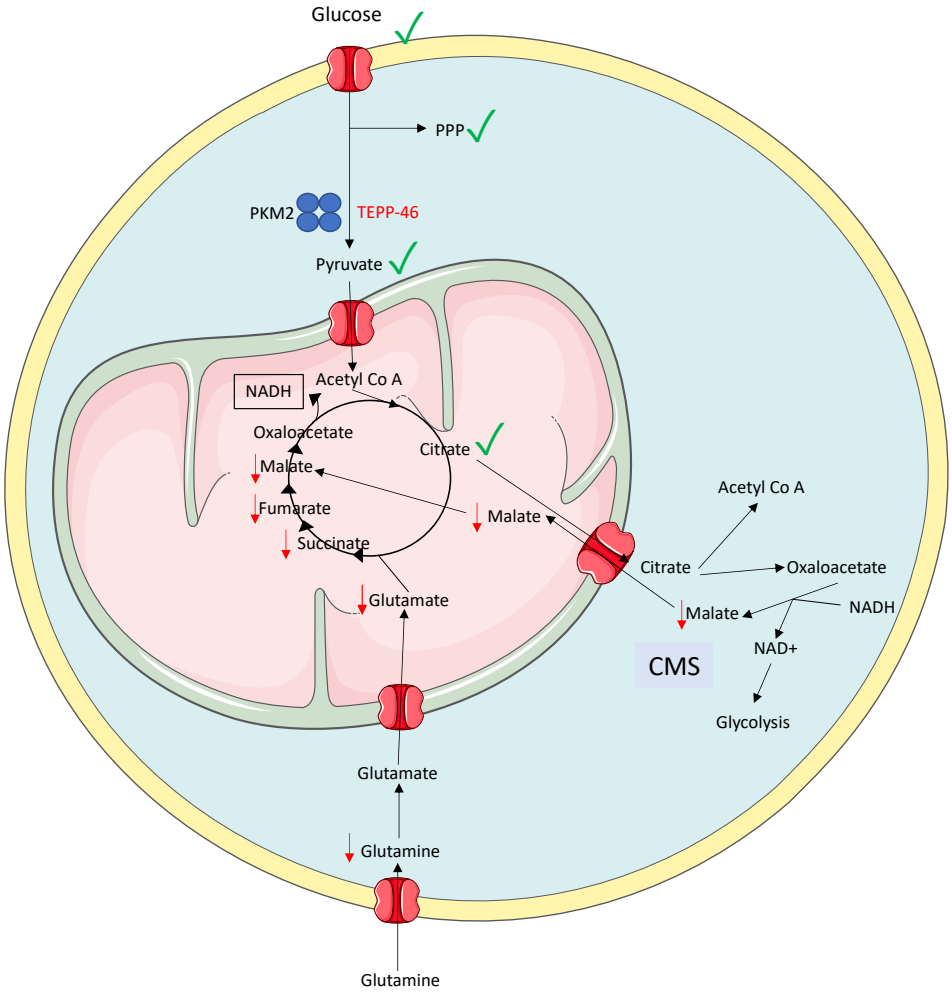

Figure 5. 24. Visual graphic of metabolic changes of IL-2/12 activated NK cells treated with TEPP-46 relative to IL-2/12 vehicle

Metabolites marked with a downward arrow denotes less accumulation of metabolite in NK cells co-cultured with IL-2/12 and TEPP-46 compared with IL-2/12 + Vehicle alone. Metabolites marked with green tick are found unchanged with TEPP-46 treatment. Metabolites with no mark indicate that their levels were not measured in the metabolomics panel. Potentially, reduced malate production in TEPP-46 treated NK cells results in reduced fuelling of the citrate-malate shuttle and reduced NADH generation from oxaloacetate. Metabolites with a downward red arrow are significantly reduced with TEPP-46.. PPP: pentose phosphate pathway. CMS: citrate malate shuttle.

Discussion

Chapter 3 and chapter 4 showed that PKM2 deficient NK cells function normally *in vivo* and *in vitro.* This is due to metabolic compensation by the alternate splice isoform, *Pkm1*. PKM1 is a more active isoform, and so it would have been expected that these PKM1 expressing NK cells would have a higher rate of overall pyruvate kinase activity. However, the findings here show that PKM1 expressing NK cells match their overall pyruvate kinase rate. This highlights the caveat of using genetic models in scientific investigations. Cells can sometimes compensate for genetic deletion. For this reason, pharmacological manipulation of PKM2 was a useful and complementary experimental approach to dissect the function of PKM2 in NK cells

There is increasing evidence that NK cell glycoysis is required for function, in both humans and mice [52, 105]. However, studies that investigated this have mainly focused on inhibition of glycolysis using inhibitors such as 2-DG and galactose. This is the first study in NK cells that focused on a potential method of increasing glycolysis. It may have been hypothesised that increasing glycolysis would be beneficial to NK cells but the data in this chapter indicate that perturbation of glycolysis with TEPP-46 is detrimental to NK cell function. Indeed, these data are in line with other immunological studies using TEPP-46 in cells such macrophages where TEPP-46 inhibited IL-1β production [119] . However, NK cells are unlike other immune cells in which PKM2 has been studied. PKM2 activation does not appear to control transcription through molecules such as HIF1α in NK cells. This can be explained as HIF1α has been shown to be dispensable for NK cell function [109]. Similarly, through RNA sequencing this study revealed no enrichment for the STAT3 target genes, of which PKM2 has been previously shown to control [163]. This indicates that PKM2 is not required for transcriptional control in NK cells.

It is clear from the data presented in this chapter that PKM2 is important for metabolic regulation in NK cells. Indeed, activation of PKM2 pyruvate kinase activity with TEPP-46 profoundly impaired oxidative metabolism. This may be due to reduced TCA intermediates – succinate, fumarate and malate. These data are interesting as our group has previously published that the traditional TCA cycle is not operational in NK cells and instead NK cells utilise the citrate-malate shuttle to make NADH. The citrate malate shuttle makes mitochondrial NADH from the conversion of malate to oxaloacetate (as shown in figure 5.24. The reduced levels of malate observed in this study may explain the reduced levels of OxPhos in these cells. Indeed, the citrate malate transported is an obligate antiporter, and the reduced levels of malate would be predicted to inhibit citrate export from the mitochondria [86]. As to why malate is reduced, it is most likely due to reduced glutamine uptake leading to defects in early export of citrate. It is most intriguing as to why glutamine uptake is decreased. Indeed, the levels of the key glutamine transporter in NK cells, ASCT2, are normal in the presence of TEPP-46 according to RNAseq data. A possible explanation is that the activity of the transporter is reduced. One possible mechanism is through post translational modification. The glutamine transporter is known to be subjected to N-linked glycosylation [164]. In low glucose, ASCT2 glycosylation is reduced which increases glutamine uptake. It is intriguing to think that the opposite could be true, and high rates of glycolysis could inhibit glutamine transporter function.

In line with previous studies, we have also observed a potential link between PKM2 activity and reactive oxygen species . Indeed, PKM2 conformation is regulated by ROS. In cells where ROS levels are high, PKM2 is inactivated (monomers/dimers) [165]. This functions as a feedback loop to limit ROS production. Indeed, inhibition of PKM2 by ROS is thought to facilitate the production of antioxidant molecules such as NADPH [166]. It is intriguing to hypothesise that maybe a similar feedback loop is present in NK cells and this is why ROS is elevated in cells treated with TEPP-46. This could be addressed by directly analysing cellular NADPH levels in the presence or absence of TEPP-46.

The direct implications of increased cellular ROS treatment can be visualised in the reduced Myc expression, which can be partially rescued by the addition of the exogenous antioxidant, MitoQ. These data of ROS inhibition of cMyc expression are in line with previous data from the Brenner group that shows ROS is inhibitory to cMyc expression in T cells [167]. However, supplementation in this study did not rescue effector molecule production. This is most likely due to the weak antioxidant capacity of MitoQ. It is likely that the use of stronger non-mitochondria targeted antioxidants such as N-acetylcysteine may be protective to TEPP-46 induced NK cell ROS.

Overall, this chapter demonstrated that TEPP-46 is detrimental to NK cell function *in vitro.* These data have profound physiological relevance as TEPP-46 is currently being investigated for the treatment of tumours, due to the high level of PKM2 expression in tumour cells. Indeed, administration of TEPP-46 *in vivo* has been shown to supress tumorigenesis in a xenograft model [133]. Although PKM2 is inhibitory to tumour growth this current study argues tat it will be important to consider the impact of such strategies on anti-tumour immunity. This is particularly relevant in blood borne cancers

such as chronic myeloid leukamia, where NK cells are showing increasing promise in therapies.

Chapter 6: Final Discussion

To date, there has been extensive research on the role of PKM2 in cancer cells. Numerous studies have characterised its role as both a metabolic enzyme and as a signalling molecule. However, our knowledge of the role for PKM2 in immunological settings is still in its infancy. This study has characterised a role for PKM2 in regulating NK cell metabolism and function. Overall, this study has revealed that NK cells have a differential requirement for PKM2 than other immune cells. Unlike cells such as macrophages and T cells, PKM2 is not required for transcriptional regulation. However, regulation of pyruvate kinase metabolic activity by PKM2 is required for normal NK cell function. Dysregulation of pyruvate kinase metabolic activity is detrimental to NK cell oxidative metabolism, and appears to impair NK cell mitochondrial function. These data potentially implicate PKM2 as a ROS defence mechanism for NK cell metabolism.

The data presented in this study crucially support a non-transcriptional role for PKM2 in NK cells. Numerous other studies have characterised a role for monomeric/dimeric PKM2 as a signalling molecule and transcriptional co-activator. Indeed, PKM2 has been shown to act as a signalling molecule in macrophages through regulation of HIF1α [119]. PKM2 has also been shown to regulate the expression of PD-L1 on macrophages, T cells, DC and tumour cells through a HIF1α mediated mechanism [134]. Similarly, it was shown by Gao et. al that PKM2 acts as a protein kinase in cancer cells and can directly phosphorylate STAT3 [131]. RNA sequencing performed in chapter 4 revealed that there was very little alteration in the transcriptome in PKM2 deficient NK cells, and no gene signature consistent with altered STAT5 or HIF1α activities. This indicates that PKM2 is not involved in the regulation of these pathways.

There are several possible explanations for why this transcriptional role is important in other cells but not in NK cells. Firstly, this can be explained experimentally. This study is

one of the first to utilise an immune cell specific conditional knockout to assess a role for PKM2. Previous studies, e.g. Palsson-McDermott *et*. *al* used a tamoxifen Cre model of PKM2 deletion *in vitro* whereby cells containing a floxed allele for PKM2 are treated with tamoxifen, leading to acute excision of the PKM2 gene. Gao et. al used an overexpression model of PKM2 and showed increased levels of STAT3 phosphorylation. It is possible that in the more long term model of deletion used in this study (*Ncr1*^{Cre}), that the cells may be genetically compensating for loss of PKM2 signalling functions. However, this is unlikely as if PKM2 was absolutely required for transcriptional regulation and not redundant, then there would be a transcriptional signature in the RNAseq data. The absence of a transcriptional role for PKM2 in NK cells was confirmed using the pharmacological compound TEPP-46, whereby there were few gene changes and no enrichment for pathways associated with HIFα or STAT signalling. These data highlight the importance not extrapolating metabolic and signalling regulation between different cell types. It is clear that NK cell signalling and metabolism is different from that of other immune cells.

The data are clearer as to why PKM2 is not required for modulation of HIF1α in NK cells. It is probable that PKM2^{KO} NK cells showed no overt HIF1α transcriptional phenotype as HIF1α is dispensable for regulation of NK cell metabolism [109]. It is interesting, however, to note that IL-2 signals through STAT3. As the main method of *in vitro* NK cell activation in this study is IL-2/12, it is intriguing therefore that STAT3 signalling was not altered upon PKM2 manipulation as determined by RNAseq pathway analysis. This suggests that the PKM2-STAT3 axis is not active in NK cells and further supports that PKM2 does not play a direct signalling role in NK cells.

It is also interesting to note that there are already some conflicting results in the PKM2 field. Indeed, the Vander Heiden lab has published that there is no intrinsic protein kinase activity of PKM2. They added recombinant PKM2 to PKM2$^{-/-}$ lysates in the presence of radiolabelled PEP and observed no PKM2 and PEP dependent phosphorylation events [168]. It is therefore possible that other studies showing PKM2 protein kinase activity may not be directly due to pyruvate kinase and may be due to an off-target effect or an alteration in ATP availability.

Aside from its lack of transcriptional role, the data presented here support the idea that regulation of pyruvate kinase enzymatic activity is required for NK cell function through control of metabolism. Treatment of IL-2/12 activated NK cells with TEPP-46 caused profound metabolic and functional defects. Although the mechanistic insight into these data were discussed at the end of chapter 5, it is interesting to compare the data generated using genetic and pharmacological approaches. The genetic knock out of PKM2 showed no overt phenotype due to genetic compensation of PKM1 and regulation of overall pyruvate kinase activity. However, the data using TEPP-46 in chapter 5 revealed a key metabolic role for PKM2 in regulating overall pyruvate kinase activity (**Figure 6.1)**. Using the genetic knock out only would have led to no observable phenotype, and the conclusion that PKM2 is not important for NK cell function. Whereas a two pronged approach using a pharmacological activator allowed to reveal a role for PKM2 in regulating NK cell metabolism. This indicates that moving forward, studies on immune metabolism should not rely only on genetic approaches to dissect enzymatic function, and a complimentary approach using of both genetics and drugs would be the most informative.

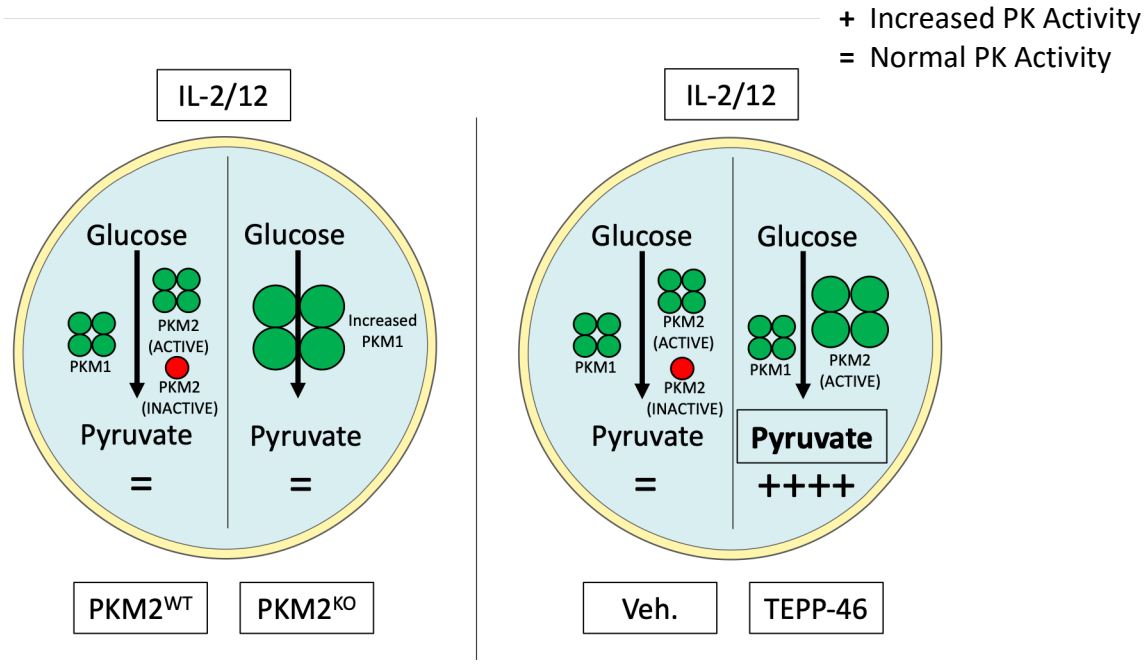

Figure 6.1 Different pyruvate kinase activity outcomes from PKM2 deletion vs pharmacological activation on IL-2/12 activated NK cells

The left panel shows the overall pyruvate kinase activity of PKM^{WT}NK cells and $PKM2^{KO}$ NK cells. The total pyruvate kinase activity in a cell can be contributed to by PKM1, active PKM2 or inactive PKM2. With PKM2 deletion, PKM1 makes up the whole pyruvate kinase pool and regulates the overall activity. The two genotypes have equal pyruvate kinase activity due to this compensatory PKM1 expression The right panel shows the effect of TEPP-46 treatment of wild-type NK cells. Their pyruvate kinase pool consists of PKM1 and only active PKM2. Wildtype NK cells treated with TEPP-46 show heightened overall pyruvate kinase activity relative to vehicle (Veh.) controls. '=' denotes normal pyruvate kinase activity '++++' denotes increased pyruvate kinase activity.

The data generated using pharmacological approaches support the emerging idea that targeting of PKM2 may be useful as a treatment for inflammatory diseases. One recent paper showed that PKM2 was required for the differentiation of Th1 and Th17 cells [121]. This is important as the authors also demonstrated that pharmacological PKM2 inhibition prevented a mouse model of experimental autoimmune encephalomyelitis (EAE).

PKM2 activators were also found to be protective in a mouse model of sepsis. Mice injected with LPS normally show a sharp increase in circulating IL-1β . When mice were treated with TEPP-46 in combination with LPS, there was a marked decrease in the expression of IL-1β [119]. Interestingly, PKM2 protein has also been found to be elevated in stool samples from patients with Crohn's disease [169]. It is intriguing to predict that TEPP-46 treatment in a model of Crohn's disease might offer some protection. This indicates that PKM2 targeting may show promise for the treatment of inflammatory diseases.

All of these data support the hypothesis that TEPP-46 could be used as an anti-inflammatory molecule. Indeed, the data presented in this study indicated that TEPP-46 was inhibitory to NK cell proinflammatory cytokine production. It is intriguing to hypothesise that inhibition (as opposed to activation) of PKM2 may boost immune function. Although less well characterised than TEPP-46, there is a potential inhibitor of PKM2 described called shikonin [170]. This inhibitor has primarily been studied in the context of cancer. However, there is also one study on human NK cells showing that shikonin treatment of IL-2 activated NK cells resulted in increased proliferation, perforin and granzyme B production [171]. Shikonin has also been shown to have low toxicity in

rats *in* vivo [172]. It is therefore possible that shikonin treatment may boost NK cell responses in tumour and viral models *in vivo.*

The importance of understanding immunometabolism is becoming apparent as the tumour microenvironment is likely to be deficient in various nutrients. The evidence for this is strongest for glucose; the concentration of glucose in the tumour microenvironment has been found to be 10-times less than the spleen or blood [115]. Similarly, tumours utilise huge amounts of glutamine and so it might be expected that glutamine levels will be low in certain tumours [173]. Such nutrient restrictive conditions will affect immune cell function. NK cells for example require both of these nutrients for optimum effector function [52, 109]. The appeal of targeting metabolism in tumours is that it offers the potential for targeted therapies, especially when focusing on pathways that are important for cancer growth but not immune cell growth. Current chemotherapeutic drugs often target highly proliferative cells, which is detrimental to tumour growth. Indeed, some of the earliest used chemotherapeutic drugs such as 5-flurouracil, methotrexate and gemcitabine all have metabolic targets [174]. However, a downside of this is that immune cells can also be highly proliferative as well and are sensitive to metabolic perturbation. Indeed, some of these chemotherapies cause bone marrow suppression [175]. PKM2 is a metabolic target for cancer. Indeed, TEPP-46 has been shown to inhibit tumour growth in a xenograft model in mice [133]. Based on the data in this current study showing detrimental effects of PKM2 activation on NK cells, it is important to recognise that targeting tumours with this drug might also have off target effects on the immune system. Therefore, for future therapies it is important to find metabolic targets that will inhibit tumour cells but not affect the antitumour

immune response. This could be achieved with more direct collaboration between immunologists and cancer researchers.

Bibliography

1. Boyiadzis, M., K.A. Foon, and R.B. Herberman, *NK cells in cancer immunotherapy: three decades of discovery.* Discov Med, 2006. **6**(36): p. 243-8.
2. Moffett, A. and C. Loke, *Immunology of placentation in eutherian mammals.* Nat Rev Immunol, 2006. **6**(8): p. 584-94.
3. Cavalcanti, Y.V.N., et al., *Role of TNF-Alpha, IFN-Gamma, and IL-10 in the Development of Pulmonary Tuberculosis.* Pulmonary Medicine, 2012. **2012**: p. 10.
4. Gordy, C. and Y.-W. He, *Endocytosis by target cells: an essential means for perforin- and granzyme-mediated killing.* Cellular and Molecular Immunology, 2012. **9**(1): p. 5-6.
5. Colucci, F., J.P. Di Santo, and P.J. Leibson, *Natural killer cell activation in mice and men: different triggers for similar weapons?* Nat Immunol, 2002. **3**(9): p. 807-13.
6. Woolthuis, C.M. and C.Y. Park, *Hematopoietic stem/progenitor cell commitment to the megakaryocyte lineage.* Blood, 2016. **127**(10): p. 1242-1248.
7. Yu, J., A.G. Freud, and M.A. Caligiuri, *Location and cellular stages of natural killer cell development.* Trends in Immunology. **34**(12): p. 573-582.
8. Luci, C., et al., *Natural Killer Cells and Type 1 Innate Lymphoid Cells Are New Actors in Non-alcoholic Fatty Liver Disease.* Frontiers in Immunology, 2019. **10**(1192).
9. Carotta, S., et al., *Identification of the earliest NK-cell precursor in the mouse BM.* Blood, 2011. **117**(20): p. 5449-52.
10. Kim, S., et al., *In vivo developmental stages in murine natural killer cell maturation.* Nat Immunol, 2002. **3**(6): p. 523-528.
11. Suzuki, H., et al., *Abnormal development of intestinal intraepithelial lymphocytes and peripheral natural killer cells in mice lacking the IL-2 receptor beta chain.* J Exp Med, 1997. **185**(3): p. 499-505.
12. Yokoyama, W.M., et al., *Tissue-Resident Natural Killer Cells.* Cold Spring Harbor Symposia on Quantitative Biology, 2013. **78**: p. 149-156.
13. Vivier, E., et al., *Functions of natural killer cells.* Nat Immunol, 2008. **9**(5): p. 503-510.
14. Guillerey, C., N.D. Huntington, and M.J. Smyth, *Targeting natural killer cells in cancer immunotherapy.* Nat Immunol, 2016. **17**(9): p. 1025-1036.
15. Antonangeli, F., et al., *Senescent cells: Living or dying is a matter of NK cells.* J Leukoc Biol, 2019. **105**(6): p. 1275-1283.
16. Souza-Fonseca-Guimaraes, F., M. Adib-Conquy, and J.-M. Cavaillon, *Natural killer (NK) cells in antibacterial innate immunity: angels or devils?* Molecular medicine (Cambridge, Mass.), 2012. **18**(1): p. 270-285.
17. Horst, D., et al., *Viral evasion of T cell immunity: ancient mechanisms offering new applications.* Curr Opin Immunol, 2011. **23**(1): p. 96-103.
18. Chambers, W.H. and C.S. Brissette-Storkus, *Hanging in the balance: natural killer cell recognition of target cells.* Chem Biol, 1995. **2**(7): p. 429-35.

19. Biron , C.A., K.S. Byron , and J.L. Sullivan *Severe Herpesvirus Infections in an Adolescent without Natural Killer Cells.* New England Journal of Medicine, 1989. **320**(26): p. 1731-1735.
20. Biron, C.A., et al., *Natural killer cells in antiviral defense: function and regulation by innate cytokines.* Annu Rev Immunol, 1999. **17**: p. 189-220.
21. Sathe, P., et al., *Innate immunodeficiency following genetic ablation of Mcl1 in natural killer cells.* Nature Communications, 2014. **5**(1): p. 4539.
22. Imai, K., et al., *Natural cytotoxic activity of peripheral-blood lymphocytes and cancer incidence: an 11-year follow-up study of a general population.* The Lancet. **356**(9244): p. 1795-1799.
23. Smyth, M.J., et al., *Activation of NK cell cytotoxicity.* Molecular Immunology, 2005. **42**(4): p. 501-510.
24. Mullbacher, A., et al., *Granzymes are the essential downstream effector molecules for the control of primary virus infections by cytolytic leukocytes.* Proc Natl Acad Sci U S A, 1999. **96**(24): p. 13950-5.
25. Sutton, V.R., et al., *Caspase Activation by Granzyme B Is Indirect, and Caspase Autoprocessing Requires the Release of Proapoptotic Mitochondrial Factors.* Immunity, 2003. **18**(3): p. 319-329.
26. Stinchcombe, J.C., et al., *Centriole polarisation to the immunological synapse directs secretion from cytolytic cells of both the innate and adaptive immune systems.* BMC Biology, 2011. **9**(1): p. 45.
27. Gardiner, C.M. and D.J. Reen, *Differential cytokine regulation of natural killer cell-mediated necrotic and apoptotic cytotoxicity.* Immunology, 1998. **93**(4): p. 511-7.
28. Blom, W.M., et al., *Interleukin-2-activated natural killer cells can induce both apoptosis and necrosis in rat hepatocytes.* Hepatology, 1999. **29**(3): p. 785-92.
29. Daniels, R.A., et al., *Expression of TRAIL and TRAIL receptors in normal and malignant tissues.* Cell Res, 2005. **15**(6): p. 430-438.
30. Schneider, P., et al., *Identification of a new murine tumor necrosis factor receptor locus that contains two novel murine receptors for tumor necrosis factor-related apoptosis-inducing ligand (TRAIL).* J Biol Chem, 2003. **278**(7): p. 5444-54.
31. Wang, S. and W.S. El-Deiry, *TRAIL and apoptosis induction by TNF-family death receptors.* Oncogene, 0000. **22**(53): p. 8628-8633.
32. Barber, G.N., *Host defense, viruses and apoptosis.* Cell death and differentiation, 2001. **8**(2): p. 113.
33. Orange, J.S., et al., *Requirement for natural killer cell-produced interferon gamma in defense against murine cytomegalovirus infection and enhancement of this defense pathway by interleukin 12 administration.* J Exp Med, 1995. **182**(4): p. 1045-56.
34. Zhu, J., H. Yamane, and W.E. Paul, *Differentiation of effector CD4 T cell populations (*).* Annual review of immunology, 2010. **28**: p. 445-489.
35. Ni, L. and J. Lu, *Interferon gamma in cancer immunotherapy.* Cancer medicine, 2018. **7**(9): p. 4509-4516.
36. Becher, B., S. Tugues, and M. Greter, *GM-CSF: from growth factor to central mediator of tissue inflammation.* Immunity, 2016. **45**(5): p. 963-973.

37. Walzer, T., et al., *Natural-killer cells and dendritic cells:"l'union fait la force".* Blood, 2005. **106**(7): p. 2252-2258.
38. Vivier, E., J.A. Nunes, and F. Vely, *Natural killer cell signaling pathways.* Science, 2004. **306**(5701): p. 1517-9.
39. Sawicki, M.W., et al., *Structural basis of MHC class I recognition by natural killer cell receptors.* Immunol Rev, 2001. **181**: p. 52-65.
40. Petersen, J.L., C.R. Morris, and J.C. Solheim, *Virus Evasion of MHC Class I Molecule Presentation.* The Journal of Immunology, 2003. **171**(9): p. 4473-4478.
41. Sivori, S., et al., *TLR/NCR/KIR: Which One to Use and When?* Frontiers in Immunology, 2014. **5**(105).
42. Cassidy, S.A., K.S. Cheent, and S.I. Khakoo, *Effects of Peptide on NK cell-mediated MHC I recognition.* Front Immunol, 2014. **5**: p. 133.
43. Pegram, H.J., et al., *Activating and inhibitory receptors of natural killer cells.* Immunol Cell Biol, 2011. **89**(2): p. 216-224.
44. Dimasi, N. and R. Biassoni, *Structural and functional aspects of the Ly49 natural killer cell receptors.* Immunol Cell Biol, 2005. **83**(1): p. 1-8.
45. Scarpellino, L., et al., *Interactions of Ly49 family receptors with MHC class I ligands in trans and cis.* J Immunol, 2007. **178**(3): p. 1277-84.
46. Corbett, A.J., et al., *Functional Consequences of Natural Sequence Variation of Murine Cytomegalovirus m157 for Ly49 Receptor Specificity and NK Cell Activation.* The Journal of Immunology, 2011. **186**(3): p. 1713-1722.
47. Ravetch, J.V. and L.L. Lanier, *Immune inhibitory receptors.* Science, 2000. **290**(5489): p. 84-9.
48. Tassi, I., et al., *Phospholipase C-gamma 2 is a critical signaling mediator for murine NK cell activating receptors.* J Immunol, 2005. **175**(2): p. 749-54.
49. Antonangeli, F., et al., *How Mucosal Epithelia Deal with Stress: Role of NKG2D/NKG2D Ligands during Inflammation.* Frontiers in immunology, 2017. **8**: p. 1583-1583.
50. Raulet, D.H., et al., *Regulation of ligands for the NKG2D activating receptor.* Annu Rev Immunol, 2013. **31**: p. 413-41.
51. Marçais, A., et al., *Regulation of Mouse NK Cell Development and Function by Cytokines.* Frontiers in Immunology, 2013. **4**(450).
52. Donnelly, R.P., et al., *mTORC1-dependent metabolic reprogramming is a prerequisite for NK cell effector function.* J Immunol, 2014. **193**(9): p. 4477-84.
53. Zanoni, I., et al., *IL-15 cis Presentation Is Required for Optimal NK Cell Activation in Lipopolysaccharide-Mediated Inflammatory Conditions.* Cell Reports. **4**(6): p. 1235-1249.
54. Jabri, B. and V. Abadie, *IL-15 functions as a danger signal to regulate tissue-resident T cells and tissue destruction.* Nat Rev Immunol, 2015. **15**(12): p. 771-783.
55. Waldmann, T.A., *The biology of interleukin-2 and interleukin-15: implications for cancer therapy and vaccine design.* Nat Rev Immunol, 2006. **6**(8): p. 595-601.
56. Gotthardt, D., et al., *STAT5 Is a Key Regulator in NK Cells and Acts as a Molecular Switch from Tumor Surveillance to Tumor Promotion.* Cancer Discov, 2016. **6**(4): p. 414-29.

57. Koka, R., et al., *Cutting edge: murine dendritic cells require IL-15R alpha to prime NK cells.* J Immunol, 2004. **173**(6): p. 3594-8.
58. Ross, S.H. and D.A. Cantrell, *Signaling and Function of Interleukin-2 in T Lymphocytes.* Annual Review of Immunology, 2018. **36**(1): p. 411-433.
59. Kobayashi, M., et al., *Identification and purification of natural killer cell stimulatory factor (NKSF), a cytokine with multiple biologic effects on human lymphocytes.* Journal of Experimental Medicine, 1989. **170**(3): p. 827-845.
60. Wu, Y., Z. Tian, and H. Wei, *Developmental and Functional Control of Natural Killer Cells by Cytokines.* Frontiers in Immunology, 2017. **8**(930).
61. Griffiths, P., I. Baraniak, and M. Reeves, *The pathogenesis of human cytomegalovirus.* The Journal of Pathology, 2015. **235**(2): p. 288-297.
62. Zuhair, M., et al., *Estimation of the worldwide seroprevalence of cytomegalovirus: A systematic review and meta-analysis.* Reviews in Medical Virology, 2019. **29**(3): p. e2034.
63. Thackeray, R., A. Wright, and K. Chipman, *Congenital cytomegalovirus reference material: a content analysis of coverage and accuracy.* Maternal and child health journal, 2014. **18**(3): p. 584-591.
64. Brown, M.G., et al., *Vital involvement of a natural killer cell activation receptor in resistance to viral infection.* Science, 2001. **292**(5518): p. 934-937.
65. Scalzo, A.A., et al., *Cmv-1, a genetic locus that controls murine cytomegalovirus replication in the spleen.* The Journal of Experimental Medicine, 1990. **171**(5): p. 1469-1483.
66. Arase, H., et al., *Direct Recognition of Cytomegalovirus by Activating and Inhibitory NK Cell Receptors.* Science, 2002. **296**(5571): p. 1323-1326.
67. Smith, K.M., et al., *Ly-49D and Ly-49H associate with mouse DAP12 and form activating receptors.* J Immunol, 1998. **161**(1): p. 7-10.
68. Orange, J.S. and C.A. Biron, *Characterization of early IL-12, IFN-alphabeta, and TNF effects on antiviral state and NK cell responses during murine cytomegalovirus infection.* The Journal of Immunology, 1996. **156**(12): p. 4746-4756.
69. Dokun, A.O., et al., *Specific and nonspecific NK cell activation during virus infection.* Nature Immunology, 2001. **2**(10): p. 951-956.
70. Kamimura, Y. and L.L. Lanier, *Rapid and sequential quantitation of salivary gland-associated mouse cytomegalovirus in oral lavage.* Journal of virological methods, 2014. **205**: p. 53-56.
71. Lin, A.W., et al., *CD56(+dim) and CD56(+bright) cell activation and apoptosis in hepatitis C virus infection.* Clin Exp Immunol, 2004. **137**(2): p. 408-16.
72. Miller, J.S., *Therapeutic applications: natural killer cells in the clinic.* ASH Education Program Book, 2013. **2013**(1): p. 247-253.
73. Rezvani, K. and R.H. Rouce, *The Application of Natural Killer Cell Immunotherapy for the Treatment of Cancer.* Frontiers in Immunology, 2015. **6**: p. 578.
74. Rubnitz, J.E., et al., *NKAML: a pilot study to determine the safety and feasibility of haploidentical natural killer cell transplantation in childhood acute myeloid leukemia.* J Clin Oncol, 2010. **28**(6): p. 955-9.
75. Miller, J.S., et al., *Successful adoptive transfer and in vivo expansion of human haploidentical NK cells in patients with cancer.* Blood, 2005. **105**(8): p. 3051-7.

76. Weiner, G.J., *Rituximab: mechanism of action.* Seminars in hematology, 2010. **47**(2): p. 115-123.
77. Dall'Ozzo, S., et al., *Rituximab-dependent cytotoxicity by natural killer cells: influence of FCGR3A polymorphism on the concentration-effect relationship.* Cancer Res, 2004. **64**(13): p. 4664-9.
78. Leidi, M., et al., *M2 macrophages phagocytose rituximab-opsonized leukemic targets more efficiently than m1 cells in vitro.* J Immunol, 2009. **182**(7): p. 4415-22.
79. Li, Y., et al., *Human iPSC-Derived Natural Killer Cells Engineered with Chimeric Antigen Receptors Enhance Anti-tumor Activity.* Cell Stem Cell, 2018. **23**(2): p. 181-192.e5.
80. Kloess, S., et al., *CAR-Expressing Natural Killer Cells for Cancer Retargeting.* Transfusion Medicine and Hemotherapy, 2019. **46**(1): p. 4-13.
81. Klingemann, H., *Are natural killer cells superior CAR drivers?* OncoImmunology, 2014. **3**(4): p. e28147.
82. Tonn, T., et al., *Treatment of patients with advanced cancer with the natural killer cell line NK-92.* Cytotherapy, 2013. **15**(12): p. 1563-70.
83. Vitko, N.P., N.A. Spahich, and A.R. Richardson, *Glycolytic Dependency of High-Level Nitric Oxide Resistance and Virulence in Staphylococcus aureus.* mBio, 2015. **6**(2): p. e00045-15.
84. O'Neill, L.A.J., R.J. Kishton, and J. Rathmell, *A guide to immunometabolism for immunologists.* Nat Rev Immunol, 2016. **16**(9): p. 553-565.
85. Lu, M., et al., *Role of the malate-aspartate shuttle on the metabolic response to myocardial ischemia.* Journal of theoretical biology, 2008. **254**(2): p. 466-475.
86. Assmann, N., et al., *Srebp-controlled glucose metabolism is essential for NK cell functional responses.* Nat Immunol, 2017. **18**(11): p. 1197-1206.
87. Lunt, S.Y. and M.G. Vander Heiden, *Aerobic glycolysis: meeting the metabolic requirements of cell proliferation.* Annu Rev Cell Dev Biol, 2011. **27**: p. 441-64.
88. Mullarky, E., et al., *Identification of a small molecule inhibitor of 3-phosphoglycerate dehydrogenase to target serine biosynthesis in cancers.* Proceedings of the National Academy of Sciences, 2016. **113**(7): p. 1778-1783.
89. Pearce, E.L. and E.J. Pearce, *Metabolic Pathways In Immune Cell Activation And Quiescence.* Immunity, 2013. **38**(4): p. 633-643.
90. Jose, C., N. Bellance, and R. Rossignol, *Choosing between glycolysis and oxidative phosphorylation: A tumor's dilemma?* Biochimica et Biophysica Acta (BBA) - Bioenergetics, 2011. **1807**(6): p. 552-561.
91. O'Neill, L.A. and E.J. Pearce, *Immunometabolism governs dendritic cell and macrophage function.* J Exp Med, 2016. **213**(1): p. 15-23.
92. Lewis, M., J.F. Tarlton, and S. Cose, *Memory versus naive T-cell migration.* Immunol Cell Biol, 2007. **86**(3): p. 226-231.
93. Billadeau, D.D., J.C. Nolz, and T.S. Gomez, *Regulation of T-cell activation by the cytoskeleton.* Nat Rev Immunol, 2007. **7**(2): p. 131-143.
94. van der Windt, G.J.W. and E.L. Pearce, *Metabolic switching and fuel choice during T-cell differentiation and memory development.* Immunological reviews, 2012. **249**(1): p. 27-42.
95. MacIver, N.J., R.D. Michalek, and J.C. Rathmell, *Metabolic regulation of T lymphocytes.* Annu Rev Immunol, 2013. **31**: p. 259-83.

96. Buck, M.D., D. O'Sullivan, and E.L. Pearce, *T cell metabolism drives immunity.* The Journal of Experimental Medicine, 2015. **212**(9): p. 1345-1360.
97. Michalek, R.D., et al., *Cutting edge: distinct glycolytic and lipid oxidative metabolic programs are essential for effector and regulatory CD4+ T cell subsets.* J Immunol, 2011. **186**(6): p. 3299-303.
98. Mascanfroni, I.D., et al., *Metabolic control of type 1 regulatory T cell differentiation by AHR and HIF1-alpha.* Nat Med, 2015. **21**(6): p. 638-46.
99. van der Windt, G.J., et al., *CD8 memory T cells have a bioenergetic advantage that underlies their rapid recall ability.* Proc Natl Acad Sci U S A, 2013. **110**(35): p. 14336-41.
100. Cui, G., et al., *IL-7-Induced Glycerol Transport and TAG Synthesis Promotes Memory CD8+ T Cell Longevity.* Cell, 2015. **161**(4): p. 750-61.
101. Tannahill, G.M., et al., *Succinate is an inflammatory signal that induces IL-1beta through HIF-1alpha.* Nature, 2013. **496**(7444): p. 238-42.
102. O'Neill, L.A.J. and M.N. Artyomov, *Itaconate: the poster child of metabolic reprogramming in macrophage function.* Nature Reviews Immunology, 2019. **19**(5): p. 273-281.
103. Keppel, M.P., et al., *Activation-Specific Metabolic Requirements for NK Cell IFN-γ Production.* The Journal of Immunology, 2015. **194**(4): p. 1954-1962.
104. Kedia-Mehta, N., et al., *Natural Killer Cells Integrate Signals Received from Tumour Interactions and IL2 to Induce Robust and Prolonged Anti-Tumour Metabolic Responses.* Immunometabolism, 2019. **1**(2): p. e190014.
105. Keating, S.E., et al., *Metabolic Reprogramming Supports IFN-γ Production by CD56^{bright} NK Cells.* The Journal of Immunology, 2016: p. 1501783.
106. Finlay, D.K., et al., *PDK1 regulation of mTOR and hypoxia-inducible factor 1 integrate metabolism and migration of CD8+ T cells.* J Exp Med, 2012. **209**(13): p. 2441-53.
107. Laplante, M. and D.M. Sabatini, *mTOR signaling in growth control and disease.* Cell, 2012. **149**(2): p. 274-93.
108. Nie, Z., et al., *c-Myc is a universal amplifier of expressed genes in lymphocytes and embryonic stem cells.* Cell, 2012. **151**(1): p. 68-79.
109. Loftus, R.M., et al., *Amino acid-dependent cMyc expression is essential for NK cell metabolic and functional responses in mice.* Nat Commun, 2018. **9**(1): p. 2341.
110. Pinz, S., S. Unser, and A. Rascle, *Signal transducer and activator of transcription STAT5 is recruited to c-Myc super-enhancer.* BMC Molecular Biology, 2016. **17**: p. 10.
111. Sinclair, L.V., et al., *Control of amino-acid transport by antigen receptors coordinates the metabolic reprogramming essential for T cell differentiation.* Nat Immunol, 2013. **14**(5): p. 500-8.
112. Kidani, Y., et al., *Sterol regulatory element-binding proteins are essential for the metabolic programming of effector T cells and adaptive immunity.* Nature immunology, 2013. **14**(5): p. 489-499.
113. O'Brien, K.L. and D.K. Finlay, *Immunometabolism and natural killer cell responses.* Nat Rev Immunol, 2019. **19**(5): p. 282-290.

114. Lenzen, S., *A fresh view of glycolysis and glucokinase regulation: history and current status.* The Journal of biological chemistry, 2014. **289**(18): p. 12189-12194.
115. Ho, P.C., et al., *Phosphoenolpyruvate Is a Metabolic Checkpoint of Anti-tumor T Cell Responses.* Cell, 2015. **162**(6): p. 1217-28.
116. Chang, C.H., et al., *Posttranscriptional control of T cell effector function by aerobic glycolysis.* Cell, 2013. **153**(6): p. 1239-51.
117. Newton, R., B. Priyadharshini, and L.A. Turka, *Immunometabolism of regulatory T cells.* Nat Immunol, 2016. **17**(6): p. 618-625.
118. Moon, J.S., et al., *mTORC1-Induced HK1-Dependent Glycolysis Regulates NLRP3 Inflammasome Activation.* Cell Rep, 2015. **12**(1): p. 102-15.
119. Palsson-McDermott, E.M., et al., *Pyruvate kinase M2 regulates Hif-1alpha activity and IL-1beta induction and is a critical determinant of the warburg effect in LPS-activated macrophages.* Cell Metab, 2015. **21**(1): p. 65-80.
120. Shirai, T., et al., *The glycolytic enzyme PKM2 bridges metabolic and inflammatory dysfunction in coronary artery disease.* J Exp Med, 2016. **213**(3): p. 337-54.
121. Kono, M., et al., *Pyruvate kinase M2 is requisite for Th1 and Th17 differentiation.* JCI insight, 2019. **4**(12): p. e127395.
122. Alves-Filho, J.C. and E.M. Palsson-McDermott, *Pyruvate Kinase M2: A Potential Target for Regulating Inflammation.* Front Immunol, 2016. **7**: p. 145.
123. Noguchi, T., H. Inoue, and T. Tanaka, *The M1- and M2-type isozymes of rat pyruvate kinase are produced from the same gene by alternative RNA splicing.* J Biol Chem, 1986. **261**(29): p. 13807-12.
124. David, C.J., et al., *HnRNP proteins controlled by c-Myc deregulate pyruvate kinase mRNA splicing in cancer.* Nature, 2010. **463**(7279): p. 364-8.
125. Mazurek, S., *Pyruvate kinase type M2: a key regulator of the metabolic budget system in tumor cells.* Int J Biochem Cell Biol, 2011. **43**(7): p. 969-80.
126. Demaria, M. and V. Poli, *PKM2, STAT3 and HIF-1alpha: The Warburg's vicious circle.* Jakstat, 2012. **1**(3): p. 194-6.
127. Keller, K.E., I.S. Tan, and Y.S. Lee, *SAICAR stimulates pyruvate kinase isoform M2 and promotes cancer cell survival in glucose-limited conditions.* Science, 2012. **338**(6110): p. 1069-72.
128. Hitosugi, T., et al., *Tyrosine phosphorylation inhibits PKM2 to promote the Warburg effect and tumor growth.* Sci Signal, 2009. **2**(97): p. ra73.
129. Tai, W.T., et al., *SH2 domain-containing phosphatase 1 regulates pyruvate kinase M2 in hepatocellular carcinoma.* Oncotarget, 2016. **7**(16): p. 22193-205.
130. Park, Y.S., et al., *AKT-induced PKM2 phosphorylation signals for IGF-1-stimulated cancer cell growth.* Oncotarget, 2016. **7**(30): p. 48155-48167.
131. Gao, X., et al., *Pyruvate kinase M2 regulates gene transcription by acting as a protein kinase.* Mol Cell, 2012. **45**(5): p. 598-609.
132. Hosios, A.M., et al., *Lack of Evidence for PKM2 Protein Kinase Activity.* Mol Cell, 2015. **59**(5): p. 850-7.
133. Anastasiou, D., et al., *Pyruvate kinase M2 activators promote tetramer formation and suppress tumorigenesis.* Nat Chem Biol, 2012. **8**(10): p. 839-47.

134. Palsson-McDermott, E.M., et al., *Pyruvate Kinase M2 Is Required for the Expression of the Immune Checkpoint PD-L1 in Immune Cells and Tumors.* Front Immunol, 2017. **8**: p. 1300.
135. Mah, A.Y., et al., *Glycolytic requirement for NK cell cytotoxicity and cytomegalovirus control.* JCI insight, 2017. **2**(23): p. e95128.
136. McCartney, S., et al., *Distinct and complementary functions of MDA5 and TLR3 in poly(I:C)-mediated activation of mouse NK cells.* J Exp Med, 2009. **206**(13): p. 2967-76.
137. Narni-Mancinelli, E., et al., *Fate mapping analysis of lymphoid cells expressing the NKp46 cell surface receptor.* Proceedings of the National Academy of Sciences, 2011. **108**(45): p. 18324-18329.
138. Chiossone, L., et al., *Maturation of mouse NK cells is a 4-stage developmental program.* Blood, 2009. **113**(22): p. 5488-96.
139. Loftus, R.M., et al., *Amino acid-dependent cMyc expression is essential for NK cell metabolic and functional responses in mice.* Nature Communications, 2018. **9**(1): p. 2341.
140. Bukowski, J.F., B.A. Woda, and R.M. Welsh, *Pathogenesis of murine cytomegalovirus infection in natural killer cell-depleted mice.* J Virol, 1984. **52**(1): p. 119-28.
141. Lee, S.-H., et al., *Activating receptors promote NK cell expansion for maintenance, IL-10 production, and CD8 T cell regulation during viral infection.* The Journal of Experimental Medicine, 2009. **206**(10): p. 2235-2251.
142. Geurs, T.L., et al., *Ly49H Engagement Compensates for the Absence of Type I Interferon Signaling in Stimulating NK Cell Proliferation During Murine Cytomegalovirus Infection.* The Journal of Immunology, 2009. **183**(9): p. 5830-5836.
143. Tanaka, K., et al., *Role of the Indigenous Microbiota in Maintaining the Virus-Specific CD8 Memory T Cells in the Lung of Mice Infected with Murine Cytomegalovirus.* The Journal of Immunology, 2007. **178**(8): p. 5209-5216.
144. El-Brolosy, M.A. and D.Y.R. Stainier, *Genetic compensation: A phenomenon in search of mechanisms.* PLoS genetics, 2017. **13**(7): p. e1006780-e1006780.
145. Jurkin, J., et al., *Distinct and redundant functions of histone deacetylases HDAC1 and HDAC2 in proliferation and tumorigenesis.* Cell Cycle, 2011. **10**(3): p. 406-12.
146. Israelsen, W.J. and M.G. Vander Heiden, *Pyruvate kinase: Function, regulation and role in cancer.* Seminars in cell & developmental biology, 2015. **43**: p. 43-51.
147. Israelsen, William J., et al., *PKM2 Isoform-Specific Deletion Reveals a Differential Requirement for Pyruvate Kinase in Tumor Cells.* Cell, 2013. **155**(2): p. 397-409.
148. Lucas, M., et al., *Dendritic cells prime natural killer cells by trans-presenting interleukin 15.* Immunity, 2007. **26**(4): p. 503-17.
149. Dubois, S., et al., *IL-15Ralpha recycles and presents IL-15 In trans to neighboring cells.* Immunity, 2002. **17**(5): p. 537-47.
150. Li, Y.H., et al., *PKM2, a potential target for regulating cancer.* Gene, 2018. **668**: p. 48-53.

151. Jiang, L. and R.J. DeBerardinis, *When more is less.* Nature, 2012. **489**(7417): p. 511-512.
152. Cruzat, V., et al., *Glutamine: Metabolism and Immune Function, Supplementation and Clinical Translation.* Nutrients, 2018. **10**(11): p. 1564.
153. Arase, N., et al., *Association with FcRγ Is Essential for Activation Signal through NKR-P1 (CD161) in Natural Killer (NK) Cells and NK1.1⁺ T Cells.* The Journal of Experimental Medicine, 1997. **186**(12): p. 1957-1963.
154. Valentini, G., et al., *The Allosteric Regulation of Pyruvate Kinase: A SITE-DIRECTED MUTAGENESIS STUDY.* Journal of Biological Chemistry, 2000. **275**(24): p. 18145-18152.
155. Xia, J., et al., *MetaboAnalyst: a web server for metabolomic data analysis and interpretation.* Nucleic acids research, 2009. **37**(Web Server issue): p. W652-W660.
156. Wang, W., et al., *Glycine metabolism in animals and humans: implications for nutrition and health.* Amino Acids, 2013. **45**(3): p. 463-77.
157. Nikiforov, M.A., et al., *A Functional Screen for Myc-Responsive Genes Reveals Serine Hydroxymethyltransferase, a Major Source of the One-Carbon Unit for Cell Metabolism.* Molecular and Cellular Biology, 2002. **22**(16): p. 5793-5800.
158. Miller, D.M., et al., *c-Myc and Cancer Metabolism.* Clinical Cancer Research, 2012. **18**(20): p. 5546-5553.
159. Eischen, C.M., et al., *Bcl-2 is an apoptotic target suppressed by both c-Myc and E2F-1.* Oncogene, 2001. **20**(48): p. 6983-6993.
160. Ruttkay-Nedecky, B., et al., *The role of metallothionein in oxidative stress.* International journal of molecular sciences, 2013. **14**(3): p. 6044-6066.
161. Iszard, M.B., J. Liu, and C.D. Klaassen, *Effect of several metallothionein inducers on oxidative stress defense mechanisms in rats.* Toxicology, 1995. **104**(1): p. 25-33.
162. Sato, M. and I. Bremner, *Oxygen free radicals and metallothionein.* Free Radical Biology and Medicine, 1993. **14**(3): p. 325-337.
163. Snaebjornsson, M.T. and A. Schulze, *Non-canonical functions of enzymes facilitate cross-talk between cell metabolic and regulatory pathways.* Experimental & Molecular Medicine, 2018. **50**(4): p. 34.
164. Polet, F., et al., *Inhibition of glucose metabolism prevents glycosylation of the glutamine transporter ASCT2 and promotes compensatory LAT1 upregulation in leukemia cells.* Oncotarget, 2016. **7**(29): p. 46371-46383.
165. Anastasiou, D., et al., *Inhibition of pyruvate kinase M2 by reactive oxygen species contributes to cellular antioxidant responses.* Science, 2011. **334**(6060): p. 1278-83.
166. Dong, G., et al., *PKM2 and cancer: The function of PKM2 beyond glycolysis.* Oncology letters, 2016. **11**(3): p. 1980-1986.
167. Mak, T.W., et al., *Glutathione Primes T Cell Metabolism for Inflammation.* Immunity, 2017. **46**(4): p. 675-689.
168. Hosios, Aaron M., et al., *Lack of Evidence for PKM2 Protein Kinase Activity.* Molecular Cell, 2015. **59**(5): p. 850-857.
169. Tang, Q., et al., *Pyruvate kinase M2 regulates apoptosis of intestinal epithelial cells in Crohn's disease.* Dig Dis Sci, 2015. **60**(2): p. 393-404.

170. Zhao, X., et al., *Shikonin Inhibits Tumor Growth in Mice by Suppressing Pyruvate Kinase M2-mediated Aerobic Glycolysis.* Scientific Reports, 2018. **8**(1): p. 14517.
171. Li, Y., et al., *Enhancement of NK cells proliferation and function by Shikonin.* Immunopharmacol Immunotoxicol, 2017. **39**(3): p. 124-130.
172. Su, L., et al., *Long-term systemic toxicity of shikonin derivatives in Wistar rats.* Pharm Biol, 2013.
173. Lukey, M.J., K.F. Wilson, and R.A. Cerione, *Therapeutic strategies impacting cancer cell glutamine metabolism.* Future Med Chem, 2013. **5**(14): p. 1685-700.
174. Chabner, B.A. and T.G. Roberts, *Chemotherapy and the war on cancer.* Nature Reviews Cancer, 2005. **5**(1): p. 65-72.
175. Wang, Y., V. Probin, and D. Zhou, *Cancer therapy-induced residual bone marrow injury-Mechanisms of induction and implication for therapy.* Current cancer therapy reviews, 2006. **2**(3): p. 271-279.